PERFORMANCE EVALUATION OF 4.75-MM NMAS SUPERPAVE MIXTURE

by

FARHANA RAHMAN

B.S., Bangladesh University of Engineering and Technology, Bangladesh, 2002
M.A.Sc., Concordia University, Montreal, Canada, 2005

AN ABSTRACT OF A DISSERTATION

submitted in partial fulfillment of the requirements for the degree

DOCTOR OF PHILOSOPHY

Department of Civil Engineering
College of Engineering

KANSAS STATE UNIVERSITY
Manhattan, Kansas

2010

Abstract

A Superpave asphalt mixture with 4.75-mm nominal maximum aggregate size (NMAS) is a promising, low-cost pavement preservation treatment for agencies such as the Kansas Department of Transportation (KDOT). The objective of this research study is to develop an optimized 4.75-mm NMAS Superpave mixture in Kansas. In addition, the study evaluated the residual tack coat application rate for the 4.75-mm NMAS mix overlay.

Two, hot-in-place recycling (HIPR) projects in Kansas, on US-160 and K-25, were overlaid with a 15- to 19-mm thick layer of 4.75-mm NMAS Superpave mixture in 2007. The field tack coat application rate was measured during construction. Cores were collected from each test section for Hamburg wheel tracking device (HWTD) and laboratory bond tests performed after construction and after one year in service. Test results showed no significant effect of the tack coat application rate on the rutting performance of rehabilitated pavements. The number of wheel passes to rutting failure observed during the HWTD test was dependent on the aggregate source as well as on in-place density of the cores. Laboratory pull-off tests showed that most cores were fully bonded at the interface of the 4.75-mm NMAS overlay and the HIPR layer, regardless of the tack application rate. The failure mode during pull-off tests at the HMA interface was highly dependent on the aggregate source and mix design of the existing layer material. This study also confirmed that overlay construction with a high tack coat application rate may result in bond failure at the HMA interface.

Twelve different 4.75-mm NMAS mix designs were developed using materials from the aforementioned but two binder grades and three different percentages of natural (river) sand. Laboratory performance tests were conducted to assess mixture performance. Results show that rutting and moisture damage potential in the laboratory depend on aggregate type irrespective of binder grade. Anti-stripping agent affects moisture sensitivity test results. Fatigue performance is significantly influenced by river sand content and binder grade. Finally, an optimized 4.75-mm NMAS mixture design was developed and verified based on statistical analysis of performance data.

PERFORMANCE EVALUATION OF 4.75-MM NMAS SUPERPAVE MIXTURE

by

FARHANA RAHMAN

B.S., Bangladesh University of Engineering and Technology, Bangladesh, 2002
M.A.Sc., Concordia University, Montreal, Canada, 2005

A DISSERTATION

submitted in partial fulfillment of the requirements for the degree

DOCTOR OF PHILOSOPHY

Department of Civil Engineering
College of Engineering

KANSAS STATE UNIVERSITY
Manhattan, Kansas

2010

Approved by:

Major Professor
Dr. Mustaque Hossain

Copyright

Abstract

A Superpave asphalt mixture with 4.75-mm nominal maximum aggregate size (NMAS) is a promising, low-cost pavement preservation treatment for agencies such as the Kansas Department of Transportation (KDOT). The objective of this research study is to develop an optimized 4.75-mm NMAS Superpave mixture in Kansas. In addition, the study evaluated the residual tack coat application rate for the 4.75-mm NMAS mix overlay.

Two, hot-in-place recycling (HIPR) projects in Kansas, on US-160 and K-25, were overlaid with a 15- to 19-mm thick layer of 4.75-mm NMAS Superpave mixture in 2007. The field tack coat application rate was measured during construction. Cores were collected from each test section for Hamburg wheel tracking device (HWTD) and laboratory bond tests performed after construction and after one year in service. Test results showed no significant effect of the tack coat application rate on the rutting performance of rehabilitated pavements. The number of wheel passes to rutting failure observed during the HWTD test was dependent on the aggregate source as well as on in-place density of the cores. Laboratory pull-off tests showed that most cores were fully bonded at the interface of the 4.75-mm NMAS overlay and the HIPR layer, regardless of the tack application rate. The failure mode during pull-off tests at the HMA interface was highly dependent on the aggregate source and mix design of the existing layer material. This study also confirmed that overlay construction with a high tack coat application rate may result in bond failure at the HMA interface.

Twelve different 4.75-mm NMAS mix designs were developed using materials from the aforementioned but two binder grades and three different percentages of natural (river) sand. Laboratory performance tests were conducted to assess mixture performance. Results show that rutting and moisture damage potential in the laboratory depend on aggregate type irrespective of binder grade. Anti-stripping agent affects moisture sensitivity test results. Fatigue performance is significantly influenced by river sand content and binder grade. Finally, an optimized 4.75-mm NMAS mixture design was developed and verified based on statistical analysis of performance data.

Table of Contents

List of Figures

List of Tables

Acknowledgements

At first, I would like to pay my outmost respect to Almighty Allah, for granting me this wonderful opportunity to work and to live.

I would like to avail this opportunity to express my sincere gratitude to my major professor Dr. Mustaque Hossain for his overall supervision, invaluable suggestions and constant encouragement at all stages of my study and research at Kansas State University. Starting from the elementary concepts, it is his keen interest and ardent inspiration that helped me to become a skilled thinker and learner. I am honored to carry out this research study under his direct supervision.

I would like to thank and express my sincere appreciation to Dr. Stefan A. Romanoschi for being in my dissertation committee and providing valuable guidance and suggestions through out the research. I am also thankful to Dr. James Neill for being my committee member and for his constructive advice during statistical analysis. I would also like to thank Dr. Sunanda Dissanayake for being in my committee and for her continuous support and encouragement.

I acknowledge the fact that the development and compilation of this research work was a team effort and I sincerely appreciate the financial support provided by Kansas Department of Transportation (KDOT) for this unique research study. I also acknowledge Mr. Cliff Hobson of KDOT for his valuable advice and support in conducting some of the material tests in KDOT laboratory.

I would also like to acknowledge my colleagues, graduate and undergraduate students who helped me in the KSU laboratory during sample preparation and testing.

Finally, I wish to express my sincere respect to my parents and sister, Afsana Rahman, for their understanding and blessings that helped me to be what I am today. I would like to express my special thanks to my husband, G. M. Osmani, for being in my life and for his patience and support.

Dedication

This dissertation is dedicated to my mother, **Mrs. Akhtar Jahan Hafiza Khanam**, and my father, **Mr. Md. Azizur Rahman**, for their endless support.

CHAPTER 1-INTRODUCTION

1.1 General

Transportation industries and infrastructure facilities such as highways consume large quantities of materials in initial construction and periodic maintenance and rehabilitation. The United States has the largest highway networks (4.04 million miles) in the world which are mainly classified into the Interstate, U.S. state and local government Highway systems. As of 2008, 94% of the highway network pavements are flexible pavement (asphalt surfaced) while the rest are either rigid (concrete) or composite pavements (asphalt layer overlaid on concrete pavement) (FHWA 2008). Kansas has about 89% of the total paved-road network which are asphalt surfaced. The common pavement distresses on asphalt pavements in Kansas can be partly addressed by proper selection of construction materials and by developing suitable mix design. The Superpave (*Su*perior *Per*forming Asphalt *Pave*ments) mix design procedure has been adopted by many state agencies including Kansas during the last decade. The Superpave procedure focuses mainly on the mixture performance corresponding to climatic conditions and expected traffic levels during pavement design life. This mix design system has design criteria for 9.5-mm to 37.5-mm nominal maximum aggregate size (NMAS) mixes. Until 2001, 9.5-mm was the smallest NMAS used in the Superpave mix design. In 2002, the National Center for Asphalt Technology (NCAT) developed Superpave mix design criteria for the 4.75-mm NMAS mix (Cooley et al. 2002). Prior to Superpave implementation, many state agencies successfully used fine mixes for various maintenance applications on low-traffic-volume roads (Williams 2006). Recently, many state agencies have expressed their interest in implementing 4.75-mm

NMAS Superpave designed mixtures for thin lift-applications, leveling courses, and for roadway maintenance.

1.1.1 Introduction to Superpave

Since the discovery of the petroleum asphalt refining process, asphalt pavement has become popular all over the world. In 1920s, the Hubbard-Field method was developed for a sheet asphalt mix with aggregates that passed fully through a 4.75-mm sieve. However, it was modified to design coarser asphalt mixtures. The method included a stability test to measure strength of the mixture using a punching-type shear load. After 1930s, the widely used Hveem method (developed by the California Department of Highways Materials and Design) and Marshall method (developed by the Mississippi Department of Transportation) were introduced in hot-mix asphalt (HMA) design. The Hveem stabilometer measures an asphalt mixture's ability to resist lateral movement under a vertical load, while the primary features of the Marshall mix design are the density/void analysis and the stability/flow test (Hossain et al. 2010).

Refinement of HMA design methods came into picture not only with the increasing use of asphalt but also with an increase in traffic volume and loading configuration. As the transportation industry grew, the demand for HMA in heavy-duty pavement applications also grew. Highway state agencies were trying to determine a fine line between mixtures that performed well and poorly (Hossain et al. 2010). The materials were the same, but the asphalt materials and pavement performances were evaluated in terms of traffic volume and load.

In 1987, the Strategic Highway Research Program (SHRP) began a significant research effort with the objective to create an improved asphalt mix design procedure. The final product of the SHRP asphalt research program was Superpave (*Su*perior *Per*forming Asphalt *Pave*ments). Traditional mix design methods, the Marshal and Hveem, were based on the

concept that if the mixture volumetric properties satisfy a set of specifications, the mix would perform well under any condition. In terms of field performance, very little testing was done to validate the claims. The design method of Superpave is based on performance-based specification. Even though it uses traditional volumetric mix design methodologies, it also includes a performance concept. The tests and analyses have direct relationships to field performance. In addition, the Superpave mix design system integrates material selection (asphalt and aggregate) and mix design into procedures based on pavement structural section, design traffic, and climate conditions. In Superpave, test procedures and performance-based models are used to estimate the performance life of HMA in terms of equivalent single-axle loads (ESALs). Since its implementation, the Superpave methodology has helped state agencies to achieve better performance of their mixes in terms of enhanced resistance to permanent deformation, fatigue, low-temperature cracking, moisture-induced damage, workability, and skid resistance to durable pavement layer (Roberts et al. 1996).

1.1.2 Fine Mix Concept in Superpave

Before the implementation of the Superpave mix design method, the mixes were fairly fine-graded. This was due to the fact that gradation of the aggregate blend prior and after Superpave is completely different. The combined aggregate gradation prior to the Superpave mix passed over the maximum density line (MDL) while some Superpave aggregate gradations passed below the restricted zone. The largest difference was evident in the material passing the intermediate sieve (No. 8 sieve). In the Superpave method, the mix contained significant amounts of both coarse and fine aggregates, with a limited amount of intermediate-size aggregates. This aggregate blending enhanced the structural capacity of the mixes. Though, the Superpave mix design included gradation specifications for 37.5-mm, 25.0-mm, 19.0-mm, and

9.5-mm NMAS mixtures, many state agencies successfully implemented smaller aggregates for rehabilitation and maintenance projects. Therefore, lack of Superpave specification for 4.75-mm NMAS mixes caused a significant gap in their implementation.

HMA mixes with smaller aggregate size can be used in thin-lift applications, commonly used in pavement preservation projects. In a corrective maintenance program, a fine-graded mixture is well accepted in leveling and shimming of the existing pavement before overlay application. The primary objective is to provide durability, workability, and smoothness. For preventive maintenance, thin-lift application of the fine mix is an excellent alternative to stretch the maintenance budget if the pavement does not experience major distresses. This application primarily improves ride quality, reduces permeability, and sometimes leads to minor crack healing.

Although the structural capacity of the fine mixes is not adequate for truck parking and loading areas, it can be utilized for low-volume highways such as rural highways, county roads, and city streets or parking lots. It is to be noted that the fine mixes are not expected to improve the structural capacity of the pavement structure and should not be placed on the weak pavement structures. As most state agencies are merging into the Superpave system, it is quite evident that complete design specifications for 4.75-mm NMAS are in great need.

Maryland and Georgia DOT have successfully used thin HMA overlays as part of their preventive maintenance program. These mixes showed excellent resistance to rutting and cracking. North Carolina is another state that has successfully implemented thin-lift overlay. They used a coarse-sand asphalt mix for paving very low-volume roadways. The target was to design a mix with higher air voids and hence, reduced optimum binder content and increased rutting resistance. Other states, such as Ohio, Missouri, Indiana, and Tennessee, have also

designed their own specifications for thin-lift HMA applications. Ohio uses a mixture known as "Smoothseal". Type A of this particular mix is extremely fine and is used for medium and urban traffic. Type B is a coarser mix and is used for heavy-duty traffic and high-speed application. Type B has a gradation similar to that of the 4.75-mm NMAS Superpave mixture. A minimum binder content of 6.4 percent is used with a minimum VMA of 15 percent and a 4 percent air void (Ohio DOT 2010). Figure 1.1 shows the Type A and Type B smoothseal.

Figure 1.1 Mixture with Type A and Type B "smoothseal" (Ohio DOT 2010)

1.2 Problem Statement

A successful pavement design ensures extended service life of the pavement structure. The design process typically includes proper selection and design of the construction materials, interface layer strength, and determination of layer thickness depending on traffic volume and climatic conditions, and finally, drainage conditions. A recent survey on Superpave-designed

pavements proves that permeability is one of the biggest problems in pavement design. The survey suggested that coarse-graded Superpave mixes result in higher permeability compared to the dense-graded mixes at the same air void (Mallick et al. 2003). It can be expected that permeability reduces durability of the pavement structure and hence, shortens the pavement life. The most critical issue is the infiltration of water into the pavement, causing stripping. The study also suggested that material selection plays a significant role in reducing the problem.

Mixes with 4.75-mm NMAS have the potential to improve riding quality and safety characteristics, extend pavement life, increase durability, and reduce permeability and road-tire noise. Many states, including Kansas, are looking at pavement preservation techniques that are cost effective due to budget constraints. Since some past experiences with thin hot-mix asphalt (HMA) overlays were positive in a few states, the 4.75-mm mixes have attracted attention from many state agencies. Since the mixes are placed in thin-lift applications, they can be used for corrective maintenance, to decrease construction time and cost, and to provide a very economical surface mix for low-traffic- volume facilities.

With the advent of Superpave, many state agencies recommended the use of a coarse-grained mixture and some agencies have begun to utilize stone-matrix asphalt (SMA) mixes (Williams 2006). Both mix types confirm their stability using the stone-to-stone contact of coarse particles, which in turn, reduces the application of fine aggregate materials. Implementation of 4.75-mm NMAS Superpave mix will reduce these screening stockpiles accumulated after the use of larger aggregates and hence provide a use for materials that could become a “by-product” of the HMA industry.

It is important to note that the aggregate source plays the most important part in pavement performance. Potential limitations for small-aggregate-size mixtures include concerns

with permanent deformation, moisture resistance, scuffing, and skid resistance. In addition, gradation criteria followed by different state agencies before 2002 were different and were put in place based on the experience of project personnel.

In 2002, the 4.75-mm NMAS designation and criteria were added to the AASHTO Superpave specifications to fit the need for small-aggregate-size mixtures. These criteria were based on a combination of experience, limited laboratory research, and engineering judgment. Thus, no study has been reported on the large-scale use of this mix in the field. A recent NCAT laboratory refinement study on 4.75-mm NMAS mix performance has been published, but the second phase of field evaluation is yet to come.

Another important issue in new pavement construction and rehabilitation projects is the bond strength at the layer interface. Poor bond between the two layers of HMA is the cause of many pavement problems. Slippage failure is one of the most common distresses that often occurs at locations where traffic accelerates, decelerates, or turns. Other pavement problems may also be attributed to the insufficient bond between the pavement layers of HMA. Compaction difficulty, premature fatigue, top-down cracking, and surface layer delamination have also been associated with a poor bond between HMA layers (West et al. 2005). An NCAT study in 2005 showed the laboratory bond-strength performance of 4.75-mm NMAS mix for new pavement layers. No study on 4.75-mm mix was performed based on a field bond-strength evaluation for a new pavement construction/pavement preservation program. Hence, research is needed in this area before widespread implementation of this mixture.

1.3 Objective

The overall objective of this research study was to evaluate various aspects of the design of 4.75-mm Superpave mixture, and to asses the relative performance of the mix in both field and

laboratory environments in terms of rutting, stripping, and long-term fatigue behavior. The step-by-step objectives were as follows:

- Investigation of laboratory 4.75-mm NMAS Superpave mixture volumetrics and performance, especially rutting, stripping, and long-term fatigue.
- Examination of the rutting performance of 4.75-mm NMAS ultra-thin overlay constructed in the field under Hamburg Wheel Tracking Device.
- Evaluation of bond strength of tack coat material at different application rates and verification of the state practice of application rate for 4.75-mm NMAS ultra-thin overlay.
- Measurement and assessment of the residual tack coat application rate in field conditions.
- Statistical analysis to identify the most influential factors affecting the laboratory mix design and to develop regression equations for laboratory mix performance.
- Development of an optimized mix design for 4.75-mm NMAS Superpave mixture based on performance regression equations to enhance performance and to extend pavement service life.

1.4 Organization of Dissertation

This dissertation is divided into six chapters. The first chapter covers a brief introduction on Superpave background and Superpave fine mixes, problem statement, study objectives, and the outline of the report. Chapter 2 covers the review of the literature and a detailed study on Superpave specifications and Superpave fine mixes, discussion of tack coat materials and bond strength test procedures at HMA interface, and some recent studies on bond strength in hot mix asphalt pavement. Chapter 3 describes the test section and data collection procedure in the field, laboratory aggregate testing and mix design procedure of 4.75-mm NMAS Superpave mixture,

and performance tests used to evaluate field cores and laboratory mixes. Chapter 4 presents the analysis of the test results. Statistical analysis of the test results are discussed in Chapter 5. Finally, Chapter 6 presents conclusions and recommendations based on the present study.

CHAPTER 2 - LITERATURE REVIEW

2.1 Superpave Compaction and Specification

One of the most significant changes made in the Superpave technology was development of the Superpave gyratory compactor (SGC). It has the combined features of the Texas gyratory compactor and the French gyratory compactor (Figure 2.1). During compaction, the mold is tilted at an internal angle of 1.16 degrees at a constant speed of 30 revolutions per minute, while being subjected to a compaction pressure of 600±6 kPa (87±0.87 psi). This compaction method simulates field conditions better than the traditional impact compaction process used in the Marshall method.

Figure 2.1 Pine Superpave gyratory compactor

Compacting effort in the SGC is expressed in terms of the number of gyrations (N) applied to the specimen. Three different gyration levels (N_{ini}, N_{des}, and N_{max}) are considered in

mix design. These three levels of gyration represent the density of the mix at different stages of the pavement over the design life. The design number of gyration (N_{des}) is a function of the project traffic level, which is 20-year design ESALs. Higher compactive effort is required for mixes that are subjected to heavy traffic condition. It is to be noted that if the initial density is too high, the mixture may show stability problems, while too high density at N_{max} may result in bleeding and rutting. Special provisions for a project provided by KDOT list N_{ini}, N_{des}, and N_{max} as shown in Table 2.1. Gyration-level values for the project are determined from the design traffic level.

Table 2.1 Gyratory Compactive Efforts in Superpave Volumetric Mix Design (Hossain et al. 2010)

20-Year Design ESALs (Million)		Compactive Effort		
		N_{ini}	N_{des}	N_{max}
< 0.3		6	50	75
0.3 - < 3		7	75	115
3 - < 30		8	100	160
> 30		9	125	205
Shoulder*	A	6	50	75
	B	**	**	**

* At the contractor's option, A or B may be used.
** Use traveled-way design properties.

2.1.1 Performance Grade of Binder

Another important change incorporated into the Superpave method is the binder performance grade. Asphalt cement binders are specified based on their expected performance at a range of temperatures. For example, if a binder has PG 64-22, it is expected that it will perform well at a high pavement temperature of 64 ^{0}C (147.2^{0}F) and a low pavement temperature of -22 ^{0}C (7.6 ^{0}F). Consideration of PG binder grade ensures good performance of the binder at the environmental conditions of that project location (AI 1994).

Binder selection in the Superpave method is totally dependent on climate and traffic-loading conditions of the paving project location. The minimum PG binder required to satisfy design reliability is selected using pavement temperature data. Pavement temperature data is obtained from the mean and standard deviation of the yearly, seven-day average, maximum pavement temperature at 20 mm (0.8 inch) below the pavement surface. The high-temperature grade of the binder is adjusted by the number of grade evaluations illustrated in Table 2.2, when traffic speed and design ESALs warrant such adjustment.

Table 2.2 Binder Selection Based on Traffic Speed and Traffic Level (Hossain et al. 2010)

Design ESALs[1] (Millions)	Adjustment to the High Temperature of the Binder[5]		
	Traffic Load Rate		
	Standing[2]	Slow[3]	Standard[4]
< 0.3	Note[6]	-	-
0.3 - < 3	2	1	-
3 - < 10	2	1	-
10 - < 30	2	1	Note[6]
≥ 30	2	1	1

(1) The anticipated project traffic level expected on the design lane over a 20-year period. Regardless of the actual design life of the roadway, determine design ESALs for 20 years.
(2) Standing traffic - where average traffic speed is less than 20 km/h.
(3) Slow traffic - where average traffic speed ranges from 20 to 70 km/h.
(4) Standard traffic - where average traffic speed is greater that 70 km/h.
(5) Increase the high-temperature grade by the number of grade equivalents indicated (one grade is equivalent to 6^0 C). Use the low-temperature grade as determined in this section.
(6) Consideration should be given to increasing the high-temperature grade by one grade equivalent.

2.1.2 Aggregate Properties

Aggregate properties are also included in Superpave specifications with respect to performance. Two types of aggregate properties are specified in the Superpave system: "consensus" and "source". Many state agencies that had already employed specifications for such properties and inclusion of these properties explained the importance of aggregate characteristics.

Consensus properties are those properties that had been selected by a group of experts during SHRP research and are critical in achieving high-performance HMA. These properties

must be met at various levels depending on traffic load and position within the pavement structure. Table 2.3 lists the consensus properties of the aggregate and the requirements specified by KDOT.

Table 2.3 KDOT Requirements for Consensus Properties of Superpave Aggregates (Hossain et al. 2010)

Design ESALs[1] (Millions)	Property					
	Coarse Aggregate Angularity (Min., %)		Fine Aggregate Angularity (Min., %)		Flat or Elongated Particles	Clay Content
	Depth from Surface		Depth from Surface		(Max., %)	(Min., %)
	≤ 100 mm	> 100 mm	≤ 100 mm	> 100 mm		
< 0.3	55	50	42	42	10	40
0.3 - < 3	75	50	42(45*)	42	10	40
3 - < 10	85/80**	60	45	42	10	45
10 - < 30	95/90	80/75	45	42	10	45
≥ 30	100/100	100/100	45	45	10	50
Shoulder	50	50	40	40	-	40

* For SM-19A mixes
** 85/80 means that 85% of the coarse aggregate has one or more fractured faces and 80% has two or more fractured faces.

Fine aggregate angularity (FAA) is more critical in dealing with fine mixes (for example, 4.75-mm NMAS). It ensures a high degree of internal friction for the fine aggregates and enhances rutting resistance. Specifications for FAA limit the use of natural sands which create a "tender" mix. The 4.75-mm mixes contain primarily fine aggregate and hence, the properties of fine-aggregate angularity are important to the performance of such mixes.

Source properties are also believed to be critical to pavement performance, but they are project–specific. Thus, critical values are basically established by local agencies based on source type. These properties are often used to qualify local sources of aggregates. Source properties included in the KDOT Superpave methods are toughness (40 to 45% L.A. abrasion test), soundness (0.85 to 0.95), and deleterious materials. In addition, specific gravities of the

aggregates (both bulk and apparent) used in the mix design need to be evaluated by Kansas Test Method KT-6.

2.1.3 Aggregate Gradation

The structure of the aggregate blend is also important to ensure mixture performance. Traditional specifications typically included a "band" for acceptable gradations so that the entire gradation curve could be plotted within that band width. In Superpave mix design, the blended aggregate gradation curves can take any shape as long as they lie within the control points. The control points refer to the maximum aggregate size (MAS), nominal maximum aggregate size (NMAS), an intermediate sieve size (normally 2.36 mm, except 1.18 mm for 4.75-mm NMAS), and the dust size (US No. 200 or 0.075 mm sieve) (Cooley et al. 2002).

Superpave uses a 0.45-power gradation chart to define a permissible gradation. The chart is a unique graphing technique to evaluate the cumulative particle-size distribution of the aggregate blend. An important feature of this power chart is the maximum density gradation. The maximum density gradation is a gradation where the aggregate particles fit themselves in the densest possible arrangement.

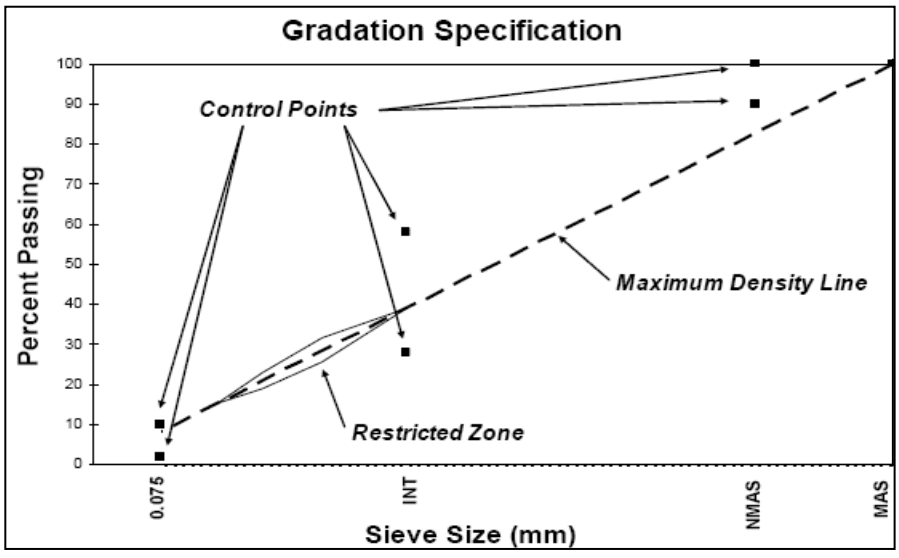

Figure 2.2 Superpave gradation specifications (Williams 2006)

The plot of the maximum density line (MDL) is a straight line from the maximum aggregate size to the origin. While designing aggregate structures, this gradation line should be avoided to obtain the optimum asphalt film thickness and thereby, to produce a durable mixture. Figure 2.2 shows the gradation specifications in Superpave mix design.

Early Superpave gradations were restricted by the control points, as well as an area called the restricted zone (RZ). Several highway agencies successfully used gradations passing above the restricted zone (ARZ), below the restricted zone (BRZ), and through the restricted zone (RZ) and these mixes performed well. Hence, the highway agencies were encouraged to eliminate use of a restricted zone (Kandhal and Cooley 2002, Hand and Epps 2001).

The Superpave method defines six mixture gradations of design aggregate structure by their nominal maximum aggregate sizes shown in Tables 2.4 and 2.5. Table 2.5 illustrates numerical gradation limits (% retained) of mixtures for major modification and overlay projects in Kansas. It incorporates the control points described by Superpave. KDOT uses the NMAS to define each mix, and mixes ending in A (for example SM-4.75A) pass above the maximum density line in the finer sieve sizes. Mixes ending with B or T (such as SM-9.5B and SM-9.5T) go below the maximum density line in the gradation chart.

Table 2.4 Superpave Mixture Sizes

Superpave Designation	Nominal Maximum Size (mm)	Maximum Size (mm)
37.5 mm	37.5	50
25 mm	25	37.5
19 mm	19	25
12.5 mm	12.5	19
9.5 mm	9.5	12.5
4.75 mm	4.75	9.5

Table 2.5 KDOT Superpave Designed Aggregate Gradations (% Retained) for Major Modification and 1R Overlay Projects (Hossain et al. 2010)

Nominal Max. Size Mix Designation	Percent Retained-Square Mesh Sieves								Min. VMA (%)
	25.0 mm	19.0 mm	12.5 mm	9.5 mm	4.75 mm	2.36 mm	1.18 mm	0.075mm	
SM-4.75A			0	0-5	0-10		40-70	90-98	16.0
SM-9.5A & SR-9.5A			0	0-10	10 min	33-53		90-98	15.0
SM-9.5B & SR-9.5B			0	0-10	10 min	53-68		90-98	15.0
SM-9.5T & SR-9.5T			0	0-10	10 min	53-68		90-98	15.0
SM-12.5A & SR-12.5A		0	0-10	10min		42-61		90-98	14.0
SM-12.5B & SR-12.5B		0	0-10	10 min		61-72		90-98	14.0
SM-19A & SR-19A	0	0-10	10 min			51-65		92-98	13.0
SM-19B & SR-19B	0	0-10	10 min			65-77		92-98	13.0

2.1.4 Volumetric Design Specifications

Requirements for volumetric mix design protocol are another vital part in the Superpave method. Volumetric mix properties of a compacted paving mixture include percent air voids in the compacted mix, voids in the mineral aggregate (VMA), voids filled with asphalt (VFA), in-place density at the initial number of gyrations (N_{ini}), and in-place density at the final number of gyrations (N_{max}). Similar to the traditional mix design methods, Superpave has also specified the limiting values of these volumetric properties that significantly affect mixture performance.

2.1.4.1 Air Voids

Air void is a major volumetric property that significantly affects pavement performance. Air void is the total volume of the small pockets of air between the coated aggregate particles throughout a compacted paving mixture. It can be computed using the following formula:

$$V_a = 100 \times \left[\frac{(G_{mm} - G_{mb})}{G_{mm}} \right] \tag{2.1}$$

where,

G_{mm} = maximum specific gravity of the mix, and

G_{mb} = bulk specific gravity of the mix.

Kansas Superpave specifications state that the mixture with percent air voids between 2 to 6 percent is a stable mix. Air voids below and beyond this range can result in rutting problems during service. Very low air voids indicate that the mixture has experienced overcompaction or premature densification during compaction or traffic operation (Williams 2006). At a very high air void content, the pavement may experience permeability problems and the presence of water may also cause stripping in the asphalt layer. Another external detrimental factor is that excess air promotes oxidation of the asphalt binder and results in a weak and brittle pavement structure.

2.1.4.2 Voids in Mineral Aggregate (VMA)

VMA is the volume of the intergranular void spaces between the aggregate particles in compacted paving mixes. The void space includes air voids and the effective asphalt content and is expressed as a percent of the total volume. VMA can be computed using the following formula:

$$VMA = 100 - \left[\frac{(G_{mb} \times P_s)}{G_{sb}} \right] \tag{2.2}$$

where,

VMA = voids in mineral aggregates;

G_{sb} = bulk specific gravity of the aggregate blend;

G_{mb} = bulk specific gravity of the compacted HMA; and

P_S = percent of aggregate.

It is important in the Superpave mix design method to select an appropriate binder content to enhance mixture durability as well as rut resistance. VMA of the mix decreases to a minimum value with increasing binder content. While the film thickness of the binder increases, the aggregate particles are forced apart from each other and again, VMA volume increases. The optimum binder content is selected from the corresponding minimum value of VMA. Asphalt mixes with binder content less than the optimum binder (on the dry side of the VMA curve) have smaller film thickness and are susceptible to durability problems in the field. Mixes designed with asphalt beyond the optimum value (on the wet side of the VMA curve) are not desirable as they cause rutting, bleeding, and flushing problems in the field. The Superpave mix design procedure incorporates minimum VMA criteria to ensure adequate binder as well as a proper air

void content. With this minimum VMA requirement, it is expected that bleeding and rutting will be minimized and the mix will be durable.

2.1.4.3 Voids Filled with Asphalt (VFA)

VFA is a property of the compacted mix which relates VMA and percent air voids. It is the percentage portion of the volume of intergranular void space between the aggregate particles that is occupied by the effective asphalt. It is calculated using the following equation:

$$VFA = 100 \times \left[\frac{VMA - V_a}{VMA} \right] \tag{2.3}$$

where,

VFA = voids filled with asphalt;

VMA= voids in mineral aggregate; and

V_a = air voids content.

2.1.4.4 Dust-to-Binder Ratio

Dust proportion is an indicator of the amount of mineral materials passing 0.075 mm (US No. 200) sieve with respect to effective asphalt content. These are very fine particles and when combined with binder, can make a major contribution to mix cohesion (Williams 2006). In general, this material has the ability to stiffen the binder, although the performance is also dependent on material types. Thus, dust content can affect rutting potential of a mix (Kandhal and Cooley 2002). The dust proportion (DP) of an HMA compacted paving mix is calculated from the following relation:

$$DP = \left[\frac{P_{0.075}}{P_{be}} \right] \tag{2.4}$$

Where,

$P_{0.075}$ = materials passing 0.075 mm (US No. 200) sieve (%); and

P_{be} = effective binder content (%).

Considering all volumetric properties of HMA paving mix, the Superpave system has also specified the limiting values of the abovementioned properties. Table 2.6 shows a summary of Superpave mixture volumetric property requirements by KDOT.

Table 2.6 KDOT Volumetric Mixture Design Requirements

Design ESAL's (Million)	Req[d]. % Density			Minimum VMA (%)*						VFA Range	DP
				NMAS, (mm)							
	N_{ini}	N_{des}	N_{max}	37.5	25.0	19.0	12.5	9.5	4.75		
< 0.3	≤91.5	96.0	≤98.0	11.0	12.0	13.0	14.0	15.0	16.0	66-80	
0.3 - < 3	≤90.5	96.0	≤98.0	11.0	12.0	13.0	14.0	15.0	16.0	65-78	0.6-1.2[a]
3 - < 10	≤90.0	96.0	≤98.0	11.0	12.0	13.0	14.0	15.0	16.0	65-76	0.6-1.6[b]
10 - < 30	≤89.5	96.0	≤98.0	11.0	12.0	13.0	14.0	15.0	16.0	65-76	0.8-1.6[c]
≥ 30	≤89.0	96.0	≤98.0	11.0	12.0	13.0	14.0	15.0	16.0	65-76	0.9-2.0[d]
Shoulder	≤91.5	96.0	≤98.0	11.0	12.0	13.0	14.0	15.0	16.0	66-80	

[a] = SM-9.5A; [b]= SM-12.5A, SM-19A; [c] = SM-9.5B, SM-9.5T, SM-12.5B, SM-19B; [d] = SM-4.75A
* = Values may be reduced by 1% for 1-R HMA overlay.

2.2 Performance Tests of Superpave Mix Design

Volumetric properties in the Superpave method significantly affect performance of the paving mix; however, the relationships are empirical and based on the experience. The Superpave system developed new equipment to asses the performance of the designed mixes. The purpose was to obtain future predictions of pavement performance over design life, especially targeting failure modes of rutting, fatigue cracking, and low-temperature cracking. The Superpave shear tester (SST) was developed to determine rut resistance and fatigue cracking, while the indirect tensile tester (IDT) was introduced to measure susceptibility to low-temperature cracking. However, these devices are very expensive and are not widely used. In the meantime, wheel-tracking testing has become more popular as one of the most acceptable options for measuring rut resistance. Again, universal testing machine (UTM) is widely used to analyze "fatigue" and

"creep" characteristics. A detailed discussion of these tests will be done in the methodology section in Chapter 3.

2.3 Initial Phase of Fine-Mix Applications

The National Center for Asphalt Technology (NCAT) first started to investigate a smaller size mixture with a motivation to use fine aggregate stockpiles (also known as screenings) for thin-lift HMA application (Cooley et al. 2001). The NCAT researchers noted that probable applications for an HMA with a higher percentage of screenings would be to extend pavement life, improve ride quality, correct surface defects, reduce road-tire noise, and enhance appearance. Another potential area to implement these types of mixes would be for low-volume roads.

2.3.1 Georgia and Maryland Experience

In Maryland, fine mixes are used as part of a preventive maintenance program and have shown excellent rutting and cracking resistance. Maryland's thin HMA overlay mixes generally contain about 65 percent manufactured screenings and 35 percent natural sand. Gradation requirements for these mixes are shown in Table 2.7. Table 2.8 shows that the gradation can have either a 4.75-mm or 9.5-mm NMAS gradation. Typical lift thicknesses in the field are in between 19 and 25 mm (0.75 and 1 inch) (Cooley et al. 2002).

Table 2.7 Design Specifications for 4.75-mm Mixtures for Maryland and Georgia

Gradation	Georgia (% passing sieve size)	Maryland (% passing sieve size)
12.5 mm	100	-
9.5 mm	90-100	100
4.75 mm	75-95	80-100
2.36 mm	36-76	60-65
0.30 mm	20-50	-
0.075 mm	4-12	2-12
Design Requirements		
Asphalt Content (%)	6-7.5	5-8
Optimum Air Voids (%)	4-7	4
Voids Filled with Asphalt (VFA)	50-80	-

The Georgia DOT has used a 4.75-mm NMAS-like mix for more than 30 years for low-volume roads and leveling purposes. Good performance has been shown by the mix that is placed in thin (approximately 25-mm or 1 inch thick) lifts. These Georgia mixes have been primarily composed of screenings with a small amount of 2.36-mm-sized chips. This results in approximately 60 to 65 percent passing a 2.36-mm sieve and an average of about 8 percent dust as shown in Table 2.8 (Cooley et al. 2002).

It is to be noted that both states have very good aggregate sources. Potential limitations for small NMAS mixtures include concerns with permanent deformation, moisture resistance, scuffing, and skid resistance. Also, gradation and design criteria are not similar for the two mixtures, and apparently, were put in place based on experience.

Michigan Department of Transportation (MDOT) has implemented ultra-thin HMA overlay as an alternative to micro-surfacing for lift thickness less than 25 mm (1 inch). They recommended polymer modified binder (PG 76-22) for medium to high-traffic volume. The mix design requirements use the Marshall method of mix design with air voids of 4.5 to 5%, VMA of less than or equal to 15.5%, and maximum dust-to-binder ratio of 1.4. The Marshall flow for the mix should be within 8 to 16 and a Marshall stability of at least 545 kg (1200 lbs) (MDOT 2005).

2.3.2 NCAT Research on Screening Materials

The main objective of this study (Cooley et al. 2001) was to determine if rut-resistant HMA mixtures could be achieved with the aggregate portion of the mixture consisting solely of screenings. Two fine aggregate stockpiles (screenings), two grades of asphalt binder, and a fiber additive were selected. The two aggregate sources selected were both manufactured aggregates: granite and limestone. The granite screenings material was relatively cubical and had a rough surface texture with a fine aggregate angularity (FAA) value of 49.3. The limestone screenings

were also considered to be angular with an FAA value of 45.8. The granite screenings were much finer than the limestone screenings. The limestone was more absorptive (1.8%) compared to granite (0.2%). The two asphalt binder grades chosen were also commonly used: PG 64-22 and PG 76-22 (SBS modified). Cellulose fiber was added at 0.3% ratio by weight of the total mixture. The material variables, when combined, resulted in eight test mixtures (2 aggregate sources x 2 binders x 2 fiber contents). Each of these mixtures was designed at three different air void contents (4, 5, and 6 percent) and then tested in the asphalt pavement analyzer (APA). Compaction level for the mixes was selected to be 100 gyrations. This level of compaction was based on the 1 to 3 million design ESALs.

Conclusions

The following conclusions were obtained from this research:

- Mixes having screenings as the sole aggregate portion can be successfully designed in the laboratory for some screenings but may be difficult for others.
- Screening type, cellulose fiber, and design air void content significantly affected optimum binder content. Of these three factors, screening type had the largest impact on optimum binder content, followed by the existence of cellulose fiber and design air void content, respectively.
- Screening type and cellulose fiber significantly affected voids in mineral aggregate (VMA). However, screening materials had a larger impact.
- Screening materials and design air void content significantly affected % G_{mm} @ N_{ini} results. Again, screening materials had the largest impact.
- Screening materials, design air void content, and binder type significantly affected laboratory rut depths. Out of these three, binder type had the largest impact followed by

screening materials and design air void content, respectively. Mixes containing PG 76-22 binder had significantly lower rut depths than mixes containing PG 64-22. Mixes designed at 4 percent air voids had significantly higher rut depths than mixes designed at 5 or 6 percent air voids.

Recommendations

Based upon the conclusions of the study, the following recommendations were provided:

- Mixes using a screening stockpile as the sole aggregate portion and having a gradation that meets the requirements for 4.75-mm Superpave mixes should be designed according to the recommended Superpave mix design system.
- Mixes using a screening stockpile as the sole aggregate portion but with gradations not meeting the requirements for 4.75-mm Superpave mixes should be designed using the following criteria:
  - Design Air Void Content (%): 4 to 6
  - Effective Volume of Binder (%): 12 min.
  - Voids Filled with Asphalt (VFA) (%): 67-80

2.3.3 NCAT Mix Design Criteria for SM 4.75-mm NMAS

The objective of this study (Cooley et al. 2002)was to develop mix design criteria for 4.75-mm NMAS mixes. Criteria targeted in the research were gradation controls and volumetric property requirements (air voids, VMA, VFA, and dust-to-effective binder ratio).

Two commonly used aggregate types were used in this study: granite and limestone. For each aggregate type, three general gradation shapes were evaluated: coarse (passing below the maximum density line), medium (passing near the maximum density line), and fine (passing above the maximum density line) as shown in Figure 2.3. Both aggregates had similar bulk

specific gravity values; however, the limestone had a slightly higher absorption value (1.0 percent compared to 0.6 percent). The granite had a higher fine aggregate angularity value (49 percent) than did the limestone (46 percent). For each of the three gradation shapes, three dust (passing a 0.075 mm sieve) contents were evaluated: 6, 9, and 12 percent. The varying dust contents were investigated to evaluate the effect of dust on the volumetric properties and rutting resistance of these 4.75-mm NMAS mixes and also for the fact that different stockpiles to be used to blend 4.75-mm NMAS mixes will likely have varying degrees of dust. When designing 4.75-mm NMAS mixes, the design air voids could be increased from the Superpave target of 4 percent, while providing an acceptable performing mix. This was evaluated by designing mixes to 4 and 6 percent air voids. The design compactive effort (N_{des}) used in this study was 75 gyrations which corresponds to a design traffic range of 0.3 to 3 million ESALs under current Superpave specifications. A PG 64-22 was used for all mixes. Thus, for the study, there were a total of 36 designed mixes (2 aggregate types x 3 general gradation shapes x 3 dust contents x 2 design air void levels).

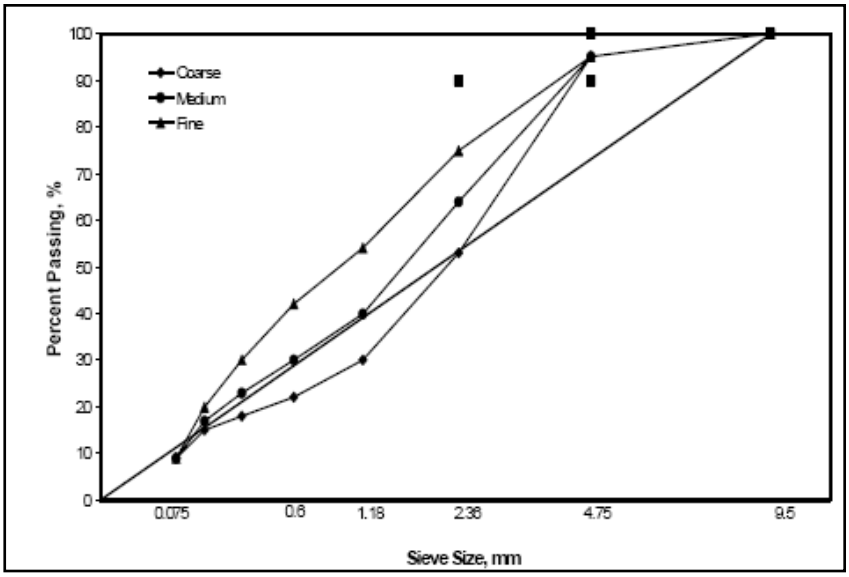

Figure 2.3 Gradations used in the 4.75-mm mix design development (Cooley et al. 2002)

Results

The results showed that the optimum binder contents ranged from a low of 4.2 percent to a high of 8 percent. On average, the granite (water absorption 0.6%) mixes had higher optimum binder content (average of 5.9 percent) than the limestone (water absorption 0.6%) mixes (average of 5.4 percent). The higher optimum binder contents for the granite mixes were likely due to the granite aggregates having more surface texture than the limestone aggregates. As the percent passing the 0.075-mm sieve (dust) increased, optimum binder content decreased. On average, increasing the dust content by 3 percent reduced optimum binder content by about 0.5 percent. Optimum binder content was also affected by the general gradation. Mixes (both 4% design air voids and with fine gradation) had the highest average optimum binder content (6 percent), followed by coarse gradation (5.7 percent) and medium gradation (5.2 percent). Also, as expected, the mixes designed at 4 percent air voids had a higher average optimum binder content (6 percent) than the mixes designed at 6 percent air voids (5.3 percent).

The VMA at optimum binder content was affected by the aggregate type, dust content, and gradation. Design air voids did not appear to significantly affect overall average VMA values. As dust content increased, average VMA values decreased. The medium gradation produced the lowest average VMA value (15.9 percent), which was expected since the gradation approached the maximum density line.

The %Gmm @N_{ini} values were most affected by aggregate type, gradation, and design air void content. On average, the granite mixes showed higher %Gmm @N_{ini} value (87.5 percent) than the limestone mixes (86.1 percent). This was likely due to the higher overall optimum binder contents for the granite mixes. As the design air void content increased (optimum binder

content decreased), the average %Gmm @N_{ini} values decreased. None of the 36 mixes failed the %Gmm @N_{ini} maximum requirement (90.5 percent maximum) for mix designs.

The binder film thicknesses ranged from 3.64 to 8.87 microns for the 36 mixes. Typical film thicknesses for these mixes were expected to be relatively lower. All four experimental factors (aggregate type, dust content, gradation, and design air void content) affected film thickness. As expected, dust content had the greatest effect on film thickness because dust has the largest effect on the calculated aggregate surface area used in calculating film thickness. Coarse gradation provided the largest film thickness (average film thickness of 6.51 microns) compared to the medium gradation, and mixes using the fine gradation fell in the middle at an average film thickness of 5.41 microns.

Analysis of the APA rut depth data was performed by conducting an analysis of variance (ANOVA) to evaluate the effect of the main factors (aggregate type, gradation, dust content, and design air voids) and any interactions between the main factors on rut depth. Results showed that all four of the experiment's main factors significantly affected rut depths. On average, the granite mixes had larger rut depths (9.1 mm) than did the limestone mixes (8.3 mm). This was likely caused by higher optimum binder contents for the granite mixes. The coarse gradations resulted in higher rut depths (10.14 mm) than did the fine gradations (9.72 mm) or the medium gradations (6.29 mm). Decreasing dust content led to higher rut depths. Because of a very wide range, on average, the mixes designed at 4 percent air voids had slightly higher rut depths (9.13 mm) than the mixes designed at 6 percent air voids (8.30 mm). Again, this is likely due to the higher optimum binder contents for mixes designed at 4 percent air voids.

Conclusions

The following conclusions were obtained from the research:

- Mixes with a 4.75-mm NMAS can be successfully designed in the laboratory.
- Optimum binder contents of designed mixes were affected by aggregate type, gradation, dust content, and design air void content.
- Voids in mineral aggregate values were affected by aggregate type, gradation, and dust content.
- The cause of excessive laboratory rutting was high optimum binder content.
- A good relationship existed between VMA and dust-to-effective binder ratio. The VMA decreased with increasing dust-to-effective binder ratio. However, this relationship may vary when different aggregate types are used.
- Based upon the relationship and mix design criteria from Maryland and Georgia, a minimum VMA criterion of 16 percent appears reasonable. For mixes designed at 75 gyrations and above, a maximum VMA value of 18 percent is rational and highly related to the rutting performance.

Recommendations

Based upon the findings in this study, Superpave mix design criteria were recommended for a 4.75-mm NMAS mixture:

- Gradations for 4.75-mm NMAS mixes should be controlled on the 1.18 mm (No. 16) and 0.075 mm (US No. 200) sieves. On the 1.18 mm sieve, gradation control points are recommended as 30 to 54 percent passing. On the 0.075 mm sieve, control points are recommended as 6 to 12 percent passing.
- An air void content of 4 percent should be used during mix design.

- For all traffic levels, a VMA minimum limit of 16 percent can be utilized. For mixes designed at 75 gyrations and above, maximum VMA criteria of 18 percent should be used to prevent excessive optimum binder contents. For mixes designed at 50 gyrations, no maximum VMA criteria should be used.
- For mixes designed at 75 gyrations and above, VFA criteria should be 75 to 78 percent. For mixes designed at 50 gyrations, VFA criteria should be 75 to 80 percent.
- $\%G_{mm}$ @N_{ini} values currently used for different traffic levels are recommended.
- Criteria for dust-to-effective binder ratio are recommended as 0.9 to 2.2.

Criticism

There are two major criticisms of this study. First, it used 100% crushed materials for two good, low-absorptive aggregate types. The effect of any natural material (like river sand) that can be used in the mixture is virtually unknown. The second criticism is the use of only one grade of PG binder (PG 64-22). Although AASHTO has adopted most of the recommendations of this study, more research is needed before widespread application.

2.3.4 NCAT Research on 4.7- mm SMA Mix Design

The objective of this research study (Hongbin et al. 2003) was to further refine the design of 4.75-mm NMAS stone matrix asphalt (SMA). Specifically, the fraction passing the 0.075 mm sieve and the requirements for the draindown basket were evaluated. The research approach entailed designing four different SMA mixes with a 4.75-mm NMAS considering granite and limestone. A single gradation was used in this study, except that two fractions passing the 0.075 mm sieve were investigated: 9 and 12 percent.

In this study, 4 and 6 percent design air voids were utilized. The design compactive effort (N_{des}) was 75 gyrations. A PG 64-22 asphalt binder, meeting Superpave high-temperature

requirements above 67ºC, was used for all mixes. Thus, for the study, there were a total of eight designed mixes (2 aggregate types x 2 dust contents x 2 design air void levels). In order to evaluate the stability of each mix, rut tests were conducted with the APA. The draindown characteristics were evaluated using two different baskets: the standard 6.3 mm (0.25 inches) wire cloth and a 2.36-mm (0.1 inch) wire cloth.

Conclusions

Based upon test results and analyses from this limited study, the following were concluded:

- Based on draindown test results, durability consideration, and relative comparison of APA testing results, SMA mixes with a 4.75-mm NMAS can sometimes be successfully designed having gradations with aggregate fractions passing the 0.075 mm sieve less than 12 percent. Gradations with aggregate fractions passing the 0.075 mm sieve of 9 percent can be utilized as long as all other requirements are met.
- APA rutting results of 4.75-mm SMA were relatively high for all mixtures tested. This was mainly because the non-modified asphalt was used and a high ratio of sample height and NMAS was used for APA testing. Based on the APA test results, 4.75-mm SMA with non-modified asphalt is not recommended for high-volume-traffic roads but was not tested in the lab.
- Aggregate shape, angularity, and texture played an important role in achieving the required design volumetric criteria required for the 4.75-mm NMAS SMA mixes. The SMA mixes with granite aggregate passed all volumetric criteria, while SMA mixes with limestone aggregate failed VMA criteria.
- As Expected, draindown tests conducted using a wire mesh basket of 2.36 mm (0.1 inch) openings produced test results with less draindown than tests conducted with a wire mesh

basket having 6.3 mm (0.25 inch) openings. It was concluded that the difference in draindown results between the two basket types was related to the amount of aggregate that could fall through the different mesh size openings.

Recommendations

Based on this study, it was recommended to change the gradation criteria on the 0.075 mm sieve to between 9 and 15 percent from 12 to 15 percent. It was also recommended that a draindown basket having a 2.36-mm wire mesh size be used for 4.75-mm NMAS SMA, instead of the current standard basket size of 6.3 mm. The specification limit of 0.3 percent for the draindown test when using a 2.36 mm basket appeared reasonable but would need further refinements.

2.3.5 NCAT Refinement Study on 4.7-mm NMAS Mix Design

The main objective of this study (West and Rausch 2006, West, Rausch, and Takahashi 2006) was to refine the mix design procedure and criteria for the 4.75-mm NMAS Superpave mixture. The considered criteria were the minimum VMA requirements and a workable range for VFA, % G_{mm} @N_{ini}, some fine aggregate properties such as sand equivalent and fine aggregate angularity of the mixture, appropriate design air voids for a given compaction effort, dust-to-effective binder ratio, and a recommendation on the usage of "modified binders" to enhance performance of the 4.75-mm NMAS mix. This study only described laboratory findings and did not mention performance of the mixes in the field.

This study received materials from eight different states (Alabama, Connecticut, Florida, Missouri, Minnesota, Tennessee, Virginia, and Wisconsin). It also included four plant-produced, 4.75-mm mixes that had been successfully implemented in the field. These baseline mixtures were obtained from Mississippi, Maryland, Georgia, and Michigan. Twenty-nine mixes were designed considering N_{des} at 50 and 75 gyrations and air voids at 4 and 6 percent. The 50 and 75

gyrations were selected based on Equivalent Single Axle Load (ESAL) values on low-volume roads (< 3 million). Four and six percent design air voids were used to assess the concern of higher asphalt percentage due to high VMA values. However, higher design air voids may lead to durability and moisture susceptibility problems. For each mix design, four performance tests were conducted: permanent deformation, durability to evaluate volumetric criteria (VMA and VFA), permeability to assess in-place density, and moisture sensitivity. Though the mix is recommended for thin-lift applications with low-speed, light traffic, rutting may not be a major concern. However, tests for permanent deformation were suggested to evaluate the stability of the mix.

Conclusions

The following conclusions were made based on this study:

- Material source properties and gradation significantly influenced optimum asphalt content.
- Change in air voids had little influence on VMA, while compaction efforts had potentially decreased the VMA. Coarser gradation among the fine mixes (one near the maximum density line) had lower VMA. Higher dust content lowered the VMA.
- Increasing design air voids reduced VFA, while change in compacting efforts had no effect on VFA.
- High VMA caused elevated asphalt mix and excessive material verification tester (MVT) rutting. Mix with a dust ratio lower than 1.5 had higher rut depth. Mix with 6% air void had better rut resistance compared to 4 %. Effective asphalt volume more than 13.5% resulted in higher MVT rut depth.

- In general, the tensile strength ratio (TSR) decreased slightly with decreasing effective asphalt content. The study showed that 4.75-mm mixes were practically impermeable, even at lower in-place density. Lower permeability may reduce exposure to moisture.
- Fracture energy ratio increases with increasing asphalt content. The study concluded that a 4.75-mm NMAS mixture's ability to resistance to cracking is a function of both asphalt content and dust content.
- Natural sand ratio over 15% adversely affected the TSR, rutting susceptibility, and permeability. FAA values above 45 lowered rutting and permeability.

Recommendations

Based on results of this study, the following recommendations were made:

- The study recommended AASHTO specifications should be modified to allow air void range of 4 to 6 percent.
- Criteria for VMA should be based on the minimum and maximum range with respect to the effective asphalt content.
- For design ESALs greater than 3 million, 4.75-mm mix should have the effective asphalt volume (ρ_{be}) of a minimum 11.5% to a maximum of 13.5%. These recommended values were based on MVT rut testing and fatigue energy testing. For design traffic less than 3 million ESALs, the effective asphalt should range from 12 to 15%.
- It is recommended that current AASHTO recommendations for % G_{mm} @ N_{ini} should be maintained as is (i.e. $\geq$ 89%).
- The aggregate blend designed for ESALs over 0.3 million, the FAA value of 45, is recommended for better rut resistance.

- For ESALs less than 3 million, the minimum dust proportion of 4.75-mm mix should be increased from 0.9 to 1.0, while ESALs greater than 3 million should have a minimum dust proportion of 1.5. The maximum range should be considered as is (i.e. 2.0).
- Minimum sand equivalent value should be maintained as specified by AASHTO.
- Current gradation limit for 1.18-mm (No. 16) sieve and 0.075-mm (US No. 200) sieve should be 30-55 and 6-13 percent passing, respectively.
- Not more than 15% natural sand with an FAA under 45 is recommended to improve rut resistance and moisture damage, and to maintain low permeability.

2.3.6 NCAT Survey Report on 4.7-mm NMAS Superpave Mix

The National Center for Asphalt Technology (NCAT) performed a survey on current usage and possible future application of the fine mix. Of 50 highway state agencies, around 21 states responded (Figure 2.4) (West and Rausch 2006).

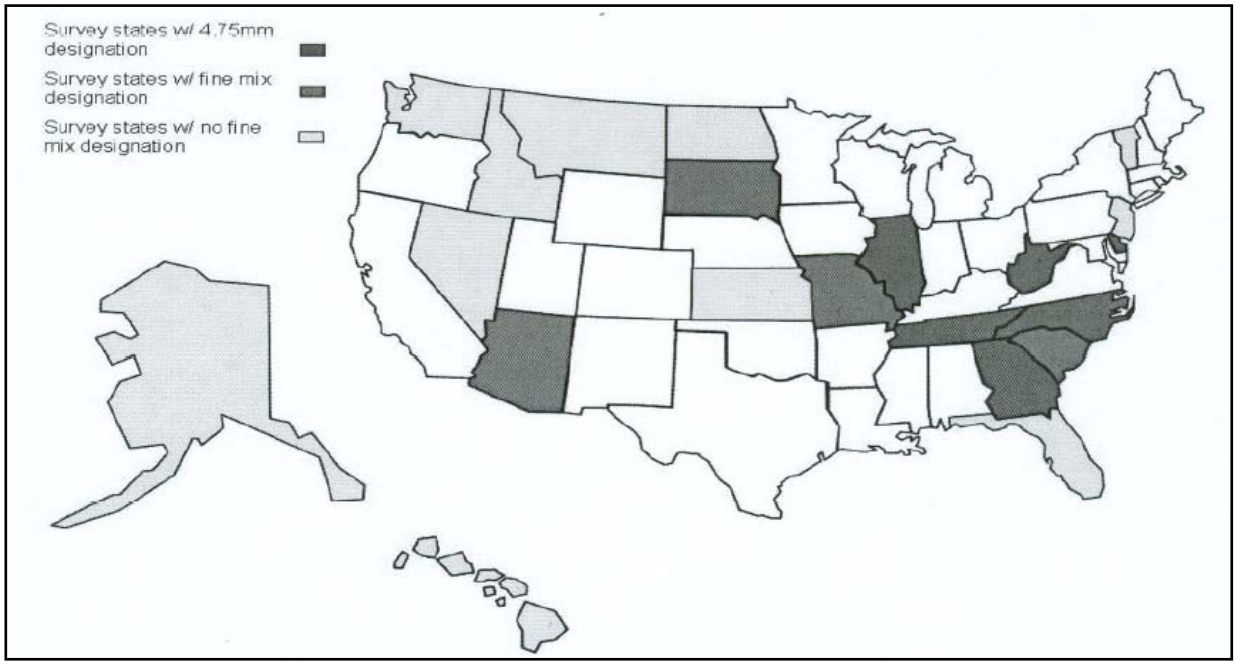

Figure 2.4 State responses to NCAT fine-mix survey (West and Rausch 2006)

The summary of the survey report from the responded states includes the following:

1 Three types of aggregates were common in this 4.75-mm mixture: (i) rock or chip (0 to 30%), (ii) screenings (0-50% typical), and (iii) natural sand (0-30% typical).

2 The common grade of asphalt used in the mix was 64-22. Hydrated lime mixed at 1% was commonly used as a liquid anti-stripping additive.

3 Both Superpave and Marshall methods were used for designing the 4.75-mm NMAS mix. For the Superpave method, the compactive effort (N_{des}) of 50 gyrations was typical. Of states using the Marshall mix design method, only Missouri disclosed its design criteria (35 blows). Most of the states did not have any in-place density requirements.

Table 2.8 State Response Regarding Production Quantity and Usage (West and Rausch 2006)

Approximate Production Quantity of 4.75-mm NMAS Mixture	
State Agencies	Quantity
Delaware	< 1,000 tons
Georgia	320,000 tons for FY 2004
Illinois	(N/A)
Tennessee	225,000 tons
West Virginia	15,000 – 20,000 tons
Arizona	250,000 – 350,000 tons
South Carolina	Approximately 5% of the total tonnage
South Dakota	75,000 tons
Missouri	1.7 million surface level, and 750,000 tons
North Carolina	75,000 tons
Usage and Further Development	
Florida	Leveling and thin overlay
New Jersey	Leveling on concrete pavement overlay
Vermont	Low ESAL Superpave
Hawaii	Thin overlay for preventive maintenance
Nevada	Fill substantial cracking (attempt failed and discontinued)
North Dakota	Bike trails
Washington	Thin-wearing surface over structurally sound pavement
Delaware	Subdivision overlay work
Georgia	Low-volume local roads and parking lots
Illinois	Explore way to add macro texture as a surface course
South Dakota	All type of roads (surface mix)
Missouri	Long-lasting surface mixtures for low-volume roadways
Iowa	Application as scratch course mix

The other two responses from the survey report are presented in Table 2.8. The important findings from this survey were that the 4.75-mm NMAS mix had been commonly used as surface mixture, leveling course and thin overlay. Most state agencies found appreciable benefit in using this mix type and responded positively for further development of the mix to improve structural capacities and rut resistance.

2.3.7 Arkansas Mix Design Criteria for 4.75-mm NMAS Mixes

This study was done to develop guidelines for designing a 4.75-mm Superpave mix for Arkansas; to assess aggregate properties relating to the design of a 4.75-mm mixture; to evaluate the applicability of a 4.75-mm mixture for medium and high volume roadways; to evaluate design air void levels for the mix; and finally, to assess the performance of rutting, stripping, and permeability of the mix (Williams 2006).

This research study was designed considering three different compactive efforts (N_{des} = 50, 75, and 100 gyrations) and two design air void levels (4.5 and 6.0%). The relationship of these factors to the rutting, stripping, and permeability of the mix was evaluated. The performance was also compared with the 12.5-mm NMAS mixture. In order to apply the results under different field conditions, aggregates were selected to cover the typical range of materials found in Arkansas. In addition, the effect of natural sand was also investigated. In order to assess rutting and stripping resistance, the evaluator of rutting and stripping in asphalt (ERSA) and the rotary asphalt wheel tester (RAWT) were used. The specified in-place density was 93%, the test was conducted at 50^0 C, and the target rut depth was 20 mm. The permeability was determined at 7% air voids using the Karol-Warner laboratory asphalt device as outlined in ASTM PS-129. Permeability was tested at variable heights (75 mm, 50 mm, and 25 mm).

Results and Conclusions

During the mix design process, the following conclusions were made:

- No successful mix design was achieved using three different aggregate sources. For the single material source meeting the gradation requirement, other volumetric properties proposed by AASHTO were not satisfied.
- Comparative study showed that the binder requirement in 4.75-mm mix was higher (6.7 to 8.7%) than that of 12.5-mm mix.
- Angular aggregates and natural sand were used to control the VMA, though it was difficult to achieve.
- Design parameters were relatively insignificant in rutting evaluation.
- Mixes with 4.5% design air void and 100 gyrations and 6% air voids with 50 gyrations performed better in stripping evaluations.
- Aggregate source was the most significant variable among all design parameters.
- Natural sand content reduced the performance level of the designed mix.
- All 4.75-mm mixes exhibited very low levels of permeability. A 25-mm sample provided a more realistic measure of permeability as it is a recommended thickness for the 4.75-mm mix.
- The research showed that it is possible to design a 4.75-mm mix with rutting resistance, which is comparable or better than the 12.5-mm mix.
- Comparison of mixes with different NMAS was significantly affected by the aggregate source. Rutting resistance was potentially influenced by the NMAS, while its effect on stripping was insignificant.

Recommendations

- Mixes can be successfully designed using 4.75 mm NMAS in Arkansas with aggregates from the existing aggregate sources. But, in some cases, sources can be improved by making minor adjustments to the aggregate gradation.
- Mixes for low and medium volumes of traffic should be designed at 6% air voids while heavy traffic roadway mix should be designed at 4.5% air voids.
- The use of natural sand should be limited. Based on the conclusions, some specifications for 4.75-mm NMAS were suggested for the State of Arkansas. The recommended specifications for 4.75-mm NMAS mixture for State of Arkansas were the design air voids should be 6% for low-to-medium volume traffic and 4.5% for heavy traffic condition. The suggested VMA and VFA ranges were 18 to 20% and 67 to 70% for low-to-medium traffic, respectively while 16 to 18% and 72 to 75 were allowed for heavy traffic volume facilities. The suggested dust ratio was 0.9 to 2.0 as specified by AASHTO (Williams 2006).

2.4 Recent Research on Fine-Mix Overlay

This section will discuss some recent findings and field experience with 4.75-mm Superpave mixture as an ultra-thin overlay. Almost all studies evaluated the performance of this fine mixture as a technique for preventive maintenance of existing pavements under prevailing traffic. Results from each research study are weather and material source-specific.

The Texas Department of Transportation (TxDOT) (Walubita and Scullion 2008) performed a study to evaluate fine mixes for their potential application in a very thin surface overlay. The research methodology incorporated extensive field and laboratory testing such as Hamburg wheel tracking device tester, overlay, and ground penetration radar. Laboratory

performance in dry conditions and at ambient temperature performed very well in the HWTD tests, while wet conditions were potentially susceptible to moisture. The fine-graded mixes with a higher percentage of rock and screening material with design asphalt content over 7% performed best in the HWTD tests. The test results also suggested that high-quality, clean aggregate with low soundness (<20) value (i.e. granite and sandstone) might result in superior performance based on HWTD and overlay tests (Walubita and Scullion 2008).

Research on 4.75-mm HMA for thin overlay application was performed by the North Dakota Department of Transportation and the University of North Dakota (Suleiman 2009). The objectives of this research study were to evaluate the rutting resistance of the 4.75-mm mixture using The Asphalt Pavement Analyzer (APA), to evaluate benefits and impacts associated with these fine mixes when applied as thin overlay for medium to low-traffic volume, and finally to find a new alternative and rehabilitation strategy (Suleiman 2009). The proposed project criteria considered optimum binder content, gradation with no material retained by the 4.75 mm (No. 4) sieve, and 0%, 20%, and 40% dust in the mix design. Results showed that mixes with higher crushed fines performed better than the mixes with lower crushed fines. Since the mixes with higher amount of dusts will need higher design asphalt content, the study suggested producing mixes with design asphalt content lower than 8%.

Another study (Mogawer et al. 2009) introduced thin-lift HMA construction with a high percentage reclaimed asphalt pavement (RAP), with fine mix and warm mix asphalt technology. Mixes with a 4.75-mm Superpave mixture and highway surface-treatment mixture containing 0%, 15%, 30%, and 50% RAP were used. Two binder grades (PF 64-28 and PG 52-33) were used for each mix, which was evaluated for stiffness and workability. Research study showed that mixes with higher percentages of RAP could satisfy the design criteria for both gradation

and volumetric properties. The master curves developed based on dynamic modulus testing showed a correlation between the virgin binder and the aged binder used from the RAP. Studies also showed that mixtures with softer binders (PG 52-33) did not experience a reduction in stiffness compared to the binder grade PG 64-28, when the amount of RAP increased from 30% to 50%. The workability of mixes with higher percentages of RAP reduced significantly. The study proposed to increase the additive dose in warm mix asphalt mix. A field trial with 4.75-mm mix with 30% RAP was laid in Wellesley, Massachusetts, in 2007 and no visible distresses were observed in the test section for the first two years (Mugawer et al. 2009, Mugawer, Austerman, and Bonaquist 2009).

Another field study with a very thin overlay with fine mix was performed by the Texas Transportation Institute (TTI) (Scullion et al. 2009). An ultra-thin overlay was placed as a surface layer on five major highways in Texas. The mixes were well designed and had a very good rut resistance measured by the Hamburg wheel tracking device tester and reflective crack resistance measured by TTI's Overlay Tester. The study called these mixes crack-attenuating mixes (CAM), which were designed and constructed based on a special specification called SS 3109. The significant limitation of this new method is that this approach works well with stiff binder and high-quality aggregate structure. The mixes with a transition to a softer binder and locally available materials were also investigated. It proposed a design window for a range of design asphalt content where both rutting and reflective crack criteria had been met. Construction problems associated with low-density pockets due to thermal segregation and areas of raveling occurred in few areas with fine mixed overlays. The skid resistance of the newly laid mat was fairly reasonable and TxDOT was updating the SS 3109 specifications (Scullion et al. 2009).

2.5 Introduction to HMA Bond Strength

In the modeling and calculation of the structural response of flexible pavements, one important assumption is that the asphalt layers are completely bonded. However, in reality, it may not be true. Again, no widely accepted test method is available to measure the degree of bonding between the pavement layers.

In field conditions, the asphalt pavement layer cannot be constructed in a single lift if the lift thickness is higher than 2.5 to 3.0 inches. Asphalt pavements are basically constructed in lifts with a maximum thickness of 2.0 to 2.5 inches for ease of compaction. Thus, interfaces between lifts and between layers are unavoidable. Adequate bond between the layers must be ensured so that multiple layers perform as a composite structure. To achieve good bond strength, a tack coat is usually sprayed in between the asphalt pavement layers. As a result, the applied stresses are distributed in the pavement and subsequently, reduce structural damage of pavements. Lack of such bonding may result in catastrophic loss of structural capacity of the asphalt layer.

2.5.1 Background on Tack Coat

A tack coat is a light application of an asphaltic emulsion or asphalt binder between the pavement lifts, most commonly used between an existing surface and a newly constructed overlay. Typically, tack coats are emulsions consisting of asphalt binder particles, which have been dispersed in water with an emulsifying agent (Woods 2004). Asphalt particles are kept in suspension in the water by the emulsifying agent and thus asphalt consistency is reduced at ambient temperature from a semi-solid to a liquid form. This liquefied asphalt is easier to distribute at ambient temperatures. When this liquid asphalt is applied on a clean surface, the water evaporates from the emulsion, leaving behind a thin layer of residual asphalt on the

pavement surface. When the asphalt binder is used as a tack coat, it requires heating for application.

Tack coat performance at interface layers is affected by many factors including emulsion set time and emulsion dilution, tack coat type and its application rate, and finally, the application temperature. Each state agency has developed its own specifications, while a few quality control methods exist to assess the tack coat performance and to evaluate the interface shear strength of the pavement layers.

2.5.2 Bond Strength Evaluation Test

The Swiss Federal Laboratories for Material Testing and Research has a standard method and criteria for evaluating the bond strength of HMA layers. The device, known as an LPDS tester, uses 150-mm (6-inch) diameter cores (Figure 2.5a). The test is a simple shear test with a loading rate of 50 mm/ min (2 inch/min). The minimum shear force criterion is 15 kN (3375 lbs) for the bond between the thin surface layer and the binder course, and 12 kN (2700 lbs) for the bond between the asphalt binder course and the base layer.

A Superpave shear tester (SST) is another device to evaluate interfacial strength (Figure 2.5b). The shear apparatus has two chambers to hold the specimen during testing, which are mounted inside the SST. The shear load is applied at a constant rate of 0.2 kN/min (50 lb/min) on the specimen until failure. The specimen can be tested at different temperatures as the environmental chamber of the SST controls the test temperature.

The in-situ torque test is popular in the UK to assess bond strength. During testing, the pavement is cored below the interface of interest and left in place. A plate is attached to the surface of the cores and torque is applied until failure, using a torque wrench. The core diameter is limited to 100 mm (4 inches) to reduce the magnitude of the moment applied. Another device

called a Luetner test which is standard in Austria, has also been adopted in the UK. Tests using the Luetner device are performed at 20^0 C (68^0 F) with a loading rate of 50 mm/min (2 inches/min).

A simple bond shear device, developed by the Florida Department of Transportation (FDOT), can be used in the universal testing machine (UTM) or a Marshall press (Figure 2.65c). The test is performed at a temperature of 25^0 C (77^0 F) with a loading rate of 50 mm/min (2 inches/min). FDOT is now using the device to evaluate pavement layer interface strength on projects which might have a chance to experience debonding due to rain during paving operations.

The Ancona shear testing research and analysis (ASTRA) device is now used in Italy to evaluate the fundamental shear behavior of bonded interfaces of multilayered pavements (Figure 2.5d). The device applies a normal load to the sample during shear with a shear displacement rate of 2.5 mm/min (0.1 inch/min). Another test that has been developed recently for testing bond strength is the ATACKER^{TM} device developed by Instrotek, Inc. During testing, the tack material is applied to a metal plate, or HMA sample, or to a pavement surface. A metal dice is then placed on the tack material to make contact with the tacked surface, and bond strength is measured in tensile or torsion mode.

In 1995, Tschegg et al. developed a new testing method called the wedge-splitting test to characterize mechanical properties of bonding agents at the HMA interface layer. The specimens are prepared with a groove at the interface and then are split with a wedge at a specified angle (Figure 2.5e). The specimens are failed in tensile stress mode at interface. Vertical and horizontal displacements and vertical loads are measured during testing, which are then converted to horizontal loads based on a specified wedge angle. The load-displacement curves are obtained by

plotting the horizontal force versus horizontal displacement, and the fracture energy of the specimen is calculated from the area under the load-displacement curve. The study suggested that the fracture energy is more appropriate to describe fracture power of the specimen at interface rather than the maximum load.

The tack coat evaluation device (TCED) (Figure 2.5f) was developed by Instro Teck, Inc. to determine the adhesive strength of tack coat materials. The TCED determines the tensile and torque or shear strength by compressing a smooth circular aluminum plate onto a prepared tack material. The device applies a normal force to detach the aluminum plate from the testing surface, either by tension or by torque or shear force. The research study shows that tack coat type and its application rate and emulsion set time significantly affect the TCED strength of the interface. A prototype study also showed that TCED can distinguish between the tack coat application rates (Woods 2004).

A summary of bond strength test methods is provided in Table 2.9.

Table 2.9 Current Bond Strength Measuring Devices (West et al. 2005)

Shear Strength Test	Tensile Strength Test	Torsion Strength Test
ASTRA (Italy)	ATACKER	ATACKER
FDOT method (Florida)	(Austrian method)	(Instro Teck, Inc.)
LPDS method (Swiss)	MTQ method (Quebec)	TCED (Instro Teck, Inc.)
Japan method	TCED (Instro Teck,	
Superpave shear tester (SST)	Inc.)	
TCED (Instro Teck, Inc.)	Pull-off test device	
Wedge-Splitting test	(UTEP)	

(a) (b)

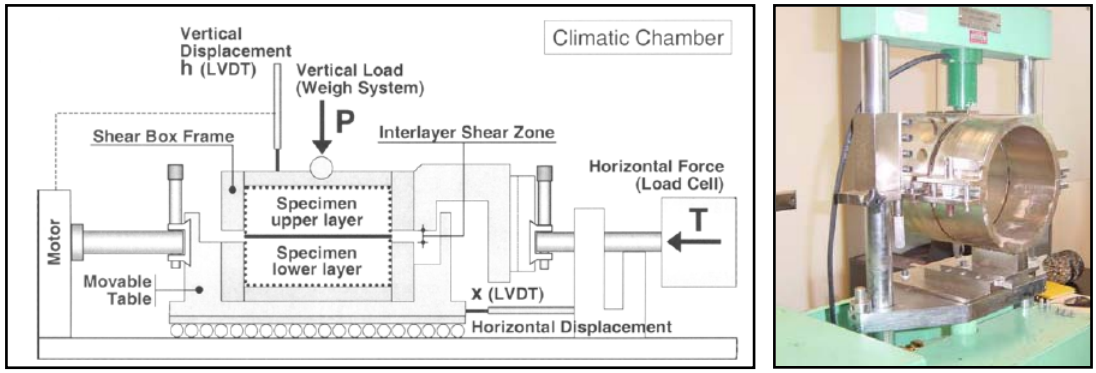

(d) (c)

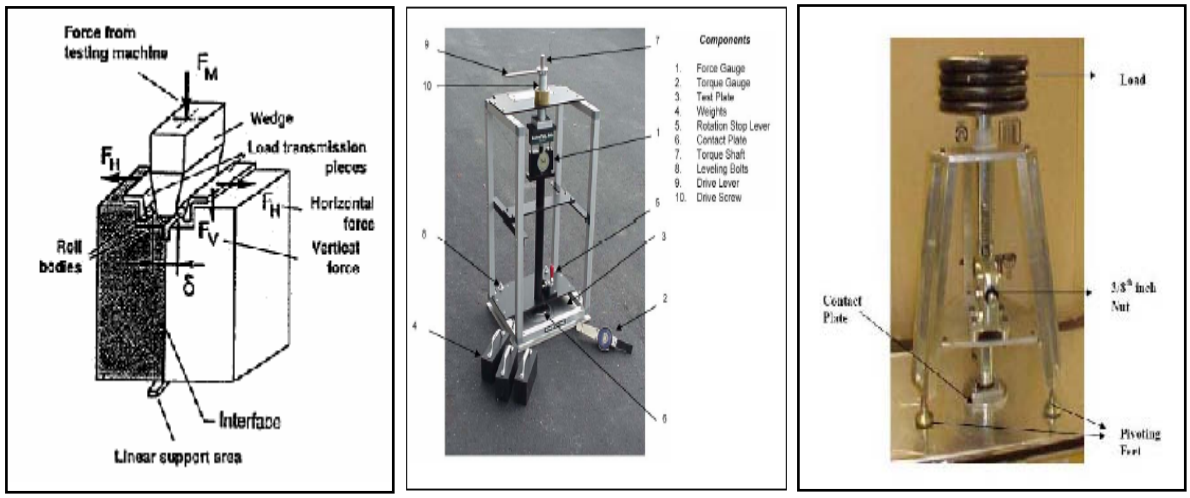

(e) (f) (g)

Figure 2.5 Bond strength testing equipments: (a) LPDS tester, (b) SST, (c) FDOT shear tester, (d) ASTRA, (e) wedge-split device, (f) TCED, (g) pull-off test device (West et al. 2005, Al-Qadi et al. 2008)

2.5.3 Study on Bond Strength Materials

In 1999, the International Bitumen Emulsion Federation (IBEF) conducted a worldwide survey on use of tack coat or interface bond materials. The survey collected information on tack material types, their application rates, curing time, test methods, and inspection methods. Responses from seven different countries confirmed that cationic emulsions are most commonly used with some use of anionic emulsion. Among seven countries, only the United States mentioned using the paving grade asphalt cement as a tack coat. The application rate generally ranged from 0.12 to 0.4 l/m^2 (0.026 to 0.088 gal/yd^2) (West et al. 2005). No other countries expect Austria and Switzerland have bond strength evaluation methods and application criteria.

2.5.3.1 Louisiana Study on Tack Coat Materials

The Louisiana study (Mohammad et al. 2001) evaluated tack coat use through a controlled laboratory simple shear test (SST) to find optimum application rate. The influence of tack coat type, application rate, and test temperature during SST were also examined. The tack coat type included two performance graded asphalt cement (PG 64-22 and PG 76-22) and four emulsions (CRS-2P, SS-1, CSS-1 and SS-1h). Application rates studied were 0. .00, 0.09, 0.23, 0.45, and 0.9 liter/m^2 (0.00, 0.02, 0.05, 0.1, and 0.2 gal/yd^2). A simple shear test was conducted at two different temperatures: 25^0 (77^0 F) and 55^0 C (131^0 F).

Summary and Conclusions

The statistical analysis indicated that among six different tack coat materials used in the study, CRS-2P provided significantly higher interface shear strength, and therefore, was identified as the best performer for Louisiana conditions. The optimum application rate for CRS-2P emulsion was 0.09 liter/m^2 (0.02 gal/yd^2). At lower temperature, increasing tack coat application rates resulted in lower interface shear strength, while the application rate of the tack coat material was

not sensitive to the interface shear strength at high testing temperatures. Test results also suggested that the best tack coat resulted in only 83% of the monolithic maximum shear strength at 25^0 C (77^0 F). It implied that the interfaces in multilayer flexible pavement are the weakest zone during construction and service.

2.5.3.2 Texas Study on Tack Coat Performance

The Texas study (Yildirim et al. 2005) was done to identify important factors affecting the performance of tack coats in laboratory conditions prior to application in the field. The study also tried to propose a suitable laboratory test procedure to examine the best combination of tack coat materials, mixture type, and application rate to be used in the field for optimum performance.

As a part of the experiment, 150-mm (6-inch), gyratory compactor-compacted asphalt specimens were bonded onto concrete specimens. Four factors, such as mix type (Type D and CMBH), tack coat type (SS1 and CSS-1H), tack coat application rate 0.11 liter/m^2 (0.024 gal/yd^2) and 0.23 liter/m^2 (0.05 gal/yd^2) and trafficking (HWTD cycles 0 and 5,000) were used in the experimental design. The Hamburg wheel tracking device (HWTD) tests were done at 50^0 C (122^0 F) and shear tests were conducted at 20^0 C (68^0 F). The shear test apparatus was developed as a part of the research, which applied a shear load to the interface of the composite specimen at a constant rate of 50 mm/min (2 inches/min).

Results and Discussions

Results of this study indicated that this testing approach may be feasible to investigate the interface shear strength of the tack coat between the AC and the PCC. Statistical analysis (Least Square Difference at 95% confidence interval) of the shear test results showed that factors considered during the experimental design significantly influenced the tack coat performance. The following conclusions were made based on the analysis of results:

- The nature of the interface, which in turn was related to the aggregate structure of the asphalt mix, had a potential influence on tack coat performance. It was found that CMHB mix specimens were more sensitive to the main factors and the interaction between them.
- Tack coat performance, in general, was better at the higher application rate.
- HWTD tests improved the shear strength response. However, the study found that 5,000 cycles were not enough to cause tack coat failure at the interface.
- Among the four responsive variables, such as maximum shear strength (S_{max}), displacement at maximum shear strength (D_{max}), area under the maximum shear-displacement curve (A_p), and total area beneath the shear-displacement curve (A_T), the A_T curve represented the better responsive factors to determine significance of the main effects and interactions.

2.5.3.3 New Brunswick Field Evaluation of Tack Coat Material)

The New Brunswick Department of Transportation (Mrawira and Yin 2006) conducted a full-scale field study of tack coats on a two-lane highway. The main objective of this study was to evaluate the structural effectiveness of tack coat in an overlay project using Dynaflect and FWD deflection testing and by laboratory testing of core samples.

During testing, a baseline structural survey and pre-overlay deflection testing were performed. Three 200 m (656 ft) homogeneous sections were subdivided into "experimental lane" and "control lane". The "experimental lane" was constructed using three different tack coat application rates (0.15, 0.20, and 0.25 l/m^2), while the "control lane" section had no tack coat at the interface layer. Dynaflect and FWD testing were performed after overlay application. Laboratory resilient modulus and splitting strength tests were also performed on the field cores. This study failed to reach any specific conclusion based on their objective.

2.5.3.4 Mississippi Study on Bond

This research was conducted to develop a tack coat evaluation device (TCED) and to perform laboratory testing on different tack coat application rates. Another aim was to develop a laboratory bond interface strength device (LBISD) for evaluation of interface bond strength. The research also investigated the evaporation rate in asphalt emulsions, and finally, assessed the tensile and torque-shear strength of emulsions at various levels of breaking (Woods 2004).

The research test plan included a series of tests to investigate the effect of application rates, tack coat set time, tack material, and other variables on tack coat tensile and torque-shear strength. The application temperature varied from 24^0 C (75^0 F) to 163^0 C (325^0 F) and the allowed set time from five minutes to an hour. The tack application rate was selected from 0.18 to 0.6 liter/m^2 (0.04 to 0.13 gal/yd^2) and dilution rate was either none (0% dilution) or diluted 1 to 1 (emulsions only). Four types of tack coat materials were selected; SS-1, CSS-1 and CRS-2 emulsions, and PG 67-22 asphalt binder. Laboratory TCED and LBISD tests were performed at different combinations of the factors.

Conclusions

The following conclusions were made based on this research study:

- Among the three emulsions (CRS-2, CSS-1, and SS-1), the CRS-2 consistently yielded highest mean strength while SS-1 was the lowest. Although statistical analysis (analysis of variance, ANOVA) showed that temperature was a significant factor affecting tensile and torque strength, it was not evident in the Tukey LSD method. This inconsistency led to the conclusion that temperature does not have any major impact on interface strength.

- Increasing set time and decreasing application rate significantly increased tensile and torque shear strength. Evaporation of water from emulsions with time and low application rates significantly increased tack coat performance at the interface.
- The performance of performance grade (PG) binder tensile strength also decreased with increasing application rate, while torsional strength showed the opposite trend.
- LBISD tests showed that tack coat type significantly affected shear strength performance and reaction index. Mix base course gradation also had a potential impact on the reaction index.
- Analysis of mass loss for emulsions proved that evaporation rates significantly increased with decreasing application rate.
- Visual breaking time potentially increased with increasing application rate. Visual breaking was achieved much faster, leaving excess moisture below the surface.
- When the emulsion was not fully broken, tensile and torque-shear strength were highest at low application rates, while fully broken emulsions yielded highest strength at 0.41 liter/m^2 (0.09 gal/yd^2).

2.5.3.5 NCAT Study on Bond Strength

An NCAT bond strength study (West et al. 2005) was performed in 2005 with the main objective to develop a test to evaluate the bond strength between pavement layers. The secondary objective was to select the best tack coat material type(s) and optimum application rates. The primary goal was to obtain a typical value of bond strength normally occurring during paving in Alabama.

The study was done in two phases. In phase one, a laboratory experiment was conducted to refine the bond test strength device and then, to establish a method to assess the factors, including tack coat material type (CRS-2, CSS-1 and PG 64-22), application rate (0.04, 0.08 and

0.12 gal/yd^2), applied normal pressure (0, 10 and 20 psi), and average test temperature (50^0, 77^0 and 140^0 F), affecting bond strength of the interface between two HMA layers. Laboratory fabricated samples were prepared and tested. In the second phase, field validation of the proposed method from phase one was performed. This phase involved setting up of tack coat application sections on seven project locations in Alabama and obtaining cores from each test section.

Conclusions

Results in phase one (laboratory experiment) indicated that a bond strength test at a low temperature (50^0 F) was not practical. The research suggested performing bond strength test at an intermediate temperature (77^0 F) compared to a high temperature (140^0 F), since the intermediate temperature yielded a wider range of bond strength for different materials. It was also recommended to use 140 kPa (20 psi) normal pressure to avoid premature failure of test samples. The experiment indicated that all main factors and several interactions among factors affect bond strength:

- Mixture type was a potential factor affecting bond strength. Overall analysis showed that a fine-graded mixture with smaller NMAS had higher bond strength compared to the coarse-graded mixture with larger NMAS. However, interactions of mixture type with other variable factors were significant, which could alter the trend of the test results.
- In general, PG 64-22 had higher bond strength compared to the emulsions.
- In general, higher tack coat application rate resulted in lower bond strength. The effect of applied vertical pressure was more pronounced at high temperature since the stiffness of the tack coat is lost at high temperature. However, 10^0 C (50^0 F) and 25^0 C (77^0 F) temperature, the bond strength was insensitive to the normal pressure.

- At the same normal pressure, the test temperature had a significant effect on bond strength. Maximum bond strength was achieved at 10^0 C (50^0 F), followed by 25^0 C (77^0 F) and 60^0 C (140^0 F).

In the field study phase, the draft procedure was successfully demonstrated. This part of the study yielded several important observations:

- ASTM D 2995, *Standard Practice for Estimating Application Rate of Bituminous Distribution,* was found to be an effective method for assessing the tack application rate.
- A milled HMA surface yielded higher bond strength with the overlaying HMA layer.
- No evidence was found regarding paving grade asphalt performing better than the asphalt emulsion in field conditions.
- The marginal bond strength in field conditions appeared to be between 50 to 100 psi. Bond strengths below 50 psi were considered to be poor.

2.5.3.6 WCAT Study on HMA Construction with Tack Coat

The State of Washington lacks unified guidelines for tack coat construction practice in its quality control and quality assurance (QA/QC) procedure. The Washington Center for Asphalt Technology (WCAT) at Washington State University performed a research study (Tashman et al. 2006 and Nam et al. 2008) to establish the guidelines for tack coat construction practices. The objective was to investigate factors that influence the adhesive bond provided by the tack coat at the pavement layer interface. These factors include surface condition, tack coat curing time, tack coat residual rate, and coring location (middle lane and wheel path). This study also aimed to assess the potential quality tests for tack coat applications.

The experimental design of the study included surface treatment (milled vs. non-milled), curing time (broken vs. unbroken), approximate target residual rate (0, 0.018, 0.048, and 0.072

gal/yd^2), and core location (wheel path vs. middle lane). A new 50-mm (2 inches) overlay was placed using a 12.5-mm NMAS Superpave mixture. A total of 14 sections were constructed incorporating the abovementioned factors. Field cores were collected from selected locations to perform the FDOT shear tester, torque bond strength and UTEP pull-off test.

Conclusions and Future Recommendations

The conclusions from the study are as follows:

- FDOT shear test and torque bond strength showed significantly higher shear strengths for milled sections compared to the non-milled sections. However, the UTEP pull-off test provided higher pull-off strength for non-milled sections.
- Curing time was an insignificant factor for all test types.
- Absence of tack coat did not have a major impact on shear strength for milled sections as it was an influential factor for non-milled sections in all tests.
- In general, the increasing residual rate did not potentially improve the shear strength for either the milled or non-milled sections. However, milled sections were more sensitive to the tack coat application rate. This finding is completely opposite to the trend obtained from NCAT bond strength study.
- Shear strength was not affected by the location of the cores.
- The study recommended the FDOT shear test be the fundamental laboratory test measure but not an in-situ test.

Criticism

The three test methods used in this study use different test mechanisms. The FDOT shear test measured the bond strength at the interface layer, the torque bond strength measured the torsional resistance of the tack materials, and the UTEP pull-off test measured the tensile

strength of the tack coat. Hence, results obtained were not consistent with each other in most cases.

2.5.3.7 Kansas Study on Bond Strength

This study on bond strength at the pavement interface layer was performed at the Civil Infrastructure Systems Laboratory (CISL) of Kansas Sate University in 2007. The objective of this research project was to evaluate the shear behavior of three asphalt-to-asphalt mix interfaces with different tack coat application rates. The target was to determine the dynamic shear reaction modulus and strength of the interfaces (Wheat 2007).

The experimental design included construction of three asphalt interfaces: (1) a coarse-coarse mix interface, (2) a coarse-fine mix interface, and (3) fine-fine mix interface. Each of these mix combination section was subdivided into four equal parts with different tack coat application rates (0, 11, 21, and 32 gram/ft^2) resulting in 12 different combinations. The BM1 coarse mix and a 12.5-mm NMAS fine mix were laid during construction. Cores of 100-mm diameter were collected and dynamic shear reaction modulus and shear strength tests were performed in a UTM-25 machine. Shear testing attachments were built to allow testing of specimen at angles from 0 to 45 degrees. The test was performed at two different angles (20 and 30 degree) and at a rate of deformation of 0.05 mm/sec (0.002 inch/sec).

Conclusions and Recommendations

Results of the laboratory experiment yielded the following conclusions:

- The interface shear strength was about the same at different normalized pressures (105 and 109 kPa) for all interface types and tack coat application rates. The study recommended not using the strength test because no effect of tack coat application rate or interface type was observed.

- The value of dynamic shear modulus of the fine-fine mixture was the minimum among the three mix types.
- Thirty degree alignment yielded significant lower dynamic shear modulus at the interface compared to a twenty degree angle.
- No tack coat condition performed the best for the coarse-coarse interface.
- The study recommended that current KDOT specifications for tack coat application rates are sufficient to produce higher strength for all three mixture type combinations. The finding suggested that the current practice is the optimum tack coat application rate during construction in a Kansas environment.

Another recommendation is that the dynamic shear reaction modulus is the best method to determine the optimum rate of tack coat application.

2.6 Current Field Evaluation of Tack Coat Performance

The Virginia Department of Transportation (VDOT) has introduced a new tack coat material called "trackless" tack. This new material uses a very hard performance graded binder and has a positive charge with break time less than a minute. The VDOT special provision for this trackless tack material is 279 kPa (40 psi) in terms of bond strength.

The VDOT research lab compared the performance of "trackless" tack with two conventional tack materials, CRS-1 and CRS-2, which are commonly used in Virginia. The objective of this study was to revise the special provisions for tack material and then to provide an approved product list for "trackless" tack materials. Findings of this study showed that trackless tack materials performed better than the CRS-1 tack coat material in the laboratory and oven-dried conditions. The materials provided better shear and tensile strength compared to CRS-1 and CRS-2 materials. The study recommended that trackless materials be evaluated in the

field conditions. The assessment should include both subjective and objective judgments. The field cores were recommended to be collected from the wheel path to see whether the dump truck removed tack materials from the pavement surface during paving operation. Finally, the study recommended evaluating the bond strength of field cores and comparing it with the laboratory data to assess the influence of weather on material performances (Trenton, Todd, and Kevin 2010).

Figure 2.6 Testing trackless tack performance on Virginia road (Trenton, Todd, and Kevin 2010)

A study on porous asphalt course interface showed that interlayer bonding had an effect on the performance of porous asphalt pavement. Identification of an optimum tack coat application rate and the Ancona shear testing research and analysis (ASTRA) test method were implemented to design the interlayer bonding. The tack coat was applied at the interface of an

existing porous asphalt layer and a newly laid open-graded course. The main objectives of this study were to investigate whether the two porous layers were independent or behaved as a twinlay, and to assess the drainage quality of the composite layer system. ASTRA results of this study showed that different tack coat application rates had achieved the acceptable interlayer bonding, while higher application rates might generate some scatter of the results. The study also showed that the existing porous asphalt layer had not increased the drainage capacity of the composite layer system (Canestrari et al. 2009).

Due to high-intensity short-duration rainfall in Florida, the Florida Department of Transportation (FDOT) conducted a study to introduce a new mixture design procedure for open-graded friction courses and thick porous friction course in Florida. This study documented the performances of bonded open graded friction courses (OGFC) from US-27, Highlands County, Florida, which were laid on a thick polymer modified tack coat. Performances of bonded OGFC were compared to OGFC laid with a regular tack material as well as a stone matrix asphalt mixture called Novachip with a thick polymer-modified tack coat. Study results showed that the newly introduced polymer modified tack material significantly improved the rutting and cracking resistance, while no adverse effects were observed in terms of noise and pavement friction (Birgission et al. 2006).

Interface bonding between HMA overlays and Portland cement concrete (PCC) pavement were studied by the Illinois Center for Transportation. Three testing phases (laboratory testing, numerical modeling, and accelerated pavement testing) were conducted to address the factors affecting interface bond strength. Factors considered during study were HMA materials (SM-9.5 surface mix and IM-19.5A binder mixture), tack coat materials (SS-1h, SS-1hP emulsions, and RC-70 cutback asphalt), tack coat application rate, PCC surface texture (smooth, longitudinal

and transverse tined, and milled), temperature, and moisture condition. A direct shear strength device at a constant loading rate of 12 mm/min (0.5 inch/min) was used to investigate the interface shear strength of HMA overlay. Test results showed that the emulsions SS-1h and SS-1hP had higher interface bond strength compared to RC-70 cutback asphalt while the SM-9.5 surface mixture was found to have better interface strength compared to the IM-19.5A mix. The 0.23 liter/m^2 (0.05 gal/yd^2) provided the maximum interface shear strength among the four application rates considered. Hence, it was selected as the optimum tack coat application rate. The direction of tining on the PCC surface did not have any significant effect on interface shear strength. At 20^0 C, the milled PCC surface provided higher shear strength than a smooth and tined surface. The smoother PCC surface produced higher interface shear strength compared to a tined surface at the optimum tack coat application rate. Moreover, bond strength decreased with increasing temperature and moisture conditions (Leng et al. 2010).

Accelerated pavement testing (APT) sections were built on the PCC surfaces mentioned above (Figure 2.7). The HMA overlay was placed on the PCC surface. A zebra section was introduced to evaluate the non-uniform tack coat application rate.

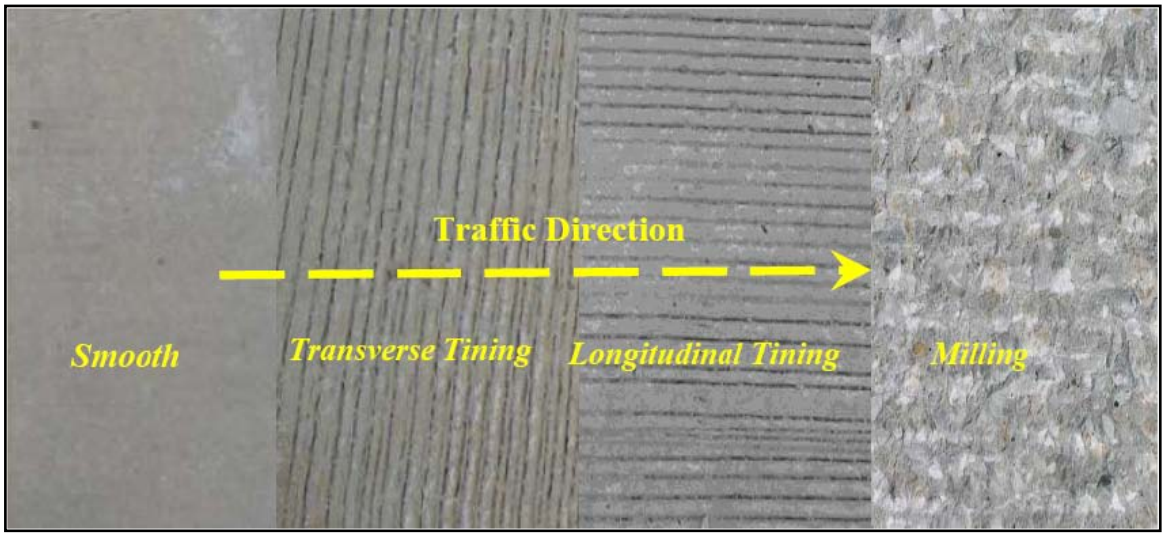

Figure 2.7 PCC surface textures in Illinois study (Al-Qadi et al. 2009)

The emulsified tack coat, SS-1hP and RC-70 cutback asphalt were applied at 0.09, 0.18, and 0.41 liter/m^2 (0.02, 0.04, and 0.09 gal/yd^2) and a binder, PG 64-22, was applied at 0.18 liter/m^2 (0.04 gal/yd^2). To quantify the potential slippage at the interface, tensile strains at the bottom of HMA layer were measured for 25 selective sections and primary rutting was analyzed for all sections (Figure 2.8). The emulsion tack material SS-1hP and PG 64-22 binder offered better rut resistance compared to cutback asphalt. In terms of rutting, a milled surface performed better compared to a transverse tined and smooth PCC surface. PCC surface cleaning methods played a significant role in interface bond strength, while a uniform tack coat application rate was the key to better bond strength between PCC and HMA overlay (Al-Qadi et al. 2009, Leng et al. 2008).

Figure 2.8 Surface profile measurements after APT runs

A study on the influence of contact surface roughness on interface bond strength focused primarily on the possible relationship between shear resistance at interface and bottom-layer

surface roughness of a double-layered asphalt concrete pavement. A laser profilometer and a profile combo were used to determine roughness of the test sections before paving. In addition, lower-layer roughness was also evaluated with the traditional sand patch method. ASTRA and LPDS testing devices were used to evaluate the relationship between interlayer shear resistance and surface roughness. Overall test results showed that the interlayer shear resistance increased when roughness of the adjacent layer was higher. However, different test methods resulted in different proportions of increments during testing (Partl et al. 2006).

2.7 Summary of Background Study

Since the advent of 4.75-mm Superpave mixture in the highway industries, several studies were done to implement this fine mixes for preventive maintenance, correct surface defects, and hence, enhance appearance. This section outlines the key findings and research gaps obtained from the extensive background study on 4.75-mm NMAS mixture and bond strength performance of thin-lift HMA surface.

- Georgia and Maryland states implemented 4.75-mm NMAS-like mixes with an average dust content of 8%. These studies identified the better performances while the mix had been placed as thin-lift rather than leveling purpose. However, the major concerns dealing with the fine mixes were rutting, moisture damage, scuffing, and road-tire friction.
- MDOT study recommended the fine mixes with polymer modified binder while implemented as micro-surfacing. The recommended maximum dust-to-binder ratio was 1.4 which is far below the range specified later by AASHTO.
- NCAT study on screening materials identified that the volumetric of such fine mixes were significantly influenced by the screening type. Rutting performance of the mix was

influenced by the binder grade rather than screening types. However, this study did not focus on other distress evaluations such as moisture susceptibility, fatigue, and low temperature cracks.

- The mix design criteria for 4.75-mm NMAS developed by NCAT showed that fine mixes had relatively higher design asphalt content. The optimum asphalt content was lower with higher dust content in the mix. VMA and film thickness of the mixes decreased with increasing dust-to-effective asphalt content ratio. Absorption of asphalt in the mix played a significant role in rutting performances of the mix. However, dust had a potential influence on rutting performance. Rut depth of such fine mixes decreased with increasing dust content. This study recommended that the gradation should be controlled by 1.18-mm and 0.075-mm sieves while 16 to 18 percent VAM was recommended for 0.3 to 3.0 million ESALs. Dust-to-binder ratio was suggested for a range of 0.9 to 2.2. However, two potential limitations were identified for this study: (1) the study used 100% crushed materials and (2) effect of binder grade on mix performance was not identified.
- NCAT study on SMA with 4.75-mm NAMS recommended limiting the dust content of the mix to 12 percent. This study indentified aggregate consensus properties played a significant role in achieving the required design volumetric criteria for 4.75-mm NMAS SMA mix. Another suggestion from this research study was that the mix with non-modified asphalt might experience excessive rutting under heavy-traffic condition.
- Further study by NCAT to refine the mix design criteria of 4.75-mm NMAS was performed to assess the minimum VMA requirement, workable VFA ranges, aggregate properties such as FAA and clay content, and dust-to-effective binder ratio. The study identified that higher dust content had lowered the VMA and higher design air voids had

resulted low VFA. Mixes with dust ratio lower than 1.5 had higher rut depth while crack resistance was a function of optimum asphalt content and dust content. This study also recommended FAA of 45 for fine mix gradation when the design ESALs is higher than 0.3 millions.

- Arkansas study on fine mixes suggested limiting the use of natural sand content. The recommended specifications for 4.75-mm NMAS mixture for State of Arkansas were the design air voids should be 6% for low-to-medium volume traffic and 4.5% for heavy traffic condition. The suggested VMA and VFA ranges were 18 to 20% and 67 to 70% for low-to-medium traffic, respectively while 16 to 18% and 72 to 75 were allowed for heavy traffic volume facilities. The suggested dust ratio was 0.9 to 2.0 as specified by AASHTO.
- TxDOT study on fine mix application for thin-lift overlay identified that fine-graded mixes with higher percentage of rocks and screening materials and design asphalt more than 7% performed very well in the HWTD in dry condition while wet conditions were susceptible to moisture. The study performed by NDOT showed that mixes with higher percentage of crushed fines had better rut resistance compared to the mix with lower crushed fines. The suggested dust content for the state practice was less than 8%.
- Texas study on tack coat material showed better tack coat performance at high application rate. Aggregate structure was another important factor affected the tack coat performance.
- Mississippi Study on bond strength of tack material postulated that tensile and torque shear strength of tack material had significantly increased when the tack material had been set for a longer period of time and the application rate was relatively lower. Study

also showed that evaporation of water from tack material had increased significantly with decreasing tack coat application rate.

- NCAT laboratory and field study on bond strength showed that mixture type of the adjacent layer materials was one of the key factors controlling the bond strength. Higher bond strength was yielded for fine-graded mixture with smaller NAMS and low tack coat application rate. Milled HMA surface resulted in higher bond strength with the overlaying HMA layer while no significant differences in performance were observed between the paving grade binder and asphalt emulsion.
- WCAT study also confirmed that absence of tack material in milled-section did not have any significant effect on shear strength. Curing time of Washington state tack material was insignificant factor for different test types.
- Kansas study on fine-mix bond strength suggested that current KDOT specification for tack application rate (0.04 gal/yd^2) should be sufficient for obtaining higher bond strength for all mixture type combination. The study also recommended dynamic shear reaction modulus is the potential method to determine the optimum tack coat application rate.

CHAPTER 3 - FIELD AND LABORATORY TESTING

3.1 Research Scope

The ultra-thin overlay of HMA with 4.75-mm NMAS is a fairly new concept in highway construction. The fine mixes in Kansas were designed according to the AASHTO specifications for the 4.75-mm NMAS. To date, no laboratory refinement study has been performed to get optimized design criteria for this fine mix. Hence, this study will result in optimized 4.75-mm NMAS Superpave mixture design criteria in Kansas. A recent NCAT study showed that reduced natural sand ratio will enhance fine-mix performance, especially against stripping. The design of this study will also investigate the applicability of these findings in Kansas environment. In Kansas, asphalt mixes mostly contain PG 64-22 and PG 70-22 binder at a design air void of 4%. This study will assess the fine mix performance for these two different binder grades. Finally and most importantly, no field evaluation on 4.75-mm NMAS mix performance has been reported to date. This research will fill that gap.

3.2 Experimental Design

In order to accomplish a statistical design and analyze an experiment, it is necessary to have a clear idea about the problem statement in advance of the method of study, data collection procedures and a qualitative understanding of data analysis procedures (Montgomery 1997). The following seven steps are equally important to design an experiment (Montgomery 1997):

1. Clear definition of the problem statement
2. Choice of design factors, levels, and the range of the design factors
3. Selection of response variables

4. Choice of experimental design means sample size or number of replicates, selection of suitable run order for experimental trials, etc.
5. Performing the experiment
6. Method of statistical analysis of experimental data
7. Conclusions and recommendations

Based on the research scope stated in the previous section, this research study developed an optimized 4.75-mm NMAS Superpave mixture using different aggregate sources, binder grade and river sand content in Kansas. The experimental design of this study was done in such a way to accomplish the investigation of volumetric parameters and performance of a 4.75-mm NMAS mixture as well as the performance of tack coat for the 4.75-mm mix overlay. Specifically, the study examined the feasibility of thin-lift surface course using fine mix in terms of rutting, stripping, and fatigue damage.

In the first phase of the experiment, the performance and bond strength of the tack coat material were planned to be evaluated in the field. Field measurements of the tack coat application rate were made and the field cores were collected in two phases to evaluate the performance (Hamburg wheel tracking device and pull-off strength tests) of the tack material. Table 3.1 shows the design matrix to evaluate the tack coat bond strength for different study parameters.

Table 3.1 Experimental Design Matrix to Evaluate 4.75-mm NMAS Core Performance

PHASE I	
Factors	**Level of Variations**
Aggregate Source	2 (US-160, K-25)
Tack Coat Application Rate	3 (0.02 gal/yd^2, 0.04 gal/yd^2, 0.08 gal/yd^2)
Performance Measure	**Response Variable**
Hamburg Wheel Tester	Number of Wheel Passes @ 20 mm rut depth
Pull-Off Strength Test	S_{max} @ 25^0 C

In the second phase of the experiment, two aggregate sources were selected in Kansas. From each aggregate source, mix design was developed using three different natural sand contents (35%, 25% and 15%). Two different binder grades (PG 64-22 and PG 70-22) were used for each design aggregate blend. A total of 12, 4.75-mm NMAS Superpave mixtures were designed and the design factors were evaluated based on rutting, moisture susceptibility, and beam fatigue failure. Table 3.2 shows the design matrix for a 4.75-mm NMAS laboratory mix design evaluation. The design blended aggregate must satisfy KDOT specifications for fine aggregate angularity (FAA≥42.0) and the compacted mix must have 4% design air voids at N_{des}.

Table 3.2 Experimental Design Matrix to Evaluate 4.75-mm NMAS in the Laboratory

PHASE II	
Factors	**Level of Variations**
Aggregate Source	2 (US-160, K-25)
Natural Sand Content	3 (35%, 25% & 15%)
PG Binder	2 (PG 64-22 & PG 70-22)
Performance Measure	**Response Variable**
Hamburg Wheel Tracking Device	Number of Wheel Passes @ 20 mm rut depth
Moisture Susceptibility Test	Tensile Strength Ratio (TSR)
Fatigue Beam Test	Change in Initial Stiffness@ 300 με and 20^0 C

The experimental design was organized in such a way to verify the KDOT specifications for 4.75-mm NMAS mix to be used in paving road projects.

3.3 Research Test Plan

Based on the extensive literature review on 4.75-mm NMAS Superpave mixture and interface bond strength, and considering the research scope and experimental design, the following research plan was developed.

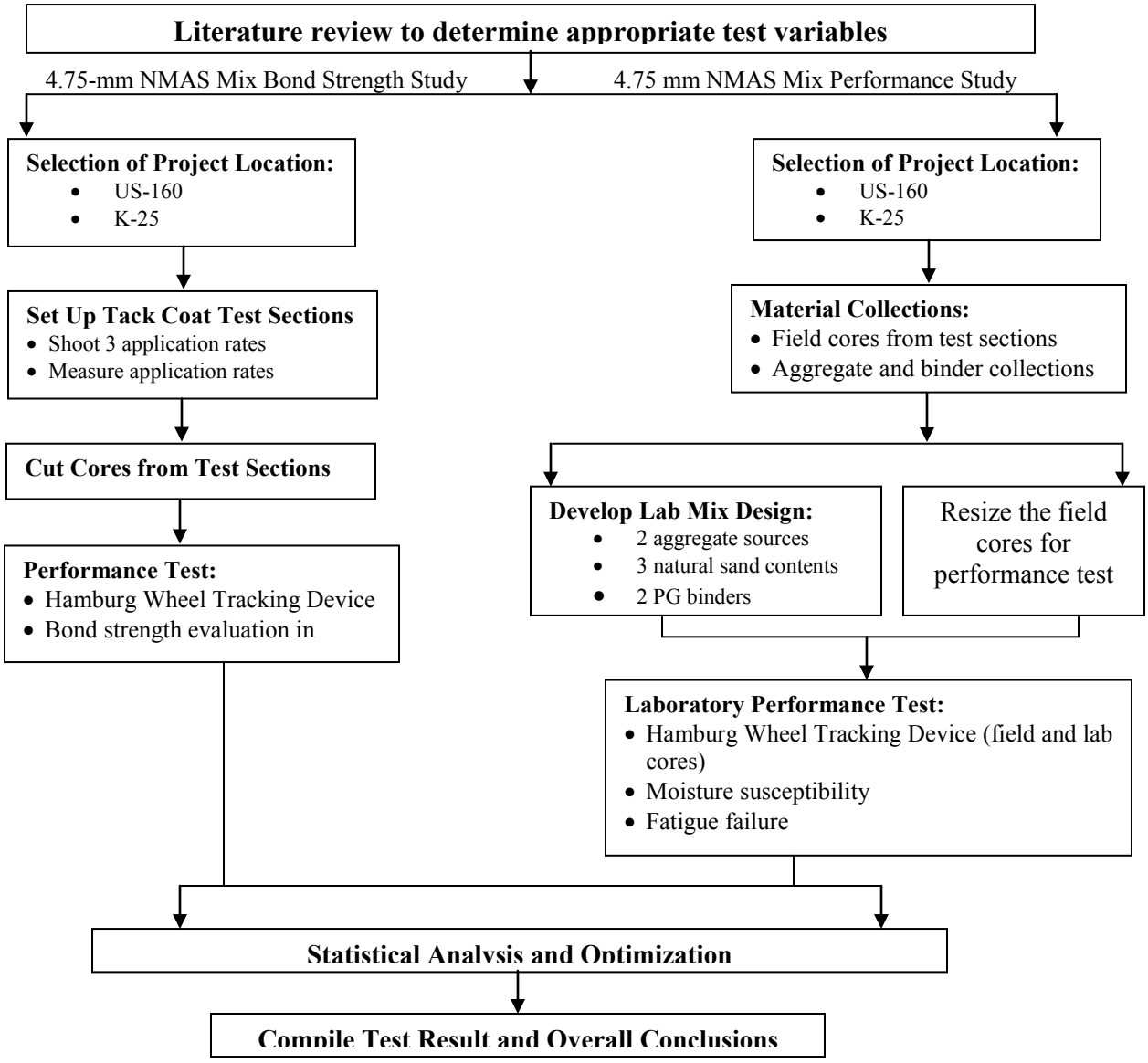

Figure 3.1 Research test plan for 4.75 mm NMAS Superpave mixture study

3.4 4.75-mm Superpave Mixture in Kansas

Currently 4.75-mm NMAS Superpave mixture is designated as SM-4.75A in Kansas. Gradation of the mixture is selected to pass over the maximum density line on a 0.45-power chart in sand sizes and thus, the mixture is considered fine. The required gradation is shown in Table 2.5. The gradation chart indicates that gradation of the SM-4.75A mixture is essentially controlled by the materials retained on 1.18-mm and 0.075-mm sieves. Current KDOT specifications also allow the use of up to 35% natural sand provided the fine aggregate angularity (FAA) of the blend meets the required criteria. The required mixture design criteria are shown in Table 3.3.

Table 3.3 Mixture Design Criteria for Kansas 4.75-mm NMAS Superpave Mix (Hossain et al. 2010)

Criteria	Specifications	Comments
	Compaction Effort	
N_{ini}, N_{des} & N_{max}	Function of 20-year design ESALs	Similar to all other Superpave mixes
	Volumetric Properties	
Air Voids	4% ± 2% at N_{des}	Similar to all other Superpave mixes
VMA	16% min. for reconstruction/major modification project	may be reduced by 1% for 1-R jobs
VFA	65-78	Function of 20-year design ESALs
$\%G_{mm}$ @ N_{ini}	90.5	Function of 20-year design ESALs and layer depth
$\%G_{mm}$ @ N_{max}	98.0	Similar to all other Superpave mixes
Dust-to-Binder Ratio	0.9 to 2.0	0.6-1.2 or 0.6-1.8
Tensile Strength Ratio, min. (%)	80	80

Table 3.3 shows that most properties of SM-4.75A blend and mixtures have requirements similar to other Superpave NMAS mixtures. Only the dust-to-effective binder ratio is higher to account for the higher fine fraction in the blend or mix. Table 3.4 shows the required aggregate

criteria. Those are similar to aggregate criteria for other Superpave mixtures with similar design traffic and position within the pavement structure.

Table 3.4 Aggregate Requirements for Kansas SM-4.75A Mixture

Aggregate Properties	Required Criteria	Project Data	
		US-160*	K-25**
Coarse Aggregate Angularity (min. %)	75	99	80
Uncompacted Voids-Fines (min. %)	42	43	44
Sand Equivalent (min. %)	40	40	78
Anti-Stripping agent	-	Yes	No

*=20-year design ESALs 1.7 million; **=20-year design ESALs 1.5 million

3.5 Design Phase-I: Field Evaluation of 4.75-mm Mix

Two rehabilitation projects on US-160 and K-25 were constructed in 2007 using 4.75-mm NMAS Superpave mixture overlay**.** The following sections describe the rehabilitation projects and their performance history, layer compositions, and field data and core collections at both locations.

3.5.1 Test Sections

3.5.1.1 US-160, Harper County

This project was on a two-lane, two-way highway. Project length was about 18 miles. Project scope consisted of a 50-mm (2-in.), hot-in-place recycling (HIPR) followed by a 19-mm (0.75-in) SM-4.75A mixture overlay. Figure 3.2 (a) shows the cross section of this project. The Annual Average Daily Traffic (AADT) was 1,011 in 2006. Daily equivalent 80-KN axle loads varied from 91 to 177. The 20-year design ESALs for the overlay was 1.7 million.

The condition survey conducted in 2006 before rehabilitation showed that the average International Roughness Index (IRI) was 1.4 m/km (89 in/mile) on the right wheel path, with a standard deviation of 0.22 m/km (14 in/mile). There was no appreciable rutting but two 1.61 km-long (mile-long) segments had 10 m and 27 linear m per 30.5 m (33 and 88 linear ft per 100 ft)

of wheel path of Code 1 fatigue cracking (hairline alligator cracking). The project had, on average, 11 Code 1 and 10 Code 2 transverse cracking, respectively. Code 1 transverse cracking in Kansas refers to full-roadway-width cracks with no roughness, 6.35-mm (0.25-in) or wider, with no secondary cracking; or any width with secondary cracking less than a 0.08 m/lane (0.25 ft/lane); or any width with a failed seal (≥1.0 ft/lane). Code 2 cracks refer to any width with noticeable roughness due to depression or bump or wide crack (one inch plus); or cracks that have more than 1.22 m (4 ft) of secondary cracking per lane but no roughness.

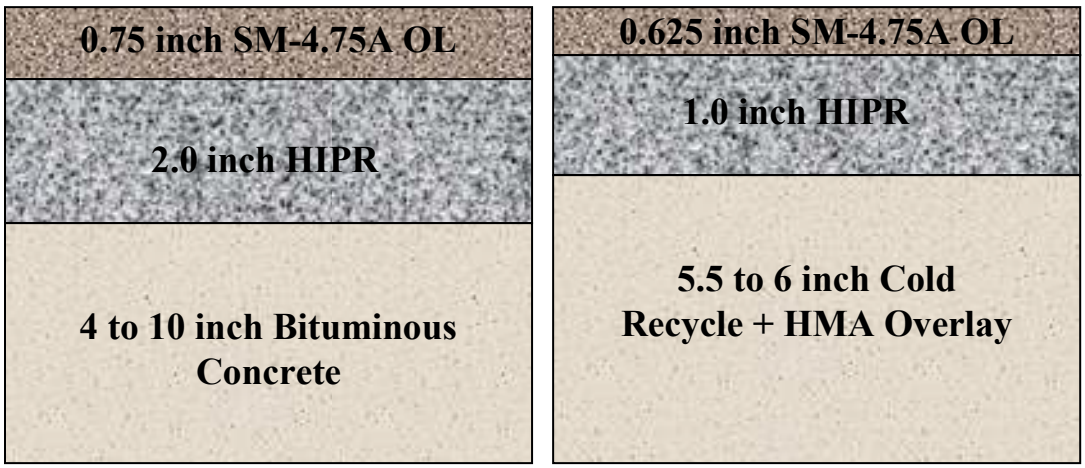

Figure 3.2 Pavement cross section of (a) US-160 and (b) K-25 project

3.5.1.2 K-25, Rawlins County

The second project was also on a two-lane, two-way highway. Project length was about 16 miles. Project scope consisted of 25-mm (1-in.) hot-in-place recycling (HIPR) followed by a 16-mm (0.625 inch) SM-4.75A mixture overlay. Figure 3.2(b) shows the cross section of this project. The annual average daily traffic (AADT) varied from 423 to 488 in 2006. Average daily equivalent 80-KN axle loads varied from 68 to 92. The 20-year design ESALs for the overlay was 1.5 million.

The condition survey conducted in 2006 before rehabilitation showed the average International Roughness Index (IRI) was 1.5 m/km (93 in/mile) on the right wheel path, with a standard deviation of 0.16 m/km (10 in/mile). There was no appreciable rutting. On average, the 16, one mile-long pavement management (PMS) segments had 27 to 28 linear m (88 to 92 linear ft) of Code 1 fatigue cracking (hairline alligator cracking with pieces which are non-removable) per 30.5 m (100 ft) of wheel path. The project had on average 17 Code 0 transverse cracks which refer to full-roadway-width sealed cracks with no roughness and sealant breaks less than 0.305 m/lane (1.0 ft/lane). Only one PMS segment had three Code 1 transverse cracks.

3.5.2 Layer Mixture Composition for Kansas' 4.75-mm Mixture

3.5.2.1 4.75-mm NMAS Mix Overlay

Table 3.5 shows the mixture on US-160 had 65% crushed limestone screening and 35% natural sand. The K-25 mixture had 63% crushed gravels, 35% natural sand, and 2% micro-silica. The design asphalt content was 7.0% for US-160 with 0.5% additive and 6.1% for K-25 by weight of total mixture. Both projects used PG 64-22 binder grade.

Table 3.5 Mixture Composition for Kansas SM-4.75A Mix on US-160 and K-25

US-160		**K-25**	
Aggregate	% in Design Mix	Aggregate	% in Design Mix
CS-1B	32	CG-2	30
CS-2	12	CG-5	33
CS-2A	7	SSG-1*	35
CS-2B	14	MFS-5	2
SSG-4*	35		
Design AC, (%)	7.0	Design AC, (%)	6.1

*Natural sand content must not exceed 35%.

3.5.2.2 Hot-In-Place Recycling (HIPR)

The US-160 project had 50 mm (2 in.) of hot-in-place recycling (HIPR). The mix design was done by SEMMaterials. The target asphalt rejuvenating agent (ARA-1P) rate based on dry

weight of reclaimed asphalt pavement (RAP) was 2.0 ± 0.2%. Thus, the recommended spread rate was 2.22 liter/m^2 ± 0.05% (0.5 ± 0.05% gal/sq. yd). The adjusted field application rate was 1.4 liter/m^2 (0.3 gals/sq. yd). The K-25 project had 25 mm (1 in.) of HIPR depth. No mix design was done to find the emulsion rate. The planned emulsion rate was 0.68 liter/m^2 (0.15 gal/sq. yd), but only 0.5 liter/m^2 (0.114 gal/sq. yd) was actually used.

3.5.2.3 Tack Coat

The tack coat used on both projects was slow-setting, high performance emulsified (SS-1HP) asphalt with about 60% asphalt residue. The target application rate was 0.18 liter/m^2 (0.04 gal/sq. yd) on both project locations. The application temperature was 77^0 C (170^0 F) to 79^0 C ($175\ ^0$ F). Tack coat properties are listed in Table 3.6.

Table 3.6 Tack Coat Properties Used on US-160 and K-25 Projects

Route	Tack Material	Shooting Temperature ^{0} F	Unit Weight (lbs/gal)	Specific Gravity	Residual Asphalt (%)
US-160 (EB)	SS-1HP	170	8.49	1.018	60.0
K-25 (SB)	SS-1HP	175	8.49	1.018	60.0

3.5.3 Field Data and Core Collection

Three test sections with variable tack coat application rates were constructed in 2007 using 4.75-mm NMAS Superpave mixture on each project. Test section lengths on US-160 and K-25 were 37 m (120 ft) and 61m (200 ft), respectively (Figure 3.3 a, and b). During construction, SS-1HP was applied at three different rates: low (0.02 gal/yd^2), medium (0.04 gal/yd^2), and high (0.08 gal/yd^2) on the hot-in-place recycled (HIPR) asphalt layer. After the tack coat sections were set up, normal pavement construction practices were followed, which included an HMA haul truck backing over the tack surfaces. A 19-mm (US-160) and 16-mm (K-25) thick overlay was laid on the hot-in-place recycled (HIPR) layer and compacted. Cores at every 6-m (20-ft) (US-160) and

4.5-m (15-ft) (K-25) intervals were collected along the right wheel path about one month after construction to evaluate the performance of both tack materials and the 4.75-mm NMAS Superpave mixture. The cores were collected again one year after construction.

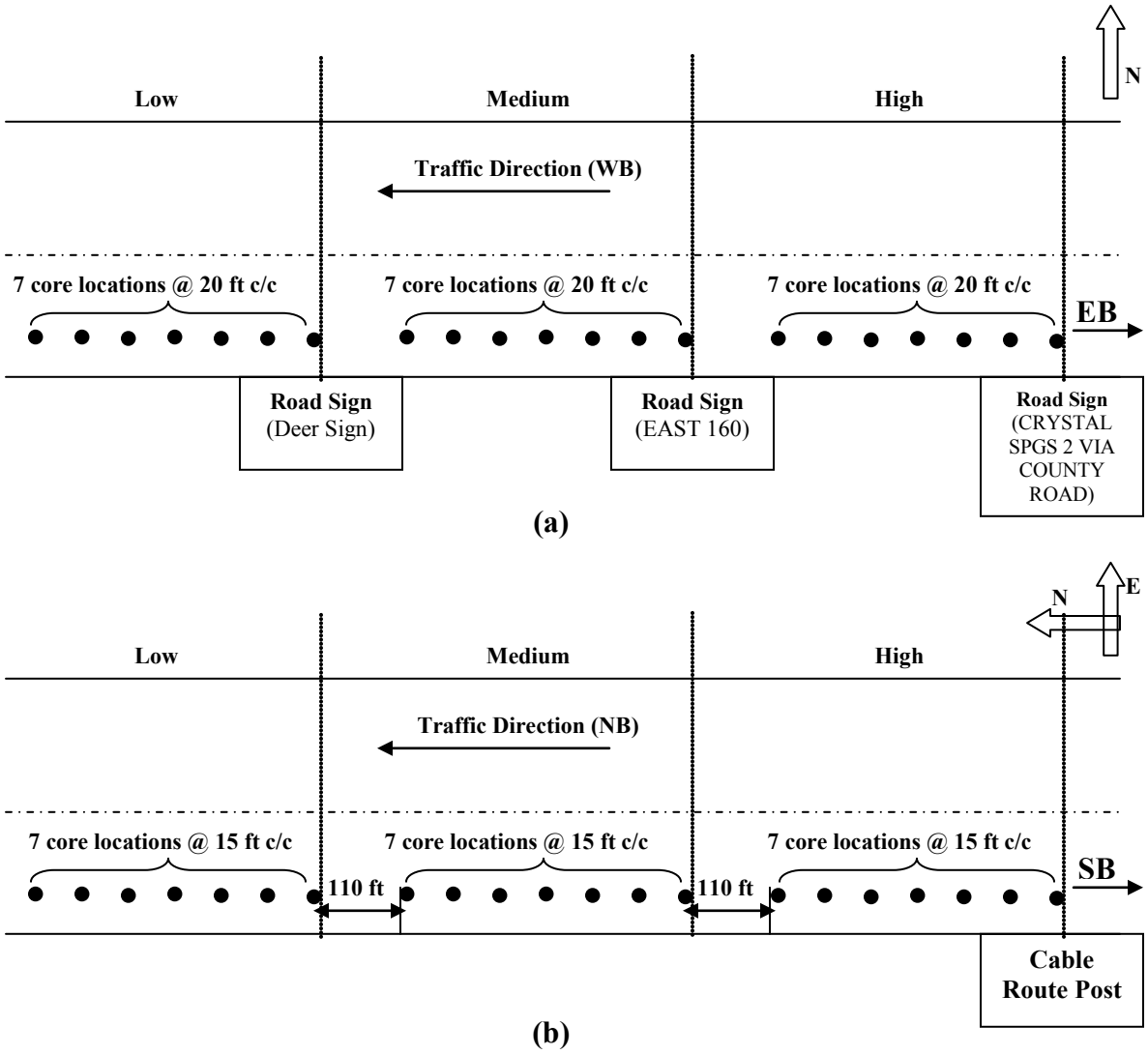

Figure 3.3 Tack coat measurement and core locations on (a) US-160 and (b) K-25

3.5.3.1 Tack Coat Application Rate Measurements

In situ residual tack application rate was measured at seven locations on each tack coat test section to check actual application rates. Measurements were taken using pre-weighed, 304 mm

× 304 mm (1ft × 1ft) dry wooden planks. A slow-setting tack (SS-1HP) was used on both project locations.

The pre-weighted wooden planks were placed near the right wheel path before the distributor truck applied the tack coat. After the passage of the distributor truck, the planks were removed and weighed again to determine the diluted application rate. Figure 3.4 shows the distribution and measurement of tack coat on the US-160 project. From Figure 3.4, it is clearly evident that the tack application rate was not uniform on the US-160 project at a higher application rate.

Figure 3.4 Tack coat application and measurement on US-160

3.5.3.2 Field Core Collections

The first phase of core collection happened one month after construction. Seven, 150-mm (6-inch) diameter cores were collected along the right wheel path from each test section (Figure 3.5a). It was observed that some cores had hairline cracks. Although this kind of cracking is often associated with tender mixes, it can also be caused by lack of bond at the interface with the underlying layer. The cores were cut to a height of 62 mm (2.4 inches) for making specimens for tests in the Hamburg wheel tracking device (HWTD). The size (height and diameter) satisfied

the requirements of Tex-242-F, the standard test method of the Texas Department of Transportation (TxDOT) (TEX 242-F 2009). The HWTD was performed to asses the rutting performance of the fine mixtures. Bulk specific gravity (G_{mb}) and maximum specific gravity (G_{mm}) were also determined to examine in-place density.

Cores in the second phase were collected in June 2008, one year after paving and traffic operation. Fourteen, 50-mm (2-inch) diameter cores were collected along the right wheel path on each test section (Figure 3.5b). No debonding occurred at the HIPR layer during core collection. The collected cores were cut to a height of 50 mm (2 inches) to perform pull-off tests. The test specimens contained only 15 mm (3/5 inch) to 19 mm (¾ inch) of 4.75-mm NMAS overlay. The rest were HIPR layers with tack coat at the interface.

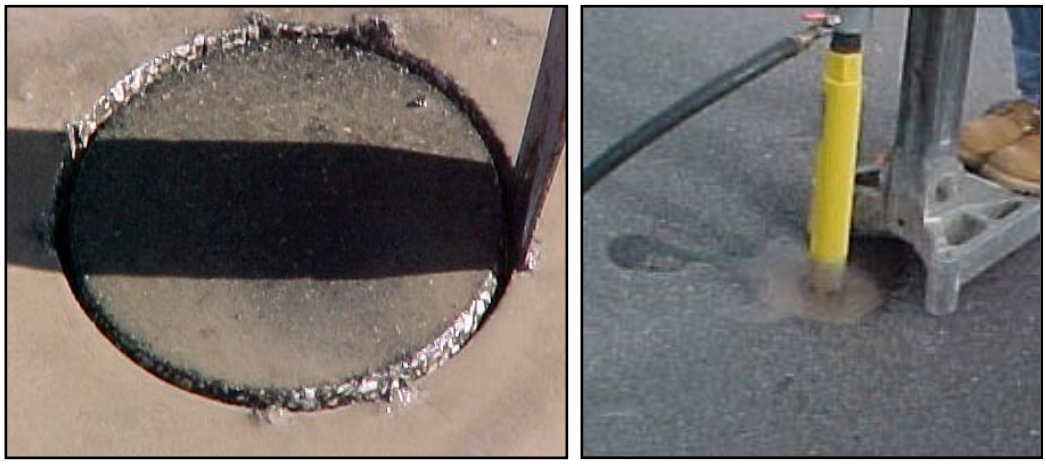

(a) **(b)**

Figure 3.5 (a) 6-inch core collection on US-160, (b) 2-inch core collection

3.6 Design Phase-II: Laboratory Performance of 4.75-mm Mixture

3.6.1 Laboratory Mix Design of 4.7- mm NMAS Superpave Mix

KDOT specification allows mix blend with maximum 35% natural sand that must meet fine aggregate angularity (FAA) requirements. As-constructed baseline mixtures served as benchmarks for comparing the results of laboratory mix designs developed in this study using

materials from the US-160 and K-25 projects. A comprehensive test plan was developed and the test matrix is shown in Table 3.7.

Table 3.7 Laboratory Mix Design and Performance Evaluation Matrix

Mix-Design Phase												
Aggregate Source	US-160						K-25					
PG Binder	64-22			70-22			64-22			70-22		
Natural Sand, (%)	35	25	15	35	25	15	35	25	15	35	25	15
Combined Gradation	G1	G2	G3	G4	G5	G6	G7	G8	G9	G10	G11	G12
FAA	FAA1		FAA2		FAA3		FAA4		FAA5		FAA6	
Selected Mix	m1	m2	m3	m4	m5	m6	m7	m8	m9	m10	m11	m12
Performance Evaluation Tests												
Rut Test (3 reps)	R1	R2	R3	R4	R5	R6	R7	R8	R9	R10	R11	R12
Moisture Test (3 reps)	T1	T2	T3	T4	T5	T6	T7	T8	T9	T10	T11	T12
Fatigue Strength (2 reps)	F1	F2	F3	F4	F5	F6	F7	F8	F9	F10	F11	F12

In the mix-design phase, all mixtures would have to have 4% air voids with N_{des} level at 75 gyrations. This compaction effort was selected as 4.75-mm NMAS mix is normally used for low-volume to medium-volume traffic conditions (ESALs less than 3 millions). Variations of these mix designs were planned by changing the binder grade and also by varying natural sand content in the combined mix for two different aggregate sources in Kansas. The baseline 4.75-mm NMAS mixture designs were obtained from the US-160 and K-25 projects. Twelve different mix designs were developed by considering two aggregate sources, two binder grades, and three different natural sand contents. An anti-stripping agent was used in the mixes for the US-160

project since the baseline mixture also had an anti-stripping agent. For each mix, tests were done for rutting, moisture sensitivity, and fatigue testing.

3.6.1.1 Aggregate Tests

Gradation analysis was performed on all materials brought to the laboratory following AASHTO T 2 and T 284, *Sampling of Coarse and Fine Aggregate*; AASHTO T27, *Sieve Analysis of Coarse and Fine Aggregate;* and AASHTO T11, *Materials Finer than 75 µm (No. 200) Sieve in Mineral Aggregate by Washing.* After selection of aggregate blends, fine aggregate angularity (FAA) of the combined gradation was determined by a KT-50 test procedure for each combination. Specific gravity (KT-59) and clay contents (KT-55) were obtained from the mix design of US-160 and K-25 projects.

3.6.1.1.1 Aggregate Sampling and Gradation by Wash Sieve

Aggregates for wash-sieve analysis were obtained by the sampling method of quartering. Approximately 4,000-gm samples were taken from individual aggregate stockpile. The mixing canvas was placed on a smooth, level surface. The sample was made into a pile near the center of the canvas and was mixed by alternately lifting each corner and rolling the aggregate particles towards the opposite corner. After mixing properly, the aggregates were centered on the canvas in a uniform pile. Using a straight-edge scoop, the pile was then flattened to a uniform thickness and diameter by pressing the apex. The diameter should be approximately four to eight times the thickness. Using a rod or straight-edge scale, the sample was divided into two equal parts. Two equally divided samples were again divided into four equal parts. Two opposite quarters were discarded and the two remaining quarter were combined, mixed and reduced to a size of a 1,000 gm sample (Figure 3.6).

After sampling the individual aggregate, the AASHTO T 11 (KT-3) procedure was followed to determine the quantity of material finer than the 75-µm (US No. 200) sieve in aggregate by the wash method. The test sample for wash-sieve analysis was selected from the material that had been thoroughly mixed. Table 3.8 shows the sample size needed to determine the aggregate particle distribution through wash-sieve analysis. It is to be noted that the material from which the sample is selected should contain sufficient moisture to avoid segregation.

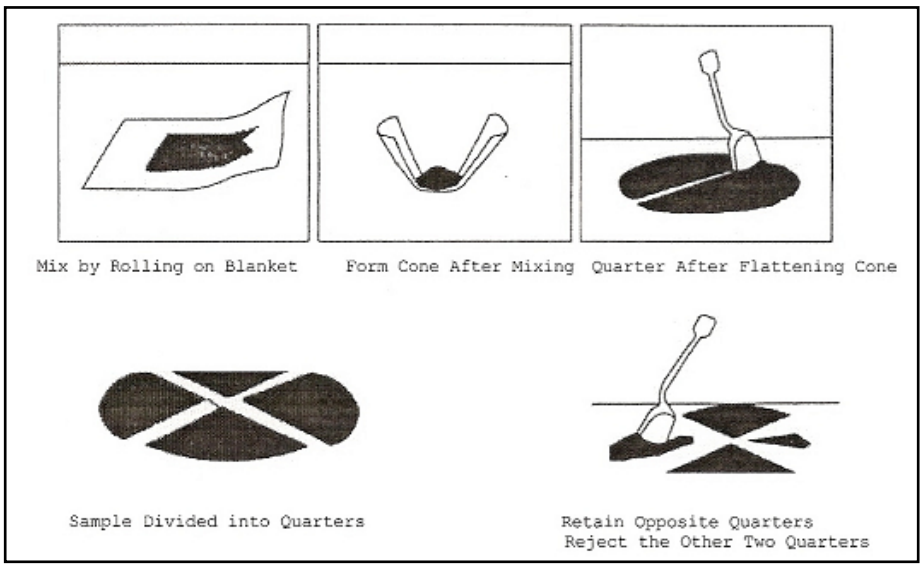

Figure 3.6 Sampling of aggregate by quartering method (Hossain et al. 2010)

Table 3.8 Sample Size for Determination of Particle-Size Distribution (Hossain et al. 2010)

Sieve Size*	Minimum Mass of Samples, (g)
1 ½ in (37.5 mm) or more	15,000
1 in (25 mm)	10,000
¾ in (19.0 mm)	5,000
½ in (12.5mm)	2,000
3/8 in (9.5 mm)	1,000
No. 4 (4.75 mm) or less	300

*Sample size based on NMAS of aggregate (5% or more retained on specified largest sieve)

At first, the sample was dried to a constant mass at a temperature of 110 ± 5^0 C (230± 9^0 F). Original dry mass was then recorded to the nearest 0.1 percent. The dry sample was then placed in a 75-μm (US No. 200 sieve) and the gentle flow of portable water was allowed to pass through the sieve with sufficient agitation. The aggregate sample was washed until complete separation of the finer particles (passing through a US No. 200 sieve) from coarser particles and the clean water comes out through the bottom of the sieve. All materials retained on the No. 200 sieve were dried to a constant mass at a temperature of 110 ± 5^0 C (230± 9^0 F) and weighed to a nearest mass of 0.1 percent. A percent finer than the No. 200 sieve was calculated using the following equation (3.1):

$$\%\,fine = \frac{(Olddrymass - Finaldrymass)\times 100}{Olddrymass} \tag{3.1}$$

U.S Standard sieves No. 4 (4.75 mm), No. 8 (2.36 mm), No. 16 (1.18 mm), No. 30 (0.6 mm), No. 50 (0.3 mm), No. 100 (0.15 mm), and No. 200(0.075 mm) were nested in order of decreasing size of opening from top to bottom. Next, 1,000 gms of re-dried samples were placed in the nested sieve piles and the sieves were agitated for 1 minute using a mechanical shaker. The mass retained on each sieve-size increment was then determined to the nearest 0.1 percent of the total original dry mass using a scale or balance. Total percent of material retained on each sieve was determined using the following equation (3.2):

$$\%\,\mathrm{Re}tained = \frac{(Mass\,\mathrm{Re}tained)\times 100}{DryMassofSampleAfterWashing} \tag{3.2}$$

3.6.1.1.2 Measurement of Fine Aggregate Angularity (KT-50/ AASHTO T-304)

This test was performed to determine the uncompacted void content of 4.75-mm NMAS aggregates based on a selected combined gradation. Test results described the angularity and texture of the aggregates compared to other gradations selected for the laboratory mix design.

Figure 3.7 describe the test apparatus and procedure needed to follow during fine-aggregate angularity testing.

(a)

(b)

(c)

(d)

Figure 3.7 (a) Sieve washed dry material, (b) sample aggregate using quartering method, (c) pour sample in 100-mL cylinder, and (d) pour sample in 200-mL flask

At first, samples from the selected aggregate gradation were washed over the No. 200 sieve and dried to a constant mass following KT-3 test procedure. The dry mass was sieved over No. 8 (2.36 mm), No. 16 (1.18 mm), No. 30 (0.6 mm), No. 50 (0.3 mm), and No. 100 (0.15 mm) sieves; and materials retained on No. 8 (2.36 mm) and passed through No. 100 (0.15 mm) were discarded. The sample was mixed thoroughly until it was homogeneous and was divided following KT-1 sampling procedure. A funnel and funnel stand were prepared to pour the sample into a 100-mL metal cylinder. The funnel had a lateral surface cone sloped 60 ± 4 degree from horizontal with an opening of 12 ± 0.6 mm (0.50 ± 0.024 inch) diameter and 1.5 in height. The funnel stand was capable of holding the funnel firmly in position by

maintaining its collinear above the top of the cylinder. The right-angle metal cylinder of approximately 6.1-in^3 (100-mL) capacity had an inside diameter of 39 ± 1 mm (1.53 ± 0.05 inch) and an inside height of approximately 85 mm (3.37 inch). The selected sample was poured into the funnel, by using a finger to block the opening of the funnel, and was allowed to fall freely into the metal cylinder (Figure 3.7c) after removing the finger. Excess and heaped aggregate in cylinder was removed by a single pass of a straight-edge spatula and cylinder contents were poured into the 200-mL volumetric flask. Distilled water at room temperature 25 ± 1^0 C (77 ± 2^0 F) was added and air bubbles were removed from the flask by rolling the flask at an angle along its base. The process continued until there were no visible air bubbles present or for a maximum 15 minutes. The water level was adjusted to the calibration mark in the flask by adding distilled water if necessary. The whole procedure was repeated four times to obtain four isolated results for the same aggregate gradation. The uncompacted void content, also known as fine aggregate angularity was calculated in 0.1 percent using equations 3.3 and 3.4.

$$U_k = \frac{U_1 + U_2 + U_3 + U_4}{4} \tag{3.3}$$

Where, U_1, U_2, U_3, and U_4 are uncompacted void content in Trial 1, 2, 3 and 4 respectively.

$$U_{1,2,3,4} = \frac{100 \times \left[V_w - \left(V_f - V_c\right)\right]}{V_c} \tag{3.4}$$

where,

V_w = volume of water, mL = $\dfrac{B - A}{0.99704}$

B = mass of flask + water + aggregate, (g)

A = mass of flask + aggregate, (g)

V_f = volume of the flask = 200-mL

V_c = calibrated volume of cylinder = 100-mL

At the end of each trial, the calculated uncompacted void content was compared with the other trial value to verify the specified limit, i.e., U_1, U_2, U_3, and U_4 cannot differ more than 1.0.

3.6.1.2 Laboratory Mix Design

The AASHTO standard practice (R 35-4), *Superpave Volumetric Design for Hot-Mix Asphalt (HMA)*, was followed during the mix-design phase of this study (AASHTO 2004). The standard practice was used to evaluate the 4.75-mm mixture properties following KDOT volumetric specifications for SM-4.75A mix. The project mix design for 4.75-mm NMAS used 35% natural sand. Mix designs with 15% and 25% natural sand were developed in this study. Once the group of aggregates was identified and the gradation was obtained on each project (Appendix B shows individual aggregate gradation), four trial aggregate blends satisfying Kansas gradations for an SM-4.75A mixture were developed. Control points for the 4.75-mm sieve (100-90% passing) were strictly observed in the blending process to maintain a true 4.75-mm NMAS Superpave mixture. Superpave consensus aggregate criterion (FAA) was also tested for the blended aggregate (Section 3.6.1.1). The most critical part in designing the aggregate structure was to meet the VMA criterion in the volumetric mix design. During the trial process, the gradation curve was kept away from the maximum density line but within the control points and optimum dust content (material finer than a No. 200 sieve) was maintained. Table 3.9 and Figure 3.8 show single point gradations of aggregates and a 0.45-power chart, respectively, developed in this study. Table 3.10 shows the selected percentage of individual aggregate in aggregate blend.

Table 3.9 Design Single Point Gradation of Aggregate Blend on US160 and K-25

Laboratory Mix Design ID	% Retained Materials on Sieves								
	12.5 mm (½ inch)	9.5 mm (3/8 inch)	4.75 mm (No. 4)	2.36 mm (No. 8)	1.18 mm (No. 16)	0.6 mm (No. 30)	0.3 mm (No. 50)	0.15 mm (No. 100)	0.075 mm (No. 200)
Max. Density Line	**0.0**	**12.1**	**36.1**	**52.8**	**65.4**	**74.5**	**81.3**	**86.4**	**90.2**
Control Points	**0**	**0-5**	**0-10**		**40-70**				**88-94**
US-160 S_35	0	0	5	36	52	64	85	93	94
US-160 S_25	0	0	6	43	60	71	86	93	94
US-160 S_15	0	0	7	49	69	78	88	93	94
K-25 S_35	0	0	10	28	47	63	80	89	93
K-25 S_25	0	0	10	28	48	63	79	88	92
K-25 S_15	0	0	10	28	48	63	78	87	92

Note: S_35 = Combined gradation with 35% natural sand content
S_25 = Combined gradation with 25% natural sand content
S_15 = Combined gradation with 15% natural sand content

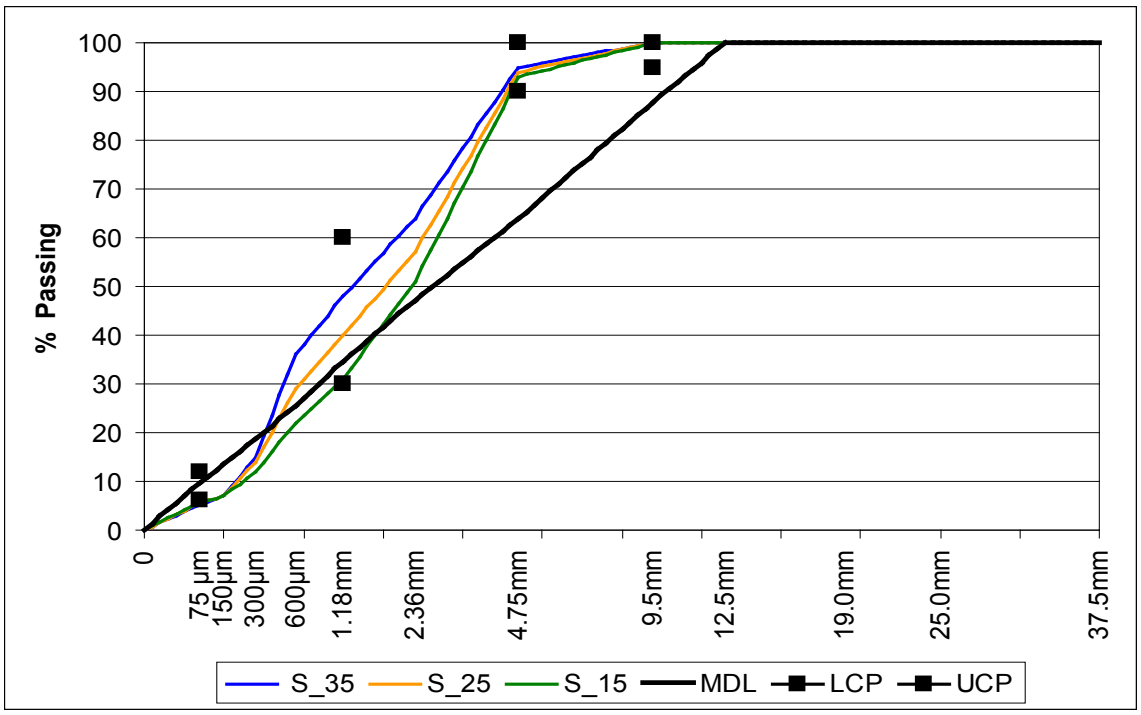

(a)

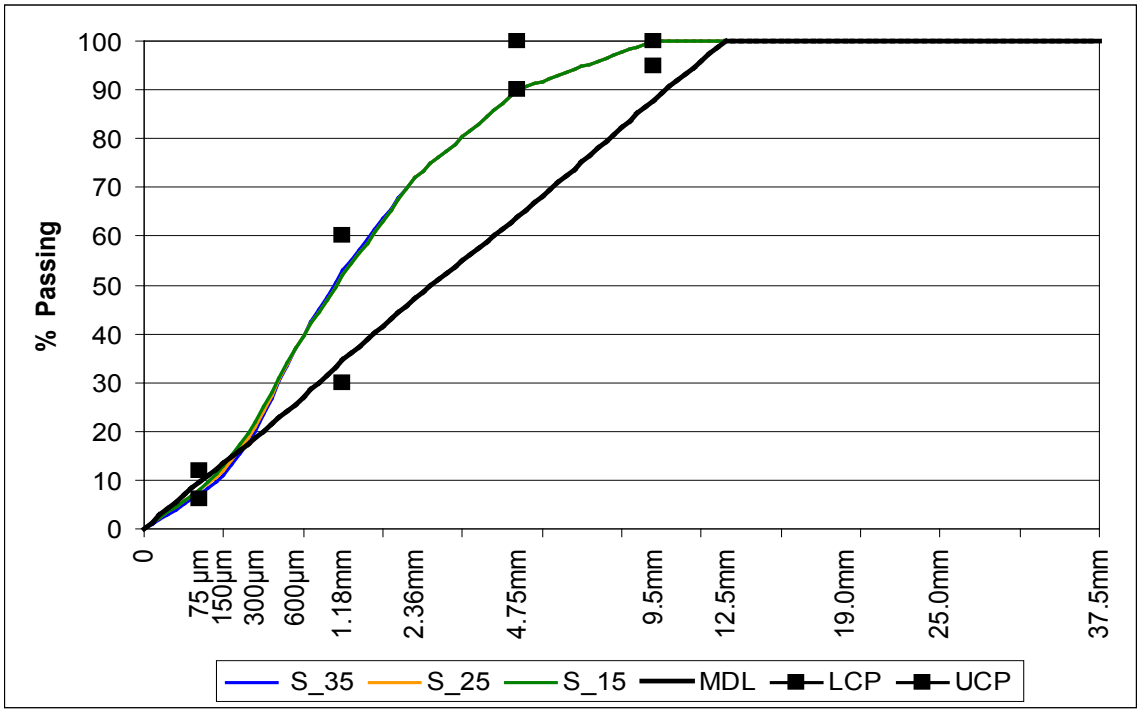

(b)

Figure 3.8 0.45 power charts for 4.75-mm NMAS Superpave laboratory mixture (a) US-160 and (b) K-25

Table 3.10 Percentage of Individual Aggregate in Combined Gradation

Source	Aggregate	% in Combined Gradation		
US-160	**CS-1B**	32	40	45
	CS-2	12	12	12
	CS-2A	7	7	7
	CS-2B	14	16	21
	SSG-4	35	25	15
K-25	**CG-2**	30	34	40
	CG-5	33	39	43
	SSG-1	35	25	15
	MFS-5	2	2	2

For experimental design purposes, aggregates from each aggregate source were again subdivided into three major categories. Based on aggregate particle-size distribution and percent fines retained on the No. 200 sieve, the subsets were defined as coarse material (among groups), screening material, and river sand (Table 3.11).

Table 3.11 Aggregate Subsets on US-160 and K-25

Source	Aggregate Subsets, (%)					
	Coarse Material[1]		**Screening Material[2]**		**River Sand[3]**	
	Max.	Min.	Max.	Min.	Max.	Min.
US-160	45	32	33	26	35	15
K-25	40	30	43	33	35	15

Note: [1] = CS-1B and CG-2 for US-160 and K-25, respectively
[2] = (CS-2 + CS-2B) and CG-5 for US-160 and K-25, respectively
[3] = SSG-4 and SSG-1 for US-160 and K-25, respectively

After selecting aggregate blends for 35%, 25%, and 15% river sand content, design asphalt content for each gradation was determined considering two different binder grades (PG 64-22 and PG 70-22). The proposed aggregate blend was combined with four different proportions of binder from -0.5% to +1% max of the trial binder content at 0.5% intervals.

Considering each binder content, preparation of each aggregate/binder mixture was defined as an individual batch. Mixing temperature ranged from 156^0 to 160^0 C (313^0 to 325^0 F). The batch mixture was then conditioned in a closed draft oven (289^0 to 300^0 F) for a minimum of 2 hours prior to compaction. This was the time needed for the aggregates to absorb the binder. Batch samples were then compacted with a Superpave gyratory compactor (SGC) at oven temperature. All samples, including the maximum specific gravity tests, were aged for the same amount of time. Theoretical maximum specific gravity (G_{mm}) of the loose mixture and bulk specific gravity (G_{mb}) of the compacted samples were then determined by KDOT standard test methods KT-39 (AASHTO T209) and KT-15 (AASHTO T166) procedure III, respectively. The G_{mm} and G_{mb} were calculated using the Equations (3.5) and (3.6), respectively.

$$G_{mm} = \frac{A}{A - C} \tag{3.5}$$

where

G_{mm} = theoretical maximum specific gravity,

A = mass of dry sample in air, (g), and

C = mass of water displaced by sample at 77^0 F (25^0 C), (g).

$$G_{mb} = \frac{A}{B - C} \tag{3.6}$$

where

G_{mb} = bulk specific gravity of a compacted specimen,

A = mass of dry sample in air, (g),

B = mass of saturated surface-dry sample in air, (g), and

C = mass of saturated sample in water, (g).

After all necessary testing had been accomplished, the volumetric parameters were calculated. Averaged results of various volumetric calculations were tabulated and design binder content was selected based on KDOT-specified volumetric criteria for SM-4.75A at 4 percent air voids. Air void of the compacted sample was calculated using the following equation (3.7):

$$\%V_a = \frac{(G_{mm} - G_{mb}) \times 100}{G_{mm}} \tag{3.7}$$

Where

V_a =air voids

Table 3.12 shows the selected design asphalt contents and other volumetric parameters obtained for 12 mixes designed in the lab.

Table 3.12 Mix Design Volumetric Properties

Aggregate Source	PG[1]	NSC[2]	Air Void (%)	ρ_b^3 (%)	VMA (%)	VFA (%)	G_{mm} @ N_{ini} (%)	DP[4]	ρ_{beff}^5 (%)
US-160	64-22	35	4.33	7.0	16.12	73.14	89.32	0.99	5.32
		25	3.95	6.8	15.32	74.24	87.84	1.09	5.09
		15	4.16	6.75	15.64	73.40	85.53	1.21	4.79
	70-22	35	4.07	6.8	15.63	73.99	89.43	1.02	5.2
		25	3.97	6.6	15.27	74.02	87.89	1.11	5.07
		15	4.07	6.6	15.28	73.35	85.6	1.15	5.03
K-25	64-22	35	3.48	6.1	16.49	78.0	89.99	1.19	5.85
		25	3.99	5.6	16.04	75.09	89.35	1.48	5.48
		15	3.96	5.4	15.65	74.72	88.96	1.53	5.24
	70-22	35	3.39	5.7	15.47	78.0	90.37	1.29	5.39
		25	4.76	5.5	16.27	70.73	88.39	1.54	5.19
		15	3.63	5.4	15.0	75.7	89.58	1.58	5.03
KDOT Spec			**4**		**Min 15**	**65-78**	**Max 90.5**	**0.9-2**	

[1]=Binder grade; [2]=natural sand content; [3]= asphalt content; [4]=Dust-to-binder ratio; [5] = Effective asphalt content

3.7 Performance Tests on Field and Laboratory Mixes

Rutting and bond strength of field cores, collected in two different phases, were evaluated by Hamburg wheel tracking device (HWTD) and laboratory pull-off strength test. Laboratory mixture performances such as rutting, moisture sensitivity, and fatigue strength of 4.75-mm

NMAS were also examined by HWTD, indirect tensile strength ratio (TSR Load Frame), and repeated flexural bending beam tests, respectively. HWTD tests were done following Tex-242-F test method of the Texas Department of Transportation, while moisture susceptibility testing followed KT-56: *Resistance of Compacted Bituminous Mixture to Moisture Induced Damage*, and long-term fatigue testing followed AASHTO T 321-03: *Determination of Fatigue Life of Compacted Hot-Mix Asphalt (HMA) Subjected to Repeated Flexural Bending*. A brief description of these field and laboratory mix performance tests is given below.

3.7.1 Hamburg Wheel Tracking Device Rutting Evaluation (TEX 242-F 2009)

Rutting or permanent deformation of the field cores and laboratory-designed mixtures was evaluated using the Hamburg wheel tracking device (HWTD) and following Tex-242-F test method of the Texas Department of Transportation. This wheel tracking equipment is operated under the mechanism that a pair of wheels apply moving loads to the specimen in order to simulate rutting in an accelerated manner. The depth of depression or rut created on the sample is measured and analyzed. Tex-242-F evaluates the premature failure susceptibility of a bituminous mixture due to weakness in the aggregate skeleton, moisture damage, and inadequate binder stiffness. The test measures the depression and number of wheel passes to failure (Figure 3.9). Each moving steel wheel of HWTD is 8 inches (203.6 mm) in diameter and 1.85 inches (47 mm) wide. The load applied by the wheel is approximately 705 ± 22 N (158 ± 5 lbs) and the wheel passes over the test specimen approximately 50 times per minute. The water control system of HWTD is capable of controlling the test temperature from 25^0 to 70^0C (77^0 to 158^0 F) with a precision of $\pm 2^0$C (4^0F). The rut depth measurement system consists of a linear variable differential transformer (LVDT) device. Rut depth is taken after every 100 passes of the wheel.

Figure 3.9 Experimental setup and failure surface on field cores

The Hamburg samples, both field and laboratory (SGC) compacted, were 150 mm (6 inch) in diameter and 62 ± 2 mm (2.4 ± 0.1 inch) tall. In-place density of the laboratory test samples must be $93 \pm 1\%$. The samples were placed together in special molds following Texas test procedure Tx-242-F as shown in Figure 3.9 and then were submerged under water at 50^0 C in the test bath. The core collected from the field also followed the diameter and height specifications as stated above. TxDOT specification allows 20,000 repetitions or number of wheel passes and 20-mm (0.8-inch) rut depth (which ever comes first) based on binder grade to evaluate the rutting performance of the HMA mix. Rut depth or deformation was measured at 11 different points along the wheel path of each sample with an Linear Variable Differential Transformer (LVDT).

Output parameters interpreted from the rut history data and plot were number of wheel passes at 20-mm(0.8 inch) rut depth, rutting/creep slope, stripping slope, and stripping inflection point (Figure 3.10).

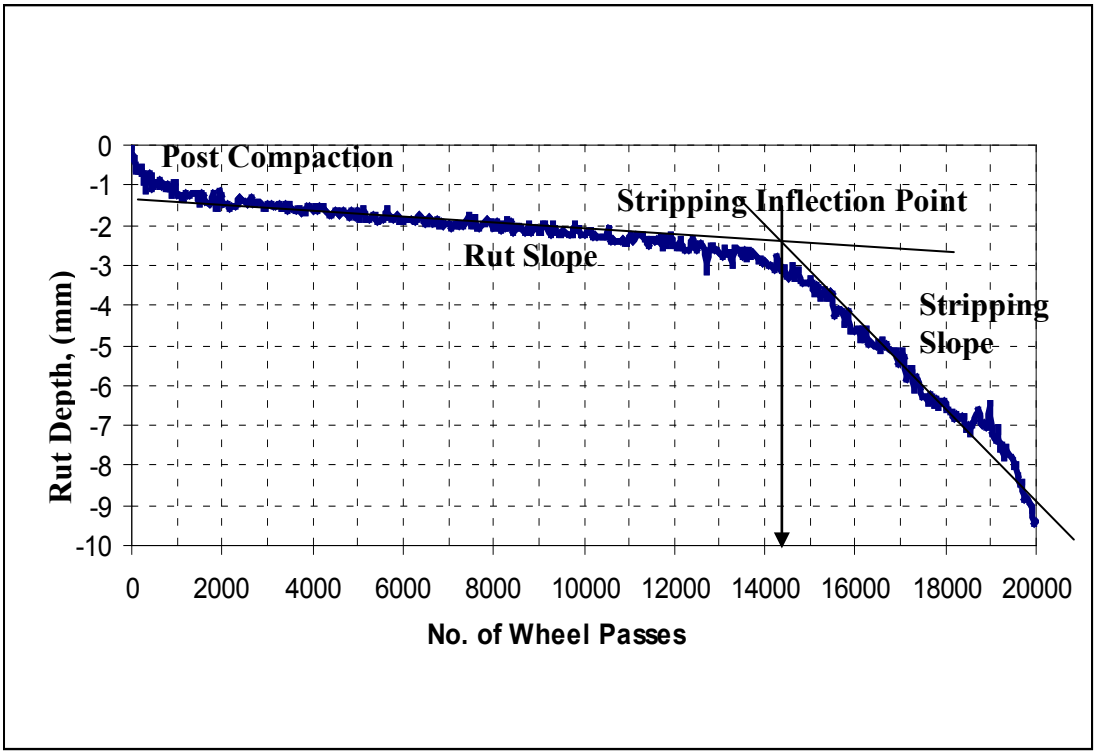

Figure 3.10 Rutting performance of laboratory mix 2 on US-160 project

Creep slope or rutting slope relates to permanent deformation from plastic flow after post-compaction effects have ended and before stripping action starts. Stripping slope is the inverse of the rutting slope and indicates the start of stripping action and continues till the end of the HWTD test. The stripping inflection point is the number of wheel passes at the intersection point of the rutting and stripping slope, which indicates the resistance of the HMA mixture to moisture damage (TEX 242-F 2009).

3.7.2 Pull-Off Tests for Bond Strength Measurement

The American Society of Testing and Materials (ASTM) has specified a standard test, "Standard Test Method for Pull-Off Strength of Coating Using Portable Adhesion Tester" (ASTM 2003). The test measures the tensile force required to pull apart two bonded, flat surfaces. The test result can be reported either as pass/fail or by recording tensile force to split the bonded layer. No

guidelines are available regarding the initial normal force or pre-compression time required to perform the test. According to the ASTM standard, these initial conditions should be assigned by the test apparatus manufacturer (ASTM 2003). KDOT has partially adopted this test procedure to evaluate in-situ bond strength in the field. During this study, the KDOT procedure was followed with a SATEC model T 5000 universal testing machine. Before testing, both faces of a core were glued to metal plates using epoxy (Pro-Poxy 300 fast A/B) as illustrated in Figure 3.11. The epoxy needed 16 to 24 hours to set and to make a perfect bonding with the bituminous mixture. The strength test was performed at 25^0 C (77^0 F). During testing, the core samples were conditioned under normal loads of 0 to 10 lbs for five seconds. The applied displacement was set to 25 mm/min (1 inch/min). The test samples were then loaded to fail in direct tension (Figure 3.11).

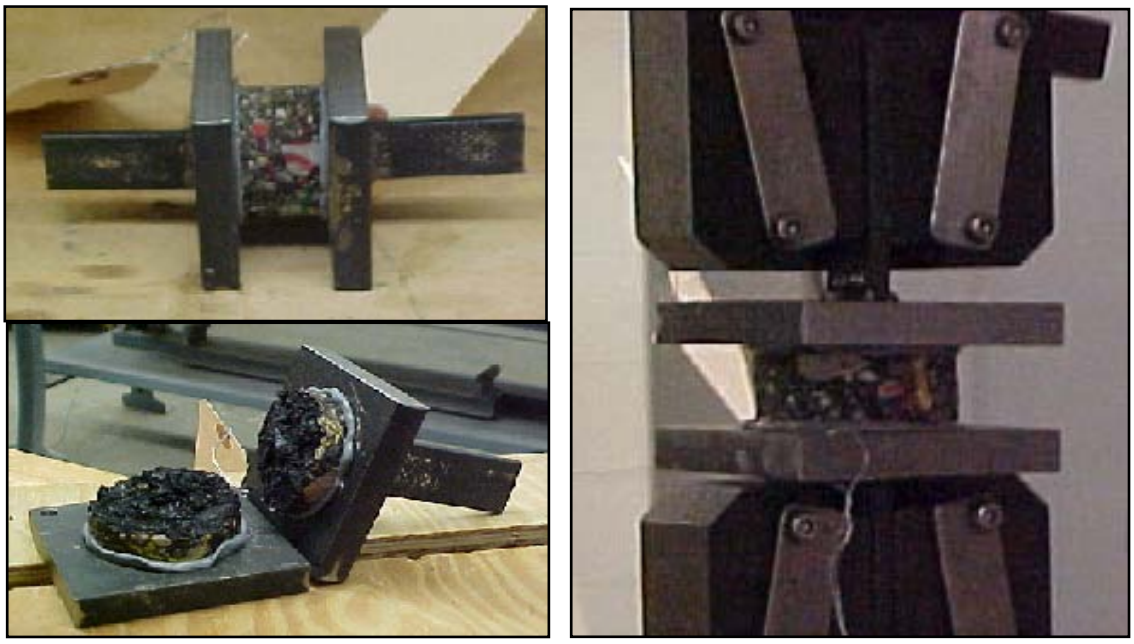

Figure 3.11 Pull-off strength test of tack coat material

3.7.3 Moisture Susceptibility Test (KT-56)

This test is used to measure the change in tensile strength resulting from the effects of saturation and accelerated water conditioning of the compacted bituminous mixture in the laboratory. It helps to evaluate the ability of the compacted bituminous mix to withstand long-term stripping action and also to asses the liquid anti-stripping additives used in the asphalt mix. Kansas test procedure KT-56, *Resistance of Compacted Bituminous Mixture to Moisture Induced Damage*, a slightly modified version of AASHTO T283, was followed in this study (Hossain et al. 2010). The test specimens were prepared using the Superpave gyratory compactor (SGC). At least six SGC-compacted specimens were prepared for each set with an air void of 7%± 0.5% (Appendix B). The specimens were 6 inches (150 mm) in diameter and 98 $\pm$ 5 mm (4 $\pm$ 0.2 inches) thick. The air void level can be obtained by adjusting the height of the specimen. After mixing and compaction, the samples were conditioned at 25 ± 1^0 C (77 ± 5^0F) for 24 $\pm$ 1 hours. The maximum specific gravity (G_{mm}), and bulk specific gravity (G_{mb}) were computed for each set to determine the air void of the test samples. Thickness and diameter of the specimens were also measured to the nearest 0.01 mm. The six compacted samples were then subdivided into two sublots. Each subset had approximately equal average air void. One subset was considered for conditioning and the other one remained unconditioned.

The conditioned subset was placed in a vacuum container with a minimum diameter of 200 mm (8 inches) and the inside height capable of holding a minimum of 25 mm (1 inch) of water above the specimen. The samples were selected to achieve percent saturation of 70% to 80%. A vacuum pump with 30 mm of Hg absolute pressure was also attached to the vacuum container (Figure 3.12). After achieving the saturation within the specified limit, the samples were sealed in a zip lock bag with 10 mL of water within 2 minutes and were kept at a freezing

temperature of -18 ± 3^0C (0 ± 5^0F) for at least 16 hours. The samples were then removed and placed in a hot water bath at 60 ± 1^0C (140 ± 2^0F) for 24±1 hours. The conditioned samples were removed from the hot water bath one at a time and damp-dried quickly. The SSD mass was measured and the samples were placed in a water bath at room temperature (25 ± 1^0C) for two hours. The mass under water was also recorded. Final height and diameter were also recorded as soon as they had been removed from water bath prior to the indirect tensile test.

Figure 3.12 Saturation and tested sample in TSR load frame

The unconditioned samples were stored at room temperature. Thickness and diameter were measured. The samples were placed in a concrete cylinder and then in water bath at 25 ± 0.5^0 C (77 ± 1^0 F) for 2 hours. The samples were then ready to be tested in a Marshall stability tester using indirect tensile strength (Figure 3.12). Average tensile strength and percent tensile strength ratio were calculated using the following equations (3.8), (3.9), and (3.10). KDOT specification requires a minimum TSR of 80% for the HMA mix not to be potentially moisture sensitive.

$$S_t(matric) = \frac{2{,}000 \times (P)}{(\pi)(t)(D)} \tag{3.8}$$

$$S_t(english) = \frac{2 \times (P)}{(\pi)(t)(D)} \tag{3.9}$$

where,

S_t = tensile strength, kPa (psi),

P = maximum load, N (lbs),

t = thickness of the samples, mm (in), and

D = diameter of the samples, mm (in).

Percent tensile strength ratio, $TSR = \frac{100 \times S_2}{S_1}$ (3.10)

where,

S_1 = average tensile strength of unconditioned subset, kPa (psi), and

S_2 = average tensile strength of conditioned subset, kPa (psi).

3.7.4 Flexural Beam-Fatigue Testing (AASHTO T321-03)

This performance test will estimate the fatigue life and failure energy of HMA pavement layer materials under repeated loading conditions. Performance of HMA can be more accurately determined when these properties are known. The failure point of the HMA beam specimen is defined as the load cycle at which the specimen exhibits a 50% reduction of its initial stiffness (AASHTO 2005). The HMA slab was prepared in the laboratory using a kneading compactor. The target air void was 7% ± 1%. The slab was 432 mm (17 inch) long by 260 mm (10 inch) wide by 50 mm (2inch) thick (Figure 3.16). The mixing and compaction temperatures were 156^0 C (313^0 F) and 146^0 C (294.5^0 F), respectively. The replicate beam samples were then sawn from the laboratory-compacted HMA slab. Approximately four beams were cut from a single slab. The beam specimen was 380 mm (15 inch) long, 50 mm (2 inch) thick and 63 mm (2.5 inch) wide. Figure 3.13 shows the slab compaction, beam specimen, test setup of the flexural beam fatigue test setup, and software output of the beam fatigue test.

The test system consisted of a loading device, an environmental chamber, and a control and data acquisition system. The test system minimum requirements are 0 to 5 kN (1,225 lb) for loading measurements and control, 0 to 5 mm (0.2 inch) displacement measurements and control, and the environmental chamber temperature should be maintained at $20^0 \pm 0.5^0$C ($68^0 \pm 0.5^0$ F). The loading frequency varies from 3 to 10 Hz.

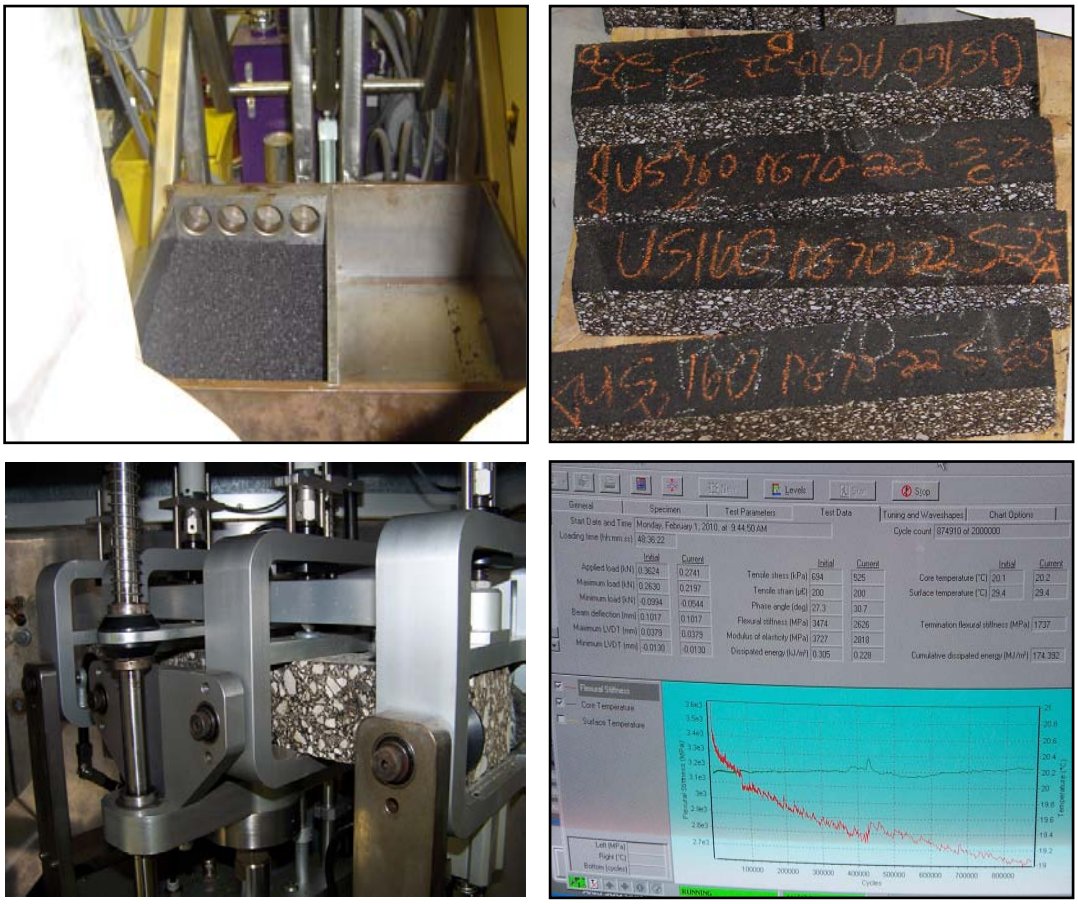

Figure 3.13 Flexural beam fatigue test sample preparation and test setup

The load was applied for 50 cycles with a constant strain of 300 micro-strains and the flexural stiffness value of the HMA beam was calculated and compared with the initial values. After completion of the test, bulk specific gravity of tested beams was measured and maximum theoretical specific gravity of the loose mixes was also determined to calculate the air voids of the beam specimen.

CHAPTER 4 - RESULTS AND ANALYSIS

4.1 General

This chapter discusses the results of field cores and laboratory mix performances of 4.75-mm NMAS Superpave mixtures. Field cores were examined with respect to permanent deformation at three different tack coat application rates. The bond strength of the layer materials was also assessed for different residual tack rates. Performances of laboratory mixes were evaluated in terms of rutting, moisture susceptibility, and fatigue damage. Volumetric properties of laboratory-designed mixes were also assessed for different binder grades, river sand contents, and aggregate types.

4.2 Tack Coat Measurement and Field Core Performance

As mentioned earlier, three application rates were selected for each project. Seven measurement points were set at 6.1-m (20-ft) and 4.5-m (15-ft) intervals near the right wheel path on the US-160 and K-25 projects, respectively. Six-inch and two-inch diameter cores from these test sections were collected and tested in the lab.

4.2.1 Performance of 4.75-mm NMAS Projects

4.2.1.1 Performance of Overlay After One Year of Construction

Figures 4.1, 4.2 and 4.3 show the performance history of the projects. The HIPR and overlay resulted in remarkable improvement in roughness (about 24% decreases in roughness). Overall, US-160 was smoother than K-25. The rutting 2.5 to 3.8 mm (0.1 to 0.15 inch) was fully addressed. K-25 had transverse cracking and that was also addressed by HIPR and the overlay.

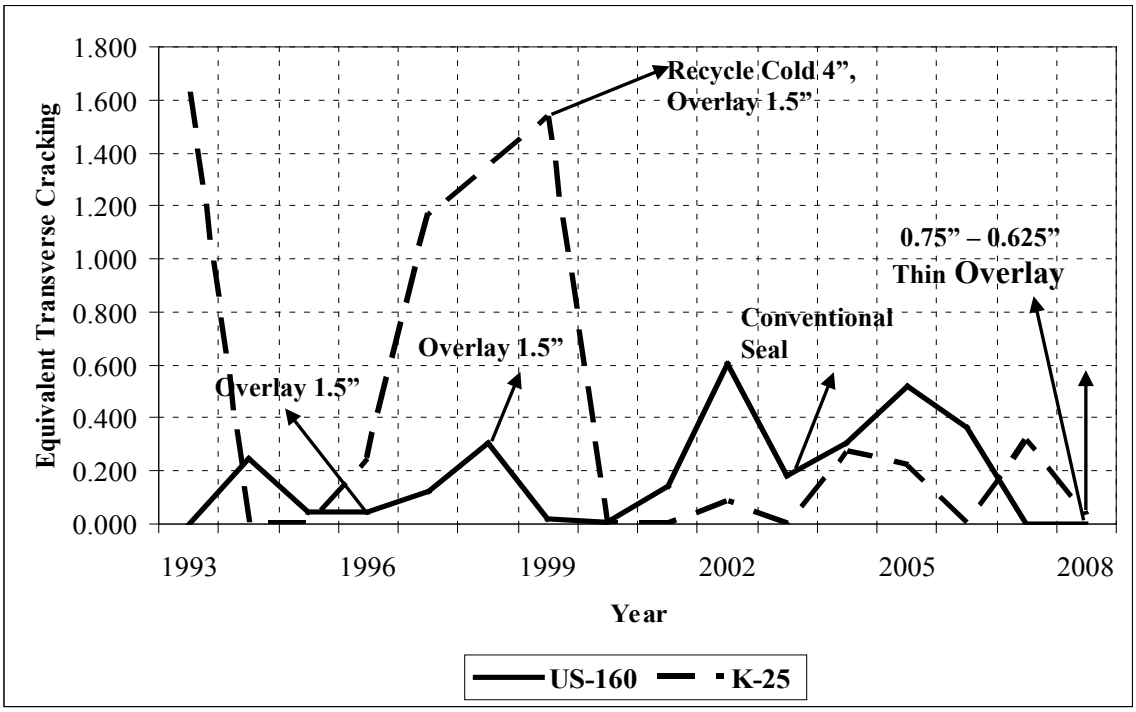

Figure 4.1 Transverse cracking progressions on US-160 and K-25, 1993-2008

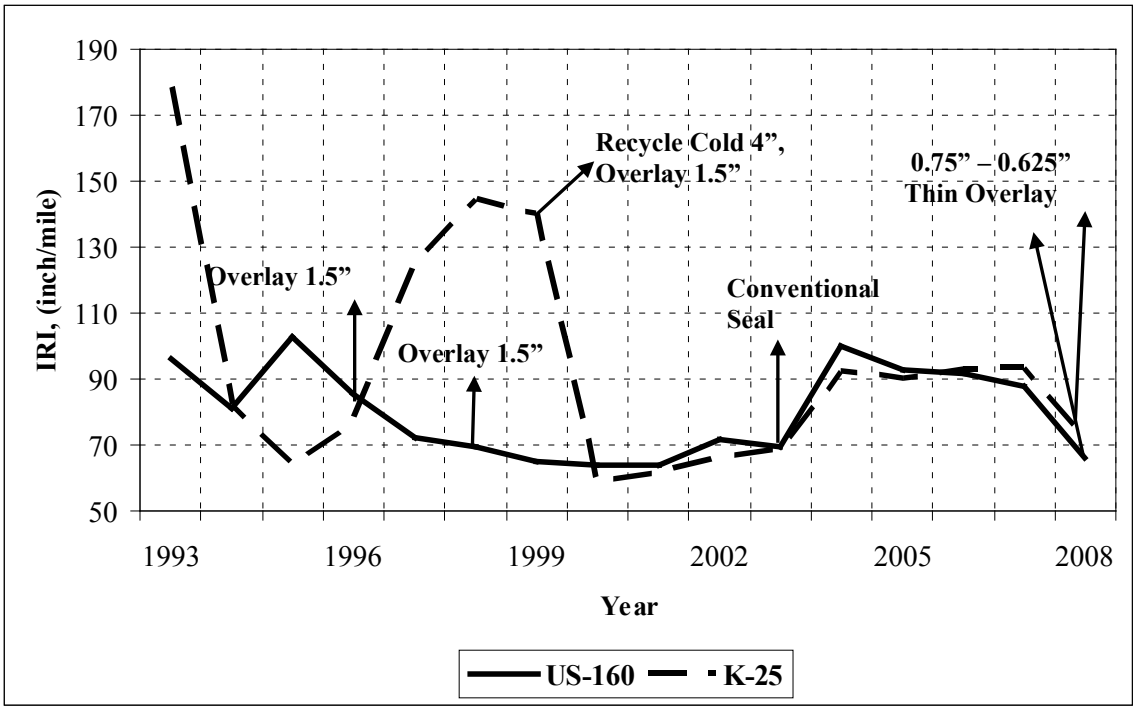

Figure 4.2 IRI progressions on US-160 and K-25, 1993-2008

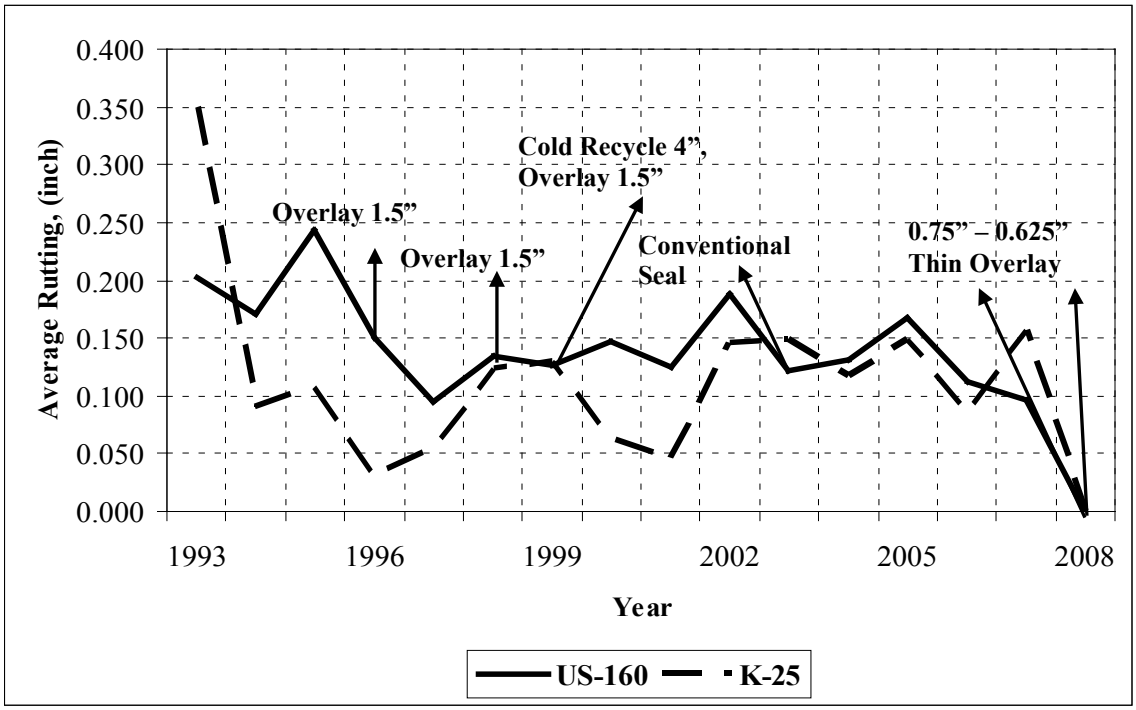

Figure 4.3 Rutting progressions on US-160 and K-25, 1993-2008

4.2.1.2 Performance of Overlay After Two Years of Construction

Kansas Pavement Management System (PMS) survey in 2009 has indicated that transverse cracks are returning on K-25 project (Figure 4.4). US-160 seems to be doing fairly well compared to K-25 project. Both projects showed good performance against rutting. Scuffing and gouging of these mixtures were the real concerns. On both projects, they were unfounded. Table 4.1 shows the equivalent transverse cracking (ETCR) and International Roughness Index (IRI in inch/mile) in each section on both projects in the year 2009. Table shows the overlay sections are fairly smooth

Table 4.1 Performance of Thin Overlay of 4.75-mm NMAS Mixture in 2009

Project	Beginning Mile Post	End Mile Post	IRI (in/mile)	ETCR
K-25	0	1	54	0.353
	1	2	53	0.000
	2	3	60	0.146
	3	4	58	0.208
	4	5	61	0.249
	5	6	59	0.104
	6	7	55	0.104
	7	8	64	0.166
	8	9	62	0.416
	9	10	60	0.146
	10	11	59	0.166
	11	12	63	0.248
	12	13	50	0.104
	13	14	46	0.062
	14	15	53	0.104
	15	16.018	71	0.000
	Average		**58**	**0.161**
US-160	0	1	42	0.104
	1	2	52	0.520
	2	3	37	0.166
	3	4	34	0.000
	4	5	39	0.000
	5	6	53	0.000
	6	6.718	51	0.146
	6.718	7.575	60	0.000
	7.575	9	39	0.000
	9	10	39	0.000
	10	11	32	0.000
	11	12	37	0.000
	12	13	41	0.000
	13	14	48	0.000
	14	15	40	0.000
	15	16	42	0.000
	16	17	43	0.000
	17	18	61	0.000
	Average		**44**	**0.052**

Figure 4.4 Visible transverse cracks on K-25 project

4.2.2 Tack Coat Application Rate Measurements

Tables 4.2 and Table 4.3 show the measured residual tack application rate at both locations. Tables show the application rate measured during construction was fairly close to the target value on the K-25 project. However, on US-160, the measured application rates were way below the targets. The high application rate was not achieved during construction. The statistical summary (mean and standard deviation) for the US-160 project showed less scattered application rates compared to the K-25 project. These tables confirm that three distinct sections, based on the tack coat application rate, were not achieved on US-160. This implies that better equipment calibration is needed in the field.

Table 4.2 Measured Tack Coat Application Rate on US-160

Route	Section	Plank #	Plank Initial Weight (lbs)	Plank Weight with Tack Coat (lbs)	Residue (lbs)	Application Rate (gal/yd^2)
US-160	High	1	0.80	0.82	0.0249	0.0264
		2	0.76	0.80	0.0344	0.0365
		3	0.77	0.81	0.0401	0.0425
		4	0.79	0.83	0.0362	0.0383
		5	0.73	0.76	0.0373	0.0395
		6	0.72	0.76	0.0392	0.0416
		7	0.75	0.79	0.0364	0.0386
		Avg.				0.038
		STDEV				0.0054
		Target				**0.08**
		% Diff.				**110.5**
	Medium	8	0.77	0.81	0.0397	0.0421
		9	0.78	0.82	0.0370	0.0393
		10	0.75	0.78	0.0375	0.0397
		11	0.78	0.81	0.0353	0.0374
		12	0.72	0.75	0.0311	0.0330
		13	0.72	0.75	0.0238	0.0252
		14	0.79	0.82	0.0302	0.0320
		Avg.				0.036
		STDEV				0.0058
		Target				**0.04**
		% Diff.				**11.1**
	Low	15	0.74	0.74	0.0053	0.0056
		16	0.80	0.82	0.0229	0.0243
		17	0.76	0.77	0.0104	0.0110
		18	0.76	0.78	0.0225	0.0238
		19	0.78	0.82	0.0355	0.0376
		20	0.78	0.81	0.0309	0.0327
		21	0.79	0.81	0.0194	0.0206
		Avg.				0.022
		STDEV				0.0113
		Target				**0.02**
		% Diff.				**9.1**

[*] 1 lb = 0.454 kg; [**] 1 gal/yd^2 = 4.527 l/m^2

Table 4.3 Measured Tack Coat Application Rate on K-25

Route	Section	Plank #	Plank Initial Weight (lbs)	Plank Weight with Tack Coat (lbs)	Residue (lbs)	Application Rate (gal/yd^2)
K-25	High	1	0.80	0.882	0.086	0.0907
		2	0.78	0.851	0.072	0.0763
		3	0.73	0.803	0.073	0.0774
		4	0.66	0.761	0.098	0.1038
		5	0.70	0.788	0.092	0.0977
		6	0.71	0.794	0.086	0.0907
		7	0.73	0.825	0.097	0.1031
		Avg.				0.09
		STDEV				0.0112
		Target				**0.08**
		% Diff.				**11.1**
	Medium	8	0.77	0.827	0.054	0.0574
		9	0.80	0.845	0.049	0.0520
		10	0.74	0.783	0.045	0.0480
		11	0.67	0.713	0.049	0.0520
		12	0.69	0.741	0.051	0.0546
		13	0.75	0.807	0.058	0.0616
		14	0.70	0.752	0.054	0.0576
		Avg.				0.05
		STDEV				0.0045
		Target				**0.04**
		% Diff.				**20.0**
	Low	15	0.72	0.748	0.026	0.0273
		16	0.68	0.713	0.035	0.0375
		17	0.67	0.693	0.021	0.0222
		18	0.74	0.759	0.021	0.0222
		19	0.82	0.836	0.016	0.0173
		20	0.79	0.796	0.008	0.0084
		21	0.76	0.759	0.001	0.0007
		Avg.				0.02
		STDEV				0.0121
		Target				**0.02**
		% Diff.				**0.0**

* 1 lb = 0.454 kg; ** 1 gal/yd^2 = 4.527 l/m^2

4.2.3 Rutting Performance of Field Cores

Rutting performance of thin overlay was evaluated to examine the effect of tack coat application rate on surface mix performance. Residual tack coat application rate at interface of thin HMA

overlay is critical as slippage or lateral movement may occur at interface under traffic at high tack coat application rate. HWTD was used to perform rut tests on all six sets of cores. Four cores from each test section (low, medium, and high tack application rates) were used to make the HWTD samples. Air voids of the field cores were determined from results of the maximum theoretical specific gravity (G_{mm}) and bulk specific gravity (G_{mb}) tests. On the US-160 project, air voids of the cores varied from 6.6% to 8.6%, while K-25 sections had a mean air void of 4.3%. Table 4.4 shows the residual tack coat application rates, percent air voids of the field cores, and number of wheel passes for all sections. Air voids of the K-25 field cores were much lower than those for the US-160 cores. However, US-160 cores carried a higher number of wheel passes before failure (19 mm rut depth) as shown in Figure 4.5. The highest number of wheel passes was observed on the low tack application rate sections on US-160. There was no appreciable difference in the number of wheel passes for the medium and high tack application rates.

Table 4.4 Rutting Performance of 4.75-mm NMAS Superpave Mix Overlay

Route	Section	Residual Application Rate (gal/yd^2)	Air Void (%)	Number of Wheel Passes
US-160	Low	0.012	6.6	5,600
	Medium	0.024	7.2	4,700
	High	0.024	8.6	5,200
K-25	Low	0.012	4.5	1,400
	Medium	0.030	4.3	1,950
	High	0.054	4.8	1,900

HWTD results showed that the number of wheel passes significantly increased at in-place density near 93%. These results also implied that compaction during paving is one of the major factors controlling performance of the mix. A well-designed HMA mixture should achieve in-place air voids within the 7% ± 1% limit immediately after construction. The air voids

determined for thin overlay on K-25 projects were way below the target value (7% ± 1%) means, the mix laid on that particular section was not well designed.

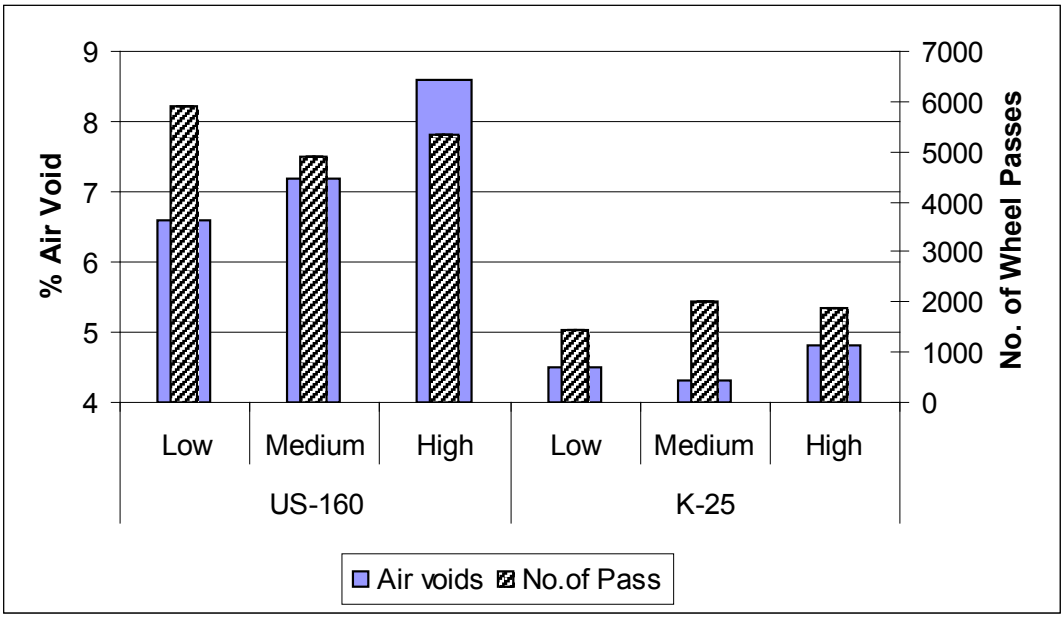

Figure 4.5 Rutting performances of field cores on US-160 and K-25

In general, the pavement with well-designed mixture is expected to have 7% to 8% air voids during construction and will achieve 4% design air voids under traffic within a 20-year design life. In-place density below 93% ± 1% immediately after construction will be permeable to air and water and will not have the required durability. Again, if the initial compaction results in air voids of approximately 4% or lower, the mix may become unstable under traffic after additional densification and hence, result in shoving and excessive rutting (AASHTO 2000). Cores from the K-25 project experienced excessive rutting and stripping during the HWTD test due to overcompaction at a very early age of the pavement. The pavement experienced extreme lateral shear at low air void under accelerated testing conditions. In addition, the US-160 mixture contained an anti-stripping additive which may be the possible cause of overall better performance in submerged conditions in HWTD.

4.2.4 Pull-Off Tests on Field Cores

Results obtained in the pull-off strength test in this study are shown in Figure 4.6. The cores were selected randomly from seven locations in each test section to get unbiased results. A very high variability in the pull-off strength was observed, even for the same coring location, tack application rate, and failure mode. In most cases, on both projects, tensile failure occurred within the HIPR layer material and/or surface material, rather than at the interface of the 4.75-mm NMAS Superpave overlay and HIPR layer. Results from US-160 implied that complete bonding was achieved between these layers regardless of tack coat application rate. Overall failure rate in the surface mix overlay was 55%, while 45% of the total failure occurred in HIPR layer material. However, test sections with higher tack coat experienced higher percentage (57%) of failure within the HIPR layer.

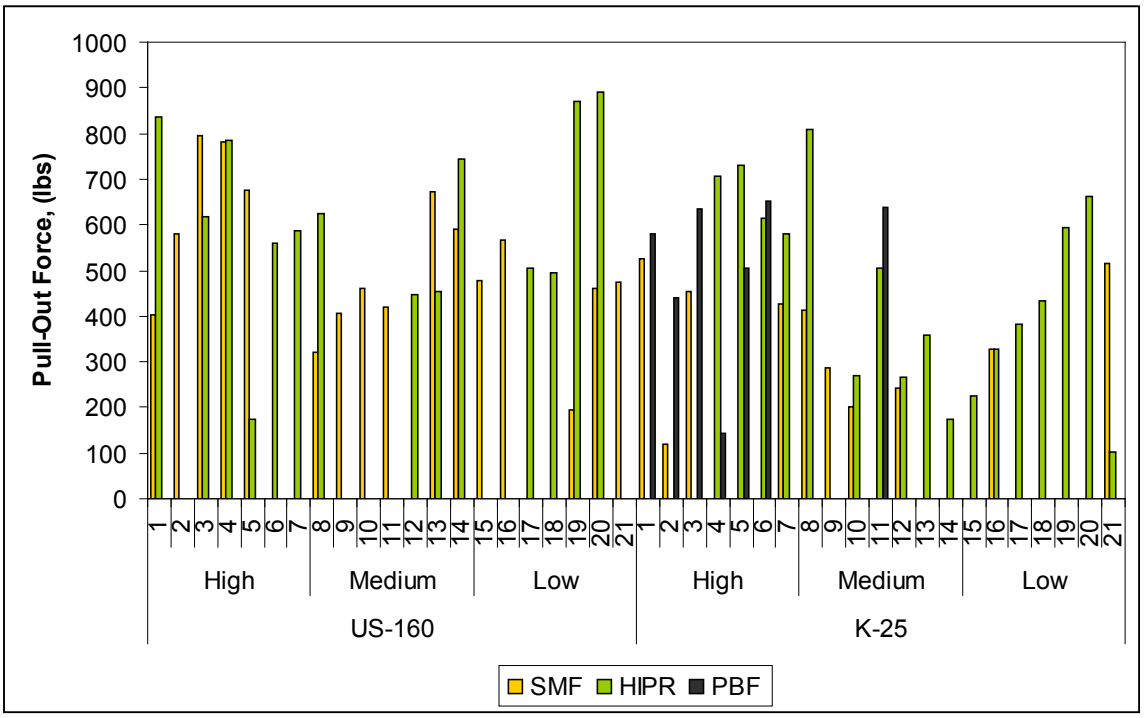

Figure 4.6 Pull-off strength at different tack application rates on US-160 and K-25

On K-25, partial debonding occurred for some cores from the test section with a high residual tack coat application rate, while only one core from the section with a medium tack application rate failed. This finding was notably important as it implied that the high tack application rate might be too high to provide sufficient bond strength for the overlay. Test results showed that the HIPR layer materials were weaker compared to the overlay mixes. Approximately 57% of the total failure occurred in HIPR, 26% failure in surface material, and 17% at the interface of these two. However, 43% of the field cores from the test section with higher tack coat application rate had failed at the layer interface. Another significant finding was that bond strength at the HMA interface was highly dependent on the aggregate source and volumetric mix design of the adjacent layer material.

4.3 Laboratory Mix Design

4.3.1 Aggregate Testing – Fine Aggregate Angularity

Table 4.5 shows the fine aggregate angularity (FAA) of the designed aggregate blend on both US-160 and K-25 projects. According to the KDOT specification for fine mix, the FAA must be higher than 42 for 0.3 to less than 3 millions design ESALs.

Table 4.5 Uncompacted Voids in Aggregate on Both US-160 and K-25

Project	Aggregate Subsets			FAA
	CA1	CA2	NSC	
US-160	32	26	35	42.9
	40	28	25	42.3
	45	33	15	43.3
K-25	30	33	35	42.8
	34	39	25	43.2
	40	43	15	42.8

Table 4.5 shows that all designed aggregate blends satisfy the KDOT specification for FAA. However, there is no significant difference in FAA among the aggregate subsets for both aggregate sources. Twenty percent reduction in natural sand content changed only 0.4% of the uncompacted void mass for the US-160 aggregate source, while no change was observed for the K-25 aggregate source.

4.3.2 Volumetric of Laboratory Mix Design

Table 3.8 in Chapter 3 shows the volumetric properties of the mix designs developed in this study. The designs corresponding to 35% natural sand content are the baseline mixtures from the US-160 and K-25 projects. The mixture characteristics are discussed below.

4.3.2.1 Design Asphalt Content

Design asphalt content (AC) was relatively higher for these mixtures due to a large amount of fine materials. It is to be noted when considering cost-effectiveness of mixtures, this must be taken into account. However, the potential high cost for the asphalt binder would be offset by the relatively low cost of aggregates used in this mixture. In general, the design asphalt content was project-specific and the difference in design asphalt content was insignificant for different sand contents and binder grades (Figure 4.7a). However, the effective asphalt content was significantly lower at lower natural sand contents for both projects. For PG 64-22 binder, it decreased approximately 10% for a 20% decrease in sand content for both projects (Figure 4.7b). However, for higher binder grade (PG 70-22), this change was relatively small.

4.3.2.2 VMA and VFA

The minimum VMA required by KDOT specifications for the SM-4.75A mixture is 16 percent, while 15 percent minimum VMA can be used for rehabilitation (1R or resurfacing) projects. All mix designs developed in this study met the minimum VMA requirements. The percent VMA, in

general, decreased with decreasing sand content with two exceptions. Mix with US-160 aggregates, PG 64-22 binder, and 25% natural sand content had lower VMA compared to the mix with 15% natural sand and the same aggregate and binder combination. However, a K-25 mix with PG 70-22 binder and 25% natural sand had significantly higher percent VMA compared to the mixes with the same binder but with 15% and 35% natural sand (Figure 4.7c). It is well known that the addition of binder in the asphalt mix will decrease VMA until a minimum is reached. Further addition of asphalt binder beyond this limit will begin to push the aggregate structure open, thereby increasing VMA. This may explain why some mixes had slightly higher and lower VMA with decreasing optimum asphalt content at a given N_{des}.

The VFA range currently specified in KDOT specifications for an SM-4.75A mixture is 65 to 78% for design ESALs of 300,000 to less than 3 million. The average VFA for all mix designs passed the required criteria by KDOT. There is no definite trend in change of VFA. Very high VFA (78%) was observed on the K-25 project with 35% natural sand for both binder grades. Lowest VFA (70%) was obtained on K-25 with 25% natural sand and PG 70-22 (Figure 4.7d).

4.3.2.3 $\%G_{mm}$ @ N_{ini} and Dust-to-Binder Ratio

All mixes met the required criteria for relative density at N_{ini} (90.5% max.) specified by KDOT for a design traffic level less than three million ESALs. Figure 4.7e shows that $\%G_{mm}$ @ N_{ini} of the laboratory mixes were project-specific and were somewhat dependent on the natural sand content. As expected, the relative density at N_{ini} slightly decreased with decreasing natural sand content. The effect of binder grade proved to be insignificant for both projects.

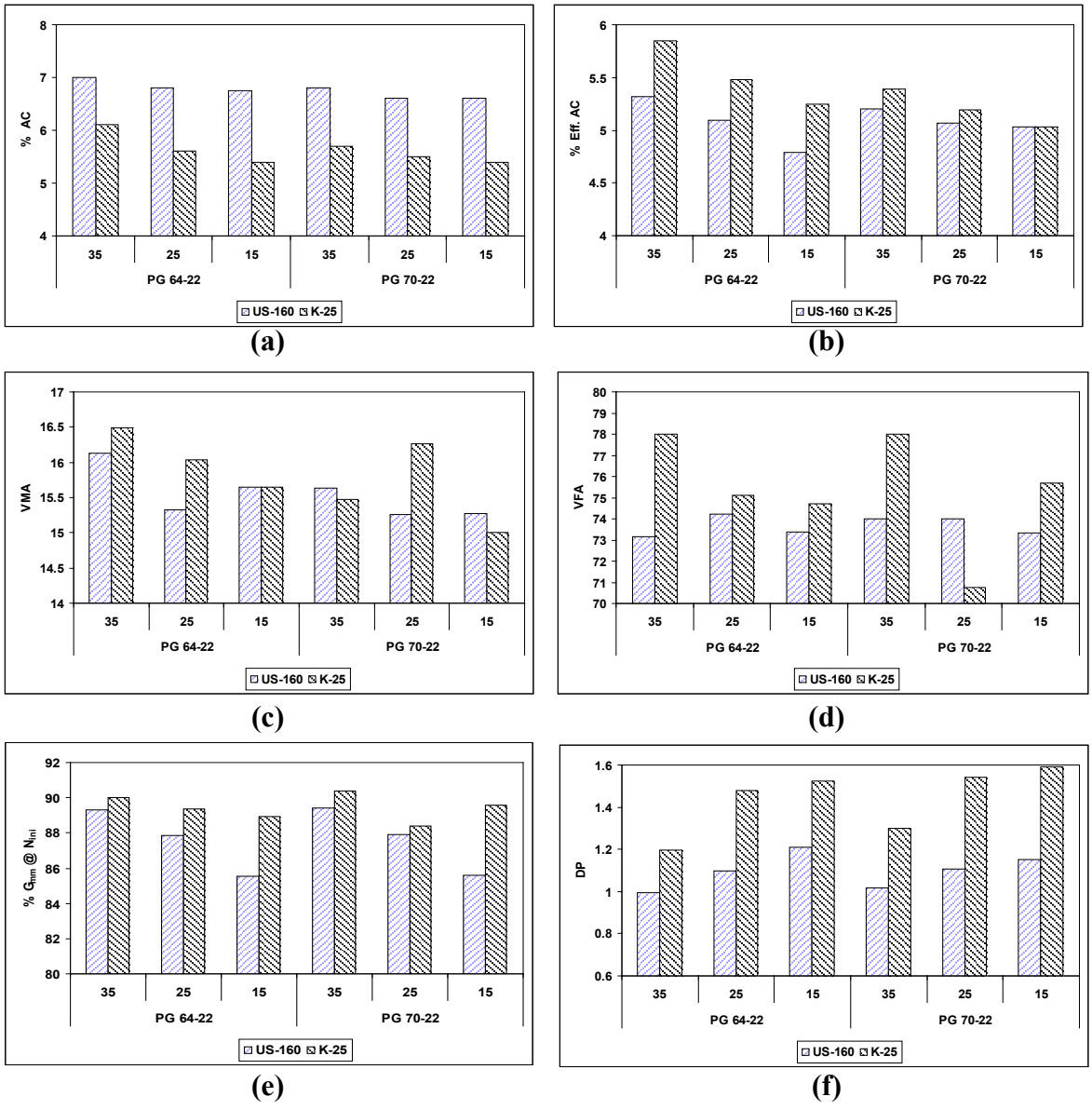

Figure 4.7 Change in volumetric properties (a) % AC, (b) % effective asphalt content, (c) % VMA, (d) %VFA, (e) % G_{mm} @ N_{ini}, and (f) dust-to-binder ratio

Dust-to-binder ratio is determined by dividing the percent materials passing a US No. 200 sieve by the effective asphalt content. The current dust-to-binder ratio or dust proportion specified by KDOT for 4.75-mm NMAS mixtures is 0.9 to 2.0. Mix designs developed in this research study satisfied these requirements. The maximum ratio was 1.58 for the mix with 15%

natural sand and PG 70-22 binder on K-25, while the minimum (0.99) was obtained for the mix with 35% sand content and PG 64-22 binder on US-160. As expected, dust proportion was influenced by the aggregate source and percent natural sand content but not by the binder grade (Figure 4.7f). On the K-25 project, dust proportion increased by 25% when sand content was decreased from 35% to 15%. For the same decrease in sand content, dust-to-binder ratio increased by 17.5% on US-160. In both cases, increase in dust-to-binder ratio was due to lower effective asphalt content.

4.4 Laboratory Mix Performance

4.4.1 Hamburg Wheel Tracking Device Rut Testing

The Hamburg wheel tracking device (HWTD) was used to evaluate rutting and stripping performance of all 12 mixes. Three replicates were produced for a particular mix design to obtain unbiased test results. The specimens had air voids of 7±1% and were tested at 50^0 C. The test was continued until an 0.8-inch (20-mm) rut depth or 20,000 wheel passes, whichever came first. Table 4.6 illustrates the rutting performance of all laboratory 4.75-mm mixtures in terms of number of wheel passes obtained during testing. Again, Figures 4.8, 4.9, 4.10, and 4.11 show the mix performances with respect to HWTD test output parameters such as the average number of wheel passes, creep slope (average no. of wheel pass per mm rut depth), stripping slope (average no. of wheel pass per mm rut depth), and stripping inflection point (number of wheel pass).

Table 4.6 and Figure 4.8 show that natural sand content was an important factor affecting rutting performance of laboratory mixes. In general, the number of wheel passes increased with decreasing natural sand content. Also, mix performance was aggregate-source specific. In most cases, there was no significant difference between the performance of the mixes with 25% and 15% natural sand. Binder grade did not appear to affect the mixture performance appreciably.

The performance of mix with PG 70-22 binder grade on US-160 was notably different than mix with PG 64-22. The number of wheel passes was significantly lower during HWTD testing.

Table 4.6 Hamburg Rutting Performance on US-160 and K-25 Laboratory Mixes

Aggregate Source	PG Binder	NSC[1]	Air Voids (%)	No. of Wheel Pass
US-160	64-22	35	6.2	8,650
		25	6.5	20,000
		15	6.7	20,000
	70-22	35	6.9	6,070
		25	6.8	5,428
		15	6.9	11,600
	64-22	35	6.9	8,500
		25	6.3	20,000
		15	6.5	15,750
	70-22	35	6.9	5,950
		25	6.6	6,200
		15	6.4	7,950
	64-22	35	6.8	4,600
		25	6.4	20,000
		15	6.8	16,450
	70-22	35	6.7	5,750
		25	6.9	7,550
		15	6.7	7,950
K-25	64-22	35	7.7	5,870
		25	7.3	15,350
		15	6.5	20,000
	70-22	35	7.1	18,200
		25	7.1	17,950
		15	6.8	20,000
	64-22	35	7.2	19,950
		25	7.1	13,450
		15	6.7	20,000
	70-22	35	7.2	10,160
		25	6.9	20,000
		15	6.9	20,000
	64-22	35	7.8	20,000
		25	6.8	17,890
		15	6.8	18,850
	70-22	35	6.1	11,700
		25	6.3	20,000
		15	6.9	20,000

Note: [1] = Natural (River) Sand Content

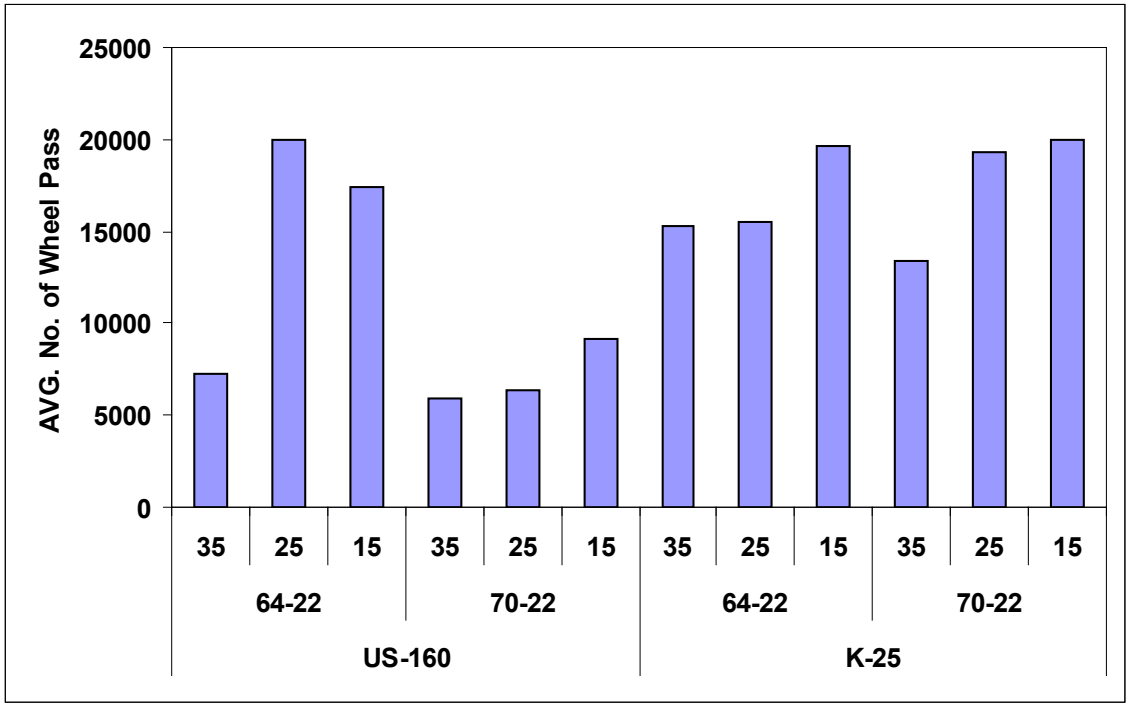

Figure 4.8 Average no. of wheel passes of 4.75-mm NMAS laboratory mixes

When other output parameters such as creep slope, stripping inflection point (SIP), and stripping slope are considered, the laboratory mixes with lower sand content performed better compared to the mixes with 35% natural sand. Higher binder grade (PG 70-22) with 25% and 15% natural sand performed relatively well on the K-25 mixes, while an opposite trend was observed in the US-160 mixes in the pure rutting phase (Figure 4.9). Higher binder grade with liquid amine (anti-strip agent) was further investigated to identify the potential cause of poor performance.

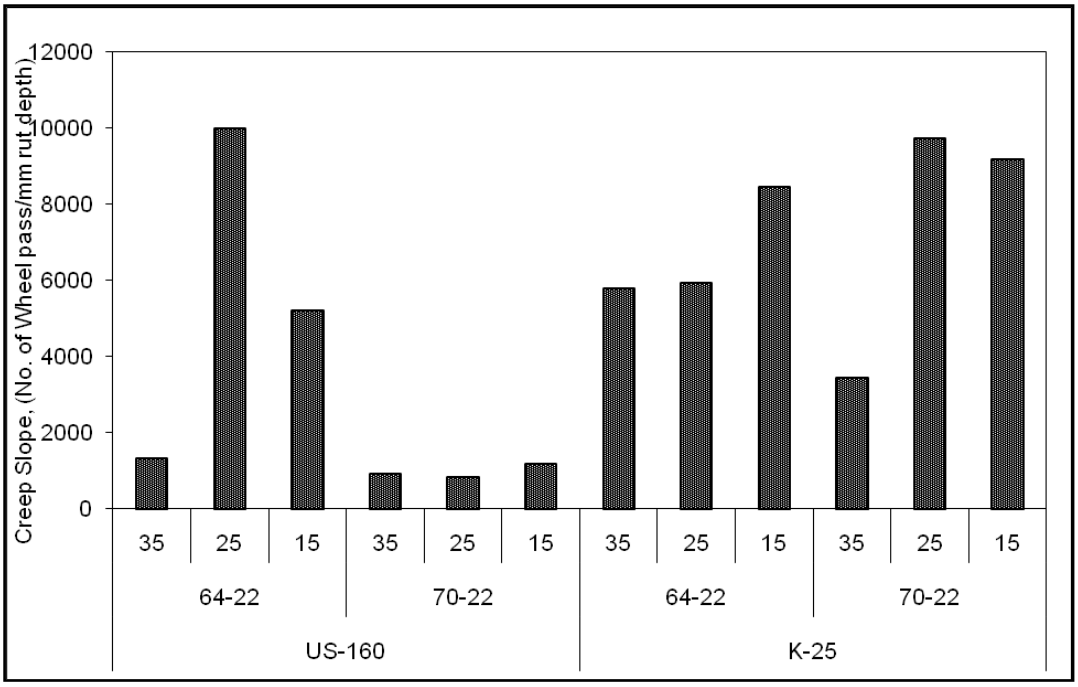

Figure 4.9 Change in creep slope at different river sand content and binder grade

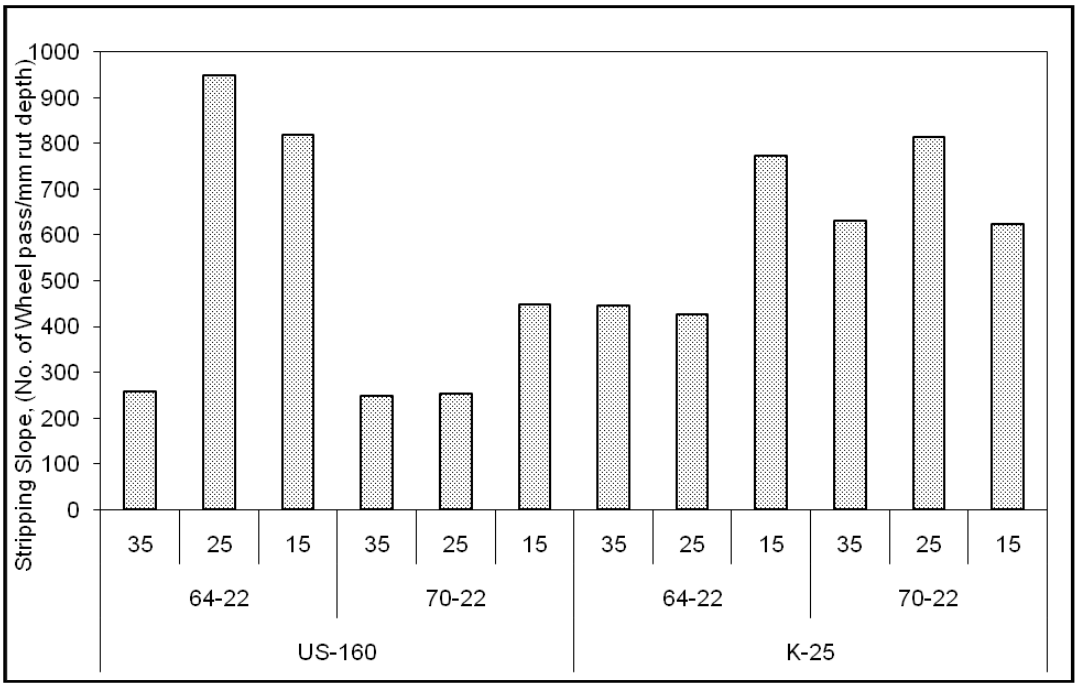

Figure 4.10 Change in stripping slope at different sand content and binder grade

As expected, stripping slope was significantly higher in the US-160 mixes with lower sand content and binder grade (Figure 4.10). Number of wheel passes per mm rut depth of mixes with PG 64-22 increased almost 68-73% with decreasing sand content from 35 to 15%, while 44% was observed with higher binder grade. On K-25, mixes with PG 64-22 and PG 70-22 had 42% and 23% higher number of wheel passes per mm rut depth, respectively. Figure 4.11 illustrates that stripping inflection point for a particular mix was highly aggregate-source specific. Better aggregate structure may help the mix to start stripping action later. Most of the K-25 mixes experienced delayed stripping distress compared to the US-160 mixes. Among all laboratory mixes, the K-25 mix with PG 70-22 and 15% to 25% sand content had allowed the major number of wheel passes before the stripping action began. The average number of wheel passes increased more than 50% compared to the mix with 35% river sand.

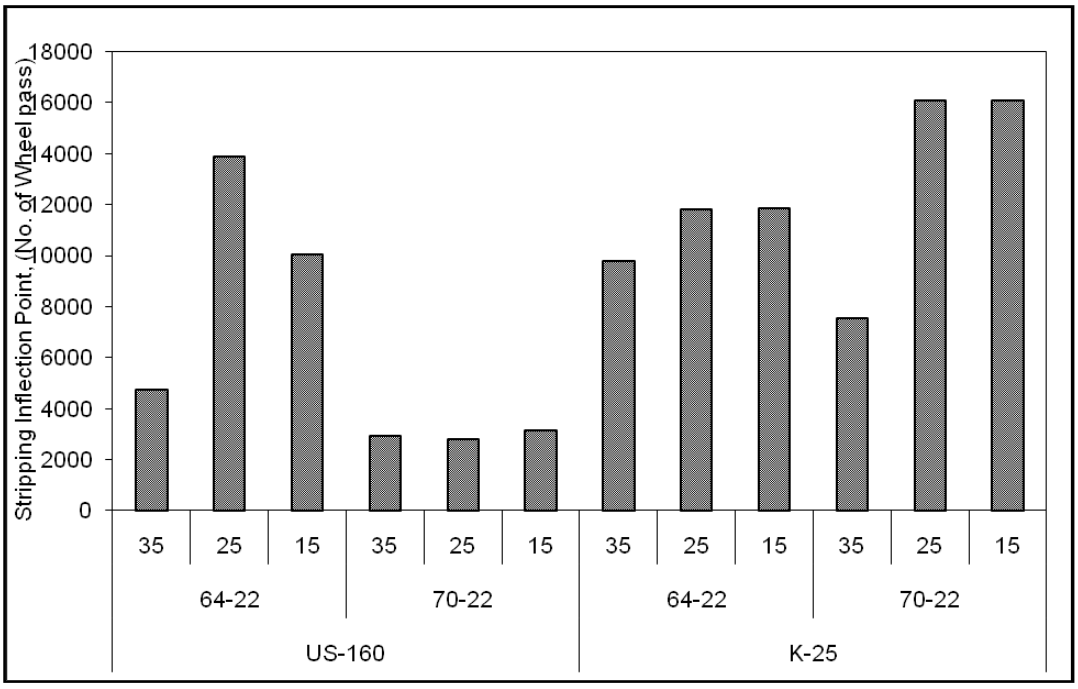

Figure 4.11 Stripping inflection point at different sand content and binder grade

Further investigation performed to evaluate the effect of an anti-stripping agent on a 70-22 binder grade is shown in Table 4.7. From the table, it is obvious that the anti-stripping agent did not have any significant effect on the binder properties except on long-term aging performance. The stiffness of the binder reduced almost 50% after adding the liquid amine. The test results also proved that the original binder PG 70-22 was not acid-modified.

Table 4.7 Verification of Binder Grade With/Without Anti-Stripping Agent

Binder Grade	Original Binder	RTFO[1]	PAV[2]		Binder Grade (after aging)
	$G^*/\sin\delta$ kPa[3]	$G^*/\sin\delta$ kPa[3]	$G^* \times \sin\delta$ kPa[3]	m @-12^0 C	
PG 70-22 (without anti-stripping)	1.12	2.64	2965	0.324	70-25
PG 70-22 (with anti-stripping)	1.18	2.66	1543	0.385	71-28

[1] RTFO = Rolling Thin Film Oven; [2] PAV = Pressure Aging Vessel; [3] 1 kPa = 0.145 psi

Another observation on the HWTD performance curves showed that stripping started early for the mixes with PG 70-22 compared to the mix with PG 64-22 for the US-160 project, while this trend was completely opposite in the K-25 mixes. With lower natural sand content (25% and 15%), the changes in SIP were almost 80% and 69%, respectively (Figure 4.12).

Figure 4.13 shows binder grade PG 70-22 had improved the rutting performance more than 25% compared to PG 64-22 on K-25. Based on laboratory test results, it is quite obvious that the binder grade PG 70-22 on US-160 was not affected by the liquid amine in short-term aging. Again, the dust content in the aggregate blend had increased with decreasing natural sand content (Figure 4.7f). Hence, further research is suggested here to investigate any chemical reaction between dust particles and higher binder grade in the presence of a liquid anti-stripping agent.

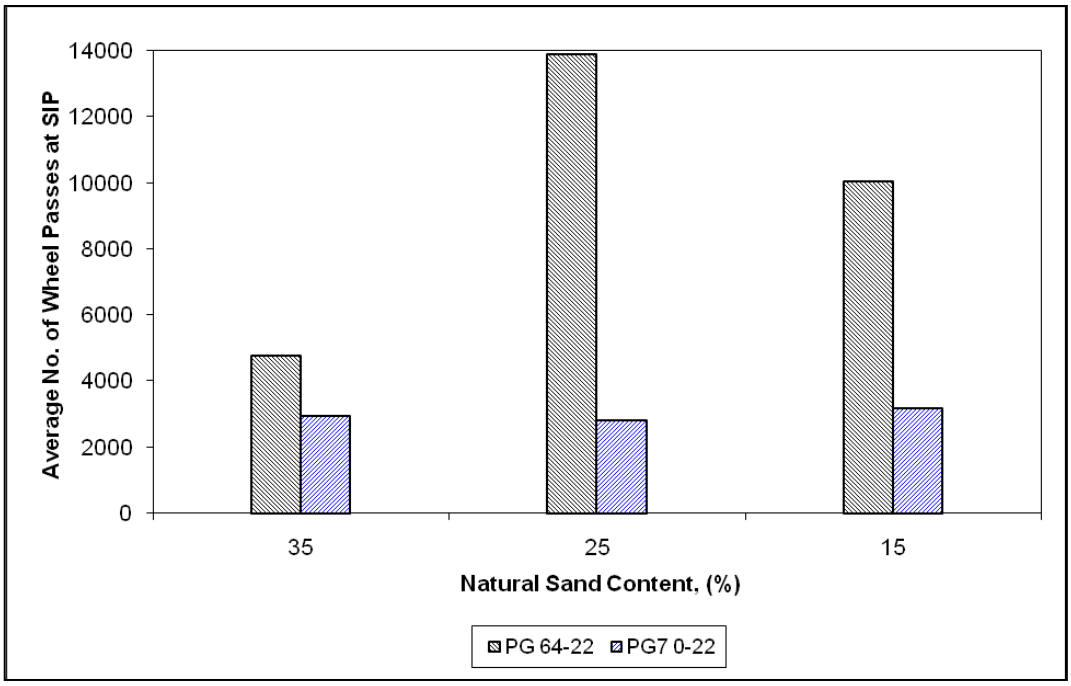

Figure 4.12 Mixture performance based on stripping inflection point on US-160

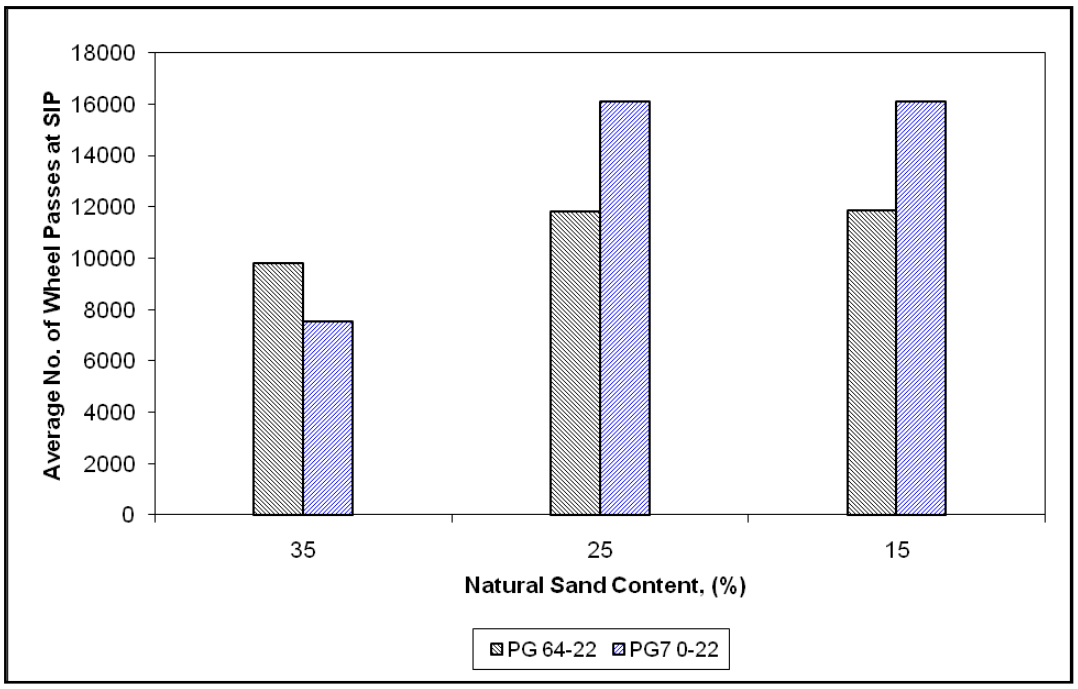

Figure 4.13 Mixture performance based on stripping inflection point on K-25

4.4.2 Tensile Strength Ratio

For all 12 mixes designed in the laboratory, tensile strength ratio (TSR) was determined as per KT-56. For this test, specimens were compacted at 7±0.5% air voids. Six samples were compacted for a particular mix design: three samples were conditioned (freeze/thaw) and three were unconditioned. All six were tested for tensile strength in indirect tension mode. The ratio of the average tensile strength of the conditioned to that of the unconditioned samples was considered as the performance measure during testing.

Figure 4.14 shows a plot of TSR and comparison of dry and wet tensile strength for all 12 mixes. In general, mixes with the anti-stripping agent (as on US-160) had higher TSR values compared to mixes with no anti-stripping agent (as on K-25). All mixes on US-160 passed the minimum TSR requirements specified by KDOT with the exception of the mix with 15% natural sand and PG 64-22 binder. The average TSR for mixes with PG 64-22 binder on US-160 was 91%, while an average of 92% was achieved for mixes with PG 70-22. This implies that the effectiveness of an anti-stripping agent depends on binder grade and aggregate source. Fifty percent of the design mixes on K-25 failed to meet the required TSR criteria. The average TSR on K-25 ranged from a minimum of 73% to a maximum of 81% for the mixes with PG 64-22 binder, and a minimum of 74% to a maximum of 82% for the mixes with PG 70-22 binder. Although the dry and wet strength of mixes on K-25 were significantly higher than those of US-160, their ratio failed to meet the minimum TSR requirement.

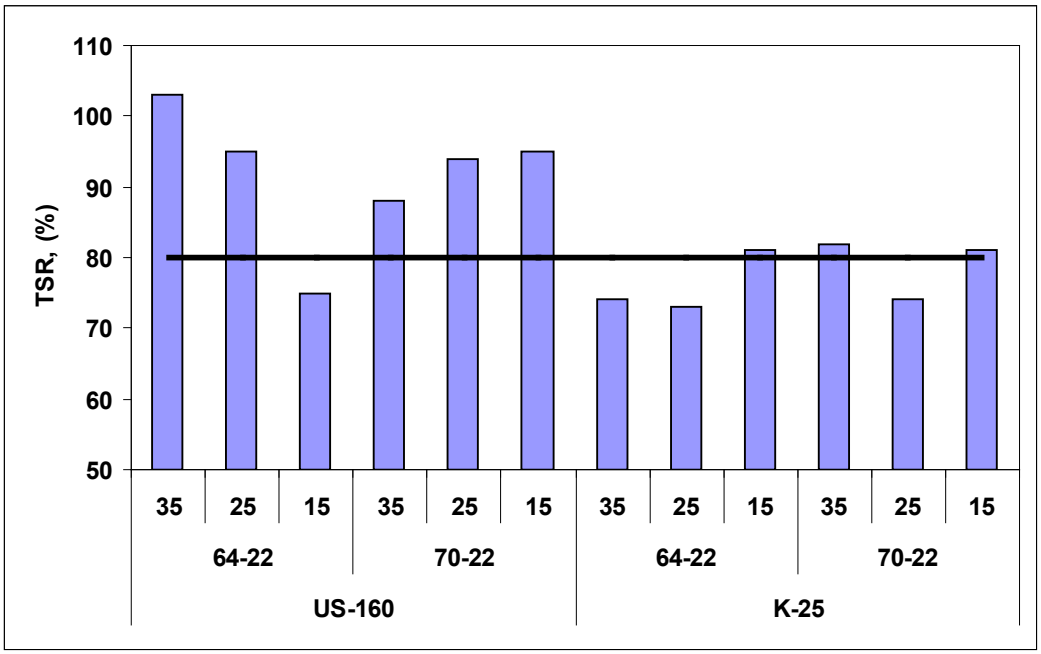

(a)

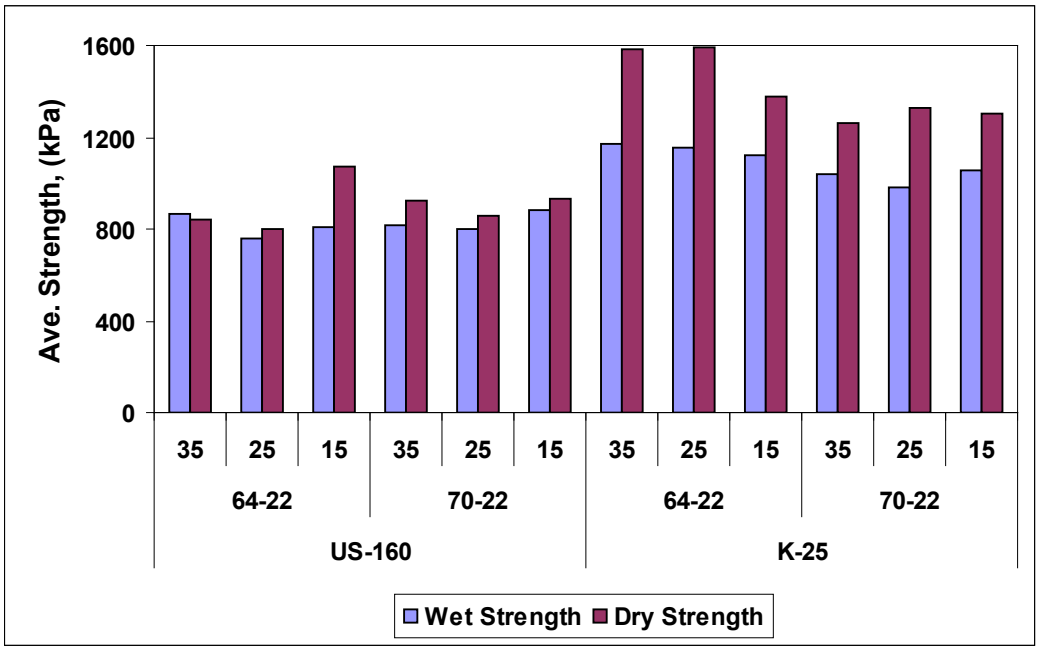

(b)

Figure 4.14 (a) Tensile strength ratios (b) dry and wet strength of 12 mixes on US-160 and K-25 projects

In general, mixes with the anti-stripping agent (as on US-160) had higher TSR values compared to mixes with no anti-stripping agent (as on K-25). All mixes on US-160 passed the

minimum TSR requirements specified by KDOT with the exception of the mix with 15% natural sand and PG 64-22 binder. The average TSR for mixes with PG 64-22 binder on US-160 was 91%, while an average of 92% was achieved for mixes with PG 70-22. This implies that the effectiveness of an anti-stripping agent depends on binder grade. Fifty percent of the design mixes on K-25 failed to meet the required TSR criteria. The average TSR on K-25 ranged from a minimum of 73% to a maximum of 81% for the mixes with PG 64-22 binder, and a minimum of 74% to a maximum of 82% for the mixes with PG 70-22 binder. Although the dry and wet tensile strength of mixes on K-25 were significantly higher than those of US-160, their ratio failed to meet the minimum TSR requirement.

4.4.3 Beam Fatigue Testing

The AASHTO T321-03 test procedure was followed to determine the change in flexural stiffness of the laboratory-designed 4.75-mm mixtures. For this test, specimens were compacted at 7±0.5% air voids. Twelve slabs were compacted for a particular mix design: two beams were cut from each slab. All beams were tested for flexural stiffness in a two-point loading arrangement in a conditioned chamber at 300 micro-strain. The change between the initial flexural stiffness (at 50 cycles) and final stiffness (at 2×10^6 cycles) was considered as the performance measure during testing.

Tables 4.8 and Table 4.9 and Figure 4.15 show the test results and change in fatigue strength for all 12 mixes.

Table 4.8 Fatigue Strength Test on US-160 Laboratory Mixes

Aggregate Source	Binder Grade	NSC	Cycle	Initial Flexural Stiffness, MPa	Final Flexural Stiffness, MPa	% Changes in Flexural Stiffness
US-160	64-22	35	50	3411		
			2×10^6		2647	22
			50	3794		
			2×10^6		2771	27
		25	50	3799		
			2×10^6		2567	32
			50	4199		
			2×10^6		2520	40
		15	50	3943		
			2×10^6		2485	37
			50	4039		
			2×10^6		2634	35
	70-22	35	50	3988		
			2×10^6		2927	27
			50	3848		
			2×10^6		2760	28
		25	50	4548		
			2×10^6		3460	24
			50	5299		
			2×10^6		3609	32
		15	50	3839		
			2×10^6		2950	23
			50	4225		
			2×10^6		3003	29

Table 4.9 Fatigue Strength Test on K-25 Laboratory Mixes

Aggregate Source	Binder Grade	NSC	Cycle	Initial Flexural Stiffness, MPa	Final Flexural Stiffness, MPa	% Changes in Flexural Stiffness
K-25	64-22	35	50	4751		
			2×10^6		3554	25
			50	4756		
			2×10^6		3561	25
		25	50	5145		
			2×10^6		3547	31
			50	4582		
			2×10^6		3116	32
		15	50	5196		
			2×10^6		3120	40
			50	5275		
			2×10^6		3442	35
	70-22	35	50	5737		
			2×10^6		4029	30
			50	4058		
			2×10^6		2821	30
		25	50	4890		
			2×10^6		3535	28
			50	5315		
			2×10^6		3650	31
		15	50	4726		
			2×10^6		3253	31
			50	4728		
			2×10^6		3267	31

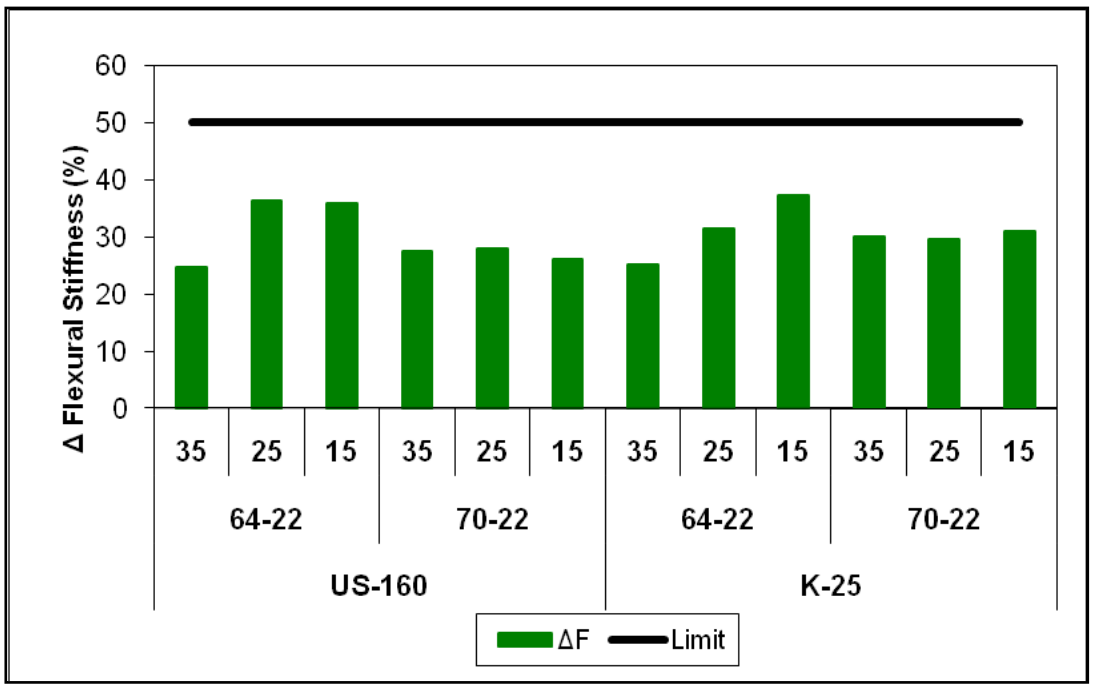

Figure 4.15 Fatigue performance of laboratory-designed mix on US-160 and K-25

Tables 4.8 and 4.9 show that laboratory-designed mixes on US-160 and K-25 passed the test criterion set by AASHTO 321-03 test procedure in beam fatigue testing. The percent change in initial and final stiffness for all mixes was less than 50% at 2 million cycles. Figure 4.15 shows that the change in initial stiffness increased with decreasing natural sand content for mixes with lower binder grade (PG 64-22) on both US-160 and K-25 at 20^0 C and 300 με. The changes were 33% and 31% for the US-160 and K-25 mixes, respectively. However, at a higher binder grade, the change in initial stiffness was almost constant, regardless of the percent of natural sand content in the mixture. This finding is significant because the results indicate that the fatigue strength of the tender mix can be improved by using a higher binder grade.

CHAPTER 5 - STATISTICAL ANALYSIS AND OPTIMIZATION

5.1 General

In general, there are two aspects to any experimental problem. One is design of the experiment and the other is statistical analysis of the experimental data. These two approaches are closely related, since the method of analysis depends directly on the design employed (Montgomery 1997). During this research study, the statistical design of the experiment (Section 3.2) was developed to plan the experiments and hence, collect the appropriate data for statistical analysis. The statistical approach to experimental design is necessary when the problems involve data that are subject to experimental errors and valid and objective conclusions are in demand. Results and conclusions from the statistical approach are objective rather than judgmental in nature. However, statistical methods cannot prove that a factor/factors has a particular effect, but rather provides guidelines for the reliability and validity of the test results and attaches a level of confidence to the statement/conclusions. The following articles in this chapter discuss the techniques used in analyzing the experimental data and significant statistical findings, the regression analysis of the designed experiment and performance equations developed, and finally, the optimized design process to identify the most effective mix design combinations, those capable of addressing the major distresses common to Kansas highways.

5.2 Statistical Analysis of Laboratory Mixes

The statistical analysis software package SAS was used to conduct both analysis of variance (ANOVA) and multivariate analysis of variance (MANOVA) to indentify the most significant mix design factors. Design factors in this study were aggregate source, binder grade, and natural sand content. The multivariate general linear model can be written as equation (5.1):

$$[Y]_{n\times d} = [X]_{n\times m}[\beta]_{m\times d} + \varepsilon_{n\times d} \quad (5.1)$$

where,

Y = matrix with series of multivariate measurements;

X = design matrix with independent variables;

β = parameters matrix; and

e = error matrix.

Hypothesis testing with a general linear model can be made either as a multivariate or as several independent univariate tests (UCLA 2010). In multivariate tests, response in the column matrix Y are modeled simultaneously, while in univariate tests, the responses are modeled separately. During the research study, volumetric mix design parameters such as percent of design asphalt content, VMA, VFA, percent G_{mm} at N_{ini}, percent of free asphalt, and dust-to-binder ratio were considered as the multivariate measurements or dependent variables. ANOVA and MANOVA were also conducted to test the interactions among the design factors at the α = 0.05 level.

5.2.1 Analysis of Variance

The general linear model in ANOVA can be written as the multiple linear regression equation (Equation 5.2). The equation predicts the response as a linear function of the estimated parameters and design factors.

$$Y_i = \beta_0 X_{i0} + \beta_1 X_{i1} + \beta_2 X_{i2} + ... + \beta_k X_{ik} + e_i \quad (5.2)$$

$$i = 1,2,3,.....,n$$

where,

Y_i = response variable for the *i*th observation;

β_k = unknown parameters to be estimated; and

X_{ij} = design factors.

The simplest form of general linear model in ANOVA is to fit a single mean to all observations or dependent variables (Equation 5.3). In this linear form, there is only one parameter β_0 and one design factor X_{i0}. The indicator or design factor always has the value of 1 in the simplest form of linear model.

$$Y_i = \beta_0 X_{i0} + e_i \tag{5.3}$$

The ordinary least-square (OLS) estimation of β_0, $\left(\hat{\beta}_0\right)$ is the mean of Y_i. All larger and complex models can be compared to this simple linear model, where β_0 is usually referred to as the intercept (Weisberg 2005).

Interaction or combination of design factors is often useful in statistical analysis. Interaction variables are often included in the mean function, along with other design factors, to allow the joint effect of two or more variables. When there are more than two independent variables, several interaction variables are introduced by using a pairwise-product in the regression equation. Before introducing the "interaction variable" term in the mean function, it is important to distinguish between qualitative and quantitative interaction variables. In the present study, the design factors aggregate source and binder grade are qualitative and natural sand content is a quantitative variable. Statistically, ANOVA is a more effective method to deal with the interacting variables, which are categorical rather than the real numbers. The following Equation (5.4) represents the ANOVA model used in the statistical analysis. The general assumptions of ANOVA were the model was independent, the errors were normally distributed, and the variance was constant. The residual plots of ANOVA are attached in Appendix C.

$$[Y]_{ijkl} = \mu + (agg)_i + (PG)_j + (NSC)_k + (agg \times PG)_{ij} + (PG \times NSC)_{jk} + (NSC \times agg)_{ki} + \varepsilon_{ijkl} \tag{5.4}$$

where, $[Y]_{ijkl}$ = response variables studied,

μ = overall mean,

$[Agg]_i$ = i^{th} aggregate source,

$[PG]_j$ = j^{th} PG binder grade,

$[NSC]_k$ = k^{th} natural sand content,

$[Agg]_i \times [PG]_j$ = interaction between i^{th} aggregate source and j^{th} PG binder grade,

$[PG]_j \times [NSC]_k$ = interaction between j^{th} PG binder grade and k^{th} sand content,

$[NSC]_k \times [Agg]_i$ = interaction between i^{th} aggregate source and k^{th} sand content, and

ε_{ijkl} = error term.

Table 5.1 shows the results of ANOVA of different mix volumetric and other properties. The variables were statistically analyzed with the level of significance at 5%. The p-value was set to a measure of extent to decide which design factors and interaction variables contradict with the defined null hypothesis (H_0). The smaller p-value signified the higher probability of rejecting the null hypothesis. Effective asphalt content of the design mix is significantly affected by the aggregate source, binder grade, and natural sand content, while aggregate source was the only influential factor for the design asphalt content. Interaction between aggregate sources and binder grade also affected the effective asphalt content. Based on the p-value (= 0.0095), aggregate source had the largest influence on effective asphalt followed by natural sand content (p-value = 0.0129) and binder grade (p-value = 0.0239). None of these design factors and interactions among them proved to be statistically significant at a 95% confidence level for VMA and VFA. As expected, the initial relative density was influenced by the aggregate source and percent natural sand used in the mixes. The highest effect was for aggregate source (p-value = 0.027), followed by percentage of natural sand (p-value = 0.05).

Table 5.1 Results of ANOVA

Parameter	Source	DF	R^2	p-value	Significant @ α = 0.05
Design Asphalt content	AGG[1]	1	0.9959	0.0023	Y
	PG[2]	1		0.0852	N
	NSC[3]	2		0.0589	N
	AGG*PG	1		0.8928	N
	PG*NSC	2		0.4057	N
	AGG*NSC	2		0.3209	N
VMA	AGG[1]	1	0.9623	0.1478	N
	PG[2]	1		0.0832	N
	NSC[3]	2		0.1291	N
	AGG*PG	1		0.5318	N
	PG*NSC	2		0.1868	N
	AGG*NSC	2		0.1383	N
VFA	AGG[1]	1	0.9359	0.1341	N
	PG[2]	1		0.4988	N
	NSC[3]	2		0.2061	N
	AGG*PG	1		0.3938	N
	PG*NSC	2		0.4354	N
	AGG*NSC	2		0.1528	N
% G_{mm} @ N_{ini}	AGG[1]	1	0.9779	0.027	Y
	PG[2]	1		0.7292	N
	NSC[3]	2		0.0516	Y
	AGG*PG	1		0.7555	N
	PG*NSC	2		0.7843	N
	AGG*NSC	2		0.1136	N
Effective Asphalt Content	AGG[1]	1	0.9943	0.0095	Y
	PG[2]	1		0.0343	Y
	NSC[3]	2		0.0129	Y
	AGG*PG	1		0.0239	Y
	PG*NSC	2		0.0881	N
	AGG*NSC	2		0.3272	N
Dust-to-Binder Ratio	AGG[1]	1	0.9989	0.0008	Y
	PG[2]	1		0.0716	N
	NSC[3]	2		0.0042	Y
	AGG*PG	1		0.0448	Y
	PG*NSC	2		0.2268	N
	AGG*NSC	2		0.0326	Y

[1]=Aggregate; [2]=Binder grade; [3]=Natural sand content

Two design factors considered during ANOVA had significant influence on the dust-to-binder ratio. Aggregate source (p-value = 0.0008) was the most influential factor followed by natural

sand content (p-value = 0.0042). The interaction between aggregate source and binder, as well as that between aggregate source and natural sand content were also statistically significant.

5.2.2 Multivariate Analysis of Variance

Multivariate analysis of variance is a generalized form of univariate analysis of variance. In the present study, more than two response variables were selected and hence, MANOVA was performed to identify whether any change in design factors had significant effects on response variables (UCLA 2010, Bruin 2010). MANOVA was carried out by proc REG. The MANOVA model used in the present study is presented in the equation (5.5).

$$\begin{bmatrix} \%AC \\ \%VMA \\ \%VFA \\ \%G_{mm}@N_{ini} \\ \%EffAC \\ Dust-to-binderRatio \end{bmatrix} = \begin{bmatrix} agg \\ PG \\ NSC \\ agg \times PG \\ PG \times NSC \\ NSC \times agg \end{bmatrix} \times [\beta_i] + \varepsilon \qquad (5.5)$$

where,

$\begin{bmatrix} \%AC \\ \%VMA \\ \%VFA \\ \%G_{mm}@N_{ini} \\ \%EffAC \\ Dust-to-binderRatio \end{bmatrix}$ = response, n×d matrix with d dimensional response vector

$\begin{bmatrix} agg \\ PG \\ NSC \\ agg \times PG \\ PG \times NSC \\ NSC \times agg \end{bmatrix}$ = n×q matrix of known design factors

$$[\beta_i] = \text{q×d matrix of unknown parameters} = \begin{bmatrix} \beta_{01} & \beta_{02} & ..... & \beta_{0d} \\ \beta_{11} & \beta_{12} & ..... & \beta_{1d} \\ . & . & . & . \\ . & . & . & . \\ \beta_{q1} & \beta_{q2} & ..... & \beta_{qd} \end{bmatrix}$$

ε = error n×d matrix

The null hypothesis in MANOVA tests the overall hypothesis of no difference in the means for the different groups. In present study, means of six response variables were tested simultaneously considering three design factors and their interactions. The null hypothesis of MANOVA can be written as:

$$H_0 : \begin{bmatrix} \beta_{11} & \beta_{12} & ..... & \beta_{1d} \\ . & . & . & . \\ . & . & . & . \\ \beta_{q1} & \beta_{q2} & ..... & \beta_{qd} \end{bmatrix} = 0$$

The output of MANOVA analysis is presented in Table 5.2. The table shows the MANOVA test statistics and F approximations to test the null hypothesis that the design factors (aggregate source, binder grade and sand content) did not have an overall effect on response variables.

Table 5.2 MANOVA Statistics and F Approximations

Statistics	Value	F Value	DF	p-value > F
Wilks' Lamda[2]	0.00008436	13.24	18	0.0002
Pillai's Trace	2.53657669	4.56	18	0.0024
Hotelling-Lawley Trace	277.30195843	61.62	18	0.0051
Roy's Greatest Root[1]	258.29179012	215.24	6	<0.0001

Note: [1] = F statistics for Roy's greatest root is an upper bound
[2] = F statistics for Wilks' Lamda is exact

MANOVA statistics were calculated from the characteristics roots which are the Eigen values of the product of the sum square matrix of the hypothesis (H) and inverse of the sum square matrix of residual (E^{-1}) . F values are F-statistics for the known design factors and test statistics. The null hypothesis of MANOVA analysis was evaluated with respect to the p-values obtained from different MANOVA statistics. The p-values from the table strongly reject the null hypothesis and hence suggest that the selected design factors have significant effect on the mix design volumetric. In addition, univariate outputs from MANOVA were similar to the ANOVA presented in Table 5.1.

5.2.3 Effect of Significant Parameter on Laboratory Mix Performance

Regression analysis using the statistical software SAS showed that the dust-to-binder ratio was the most significant mixture parameter influencing mix performance in HWTD rutting and KT-56 moisture sensitivity tests. Figure 5.1 shows the plot of performance of laboratory mixes versus dust-to-binder ratio.

Figure 5.1(a) shows that the number of wheel passes at the stripping inflection point increases linearly with increasing dust-to-binder ratio for all laboratory mixes. Analysis of HWTD test performance curves showed that pure rutting performance (number of wheel passes just before stripping started) improves with decreasing natural sand content (which in turn, increases the dust proportion). However, TSR obtained in the moisture sensitivity tests was inversely proportional to the dust-to-binder ratio (Figure 5.1b). Thus, it is obvious from these results that the dust-to-binder ratio of the design mix should be selected in a narrow range so that optimum rutting performance and lower moisture susceptibility are obtained. This may indicate the need for further refinement of dust-to-binder ratio range specified by AASHTO for 4.75-mm NMAS Superpave mixture.

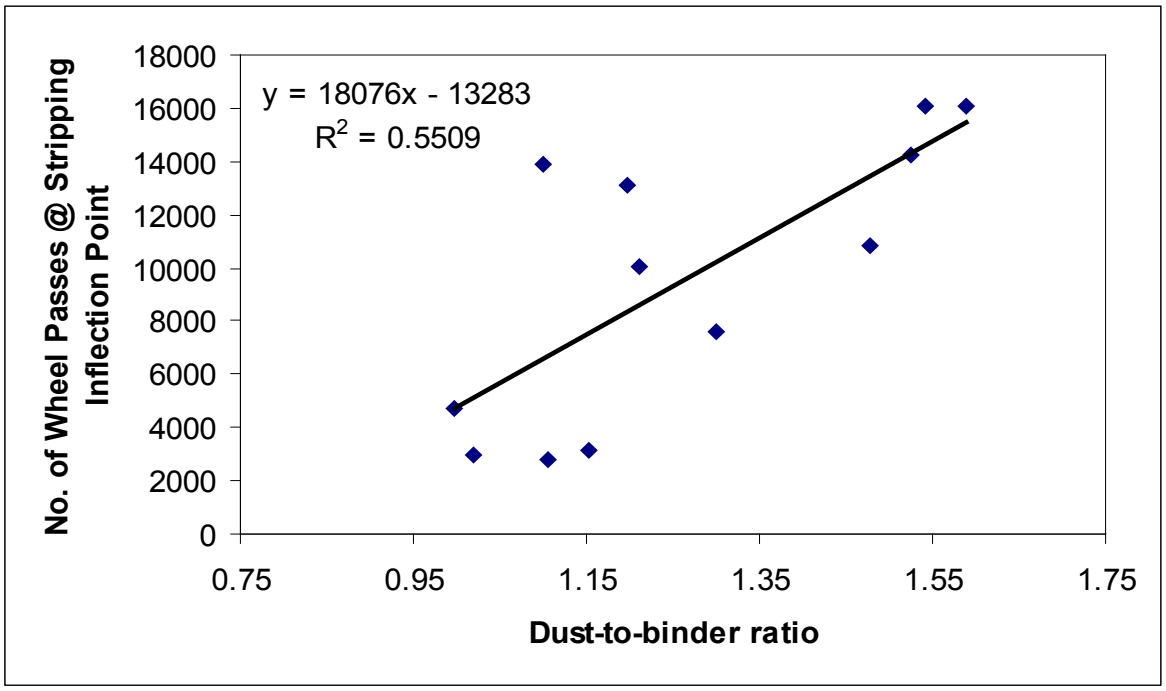

(a)

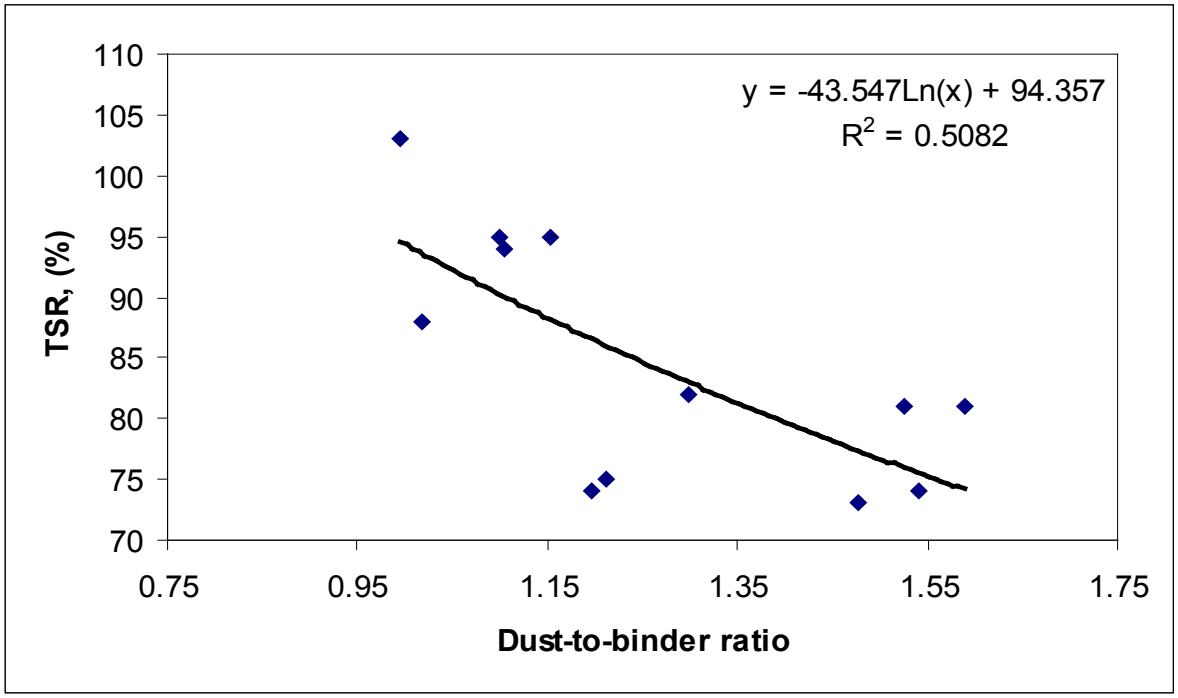

(b)

Figure 5.1 Laboratory mix performance versus dust-to-binder ratio

5.3 Regression Analysis of Mix Performance

Regression analysis is a statistical technique of modeling dependency between a response variable and one or more independent variables (Weisberg 2005). During analysis, the estimated variable is the function of the predictors called the independent variables. The goal of regression analysis of the present study is to develop the regression functions/ equations for laboratory-designed mixtures based on the performance test results and hence, to predict the distresses at different design factors. Similar to ANOVA, the aggregate source, binder grade, and natural sand content are considered as independent variables in regression functions. The number of wheels passes, tensile strength ratio, and change in initial flexural stiffness are considered as the response variables obtained from HWTD rut test, moisture sensitivity test, and fatigue test data, respectively. The following sections illustrate the regression equations obtained from the laboratory performance tests.

5.3.1 Rutting Prediction Equation

The rutting regression function was developed based on Hamburg wheel tracking device test data. Laboratory mix performance is expressed as the total number of wheel passes needed to satisfy the Tex-242 test criteria. Number of wheel passes (NWP) is always considered as the response variable. Tables 5.3 and 5.4 show the independent variables considered during analysis. The following two steps are accounted to achieve the rutting prediction equations.

Table 5.3 Variables in Regression Equation on US-160 Mix Analysis

	Independent Variables					Response Variable
Project	**Aggregate Type**				**Binder Grade**	**NWP**
US-160	Coarse Aggregate, **(CA1)**	32	40	45	64-22 (0)	8,650
	Screening Material, **(CA2)**	26	28	33		20,000
	Natural Sand Content, (NSC)	35	25	15		20,000
	Coarse Aggregate, **(CA1)**	32	40	45	70-22 (1)	6,070
	Screening Material, **(CA2)**	26	28	33		5,428
	Natural Sand Content, (NSC)	35	25	15		11,600
	Coarse Aggregate, **(CA1)**	32	40	45	64-22 (0)	8,500
	Screening Material, **(CA2)**	26	28	33		20,000
	Natural Sand Content, (NSC)	35	25	15		15,750
	Coarse Aggregate, **(CA1)**	32	40	45	70-22 (1)	5,950
	Screening Material, **(CA2)**	26	28	33		6,200
	Natural Sand Content, (NSC)	35	25	15		7,950
	Coarse Aggregate, **(CA1)**	32	40	45	64-22 (0)	4,600
	Screening Material, **(CA2)**	26	28	33		20,000
	Natural Sand Content, (NSC)	35	25	15		16,450
	Coarse Aggregate, **(CA1)**	32	40	45	70-22 (1)	5,750
	Screening Material, **(CA2)**	26	28	33		7,550
	Natural Sand Content, (NSC)	35	25	15		7,950

Note: **Reference Table 3.10 and Table 3.11**

Table 5.4 Variables in Regression Equation on K-25 Mix Analysis

	Independent Variables					Response Variable
Project	**Aggregate Type**				**Binder Grade**	**NWP**
K-25	Coarse Aggregate, **(CA1)**	30	34	40	64-22 (0)	5,870
	Screening Material, **(CA2)**	33	39	43		15,350
	Natural Sand Content, (NSC)	35	25	15		20,000
	Coarse Aggregate, **(CA1)**	30	34	40	70-22 (1)	18,200
	Screening Material, **(CA2)**	33	39	43		17,950
	Natural Sand Content, (NSC)	35	25	15		20,000
	Coarse Aggregate, **(CA1)**	30	34	40	64-22 (0)	19,950
	Screening Material, **(CA2)**	33	39	43		13,450
	Natural Sand Content, (NSC)	35	25	15		20,000
	Coarse Aggregate, **(CA1)**	30	34	40	70-22 (1)	10,160
	Screening Material, **(CA2)**	33	39	43		20,000
	Natural Sand Content, (NSC)	35	25	15		20,000
	Coarse Aggregate, **(CA1)**	30	34	40	64-22 (0)	20,000
	Screening Material, **(CA2)**	33	39	43		17,890
	Natural Sand Content, (NSC)	35	25	15		18,850
	Coarse Aggregate, **(CA1)**	30	34	40	70-22 (1)	11,700
	Screening Material, **(CA2)**	33	39	43		20,000
	Natural Sand Content, (NSC)	35	25	15		20,000

Note: **Reference Table 3.10 and Table 3.11**

5.3.1.1 Step 1 - Variable Selection

A variable selection method was used to identify the influential design factors to be considered in the regression equation. The goal of variable selection was to divide available design factors into the set of active terms and the set of inactive terms. The following mean function in Equation (5.6) was used in selection of significant independent variables (Weisberg 2005).

$$Y = \beta X = \beta_A X_A + \beta_B X_B \tag{5.6}$$

where,

X_A and X_B = variable subsets.

There are several computational methods of variables selection: forward selection, backward elimination and stepwise model selection methods. In the present study, forward selection was used and independent variables were selected based on coefficient of determination (R^2), overall F-statistics, and p-values. In the context of multiple linear regression, Mallows' C_p was also considered in SAS analysis to verify the goodness of fit or uncertainty of experimental data (Weisberg 2005). The smallest C_p value is preferred to eliminate the complexity of the regression functions. Tables 5.3 and 5.4 show the variation of response variable (NWP) with coarse material (CA1), screening material (CA2), natural sand content (NSC), and binder grades (PG) on both K-25 and US-160 mixes. For a specific mix design, the variables CA1, CA2, and NSC were dependent of each other. Hence, in a particular regression function, either CA1 or CA2 or NSC and PG were considered during the goodness test (forward selection, stepwise selection, and backward elimination). The cutoff p-value for F-statistics was set to default used in SAS (0.05) and variables having p-values higher than cutoff were excluded from the model equation. Table 5.5 shows the variables selected from the forward selection procedure.

Table 5.5 Variable Selection on US-160 and K-25

Project	Step	Variables	R^2	$C_{(P)}$	F-statistics	p-value
US-160	1	PG	0.45	14.46	13.3	0.0022
	2	**PG, CA1**	**0.71**	**3.0**	**18.56**	**<0.0001**
	1	PG	0.45	14.46	13.3	0.0022
	2	PG, CA2	0.61	3.0	11.87	0.0008
	1	PG	0.45	14.46	13.3	0.0022
	2	PG, NSC	0.68	3.0	16.04	0.0002
K-25	1	CA1	0.29	1.175	6.59	0.0206
	1	**CA2**	**0.31**	**1.178**	**6.95**	**0.0180**
	1	NSC	0.30	1.177	6.9	0.0183

The table shows that rutting performance of US-160 laboratory mixes was significantly affected by the binder grade (PG) and coarser materials (CA1) present in the aggregate blend. The R^2 (0.71) and p-value (<0.0001) prove that both PG and CA1 can be the best selected design factors to fit the design function compared to the PG, CA2 and PG, NSC combination in the regression equation. Hence, both PG and CA1 were considered as independent variables in developing the rutting performance equation. On the other hand, binder grade does not have any potential influence on K-25 mixes. Based on R^2 (0.31) and p-value (0.018), screening materials (CA2) was selected as the best design factor to develop the rutting prediction model. However, interaction between CA2 and PG was added to the regression function to check for better R^2 value.

5.3.1.2 Step 2 - Selection of Regression Equation

The next phase was to select the order of the regression equations, considering the independent variables selected in the previous phase. The selection criteria were set based on the coefficient of determination (R^2) of overall models and p-values of the estimated parameters. The multiple

linear regressions with/without interactions variables and nonlinear regression equations such as log transformation, power and higher order polynomial equations were considered during selection. The independent variables selected in Section 5.3.1.1 were used in the multiple linear and nonlinear regression models to find the best fit equations for rutting prediction of the laboratory fine mixes. Tables 5.6 and 5.7 show the rutting prediction equations developed during regression analysis for both US-160 and K-25 mixes.

Table 5.6 Rutting Prediction Models for US-160 Mixes

Response Variable	Parameters	Independent Variables	Estimated Parameters	p-value	R^2
NWP	B_0	Vertical Intercept	-18516	0.0217	0.80
	B_1	PG	16639	0.1231	
	B_2	CA1	856.395	0.0003	
	B_3	PG × CA1	-624.66	0.0294	
NWP	B_0	Vertical Intercept	-6335.23	0.2992	0.71
	B_1	PG	-7722.44	0.0002	
	B_2	CA1	148.29	0.0023	
Log(NWP)	B_0	Vertical Intercept	6.55019	<0.0001	0.78
	B_1	PG	1.12423	0.2440	
	B_2	CA1	0.07573	0.0004	
	B_3	PG × CA1	-0.04562	0.0725	
$\frac{1}{NWP}$	B_0	Vertical Intercept	3.822×10^{-4}	0.0002	0.71
	B_1	PG	-0.78×10^{-4}	0.4941	
	B_2	CA1	-0.759×10^{-5}	0.0019	
	B_3	PG × CA1	0.355×10^{-4}	0.2269	
NWP	B_0	Vertical Intercept	-101615	0.0661	0.83
	B_1	PG	4253.37	0.4216	
	B_2	CA1	5305.76	0.0701	
	B_3	PG × $CA1^2$	-7.728	0.0311	
	B_5	$CA1^2$	-58.35	0.1206	

Table 5.7 Rutting Prediction Models for K-25 Mixes

Response Variable	Parameters	Independent Variables	Estimated Parameters	p-value	R^2
NWP	B_0	Vertical Intercept	-3791.03	0.6422	0.30
	B_1	CA2	547.26	0.018	
NWP	B_0	Vertical Intercept	-3791.03	0.6505	0.31
	B_1	CA2	536.10	0.0242	
	B_2	PG×CA2	22.315	0.6298	
Log(NWP)	B_0	Vertical Intercept	8.114	<0.0001	0.29
	B_1	CA2	0.04165	0.0221	
$\frac{1}{NWP}$	B_0	Vertical Intercept	1.99×10^{-4}	0.0038	0.25
	B_1	CA2	-0.35×10^{-5}	0.0356	
NWP	B_0	Vertical Intercept	6250.79	0.9559	0.30
	B_1	CA2	10.11	0.9987	
	B_2	$CA2^2$	7.097	0.9291	

Although the nonlinear models on both projects improved the coefficient of determination (R^2) significantly, the p-values of the estimated parameters failed to reject the null hypothesis at significant level $\alpha = 0.05$. Hence, the linear regression equations with interaction variables (US-160 mixes) and without interaction (K-25) were selected to estimate the rutting. The following equations (5.7) and (5.8) represent the rutting performance models developed by regression analysis in-terms of number of wheel passes (NWP). The independent variables of regression equations such as coarse materials (CA1) and screening materials (CA2) are measured in percentage by weight of total aggregate and binder grade (PG) is considered either 0 (PG 64-22) or 1 (PG 70-22) in the following equations

$$NWP(US-160) = -18516 + 16639 \times PG + 856.4 \times CA1 - 624.66 \times PG \times CA1 \quad (5.7)$$

$$R^2 = 0.80 \quad p-value < 0.0001$$

$$NWP(K-25) = -3791.03 + 547.26 \times CA2 \quad (5.8)$$

$$R^2 = 0.30 \quad p - value = 0.0180$$

However, these prediction model equations were further verified by the laboratory-designed mixes with different percent of coarse materials, screening materials, and natural sand content combinations.

5.3.2 Moisture Sensitivity Prediction Equation

The prediction function to estimate the damage against moisture was developed based on data obtained from the field Lottman test. Laboratory mix performance was expressed in terms of wet strength to dry strength ratio, also known as tensile strength ratio (TSR), that must be higher than 0.8. TSR values were considered the dependent variable, while independent variables are presented in Table 5.8. Fifty percent of the K-25 laboratory mixes failed to meet the TSR criterion. Therefore, regression analysis was performed only for US-160 mixes.

Table 5.8 Variables in Regression Analysis for US-160 Fine Mixes

Independent Variables						Response Variable
Project	**Aggregate Type**				**Binder Grade**	**TSR**
US-160	Coarse Aggregate, **(CA1)**	32	40	45	64-22 (0)	103
	Screening Material **(CA2)**	26	28	33		95
	Natural Sand Content (NSC)	35	25	15		75
	Coarse Aggregate **(CA1)**	32	40	45	70-22 (1)	88
	Screening Material **(CA2)**	26	28	33		94
	Natural Sand Content (NSC)	35	25	15		95

The following two steps were adopted to select the independent variables and to develop the regression equation to predict the performance against moisture.

5.3.2.1 Step 1 – Independent Variables Selection

Table 5.9 shows the output of the forward selection method used to select variables from the goodness test. The table shows that moisture damage of US-160 laboratory mixes is significantly affected by the percentage of screening materials (CA2) in the aggregate blend. Other subsets of materials, such as coarser materials (CA1) and natural sand content (NSC), have the similar p-values compared to CA2 materials. The C_p values are almost similar for all three aggregate subsets. The forward selection method discarded the binder grade (PG) at a cutoff point of 0.5 in all aggregate combinations. The F-statistics (1.63) and p-value (0.2712) of the CA2 subset describe the design function better compared to CA1 and NSC, even though the R^2 (0.30) is lower than the CA1 subset (R^2 = 0.43). Since binder grade is not selected to add in the regression functions, a trial interaction between CA2 and PG was introduced into the regression function to check for improved R^2 and p-value.

Table 5.9 Variable Selection for Moisture Distress Prediction Model

Project	Step	Variables	R^2	$C_{(P)}$	F-statistics	p-value
US-160	1	CA1	0.43	1.023	1.08	0.3569
	1	CA2	0.30	1.025	1.63	0.2712
	1	NSC	0.25	1.024	1.31	0.3165

5.3.2.2 Step 2 – Development and Selection of Prediction Models

Multiple linear regressions with/without interactions and nonlinear regression equations (log transformation, power and higher order polynomials) were developed considering the CA2 material subset. The best-fit moisture damage prediction model selection criteria were set based on the coefficient of determination (R^2) of overall model and p-values of estimated parameters. Table 5.10 shows the moisture damage prediction equations in terms of TSR developed during regression analysis.

Table 5.10 Moisture Damage Prediction Models

Response Variable	Parameters	Independent Variables	Estimated Parameters	p-value	R^2
TSR	B_0	Vertical Intercept	207	0.0038	0.98
	B_1	PG	-139.205	0.0165	
	B_2	CA2	4.0	0.0119	
	B_3	PG × CA2	4.85	0.0161	
TSR	B_0	Vertical Intercept	136.73	0.0463	0.3
	B_1	PG	1.333	0.8836	
	B_2	CA2	-1.577	0.3483	
Log(TSR)	B_0	Vertical Intercept	5.83	0.0006	0.98
	B_1	PG	1.57	0.0166	
	B_2	CA2	-0.0457	0.0116	
	B_3	PG × CA2	0.055	0.0159	
$\frac{1}{TSR}$	B_0	Vertical Intercept	-0.00407	0.1399	0.98
	B_1	PG	0.01784	0.0178	
	B_2	CA2	5.3×10^{-4}	0.0122	
	B_3	PG × CA2	6.3×10^{-4}	0.017	
TSR	B_0	Vertical Intercept	-3.24	0.9902	0.98
	B_1	PG	-67.72	0.1018	
	B_2	CA2	10.3	0.6026	
	B_3	PG × $CA2^2$	-0.241	0.5002	
	B_5	$CA2^2$	0.081	0.0979	

It is interesting to note that the addition of interaction variables (between PG and CA2) in the regression equations has significantly improved the coefficient of determination (R^2) and p-values of individual estimated parameters. Almost all prediction models have $R^2 = 0.98$. However, some p-values of individual estimated parameters in nonlinear models fail to reject the null hypothesis at significant level $\alpha = 0.05$. Hence, the linear regression equation with an

interaction variable was selected to estimate the moisture damage of US-160 laboratory mixes. The following equation (5.9) represents the moisture damage prediction model in-terms of tensile strength ration (TSR) in percentage developed by regression analysis. The independent variables of regression equation such as screening material (CA2) is measured in percentage by weight of total aggregate and binder grade (PG) is considered either 0 (PG 64-22) or 1 (PG 70-22) in the following equation to estimate the percent TSR.

$$TSR = 207 - 139.205 \times PG - 4.0 \times CA2 + 4.85 \times PG \times CA2 \quad (5.9)$$

$$R^2 = 0.98 \qquad p - value < 0.0001$$

This model is further verified by the laboratory-designed mixes with different percent of natural sand content combinations.

5.3.3 Fatigue Life Prediction Equation

The fatigue strength prediction model was developed based on data obtained from a laboratory bending beam fatigue test. Laboratory mix performance is expressed in terms of change in initial flexural stiffness of the beam that must not be higher than 50%. Percent change in flexural stiffness (ΔFS) values was considered as the dependent variable, while independent variables on both projects are presented in Tables 5.11 and 5.12. The following two steps were adopted to select the independent variables and to develop the regression equation to predict the performance against moisture.

5.3.3.1 Step 1 - Independent Variable Selection

Table 5.13 shows the output of the forward selection process to identify the variables from the goodness test. The table shows that change in initial flexural stiffness of US-160 laboratory mixes was significantly affected by all material subsets in the aggregate blend. The binder grade (PG) was selected as a potential design factor for all US-160 mixes. However, CA2 and PG

combination results lowered R^2 (0.30) and raised p-value (0.2033) among the subset groups. The C_p values are similar for all three aggregate subsets. Hence, all three aggregate subsets (CA1, CA2 and NSC), along with PG, were selected to develop the trial regression functions to avoid biased results. On the other hand, the forward selection method discarded the binder grade (PG) at a cutoff point of 0.05 in all aggregate combinations for K-25 mixes. Selection criteria (F-statistics, R^2, C_p, and p-values) obtained from the computational method were almost similar among the aggregate subsets. Since binder grade was not selected to add in the regression functions, a trial interaction between CA2 and PG, CA1 and PG, and NSC and PG were introduced into the regression functions to check for improved R^2 and p-value.

Table 5.11 Variables in Regression Analysis for US-160 Fine Mixes

	Independent Variables					**Response Variable**
Project	**Aggregate Type**				**Binder Grade**	**ΔFS**
US-160	Coarse Aggregate **(CA1)**	32	40	45	64-22 (0)	22
	Screening Material **(CA2)**	26	28	33		32
	Natural Sand Content (NSC)	35	25	15		37
	Coarse Aggregate **(CA1)**	32	40	45	70-22 (1)	27
	Screening Material **(CA2)**	26	28	33		24
	Natural Sand Content (NSC)	35	25	15		23
	Coarse Aggregate **(CA1)**	32	40	45	64-22 (0)	27
	Screening Material **(CA2)**	26	28	33		40
	Natural Sand Content (NSC)	35	25	15		35
	Coarse Aggregate **(CA1)**	32	40	45	70-22 (1)	28
	Screening Material **(CA2)**	26	28	33		32
	Natural Sand Content (NSC)	35	25	15		29

Table 5.12 Variables in Regression Analysis for K-25 Fine Mixes

Independent Variables						Response Variable
Project	**Aggregate Type**				**Binder Grade**	**ΔFS**
K-25	Coarse Aggregate **(CA1)**	32	40	45	64-22 (0)	25
	Screening Material **(CA2)**	26	28	33		31
	Natural Sand Content (NSC)	35	25	15		40
	Coarse Aggregate **(CA1)**	32	40	45	70-22 (1)	30
	Screening Material **(CA2)**	26	28	33		38
	Natural Sand Content (NSC)	35	25	15		32
	Coarse Aggregate **(CA1)**	32	40	45	64-22 (0)	25
	Screening Material **(CA2)**	26	28	33		32
	Natural Sand Content (NSC)	35	25	15		35
	Coarse Aggregate **(CA1)**	32	40	45	70-22 (1)	30
	Screening Material **(CA2)**	26	28	33		28
	Natural Sand Content (NSC)	35	25	15		31

Table 5.13 Variable Selection for Fatigue Strength Analysis

Project	Step	Variables	R^2	$C_{(P)}$	F-statistics	p-value
US-160	1	PG	0.21	3.5	2.7	0.1313
	2	PG, CA1	0.38	3.0	2.8	0.1133
	1	PG	0.21	3.5	2.7	0.1313
	2	PG, CA2	0.30	3.0	1.91	0.2033
	1	PG	0.21	3.5	2.7	0.1313
	2	PG, NSC	0.35	3.0	1.98	0.1395
K-25	1	CA1	0.51	1.43	10.26	0.0095
	1	CA2	0.49	1.42	9.67	0.0111
	1	NSC	0.51	1.43	10.22	0.0095

5.3.3.2 Step 2 - Fatigue Strength Prediction Models

Trial multiple linear regression (MLR) models with/without interactions with binder grade were developed to identify the most influential aggregate subset based on R^2 and p-values of individual estimated parameters. Among the groups, the regression function with NSC and PG was selected even though the overall R^2 (0.59) was lower than the regression function with CA1 and PG ($R^2 = 0.64$). The p-values of individual estimated parameters of regression function with NSC and PG strongly rejected the null hypothesis, while in most cases, functions with PG and CA1 design factors failed to do so. After selecting the MLR models, nonlinear regression equations were developed considering PG and NSC material subsets. The best fit fatigue damage prediction models for US-160 mixes are shown in Table 5.14.

Similar to the moisture induced damage model, the addition of interaction variables (between PG and CA1, CA2 and NSC) in the regression equations in K-25 mixes significantly improved the coefficient of determination (R^2) and p-vales of the individual estimated parameters. Almost all MLR prediction models have R^2 ranging from 0.88 to 0.90. Among the groups, MLR with PG and NSC subset performed the best. Nonlinear and higher order polynomial equations were further developed considering PG and NSC design factors shown in Table 5.15.

Some p-values of individual estimated parameters in the higher order polynomial model failed to reject the null hypothesis at significant level $\alpha = 0.05$. Log transformation and power models were equally best fitted as an MLR equation. Hence, the linear regression equations with interaction variable were selected to estimate the fatigue damage laboratory mixes.

Table 5.14 Fatigue Strength Prediction Models for US-160 Mixes

Response Variable	Parameters	Independent Variables	Estimated Parameters	p-value	R^2
ΔFS	β_0	Vertical Intercept	-4.34	0.7244	0.64
	β_1	PG	35.36	0.0684	
	β_2	CA1	0.93605	0.0146	
	β_3	PG × CA1	-0.427	0.0415	
ΔFS	β_0	Vertical Intercept	-6.314	0.7523	0.48
	β_1	PG	40.73	0.1745	
	β_2	CA2	1.327	0.0803	
	β_3	PG × CA2	-1.577	0.1311	
ΔFS	β_0	Vertical Intercept	46.54	<0.0001	0.59
	β_1	PG	-21.25	0.0270	
	β_2	NSC	-0.575	0.0263	
	β_3	PG × NSC	0.65	0.0615	
ΔFS	β_0	Vertical Intercept	38.42	<0.0001	0.35
	β_1	PG	-5.0	0.1192	
	β_2	NSC	-0.25	0.1933	
Log(ΔFS)	β_0	Vertical Intercept	3.94	<0.0001	0.58
	β_1	PG	-0.721	0.0274	
	β_2	NSC	-0.0195	0.0269	
	β_3	PG × NSC	0.0226	0.0572	
$\frac{1}{\Delta FS}$	β_0	Vertical Intercept	0.0156	0.0487	0.55
	β_1	PG	0.02495	0.0302	
	β_2	NSC	6.27×10^{-4}	0.0299	
	β_3	PG × NSC	-8.025×10^{-4}	0.0568	
ΔFS	β_0	Vertical Intercept	13.81	0.1324	0.71
	β_1	PG	-14.28	0.0134	
	β_2	NSC	1.5	0.2466	
	β_3	PG × NSC^2	0.01342	0.0421	
	β_4	NSC^2	-0.042	0.1222	

Table 5.15 Fatigue Strength Prediction Models for K-25 Mixes

Response Variable	Parameters	Independent Variables	Estimated Parameters	p-value	R^2
ΔFS	β_0	Vertical Intercept	-11.32	0.0819	0.88
	β_1	PG	37.605	0.0016	
	β_2	CA1	1.23	<0.0001	
	β_3	PG × CA1	-1.118	0.0013	
ΔFS	β_0	Vertical Intercept	-16.08	0.0302	0.89
	β_1	PG	42.967	0.0011	
	β_2	CA2	1.237	<0.0001	
	β_3	PG × CA2	-1.15	0.0009	
ΔFS	β_0	Vertical Intercept	46.96	<0.0001	0.90
	β_1	PG	-15.54	0.0006	
	β_2	NSC	-0.625	<0.0001	
	β_3	PG × NSC	0.575	0.0007	
ΔFS	β_0	Vertical Intercept	39.77	<0.0001	0.53
	β_1	PG	-1.167	0.5274	
	β_2	NSC	-0.3375	0.0126	
Log(ΔFS)	β_0	Vertical Intercept	3.934	<0.0001	0.90
	β_1	PG	-0.48725	0.0005	
	β_2	NSC	-0.02016	<0.0001	
	β_3	PG × NSC	0.01852	0.0005	
$\frac{1}{\Delta FS}$	β_0	Vertical Intercept	0.01633	<0.0001	0.90
	β_1	PG	0.01552	0.0006	
	β_2	NSC	6.61×10^{-4}	<0.0001	
	β_3	PG × NSC	-6.07×10^{-4}	0.0005	
ΔFS	β_0	Vertical Intercept	45.5625	0.0018	0.90
	β_1	PG	-8.5626	0.5058	
	β_2	NSC	-0.5	0.5268	
	β_3	PG × NSC	-0.05	0.9637	
	β_4	PG × NSC^2	-0.0025	0.8713	
	β_5	NSC^2	0.0125	0.5719	

The following equations (5.10) and (5.11) represent the fatigue damage prediction model developed by regression analysis. The predicted fatigue damage is estimated in-terms of percent change in initial flexural stiffness (ΔFS) while the independent variables such as natural sand content (NSC) is measured in percentage by weight of total aggregate and binder grade (PG) is considered either 0 (PG 64-22) or 1 (PG 70-22) in the following equations to determine the fatigue life.

$$\Delta FS(US-160) = 46.54 - 21.25 \times PG - 0.575 \times NSC + 0.65 \times PG \times NSC \quad (5.10)$$

$$R^2 = 0.59 \qquad p - value < 0.0001$$

$$\Delta FS(K-25) = 46.96 - 15.54 \times PG - 0.625 \times NSC + 0.575 \times PG \times NSC \quad (5.11)$$

$$R^2 = 0.90 \qquad p - value < 0.0001$$

5.4 Validation of Prediction Model Equations

In order to validate the distress prediction models developed by regression analysis, the experimental data were generated in the KSU lab considering 20% and 30% natural sand content in the aggregate blend. Similar to experimental design, binder grades PG 64-22 and PG 70-22 were considered for the US-160 and K-25 aggregate sources. At first, the trial 4.75-mm mix designs were developed for 20% and 30% natural sand content. After selecting the mix designs, the HWTD and KT-56 samples were prepared in the lab for prediction models verification. Table 5.16 shows the mix properties obtained from the laboratory mix design.

Table 5.16 Mix Properties with 20% and 30% River Sand Content

Source	Binder Grade	CA1	CA2	NSC	Design Asphalt Content	Dust-to-binder Ratio
US-160	PG 64-22	42	31	20	6.79	1.153
		36	27	30	6.65	1.090
	PG 70-22	42	31	20	6.5	1.185
		36	27	30	6.6	1.094
K-25	PG 64-22	37	41	20	5.53	1.549
		32	36	30	5.88	1.278
	PG 70-22	37	41	20	5.45	1.571
		32	36	30	5.61	1.335

The comparison between predicted and laboratory rutting performance and moisture induced damage of the mixes with 20% and 30% river sand contents are presented in Figures 5.2 and 5.3. The goal of this comparative study was not only to validate the prediction models but also to evaluate the aggregate subsets as continuous variables for optimization.

The study shows that the rutting and moisture damage prediction models correlated very well with the test results obtained from laboratory performance testing. In the case of rutting performance of the mixes with PG 64-22 binder grade, the prediction models estimated higher number of wheel passes compared to the actual value. Average deviations between the predicted and the actual number of wheel passes were 10% and 17% for US-160 and K-25 mixes, respectively. However, the reverse trend was true for the mixes with PG 70-22 binder grade at both locations. Actual numbers of wheel passes were minimum 7% and maximum 20% more than the predicted values. The moisture damage prediction model for US-160 mixes had very good agreement with the laboratory TSR values. Only a 3% to 6% deviation was obtained between actual and predicted TSR.

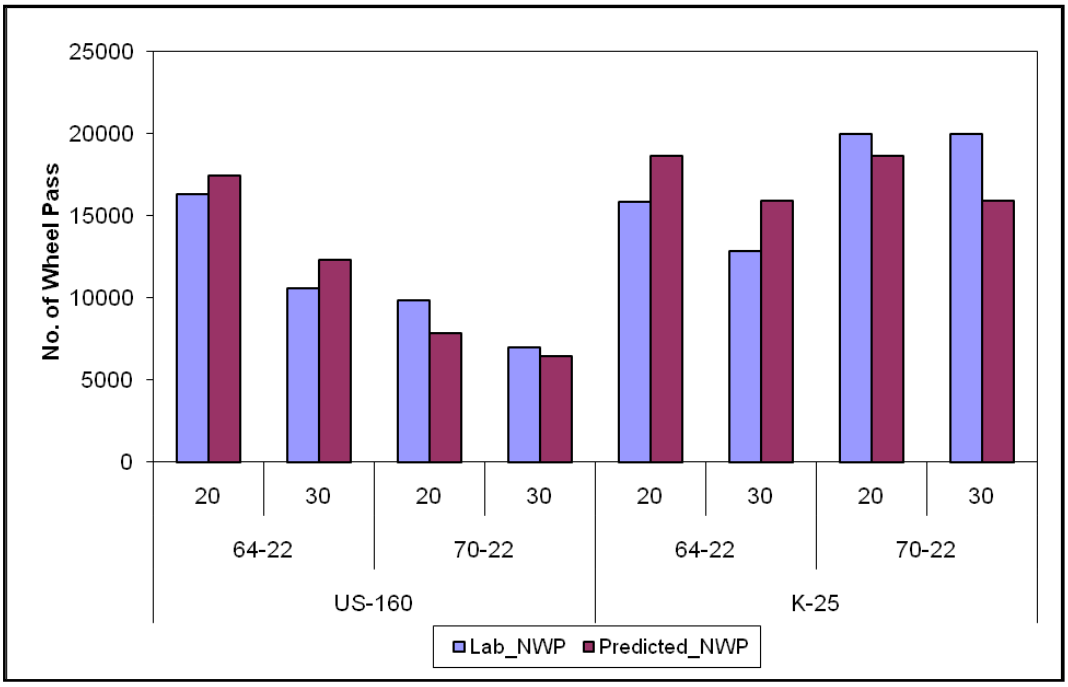

Figure 5.2 Comparison between predicted and laboratory rut data

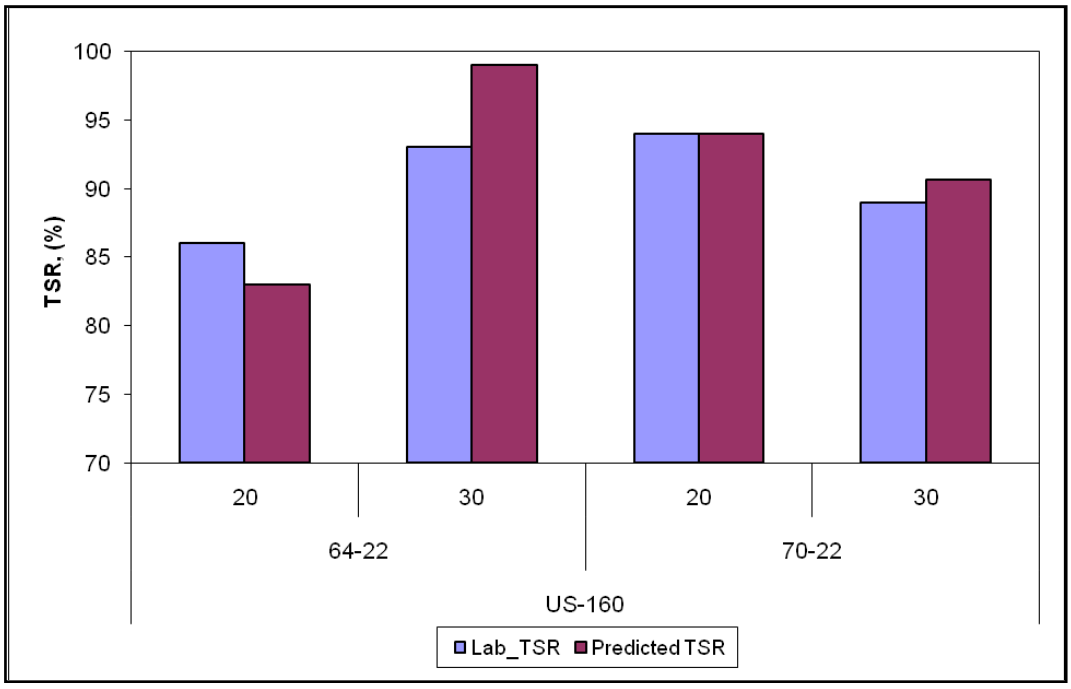

Figure 5.3 Comparison between predicted and laboratory TSR data

5.5 Optimization of 4.75-mm Laboratory Mixes

The main objective of the optimization design procedure was to select the best combination of aggregate blending from some set of available aggregate subsets. Selection technique was based on maximizing or minimizing the real functions, called objective functions, by sequentially choosing the values of real or integer variables from available subsets. In the present study, the multi-objective optimization technique was used to identify the significant aggregate subsets and binder grade combinations, which can address the major distresses common on Kansas highways. Multi-objective optimization is a simultaneous process that can optimize two or more conflicting objective functions subject to certain constraints. Table 5.17 shows the objective functions considered during the optimization process. A well-designed problem should generate more than one feasible solution, which simultaneously maximizes or minimizes each objective or goal.

Table 5.17 Objective Functions for Multi-objective Optimization

`Project	Regression Equations/Objective Functions
US-160	$NWP = -18516 + 16639 \times PG + 856.4 \times CA1 - 624.66 \times PG \times CA1$
	$TSR = 207 - 139.205 \times PG - 4.0 \times CA2 + 4.85 \times PG \times CA2$
	$\Delta FS = 46.54 - 21.25 \times PG - 0.575 \times NSC + 0.65 \times PG \times NSC$
K-25	$NWP = -3791.03 + 547.26 \times CA2$
	$\Delta FS = 46.96 - 15.54 \times PG - 0.625 \times NSC + 0.575 \times PG \times NSC$

The objective functions for the optimization process were selected from the best regression equations developed in the previous sections. Three prediction model equations (rut, moisture damage, and fatigue strength) for US-160 mixes were selected based on R^2 and p-

values, while two prediction models (rutting and fatigue strength) were used to define K-25 mixes.

Goal setting for each objective function enhanced the multi-objective optimization to get the best solutions and quantify how much better the solutions were compared to other such solutions. The goal normally measures the "target" value to be achieved. The optimization problem must satisfy the condition lists or constraints. There are two types of constraints: equality constraints and inequality constraints. In this research study, both equality and inequality constraints were introduced to define the constrained optimization problem. Table 5.18 shows the constraints and goals of the objective functions considered during analysis.

Table 5.18 Constraints and Goals for Objective Functions

Projects	Constraints Functions	Goals
US-160	$0 \le PG \le 1$ [1] $32 \le CA1 \le 45$ [1] $26 \le CA2 \le 33$ [1] $15 \le NSC \le 35$ [1] $CA1 + CA2 + NSC = 93$ [2]	$NWP \ge 20{,}000$ $TSR \ge 80\%$ $\Delta FS \le 50\%$
K-25	$0 \le PG \le 1$ [1] $30 \le CA1 \le 40$ [1] $33 \le CA2 \le 43$ [1] $15 \le NSC \le 35$ [1] $CA1 + CA2 + NSC = 98$ [2]	$NWP \ge 20{,}000$ $\Delta FS \le 50\%$

Note: [1] = Inequality Constraints
[2] = Equality Constraints

The goals for each project were set according to the objective functions. For US-160 mixes, the objective functions for rutting and moisture damage were minimized by maximizing the number of wheel passes (NWP) and tensile strength ratio (TSR) higher or equal to 20,000 repetitions and 80%, respectively. The objective function for fatigue damage was minimized by minimizing the change in initial flexural stiffness (ΔFS) less or equal to 50%. Similar to the US-160 mixes, goals for K-25 mixes were set except for TSR, because successful objective function could not be achieved for K-25 mixes as most mixes failed to reach the TSR limit. The constraints functions were based on upper and lower limits of the individual subsets. The binder grade PG was considered to be continuous within 0 to 1 limit. The summation of coarse, screening, and river sand materials within the aggregate blend were 93% and 98% for US-160 and K-25 mixes, respectively. During optimizing the problem, the feasible solutions generated unique value of binder grade, percentage of coarser material, screening material, and river sand content considering the limits and constraints of the objective functions. An output Excel sheet (Appendix D) of feasible solutions was generated to verify the possible combinations of the design factors. Tables 5.19 and 5.20 show the feasible optimized combination of aggregate subsets and binder grade for the laboratory-designed mixes.

Table 5.19 Proposed Optimized Design Combinations for US-160 Mixes

Project	Optimized Combination				
	PG	CA1 (%)	CA2 (%)	NSC (%)	Manufactured Sand (%)
US-160	64-22	45	26	22	7
	64-22	45	27	21	7
	64-22	45	28	20	7
	64-22	45	29	19	7
	64-22	45	30	18	7
	64-22	45	31	17	7

Table 5.20 Proposed Optimized Design Combinations for K-25 Mixes

Project	Optimized Combination				
	PG	CA1 (%)	CA2 (%)	NSC (%)	Manufactured Sand (%)
K-25	70-22	35	43	20	2
	70-22	36	43	19	2
	70-22	37	43	18	2
	70-22	38	43	17	2
	70-22	39	43	16	2
	70-22	40	43	15	2

The multi-objective optimization process proposed six feasible aggregate and binder combinations to address all three major distresses for asphalt pavement at each location. For US-160 mixes, binder grade PG 64-22 proved to be effective over PG 70-22. Seventeen to 22 percent river sand in the designed aggregate blend was sufficient to produce optimized design combinations rather than using 35% natural sand (state practice). The coarse material was set at 45% for optimized design purposes. Reduced sand content enhanced the usage of screening material (increase 5%) in the aggregate blend, which in turn reduced the accumulated aggregate stockpiles. On the other hand, K-25 mixes with 15 to 20 percent natural sand content were suggested to produce the optimized mix design. Higher binder grade PG 70-22 was more effective for the K-25 aggregate source compared to PG 64-22. The percentage of screening material was set at 43%, regardless of the natural sand content in the aggregate blend to control the dust content in the combined gradation. The percentage of coarse material can be increased by 5% to reduce the sand content from 20% to 15%. The detail output and input codes for the multi-objective optimization problem are attached in the Appendix D.

5.6 Optimization Design Procedure of Superpave Mixture

The ultimate objective of this research study was to propose an optimized design procedure for any Superpave mixture. The proposed optimal combination of aggregate subsets and binder in section 5.5 is good enough to address all types of distresses common in Kansas using the 4.75-mm NAMS Superpave mixture. The prediction model equations developed in section 5.3 are competent to estimate the performances of Kansas fine mix for those two aggregate sources and binder grade. Based on the optimized design procedure followed during the research study, the flow chart shown in Figure 5.4 is suggested to develop the optimal design for the Superpave mixture with any nominal maximum aggregate size. Four consecutive steps must be followed to obtain the best aggregate-binder combination in Superpave mixtures with any NMAS. The steps are as follows:

1. **Step – 1:** In the initial phase of the design procedure, a statistical experimental design must be performed to select the design factors and corresponding response variables. For example, in present study, the design factors (aggregate types and binder grades) and their number of replicates were selected in the statistical experimental design. The response variables, such as the number of wheel passes from the HWTD test, TSR value from the moisture susceptibility test, and change in initial flexural stiffness from the beam fatigue test were set based to fulfill the objectives of the design problem.
2. **Step – 2:** In the second phase of the design process, the aggregates subsets should be defined and the laboratory trial mix designs shall be developed considering the aggregate subsets and binder grades. After selecting the final mix design from the trial mixes, the performance test specimens will be prepared according to the appropriate test specifications. In the current study, aggregates from two different sources (US-160 and K-25) were subdivided into

coarser material, screening material, and river sand. Trial mixes were developed using theses aggregate subsets and different binder grades (PG 64-22 and PG 70-22). The samples for the performance tests were prepared knowing the mix design. The suggested performance tests were the HWTD rut test, moisture susceptibility test, and fatigue strength test.

3. **Step – 3**: The next step in the design procedure is the regression analysis of the experimental data. Performance tests data needs to be analyzed statistically and regression equations need to develop using influential design factors and response variables. Among the regression equations, the distress prediction model equations for each performance test would have to be selected based on R^2 and p-value of the regression equation. In present study, three distress prediction model equations (Equations 5.7, 5.9 and 5.10) were selected for the US-160 mixes while distresses of the K-25 mixes were defined by two prediction equations (Equations 5.8 and 5.11). Theses distress prediction equations were used as the objective functions in the optimization process.
4. **Step** – 4: The next step is to optimize the objective function based on certain constraints and goals. The constraint functions are defined by the design factors and the goals are obtained from the failure criteria of the laboratory performance tests. If the regression functions are nonlinear and have more than one goal to optimize, a multi-objective optimization process is the best technique to get more than one feasible solution. In this study, the combined gradation of the aggregate subsets and binder grades defined the five constraints of the objective functions and three goals were set based on the failure criteria of the HWTD, moisture susceptibility and beam-fatigue tests. Finally, multi-objective optimization process was used to get the feasible solutions of the design problem.

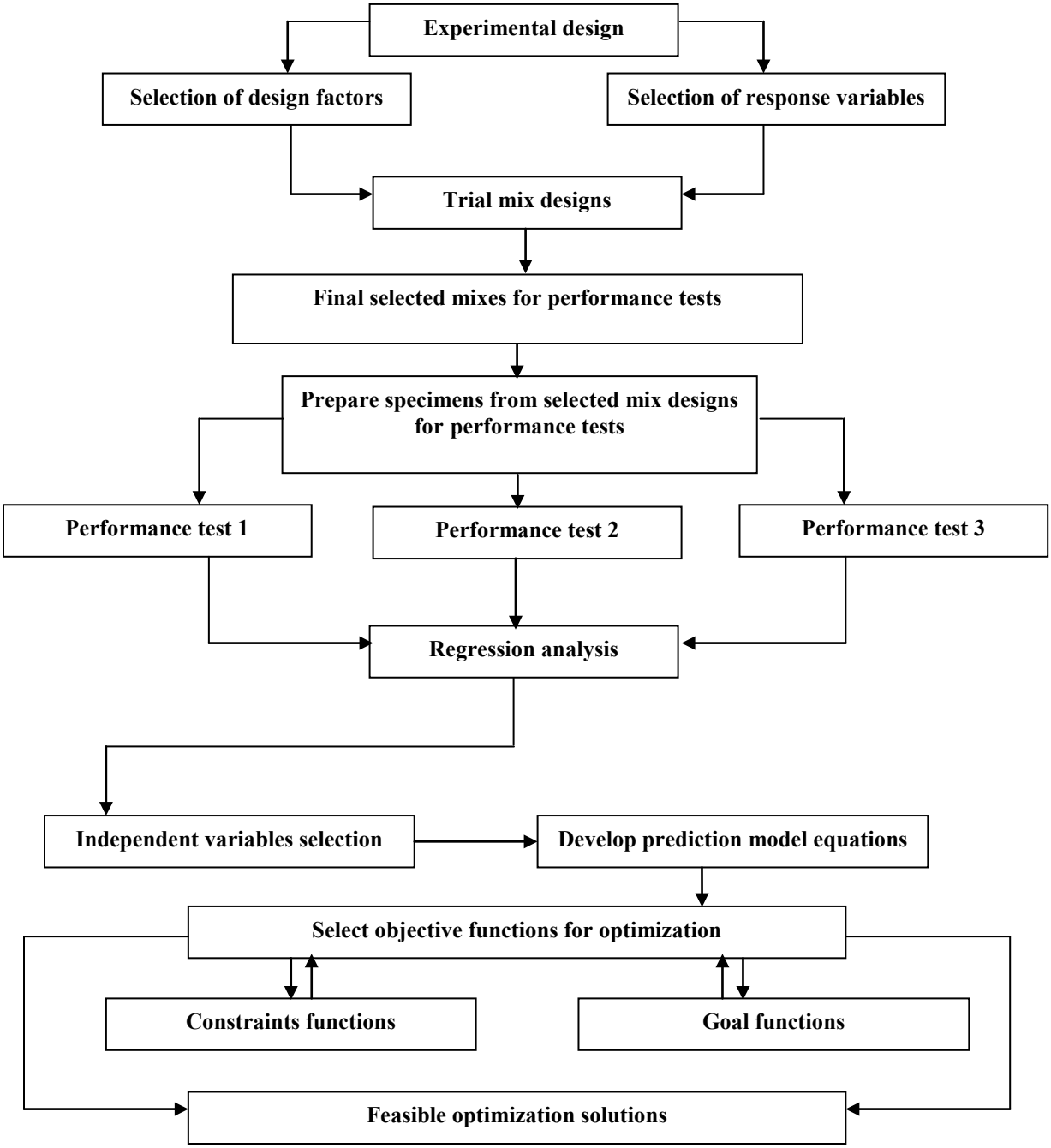

Figure 5.4 Design flow chart for multi-objective optimization process

CHAPTER 6 - CONCLUSIONS AND RECOMMENDATIONS

6.1 Conclusions

The design method of Superpave is a performance-based method. Even though it uses traditional volumetric mix design methodologies, it also includes a performance concept. The tests and analyses have direct relationships to field performance. In addition, the Superpave mix design system integrates material selection (asphalt and aggregate) and mix design into procedures based on pavement structural section, design traffic, and climate conditions. A Superpave mixture with 4.75-mm nominal maximum aggregate size (NMAS) is a promising, low-cost pavement preservation treatment. For preventive maintenance, ultra thin-lift application of this fine mix is an excellent alternative to stretch the maintenance budget if the pavement does not have any major distresses. Since past experiences with thin hot-mix asphalt (HMA) overlays were positive in a few states, the 4.75-mm mixes have attracted attention from many state agencies including Kansas. Successful implementation of this mix has benefit in-terms of construction time and cost, it can be used for corrective maintenance, and to provide a very economical surface mixture for low-to-medium traffic- volume facilities. The main objective of this research study was to evaluate various aspects of the design of Kansas 4.75-mm Superpave mixture, and to asses the relative performance of the mix in both field and laboratory environments. Based on this study, the following conclusions can be made:

- Three distinct tack coat application rates were not achieved on one project out of two studied, emphasizing the need for better equipment calibration.
- Rutting performance of field cores was project-specific and was highly dependent on the in-place density of the compacted mixture, rather than the tack application rate.

- During pull-off testing of 50-mm (two-inch) diameter field cores, most failure occurred within the 4.75-mm NMAS overlay and with HIPR materials, rather than at the interface. This implied that the overlay layer was fully bonded with the HIPR layer in most cases. However, the high tack application rate used in this study might be too high to provide sufficient bond strength for the overlay.
- Failure force during pull-off tests was highly dependent on the aggregate source and volumetric mix design of the adjacent layer material.
- Twelve 4.75-mm NMAS mixtures were successfully designed in the laboratory for two different Kansas aggregate sources, two binder grades, and three natural sand contents. Design binder content is relatively high for these fine mixes.
- The effective asphalt content in the design mix is highly influenced by the natural sand content. The percent free asphalt decreased with decreasing natural sand content.
- The relative density at the initial number of gyrations and dust-to-binder ratio were influenced by aggregate type and natural sand content in the design mix. The initial relative density decreased with decreased river sand content in the mix while the dust-to-binder ratio significantly increased with decreasing natural sand.
- Rutting performance during the Hamburg wheel tracking device tests was aggregate source specific. Higher binder grade may or may not improve rutting performance of 4.75-mm NMAS mixes.
- The anti-stripping agent affected the moisture sensitivity test results, irrespective of natural sand content, binder grade, and aggregate source. Mixes without anti-stripping agent failed to meet the Tensile Strength Ratio (TSR) criteria specified by Kansas Department of Transportation.

- Laboratory fatigue performance was significantly influenced by river sand content and binder grade. Changes in flexural strength increased with decreasing natural sand content for the mixes with lower binder grade. Higher binder grade helped to improve the fatigue strength.
- Multivariate analysis of variance (MANOVA) showed that the overall response variables from laboratory mix volumetric were highly influenced by the aggregate source type, binder grades, and percent of river sand in the aggregate blend.
- Univariate analysis of variance (ANOVA) showed that among the volumetric properties of the laboratory design mix, dust-to-binder ratio was the most statistically significant mixture parameter that highly affects mix performance.
- Five multiple linear regression equations were developed to predict the pavement performance in Kansas.
- Six optimized design combinations were proposed by the multi-objective optimization process to address major distresses. The feasible optimized solutions suggested limiting the river sand content in between 15% and 20%.
- An optimized design procedure was proposed to minimize pavement distresses, considering local materials and specifications.

6.2 Recommendations

Based on the present study and above conclusions, the following recommendations are made:

- Present study recommends limiting the river sand content currently used by KDOT. The suggested river sand content must be ranged from 15% to 20% rather than 35% (current practice) for Kansas 4.75-mm NMAS Superpave mixture.

- The research study also recommends narrowing down the dust-to-effective binder ratio specified by KDOT to design the SM-4.75A mix. Current KDOT specification uses dust-to-effective binder ratio 0.9 to 2.0. The suggested range to design the Kansas mix is 0.9 to 1.6.
- Clay content of aggregate blend plays a pivotal roll in stripping action in a Superpave mixture. Stripping started early in US-160 mixes with binder grade PG 70-22, while mixes with PG 64-22 performed essentially better. There might be a significant possibility to have a chemical reaction between PG 70-22 binder grade and dust particles in the presence of liquid amine. Possible causes of early stripping for US-160 mixes with PG 70-22 could be detachment, displacement, film rupture, hydraulic scouring, pore pressure, and especially emulsification and pH instability. Further research is needed to identify the possible causes of early stripping.
- Chemical reaction between asphalt binder and aggregate consists of acidic and basic components. Tests for acidic aggregate in the fine mix is recommended, especially when the baghouse dust is used in the aggregate blend.
- Since the dust-to-binder ratio is a statistically proven critical parameter for mix performances, an optimized 4.75-mm NMAS mixture may have a much narrower range of the dust-to-binder ratio than is allowed in the current specifications. Further study is recommended in this matter.
- Study of film thickness of these fine mixes with higher dust-to-binder ratio is recommended.
- Some tests on materials finer than US No. 200 sieve such as sand equivalent, plasticity index (Atterberg limits), and Methylene blue value are recommended.

- Since determination of creep slope, stripping inflection point, and stripping slope from the Hamburg wheel tracking test are subjective, a dynamic creep test is recommended to determine the permanent deformation of laboratory mixes.
- Pull-off strength tests at three or more different temperatures is recommended.
- Further study on bond strength at the HMA interface layer is recommended, considering different tack coat materials, tack coat curing time, and coring locations in the field.

References

AASHTO. (2004). "Specifications. Standard Specifications for Transportation Materials and Methods of Sampling and Testing." 24th Edition Part B, 444 North Capitol Street, NW, Washington, D.C.

AI. (1994). "Performance Graded Asphalt Binder Specification and Testing." *Superpave Series No.1 (SP-1)*, The Asphalt Institute, Lexington, Kentucky.

Al-Qadi, I. L., Carpenter, S. H., Leng, Z., Ozer, H., and Trepanier, J. S. (2008). "Tack Coat Optimization for HMA Overlays: Laboratory Testing." *Research Report FHWA-ICT-08-023.* Illinois Center for Transportation, University of Illinois at Urbana-Champaign, Illinois.

Al-Qadi, I. L., Carpenter, S. H., Leng, Z., Ozer, H., and Trepanier, J. S. (2009). "Tack Coat Optimization for HMA Overlays: Accelerated Pavement Test Report." *Research Report ICT-09-035.* Illinois Center for Transportation, University of Illinois at Urbana-Champaign, Illinois.

ASTM. (2003). "Standard Test Method for Pull-Off Strength of Coating Using Portable Adhesion Testers." *D4541.* West Conshohocken, Pennsylvania.

AASHTO. (2005). "Testing: Standard Specifications for Transportation Materials and Methods of Sampling and Testing." *AASHTO, 24th Edition, Part 2,* 444 North Capitol Street, NW, Washington, D.C.

AASHTO. (2000). "Hot-Mix Asphalt Paving Handbook 2000." *US Army Corps of Engineers and Federal Aviation Administration AC 150/5370-14A, Appendix 1*, USA.

Bruin, J. (2010). "New test: command to compute new test." UCLA: Academic Technology Services, Statistical Consulting Group. http://www.ats.ucla.edu/stat/stata/ado/analysis/. Accessed February 24, 2010.

Birgisson, B., Reynaldo, R., Varadhan, A., Thai, T., and Lokendra, J. (2006). "Evaluation of Thick Open Graded and Bonded Friction Courses for Florida." *FDOT Final Report 4504968-12 (00026875)*. Florida Department of Transportation, Florida.

Cooley, L. A., James, R. S., and Buchanan, M. S. (2002). "Development of Mix Design Criteria for 4.75 mm Superpave Mixes-Final Report." *NCAT Report 02-04*. National Center for Asphalt Technology, Auburn University, Auburn, Alabama.

Cooley, L. A., Huner, Jr., M. H., and Brown, E. R. (2001). "Use of Screening to Produce HMA Mixture." *NCAT Report 02-10.* National Center for Asphalt Technology, Auburn University, Auburn, Alabama.

Canestrari, F., Ferrotti, G., Graziani, A., and Baglieri, O. (2009). "Interlayer Bonding Design of Porous Asphalt Course Interface." Conference Proceeding CD-ROM. *Sixth International Conference on Maintenance and Rehabilitation of Pavements and Technological Control (MAIREPAV6),* Turin, Italy, 2009.

FHWA. (2008). Highway Statistics 2008, Federal Highway Administration, U.S. Department of Transportation. http://www.fhwa.dot.gov/policyinformation/statistics/2008/hm220.cfm Accessed April 25, 2010.

Hand, A., and Epps. A. (2001). "Impact of Gradation Related to Superpave Restricted Zone on Hot Mix Asphalt Performance." *Transportation Research Record: Journal of the Transportation Research Board*, n 1767, Transportation Research Board of the National Academics, Washington, D.C., p 158-166.

Hongbin, X., Cooley, L. A., and Huner, M. H. (2003). "4.75-mm NMAS Stone Mastic Asphalt (SMA) Mixture." *NCAT Report 03-05.* National Center for Asphalt Technology, Auburn University, Auburn, Alabama.

Hossain, M., Maag, R. G., and Fager, G. (2010). "Handbook of Superpave Volumetric Asphalt Mixture Design and Analysis." *Superpave Certification Training Manual*, Kansas State University, Manhattan, Kansas.

Kandhal, P. S. and Cooley, L. A. (2002). "Coarse vs. Fine-Graded Superpave Mixtures: Comparative Evaluation of Resistance to Rutting." *NCAT Report 02-02.* National Center for Asphalt Technology, Auburn University, Auburn, Alabama.

Leng, Z., Al-Qadi, I. L., Carpenter, S. H., and Ozer, H. (2010). "Interface Bonding Between Hot-Mix Asphalt and Various Portland Cement Concrete Surfaces." *Transportation Research Record: Journal of Transportation Research Board*, vol. 2127, pp 20-28.

Leng, Z., Al-Qadi, I. L., Carpenter, S. H., and Ozer, H. (2008). "Tack Coat Type and Application Rate Optimization to Enhance HMA Overlay- PCC Interface Bonding." *Third International Conference on Accelerated Pavement Testing. APT 2008. Impacts and Benefits from APT Programs,* Madrid, Spain.

Mallick, R. B., Cooley, L. A., Bradbury, R. L., and Peabody, D. (2003). "An Evaluation of Factors Affecting Permeability of Superpave Designed Pavements." *NCAT Report 03-02.* National Center for Asphalt Technology, Auburn University, Auburn, Alabama.

MDOT. (2005). "Guide Specification for HMA Ultra-Thin." Michigan Department of Transportation, Michigan.

Mogawer. W. S., Austerman, A. J., Engstrom, B., and Bonaquist, R. (2009). "Incorporating High Percentages of Recycled Asphalt Pavement and Warm-Mix Asphalt Technology into Thin Hot-Mix Asphalt Overlays as Pavement Preservation Strategy." *TRB Preprint DVD*

Paper #09-1275, 88th Annual Meeting of the Transportation Research Board, Washington, D.C.

Mogawer. W. S., Austerman, A. J., and Bonaquist, R. (2009). "Laboratory Development and Field Trials of Thin-Lift Hot Mix Asphalt Overlays Incorporating High Percentages of Reclaimed Asphalt Pavement with Warm Mix Asphalt Technology." *Proceedings of the 54th Annual Conference of the Canadian Technical Asphalt Association (CTAA)*, pp. 73-97, Moncton, NB.

Mohammad, L. N., Raqib, M. A., and Haung, B. (2001). "Influence of Asphalt Tack Coat Materials on Interface Shear Strength." *Transportation Research Record: Journal of the Transportation Research Board*, n 1789, Transportation Research Board of the National Academics, Washington, D.C. p 56-65.

Montgomery, D. C. *Design and Analysis of Experiments.* 4th Edition, John Wiley & Sons Inc. Publication, New York, USA, 1997

Mrawira, D. and Yin, D. (2006). "Field Evaluation of Effectiveness of Tack Coats in Hot Mix Asphalt Paving." *TRB Preprint CD-ROM Paper #06-1248,* 85th Annual Meeting of the Transportation Research Board, Washington, D.C.

Nam, K., Tashman, L., Papagiannakis, T., Willoughby, K., Pierce, L. M., and Baker, T. (2008). "Evaluation of Construction Practices That Influence the Bond Strength at the Interface between Pavement Layers." *ASCE: Journal of Performance of Constructed Facilities,* vol. 22, n 3, pp 154-161, May, 2008.

Ohio Department of Transportation. *Flexible Pavements of Ohio*. *http://www.flexiblepavements.org/smoothseal.cfm.* Accessed March, 2010.

Partl, M. N., Canestrari, F., Ferrotti, G., and Santagata, F. A. (2006). "Influence of Contact Surface Roughness on Interlayer Shear Resistance." *10th International Conference on Asphalt Pavement,* vol. 1, pp. 358-367, Quebec City, Canada.

Roberts, F. L., Kandhal, P. S., Brown, E. R., Lee, D., and Kennedy, T. W. (1996). "Hot Mix Asphalt Materials, Mixture Design and Construction." National Asphalt Pavement Association Research and Education Foundation, *2nd Edition*, Lanham, Maryland.

Scullion, T., Zhou, F., Walubita, L. F., and Sebesta, S. (2009). "Design and Performance Evaluation of very Thin Overlays in Texas." *FHWA/TX Report 0-5598-2,* Texas Transportation Institute, Texas.

State Testing Procedures, TEX 242-F Draft. http://www.pmw-wheeltracker.com/test_procedures/Tex-242-F%20DRAFT.pdf. Accessed July 15, 2009.

Suleiman, N. "Evaluation of North Dakota's 4.75 mm Local Gyratory HMA Mixtures for Thin Overlay Applications." *NDDOT Final Report.* North Dakota Department of Transportation, Bismarck.

Tashman, L., Nam, K., and Papagiannakis, T. (2006). "Evaluation of the Influence of Tack Coat Construction Factors on the Bond Strength Between Pavement Layers." *WCAT Report # 06-002.* Washington Center for Asphalt Technology, Washington.

Trenton, M. C., Todd, M. R., and Kevin, K. M. (2010). "Trackless Tack Coat Materials – A Laboratory Evaluation for Performance Acceptance." *TRB Preprint DVD Paper #10-0985,* 89th Annual Meeting of the Transportation Research Board, Washington, D.C.

UCLA. "Introduction to SAS." UCLA: *Academic Technology Services, Statistical Consulting Group.*http://www.ats.ucla.edu/stat/sas/notes2/. Accessed February 24, 2010.

Walubita, L. F. and Scullion, T. (2008). "Thin HMA Overlays in Texas: Mix Design and Laboratory Material Property Characterization." *FHWA/TX Report 0-5598-1*. Texas Transportation Institute, Texas.

Weisberg, S. (2005). "Applied Linear Regression." *3rd Edition*, John Wiley & Sons Inc. Publication, 111 River Street, Hoboken, New Jersey, USA.

West, R. C., Zhang, J., and Moore, J. (2005). "Evaluation of Bond Strength Between Pavement Layers." *NCAT Report 05-08.* National Center for Asphalt Technology, Auburn University, Auburn, Alabama.

West, R. C., and Rausch, D. M. (2006). "Laboratory Refinement of 4.75 mm Superpave Designed Asphalt Mixture." *NCAT Phase I Draft Report.* National Center for Asphalt Technology, Auburn University, Auburn, Alabama.

West, R. C., Rausch, D. M., and Takahashi, O. (2006)." Refinement of Mix Design Criteria for 4.75mm Superpave Mixes." *10th International Conference on Asphalt Pavement*, vol. 1, pp. 161-170, Quebec City, Canada.

Wheat, M. (2007). "Evaluation of Bond Strength at Asphalt Interface." A M.S Thesis. Department of Civil Engineering, Kansas State University, Manhattan, Kansas.

Williams, S. G. (2006). "Development of 4.75 mm Superpave Mixes." *MBTC Report 2030.* Department of Civil Engineering, University of Arkansas, Arkansas.

Woods, M. E. (2004) "Laboratory Evaluation of Tensile and Shear Strength of Asphalt Tack Coats." *An M.S Thesis*, Civil Engineering, Mississippi State University, Mississippi.

Yildirim, Y., Smit, A. F., and Korkmaz, A. (2005). "Development of a Laboratory Test Procedure to Evaluate Tack Coat Performance." *Turkish Journal of Engineering & Environmental Science*, n 29, p 195-205.

Appendix A - QA/QC of 4.75-mm NMAS Plant Mix and Laboratory Testing of Field Cores

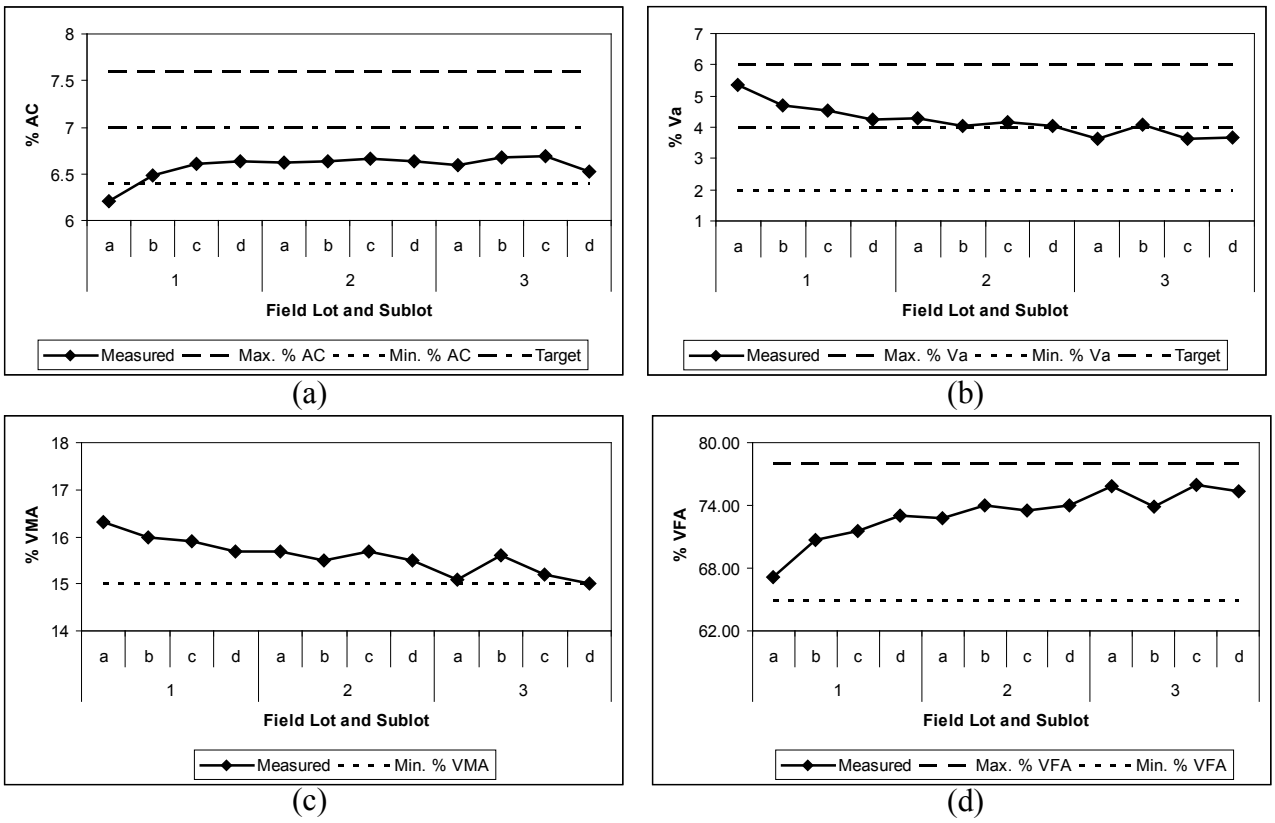

Figure A.1 Field quality control of SM-4.75A, US-160 mix based on (a) % AC, (b) % Va, (c) % VMA, and (d) % VFA

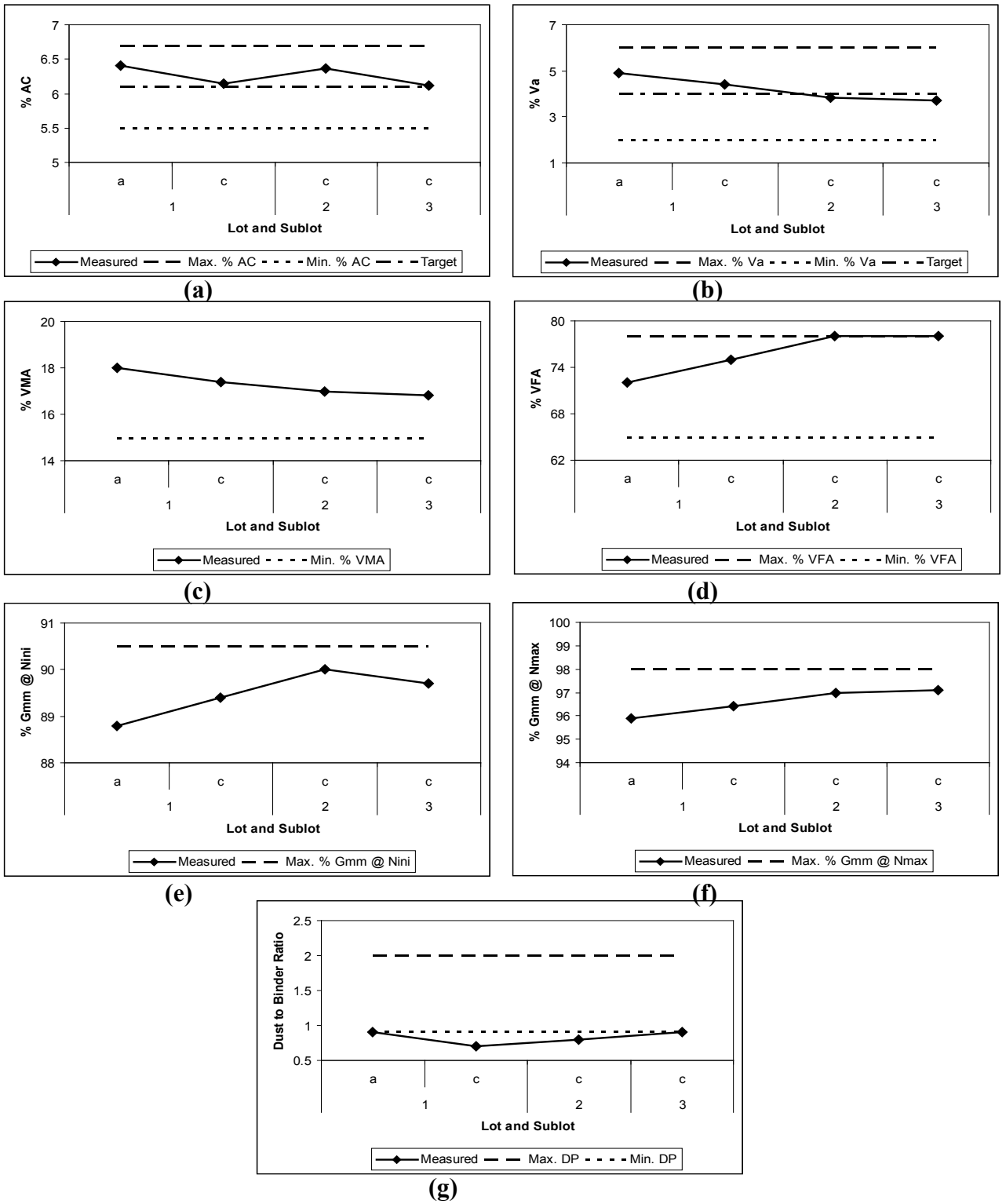

Figure A.2 Quality assurance of SM-4.75A mix on K-25 project based on (a) %AC, (b) %Va, (c) %VMA, (d) %VFA, (e) %G_{mm} @N_{ini}, (f) %G_{mm} @N_{max}, and (g) dust-to-binder ratio

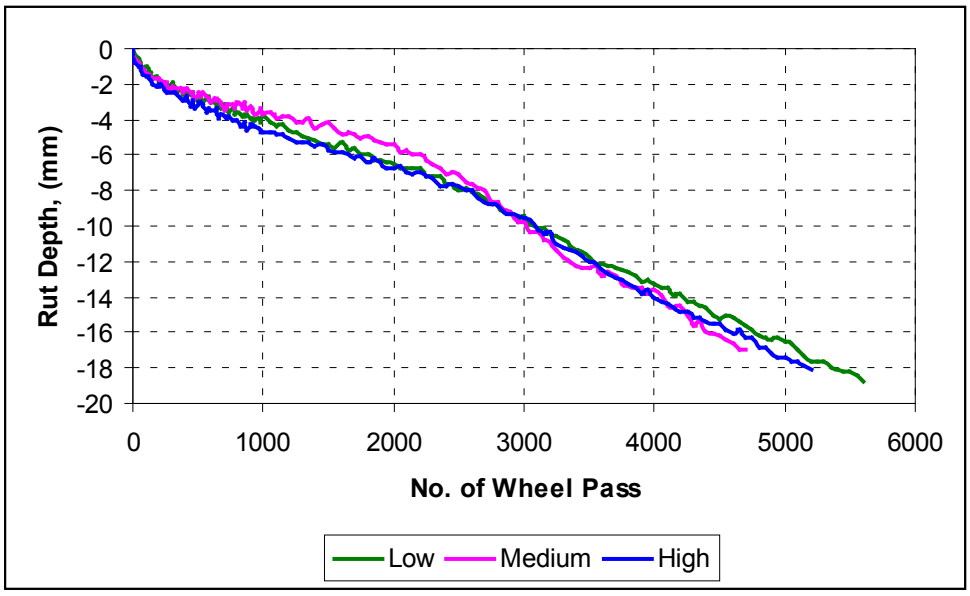

Figure A.3 HWTD testing of field cores from US-160 project with low, medium, and high tack coat application rate

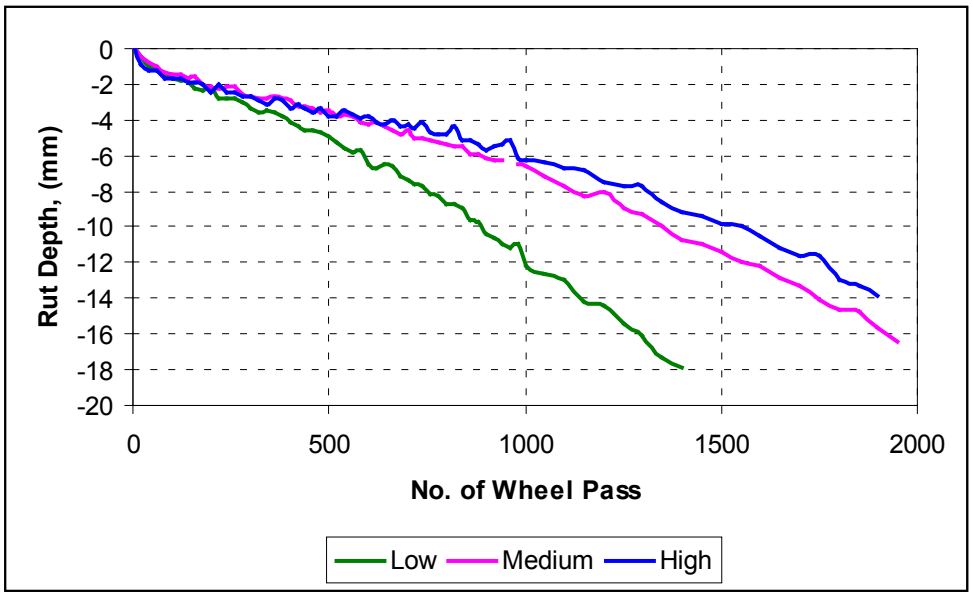

Figure A.4 HWTD testing of field cores from K-25 project with low, medium, and high tack coat application rate

Table A.1 Pull-Off Strength Test on US-160 and K-25 Projects

Test sections	Core Location	Pull-out/Tensile Force (lbs)			
		US-160		K-25	
High	1	404 (SMF)	836 (HIPR)	581 (PBF)	527 (SMF)
	2	356 (SMF)	801 (SMF)	120 (SMF)	439 (PBF)
	3	617 (HIPR)	795 (SMF)	453 (SMF)	635 (PBF)
	4	786 (HIPR)	780 (SMF)	707 (HIPR)	142 (PBF)
	5	174 (HIPR)	676 (SMF)	730 (HIPR)	505 (PBF)
	6	660 (HIPR)	459 (HIPR)	615 (HIPR)	652 (PBF)
	7	645 (HIPR)	531 (HIPR)	427 (SMF)	580 (HIPR)
Medium	8	624 (HIPR)	321 (SMF)	808 (HIPR)	412 (SMF)
	9	420 (SMF)	389 (SMF)	374 (SMF)	199 (SMF)
	10	461 (SMF)	459 (SMF)	202 (SMF)	270 ((HIPR)
	11	253 (SMF)	585 (SMF)	504 (HIPR)	637 (PBF)
	12	668 (HIPR)	229 (HIPR)	242 (SMF)	266 (HIPR)
	13	454 (HIPR)	673 (SMF)	210 (HIPR)	505 (HIPR)
	14	743 (HIPR)	590 (SMF)	201 ((HIPR)	146 (HIPR)
Low	15	502 (SMF)	452 (SMF)	224 (HIPR)	225 (HIPR)
	16	675 (SMF)	456 (SMF)	326 (SMF)	328 (HIPR)
	17	311 (HIPR)	696 (HIPR)	305 (HIPR)	457 (HIPR)
	18	570 (HIPR)	420 (HIPR)	646 (HIPR)	219 (HIPR)
	19	869 (HIPR)	196 (SMF)	795 (HIPR)	395 ((HIPR)
	20	890 (HIPR)	460 (SMF)	821 (HIPR)	502 (HIPR)
	21	716 (SMF)	230 (SMF)	517 (SMF)	103 (HIPR)

Note: SMF = Surface Material Failure
HIPR = Hot-In-Place Recycle Material Failure
PBF = Partial Bond Failure

Appendix B - Laboratory Mix Design and Performances of 4.75-mm NMAS Mixture

Table B.1 Sieve Analysis of Individual Aggregate on US-160 Project

CS-1B			
Sieve Openings, (mm)	**Retained, (gm)**	**% Retained**	**Cumulative % Retained**
4.75	81.6	11.83	11.83
2.36	386.5	56.01	67.84
1.18	146.8	21.28	89.12
0.6	31.4	4.55	93.67
0.3	8.7	1.26	94.93
0.15	2.8	0.41	95.33
0.075	3.3	0.48	95.81
Dust (passing # 200)	28.1		
CS-2			
4.75	45.2	7.89	7.89
2.36	107.9	18.82	26.71
1.18	127.8	22.30	49.01
0.6	86.6	15.11	64.11
0.3	57.8	10.08	74.20
0.15	30	5.23	79.43
0.075	20.3	3.54	82.97
Dust (passing # 200)	96.4		
CS-2A			
4.75	2.5	0.57	0.57
2.36	51.9	11.78	12.35
1.18	96.3	21.86	34.21
0.6	79.4	18.02	52.24
0.3	61.7	14.01	66.24
0.15	33.6	7.63	73.87
0.075	21.2	4.81	78.68
Dust (passing # 200)	92.4		
CS-2B			
4.75	27.4	4.21	4.21
2.36	431.6	66.30	70.51
1.18	144.9	22.26	92.76
0.6	31	4.76	97.53
0.3	6.1	0.94	98.46
0.15	1.3	0.20	98.66
0.075	1.1	0.17	98.83
Dust (passing # 200)	7.3		
SSG-4			
4.75	0	0.00	0.00
2.36	2	0.44	0.44
1.18	26.1	5.75	6.19
0.6	85.8	18.92	25.11
0.3	233.7	51.52	76.63
0.15	91.9	20.26	96.89
0.075	10.1	2.23	99.12
Dust (passing # 200)	2.4		

Table B.2 Sieve Analysis of Individual Aggregate on K-25 Project

CG-2			
Sieve Openings, (mm)	Retained, (gm)	% Retained	Cumulative % Retained
4.75	151.8	15.17	15.17
2.36	231.8	23.16	38.33
1.18	162.3	16.22	54.55
0.6	110.6	11.05	65.60
0.3	102.3	10.22	75.82
0.15	82.7	8.26	84.08
0.075	58.9	5.89	89.97
Dust (passing # 200)	100.9		
CG-5			
4.75	52.1	5.21	5.21
2.36	153.6	15.36	20.57
1.18	254.2	25.42	45.99
0.6	177.2	17.72	63.71
0.3	172.1	17.21	80.92
0.15	98.4	9.84	90.76
0.075	38.5	3.85	94.61
Dust (passing # 200)	53.6		
SSG-1			
4.75	115	11.5	11.5
2.36	154.4	15.44	26.94
1.18	182.2	18.22	45.16
0.6	173	17.3	62.46
0.3	235.8	23.58	86.04
0.15	100.9	10.09	96.13
0.075	17.2	1.72	97.85
Dust (passing # 200)	21.2		
MFS-5			
4.75	28.9	2.89	2.89
2.36	14.7	1.47	4.36
1.18	13.9	1.39	5.75
0.6	15.5	1.55	7.3
0.3	22	2.2	9.5
0.15	39.3	3.93	13.43
0.075	107.3	10.73	24.16
Dust (passing # 200)	759.2		

Table B.3 Combined Aggregate Gradation of US-160 Mix with 35% Natural Sand Content

Material	CS-1B		CS-2		CS-2A		CS-2B		SSG-4		Blend	Target
% Used	32		12		7		14		35			
Sieve Size	% Ret.	% Batch	% Ret.	% Batch	% Ret.	% Batch	% Ret.	% Batch	% Ret.	% Batch		
1/2	0	0.00	0	0.00	0	0.00	0	0.00			0	0
3/8	0	0.00	0	0.00	0	0.00	0	0.00	0	0.00	0	0-5
#4	11.83	3.78	7.89	0.95	0.57	0.04	4.21	0.59	0.00	0.00	5	0-10
#8	67.84	21.71	26.71	3.21	12.35	0.86	70.51	9.87	0.44	0.15	36	
#16	89.12	28.52	49.01	5.88	34.21	2.39	92.76	12.99	6.19	2.17	52	40-70
#30	93.67	29.97	64.11	7.69	52.24	3.66	97.53	13.65	25.11	8.79	64	
#50	94.93	30.38	74.20	8.90	66.24	4.64	98.46	13.78	76.63	26.82	85	
#100	95.33	30.51	79.43	9.53	73.87	5.17	98.66	13.81	96.89	33.91	93	
#200	95.81	30.66	82.97	9.96	78.68	5.51	98.83	13.84	99.12	34.69	94.7	88-94

Table B.4 Combined Aggregate Gradation of US-160 Mix with 25% Natural Sand Content

Material	CS-1B		CS-2		CS-2A		CS-2B		SSG-4		Blend	Target
% Used	40		12		7		16		25			
Sieve Size	% Ret.	% Batch	% Ret.	% Batch	% Ret.	% Batch	% Ret.	% Batch	% Ret.	% Batch		
1/2	0	0.00	0	0.00	0	0.00	0	0.00			0	0
3/8	0	0.00	0	0.00	0	0.00	0	0.00	0	0.00	0	0-5
#4	11.83	4.73	7.89	0.95	0.57	0.04	4.21	0.67	0.00	0.00	6	0-10
#8	67.84	27.14	26.71	3.21	12.35	0.86	70.51	11.28	0.44	0.11	43	
#16	89.12	35.65	49.01	5.88	34.21	2.39	92.76	14.84	6.19	1.55	60	40-70
#30	93.67	37.47	64.11	7.69	52.24	3.66	97.53	15.60	25.11	6.28	71	
#50	94.93	37.97	74.20	8.90	66.24	4.64	98.46	15.75	76.63	19.16	86	
#100	95.33	38.13	79.43	9.53	73.87	5.17	98.66	15.79	96.89	24.22	93	
#200	95.81	38.32	82.97	9.96	78.68	5.51	98.83	15.81	99.12	24.78	94.4	88-94

Table B.5 Combined Aggregate Gradation of US-160 Mix with 15% Natural Sand Content

Material	CS-1B		CS-2		CS-2A		CS-2B		SSG-4		Blend	Target
% Used	45		12		7		21		15			
Sieve Size	% Ret.	% Batch	% Ret.	% Batch	% Ret.	% Batch	% Ret.	% Batch	% Ret.	% Batch		
1/2	0	0.00	0	0.00	0	0.00	0	0.00			**0**	**0**
3/8	0	0.00	0	0.00	0	0.00	0	0.00	0	0.00	**0**	**0-5**
#4	11.83	5.32	7.89	0.95	0.57	0.04	4.21	0.88	0.00	0.00	**7**	**0-10**
#8	67.84	30.53	26.71	3.21	12.35	0.86	70.51	14.81	0.44	0.07	**49**	
#16	89.12	40.10	49.01	5.88	34.21	2.39	92.76	19.48	6.19	0.93	**69**	**40-70**
#30	93.67	42.15	64.11	7.69	52.24	3.66	97.53	20.48	25.11	3.77	**78**	
#50	94.93	42.72	74.20	8.90	66.24	4.64	98.46	20.68	76.63	11.49	**88**	
#100	95.33	42.90	79.43	9.53	73.87	5.17	98.66	20.72	96.89	14.53	**93**	
#200	95.81	43.12	82.97	9.96	78.68	5.51	98.83	20.75	99.12	14.87	**94.2**	**88-94**

Table B.6 Combined Aggregate Gradation of K-25 Mix with 35% Natural Sand Content

Material	CG-2		CG-5		SSG-1		MFS-5		Blend	Target
% Used	30		33		35		2			
Sieve Size	% Ret.	% Batch	% Ret.	% Batch	% Ret.	% Batch	% Ret.	% Batch		
1/2	0	0.00	0	0.00	0	0.00	0	0.00	0	0
3/8	0	0.00	0	0.00	0	0.00	0	0.00	0	0-5
#4	15.17	4.55	5.21	1.72	11.50	4.03	2.89	0.06	10	0-10
#8	38.33	11.50	20.57	6.79	26.94	9.43	4.36	0.09	28	
#16	54.55	16.36	45.99	15.18	45.16	15.81	5.75	0.12	47	40-70
#30	65.60	19.68	63.71	21.02	62.46	21.86	7.30	0.15	63	
#50	75.82	22.75	80.92	26.70	86.04	30.11	9.50	0.19	80	
#100	84.08	25.22	90.76	29.95	96.13	33.65	13.43	0.27	89	
#200	89.97	26.99	94.61	31.22	97.85	34.25	24.16	0.48	93	88-94

Table B.7 Combined Aggregate Gradation of K-25 Mix with 25% Natural Sand Content

Material	CG-2		CG-5		SSG-1		MFS-5		Blend	Target
% Used	34		39		25		2			
Sieve Size	% Ret.	% Batch	% Ret.	% Batch	% Ret.	% Batch	% Ret.	% Batch		
1/2	0	0.00	0	0.00	0	0.00	0	0.00	0	0
3/8	0	0.00	0	0.00	0	0.00	0	0.00	0	0-5
#4	15.17	5.16	5.21	2.03	11.50	2.88	2.89	0.06	10	0-10
#8	38.33	13.03	20.57	8.02	26.94	6.74	4.36	0.09	28	
#16	54.55	18.55	45.99	17.94	45.16	11.29	5.75	0.12	48	40-70
#30	65.60	22.30	63.71	24.85	62.46	15.62	7.30	0.15	63	
#50	75.82	25.78	80.92	31.56	86.04	21.51	9.50	0.19	79	
#100	84.08	28.59	90.76	35.40	96.13	24.03	13.43	0.27	88	
#200	89.97	30.59	94.61	36.90	97.85	24.46	24.16	0.48	92	88-94

Table B.8 Combined Aggregate Gradation of K-25 Mix with 15% Natural Sand Content

Material	CG-2		CG-5		SSG-1		MFS-5		Blend	Target
% Used	40		43		15		2			
Sieve Size	% Ret.	% Batch	% Ret.	% Batch	% Ret.	% Batch	% Ret.	% Batch		
1/2	0	0.00	0	0.00	0	0.00	0	0.00	**0**	**0**
3/8	0	0.00	0	0.00	0	0.00	0	0.00	**0**	**0-5**
#4	15.17	6.07	5.21	2.24	11.50	1.73	2.89	0.06	**10**	**0-10**
#8	38.33	15.33	20.57	8.85	26.94	4.04	4.36	0.09	**28**	
#16	54.55	21.82	45.99	19.78	45.16	6.77	5.75	0.12	**48**	**40-70**
#30	65.60	26.24	63.71	27.40	62.46	9.37	7.30	0.15	**63**	
#50	75.82	30.33	80.92	34.80	86.04	12.91	9.50	0.19	**78**	
#100	84.08	33.63	90.76	39.03	96.13	14.42	13.43	0.27	**87**	
#200	89.97	35.99	94.61	40.68	97.85	14.68	24.16	0.48	**92**	**88-94**

Table B.9 G_{mm}, G_{mb}, and Air Voids Results of HWTD Test Specimens for US-160 Laboratory Mixes with PG 64-22

Natural Sand Content	Sample ID	Design AC (%)	G_{mb}	G_{mm}	%Gmm @ N_f	% V_a	Average % V_a	Target % V_a
35	S_35 HT11	7	2.241	2.387	93.90	6.10	6.19	7% ± 1%
	S_35 HT12		2.241		93.89	6.11		
	S_35 HT13		2.238		93.76	6.24		
	S_35 HT14		2.237		93.70	6.30		
	S_35 HT21		2.227	2.392	93.09	6.91	6.95	
	S_35 HT22		2.227		93.12	6.88		
	S_35 HT23		2.228		93.14	6.86		
	S_35 HT24		2.221		92.85	7.15		
	S_35 HT31		2.236	2.398	93.23	6.77	6.84	
	S_35 HT32		2.233		93.13	6.87		
	S_35 HT33		2.233		93.10	6.90		
	S_35 HT34		2.235		93.20	6.80		
25	S_25 HT11	6.8	2.254	2.416	93.31	6.69	6.51	7% ± 1%
	S_25 HT12		2.257		93.41	6.59		
	S_25 HT13		2.261		93.57	6.43		
	S_25 HT14		2.263		93.68	6.32		
	S_25 HT21		2.255	2.408	93.66	6.34	6.25	
	S_25 HT22		2.254		93.61	6.39		
	S_25 HT23		2.260		93.86	6.14		
	S_25 HT24		2.260		93.86	6.14		
	S_25 HT31		2.250	2.408	93.42	6.58	6.38	
	S_25 HT32		2.257		93.71	6.29		
	S_25 HT33		2.256		93.71	6.29		
	S_25 HT34		2.254		93.62	6.38		
15	S_15 HT11	6.75	2.254	2.414	93.36	6.64	6.67	7% ± 1%
	S_15 HT12		2.257		93.50	6.50		
	S_15 HT13		2.250		93.21	6.79		
	S_15 HT14		2.251		93.25	6.75		
	S_15 HT21		2.250	2.407	93.49	6.51	6.52	
	S_15 HT22		2.254		93.64	6.36		
	S_15 HT23		2.248		93.38	6.62		
	S_15 HT24		2.248		93.39	6.61		
	S_15 HT31		2.245	2.41	93.17	6.83	6.83	
	S_15 HT32		2.248		93.29	6.71		
	S_15 HT33		2.241		92.98	7.02		
	S_15 HT34		2.247		93.24	6.76		

Table B.10 G_{mm}, G_{mb}, and Air Voids Results of HWTD Test Specimens for US-160 Laboratory Mixes with PG 70-22

Natural Sand Content	Sample ID	Design AC (%)	G_{mb}	G_{mm}	$\%G_{mm}$ @ N_f	% V_a	Average % V_a	Target % V_a
35	S_35 HT11	6.8	2.218	2.384	93.06	6.94	6.91	7% ± 1%
	S_35 HT12		2.222		93.22	6.78		
	S_35 HT13		2.220		93.12	6.88		
	S_35 HT14		2.216		92.95	7.05		
	S_35 HT21		2.227	2.389	93.21	6.79	6.87	
	S_35 HT22		2.225		93.12	6.88		
	S_35 HT23		2.227		93.21	6.79		
	S_35 HT24		2.221		92.98	7.02		
	S_35 HT31		2.226	2.387	93.24	6.76	6.66	
	S_35 HT32		2.229		93.37	6.63		
	S_35 HT33		2.230		93.43	6.57		
	S_35 HT34		2.228		93.33	6.67		
25	S_25 HT11	6.6	2.228	2.387	93.34	6.66	6.79	7% ± 1%
	S_25 HT12		2.223		93.13	6.87		
	S_25 HT13		2.227		93.31	6.69		
	S_25 HT14		2.222		93.08	6.92		
	S_25 HT21		2.231	2.386	93.51	6.49	6.63	
	S_25 HT22		2.228		93.37	6.63		
	S_25 HT23		2.223		93.19	6.81		
	S_25 HT24		2.229		93.40	6.60		
	S_25 HT31		2.229	2.393	93.15	6.85	6.88	
	S_25 HT32		2.229		93.15	6.85		
	S_25 HT33		2.228		93.09	6.91		
	S_25 HT34		2.228		93.09	6.91		
15	S_15 HT11	6.6	2.225	2.394	92.96	7.04	6.87	7% ± 1%
	S_15 HT12		2.231		93.21	6.79		
	S_15 HT13		2.228		93.07	6.93		
	S_15 HT14		2.233		93.27	6.73		
	S_15 HT21		2.231	2.384	93.58	6.42	6.39	
	S_15 HT22		2.234		93.70	6.30		
	S_15 HT23		2.228		93.44	6.56		
	S_15 HT24		2.234		93.71	6.29		
	S_15 HT31		2.231	2.391	93.30	6.70	6.66	
	S_15 HT32		2.234		93.43	6.57		
	S_15 HT33		2.228		93.17	6.83		
	S_15 HT34		2.234		93.44	6.56		

Table B.11 G_{mm}, G_{mb}, and Air Voids Results of HWTD Test Specimens for K-25 Laboratory Mixes with PG 64-22

Natural Sand Content	Sample ID	Design AC (%)	G_{mb}	G_{mm}	$\%G_{mm}$ @ N_f	% V_a	Average % V_a	Target % V_a
35	S_35 HT11	6.1	2.213	2.402	92.13	7.87	7.72	7% ± 1%
	S_35 HT12		2.219		92.38	7.62		
	S_35 HT13		2.214		92.19	7.81		
	S_35 HT14		2.220		92.42	7.58		
	S_35 HT21		2.224	2.401	92.61	7.39	7.20	
	S_35 HT22		2.231		92.93	7.07		
	S_35 HT23		2.230		92.90	7.10		
	S_35 HT24		2.227		92.75	7.25		
	S_35 HT31		2.216	2.404	92.16	7.84	7.82	
	S_35 HT32		2.214		92.11	7.89		
	S_35 HT33		2.216		92.18	7.82		
	S_35 HT34		2.219		92.29	7.71		
25	S_25 HT11	5.6	2.233	2.41	92.66	7.34	7.28	7% ± 1%
	S_25 HT12		2.231		92.58	7.42		
	S_25 HT13		2.239		92.90	7.10		
	S_25 HT14		2.235		92.74	7.26		
	S_25 HT21		2.236	2.408	92.84	7.16	7.12	
	S_25 HT22		2.239		93.00	7.00		
	S_25 HT23		2.237		92.91	7.09		
	S_25 HT24		2.234		92.77	7.23		
	S_25 HT31		2.234	2.398	93.17	6.83	6.77	
	S_25 HT32		2.237		93.30	6.70		
	S_25 HT33		2.239		93.35	6.65		
	S_25 HT34		2.233		93.12	6.88		
15	S_15 HT11	5.4	2.262	2.419	93.51	6.49	6.51	7% ± 1%
	S_15 HT12		2.263		93.57	6.43		
	S_15 HT13		2.259		93.40	6.60		
	S_15 HT14		2.261		93.47	6.53		
	S_15 HT21		2.253	2.416	93.24	6.76	6.68	
	S_15 HT22		2.253		93.27	6.73		
	S_15 HT23		2.256		93.36	6.64		
	S_15 HT24		2.256		93.39	6.61		
	S_15 HT31		2.254	2.417	93.24	6.76	6.83	
	S_15 HT32		2.254		93.24	6.76		
	S_15 HT33		2.250		93.09	6.91		
	S_15 HT34		2.251		93.13	6.87		

Table B.12 G_{mm}, G_{mb}, and Air Voids Results of HWTD Test Specimens for K-25 Laboratory Mixes with PG 70-22

Natural Sand Content	Sample ID	Design AC (%)	G_{mb}	G_{mm}	$\%G_{mm}$ @ N_f	% V_a	Average % V_a	Target % V_a
35	S_35 HT11	5.7	2.241	2.416	92.77	7.23	7.22	7% ± 1%
	S_35 HT12		2.240		92.70	7.30		
	S_35 HT13		2.244		92.87	7.13		
	S_35 HT14		2.242		92.80	7.20		
	S_35 HT21		2.240	2.42	92.58	7.42	7.26	
	S_35 HT22		2.242		92.65	7.35		
	S_35 HT23		2.246		92.83	7.17		
	S_35 HT24		2.248		92.90	7.10		
	S_35 HT31		2.240	2.41	92.95	7.05	7.05	
	S_35 HT32		2.237		92.84	7.16		
	S_35 HT33		2.241		92.98	7.02		
	S_35 HT34		2.242		93.03	6.97		
25	S_25 HT11	5.5	2.243	2.414	92.92	7.08	7.06	7% ± 1%
	S_25 HT12		2.244		92.95	7.05		
	S_25 HT13		2.244		92.97	7.03		
	S_25 HT14		2.243		92.93	7.07		
	S_25 HT21		2.250	2.414	93.22	6.78	6.87	
	S_25 HT22		2.249		93.16	6.84		
	S_25 HT23		2.246		93.04	6.96		
	S_25 HT24		2.247		93.08	6.92		
	S_25 HT31		2.247	2.397	93.76	6.24	6.31	
	S_25 HT32		2.245		93.65	6.35		
	S_25 HT33		2.247		93.74	6.26		
	S_25 HT34		2.244		93.60	6.40		
15	S_15 HT11	5.4	2.254	2.42	93.16	6.84	6.78	7% ± 1%
	S_15 HT12		2.256		93.24	6.76		
	S_15 HT13		2.254		93.15	6.85		
	S_15 HT14		2.258		93.32	6.68		
	S_15 HT21		2.258	2.424	93.14	6.86	6.88	
	S_15 HT22		2.259		93.18	6.82		
	S_15 HT23		2.256		93.07	6.93		
	S_15 HT24		2.257		93.10	6.90		
	S_15 HT31		2.251	2.42	93.00	7.00	6.87	
	S_15 HT32		2.250		92.98	7.02		
	S_15 HT33		2.258		93.32	6.68		
	S_15 HT34		2.256		93.22	6.78		

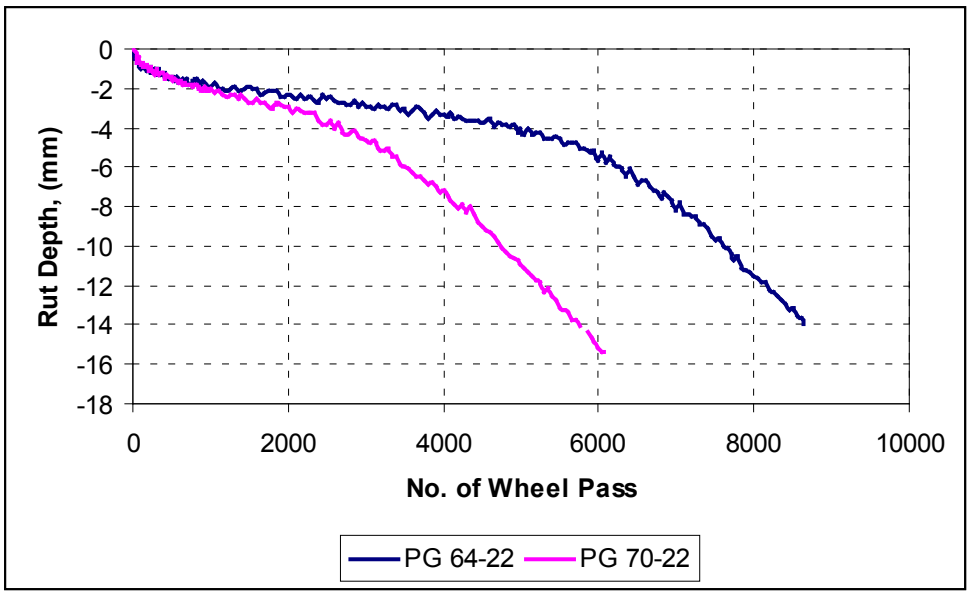

Figure B.1 HWTD performance of US-160 mixes with 35% natural sand

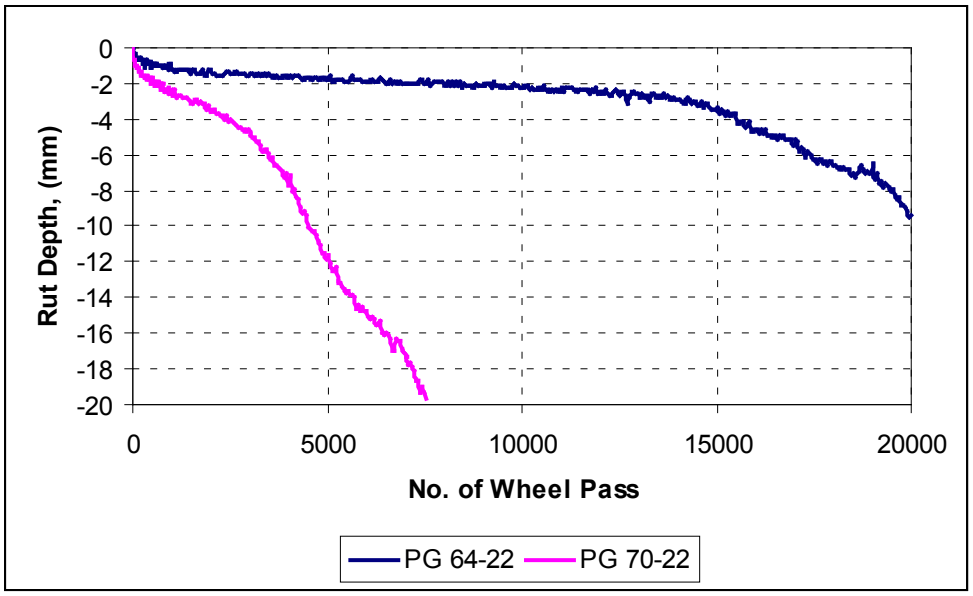

Figure B.2 HWTD performance of US-160 mixes with 25% natural sand

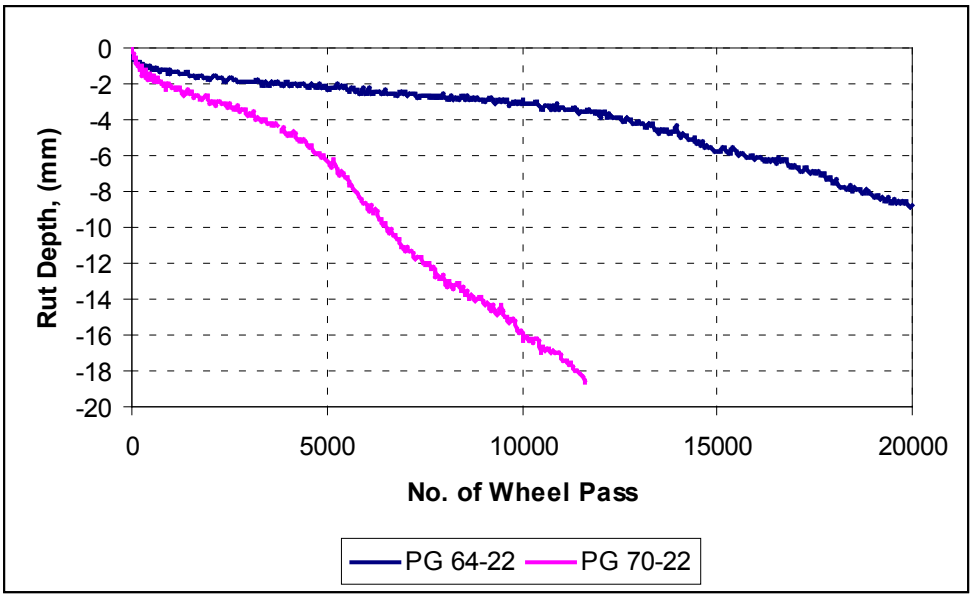

Figure B.3 HWTD performance of US-160 mixes with 15% natural sand

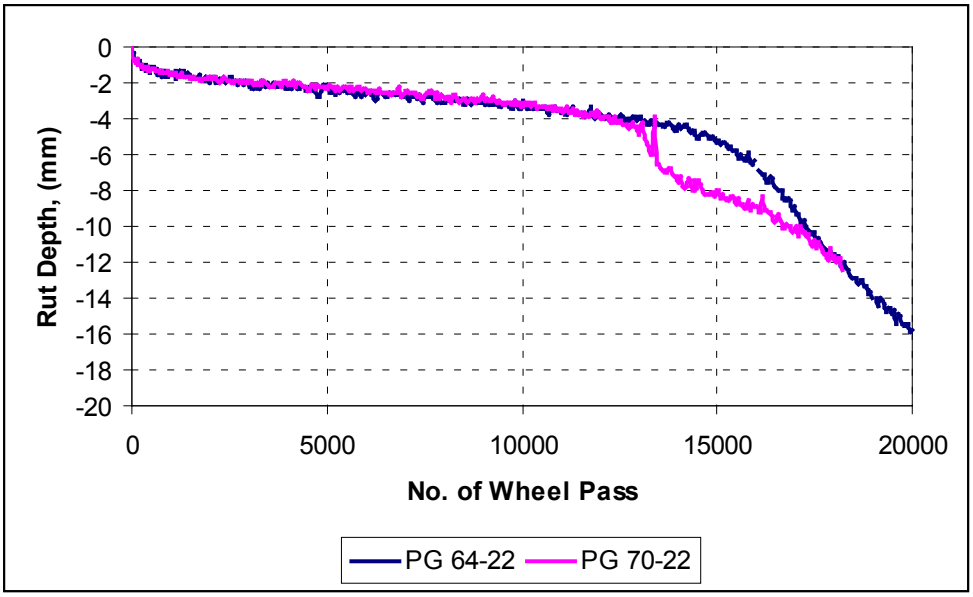

Figure B.4 HWTD performance of K-25 mixes with 35% natural sand

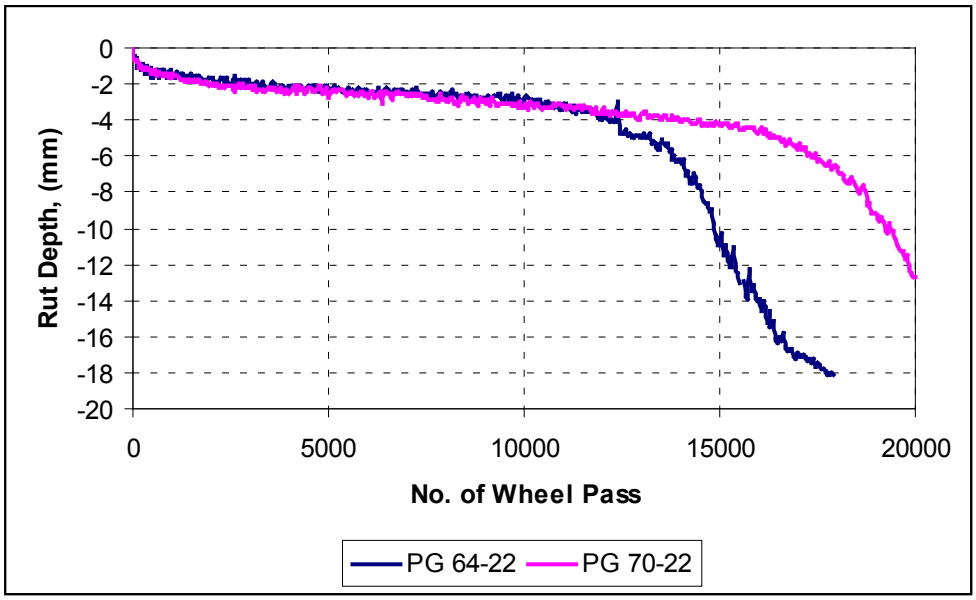

Figure B.5 HWTD performance of K-25 mixes with 25% natural sand

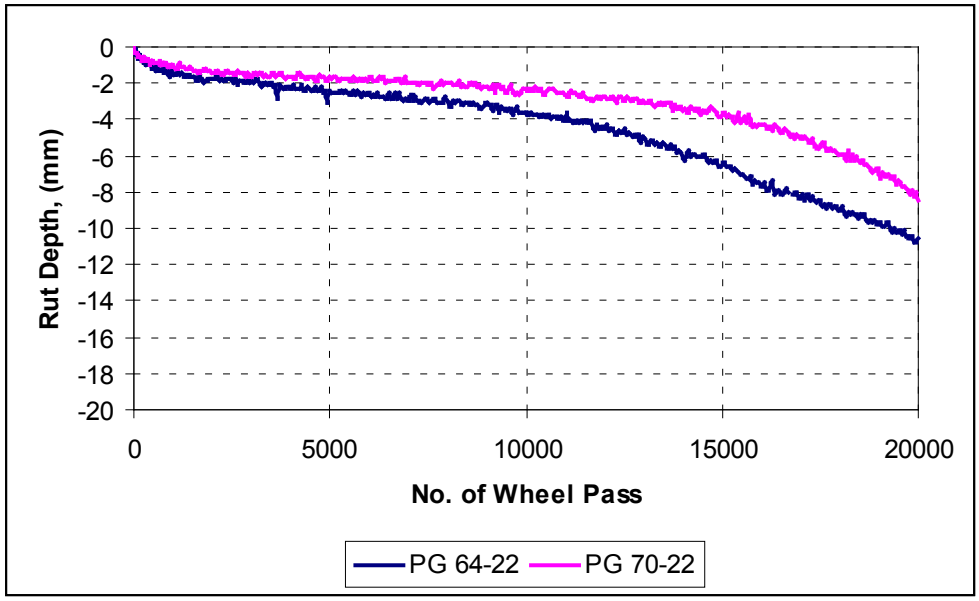

Figure B.6 HWTD performance of K-25 mixes with 15% natural sand

Table B.13 HWTD Test Output of US-160 and K-25 Mixes

Aggregate Source	PG Binder	NSC	Design Asphalt Content (%)	Creep Slope (No. of wheel pass/mm rut depth)	SIP (No. of wheel pass)	Stripping Slope (No. of wheel pass/mm rut depth)
US-160	64-22	35	7	1333	4758	259
		25	6.8	10000	13917	949
		15	6.75	5220	10050	820
	70-22	35	6.8	922	2957	250
		25	6.6	833	2817	253
		15	6.6	1185	3167	448
K-25	64-22	35	6.1	5808	9813	446
		25	5.6	5952	11833	428
		15	5.4	8472	11875	773
	70-22	35	5.7	3438	7562	631
		25	5.5	9733	16095	814
		15	5.4	9192	16095	625

Note: NSC = Natural Sand Content
SIP = Stripping Inflection Point

Table B.14 G_{mm}, G_{mb}, and Air Voids Results of KT-56 Test Specimens for US-160 Laboratory Mixes with PG 64-22

Natural Sand Content	Sample ID	Design AC (%)	G_{mb}	G_{mm}	$\%G_{mm}$ @ N_f	% V_a	Average % V_a	Target % V_a
35	S_35 HT11(C)	7	2.220	2.396	92.66	7.34	7.02	7% ± 0.5%
	S_35 HT12 (C)		2.221	2.389	92.97	7.03		
	S_35 HT13 (C)		2.228	2.389	93.27	6.73		
	S_35 HT14 (UC)		2.228	2.396	93.01	6.99		
	S_35 HT15 (UC)		2.223	2.396	92.78	7.22	7.06	
	S_35 HT16 (UC)		2.224	2.389	93.09	6.91		
25	S_25 HT11(C)	6.8	2.222	2.396	92.73	7.27	7.23	7% ± 0.5%
	S_25 HT12 (C)		2.221	2.396	92.71	7.29		
	S_25 HT13 (C)		2.227	2.403	92.67	7.33		
	S_25 HT14 (UC)		2.228	2.396	92.97	7.03		
	S_25 HT15 (UC)		2.229	2.403	92.76	7.24	7.34	
	S_25 HT16 (UC)		2.224	2.403	92.55	7.45		
15	S_15 HT11 (C)	6.75	2.244	2.406	93.27	6.73	6.79	7% ± 0.5%
	S_15 HT12 (C)		2.243	2.404	93.29	6.71		
	S_15 HT13 (C)		2.239	2.404	93.14	6.86		
	S_15 HT14 (UC)		2.241	2.406	93.13	6.87		
	S_15 HT15 (UC)		2.240	2.406	93.12	6.88	6.78	
	S_15 HT16 (UC)		2.243	2.404	93.32	6.68		

Table B.15 G_{mm}, G_{mb}, and Air Voids Results of KT-56 Test Specimens for US-160 Laboratory Mixes with PG 70-22

Natural Sand Content	Sample ID	Design AC (%)	G_{mb}	G_{mm}	$\%G_{mm}$ @ N_f	% V_a	Average % V_a	Target % V_a
35	S_35 HT11(C)	7	2.218	2.385	93.01	6.99	7.12	7% ± 0.5%
	S_35 HT12 (C)		2.213	2.384	92.84	7.16		
	S_35 HT13 (C)		2.215	2.384	92.90	7.10		
	S_35 HT14 (UC)		2.212	2.385	92.74	7.26		
	S_35 HT15 (UC)		2.221	2.385	93.12	6.88	6.95	
	S_35 HT16 (UC)		2.217	2.384	92.97	7.03		
25	S_25 HT11(C)	6.8	2.233	2.39	93.45	6.55	6.67	7% ± 0.5%
	S_25 HT12 (C)		2.225	2.389	93.12	6.88		
	S_25 HT13 (C)		2.229	2.389	93.30	6.70		
	S_25 HT14 (UC)		2.234	2.39	93.45	6.55		
	S_25 HT15 (UC)		2.226	2.39	93.14	6.86	6.86	
	S_25 HT16 (UC)		2.225	2.389	93.14	6.86		
15	S_15 HT11 (C)	6.75	2.221	2.393	92.82	7.18	7.31	7% ± 0.5%
	S_15 HT12 (C)		2.219	2.393	92.72	7.28		
	S_15 HT13 (C)		2.218	2.397	92.52	7.48		
	S_15 HT14 (UC)		2.218	2.393	92.69	7.31		
	S_15 HT15 (UC)		2.224	2.397	92.80	7.20	7.30	
	S_15 HT16 (UC)		2.220	2.397	92.60	7.40		

Table B.16 G_{mm}, G_{mb}, and Air Voids Results of KT-56 Test Specimens for K-25 Laboratory Mixes with PG 64-22

Natural Sand Content	Sample ID	Design AC (%)	G_{mb}	G_{mm}	$\%G_{mm}$ @ N_f	% V_a	Average % V_a	Target % V_a
35	S_35 HT11(C)	7	2.224	2.401	92.64	7.36	7.29	7% ± 0.5%
	S_35 HT12 (C)		2.228	2.402	92.75	7.25		
	S_35 HT13 (C)		2.229	2.402	92.79	7.21		
	S_35 HT14 (UC)		2.225	2.401	92.67	7.33		
	S_35 HT15 (UC)		2.227	2.401	92.75	7.25	7.27	
	S_35 HT16 (UC)		2.227	2.402	92.72	7.28		
25	S_25 HT11(C)	6.8	2.235	2.406	92.89	7.11	7.12	7% ± 0.5%
	S_25 HT12 (C)		2.235	2.406	92.88	7.12		
	S_25 HT13 (C)		2.245	2.419	92.80	7.20		
	S_25 HT14 (UC)		2.236	2.406	92.94	7.06		
	S_25 HT15 (UC)		2.245	2.419	92.81	7.19	7.19	
	S_25 HT16 (UC)		2.245	2.419	92.81	7.19		
15	S_15 HT11 (C)	6.75	2.242	2.401	93.38	6.62	6.81	7% ± 0.5%
	S_15 HT12 (C)		2.246	2.416	92.95	7.05		
	S_15 HT13 (C)		2.246	2.416	92.96	7.04		
	S_15 HT14 (UC)		2.245	2.401	93.48	6.52		
	S_15 HT15 (UC)		2.240	2.401	93.31	6.69	7.05	
	S_15 HT16 (UC)		2.237	2.416	92.59	7.41		

Table B.17 G_{mm}, G_{mb}, and Air Voids Results of KT-56 Test Specimens for K-25 Laboratory Mixes with PG 70-22

Natural Sand Content	Sample ID	Design AC (%)	G_{mb}	G_{mm}	$\%G_{mm}$ @ N_f	% V_a	Average % V_a	Target % V_a
35	S_35 HT11(C)	7	2.244	2.421	92.70	7.30	7.24	7% ± 0.5%
	S_35 HT12 (C)		2.242	2.417	92.77	7.23		
	S_35 HT13 (C)		2.242	2.417	92.75	7.25		
	S_35 HT14 (UC)		2.247	2.421	92.81	7.19		
	S_35 HT15 (UC)		2.244	2.421	92.70	7.30	7.30	
	S_35 HT16 (UC)		2.240	2.417	92.69	7.31		
25	S_25 HT11(C)	6.8	2.245	2.418	92.83	7.17	7.23	7% ± 0.5%
	S_25 HT12 (C)		2.243	2.419	92.74	7.26		
	S_25 HT13 (C)		2.242	2.419	92.69	7.31		
	S_25 HT14 (UC)		2.244	2.418	92.82	7.18		
	S_25 HT15 (UC)		2.242	2.418	92.71	7.29	7.29	
	S_25 HT16 (UC)		2.243	2.419	92.71	7.29		
15	S_15 HT11 (C)	6.75	2.248	2.424	92.74	7.26	7.14	7% ± 0.5%
	S_15 HT12 (C)		2.248	2.42	92.90	7.10		
	S_15 HT13 (C)		2.250	2.42	92.97	7.03		
	S_15 HT14 (UC)		2.250	2.424	92.84	7.16		
	S_15 HT15 (UC)		2.248	2.424	92.72	7.28	7.13	
	S_15 HT16 (UC)		2.251	2.42	93.02	6.98		

Table B.18 Thickness, Diameter, and Indirect Tensile Strength of KT-56, US-160 Laboratory Mixes

Sample ID		Thickness, T (mm)			AVG. T (mm)	Diameter, D (mm)			AVG. D (mm)	Load (N)	Tensile Strength, S_t, (kPa)	AVG. St, (kPa)	TSR, (%)
KS_35 C (PG 64-22)	1	97.88	97.88	97.88	97.88	150.15	150.23	150.18	150.19	18832.83	816	865	103
	4	98.02	97.83	97.88	97.91	150.16	150.28	150.19	150.21	19837.64	859		
	5	97.77	97.69	97.93	97.80	150.30	150.29	150.30	150.30	21268.11	921		
KS_35 UC (PG 64-22)	2	97.67	97.66	97.74	97.69	150.04	150.07	150.08	150.06	20855.78	906	841	
	3	97.67	97.70	97.66	97.68	150.16	150.28	150.30	150.25	17524.23	760		
	6	97.71	97.81	97.69	97.74	150.08	150.12	150.13	150.11	19727.32	856		
KS_25 C (PG 64-22)	1	97.89	97.95	97.88	97.91	150.47	150.36	150.26	150.36	17082.10	739	760	95
	2	97.89	97.94	97.92	97.92	150.56	150.45	150.11	150.37	17525.12	758		
	4	97.83	97.82	97.77	97.81	150.23	150.31	150.21	150.25	18085.57	783		
KS_25 UC (PG 64-22)	3	97.62	97.70	97.65	97.66	150.09	150.22	150.29	150.20	16467.83	715	799	
	5	97.89	98.00	98.01	97.97	150.04	150.15	150.13	150.11	19474.23	843		
	6	97.73	97.78	97.73	97.75	150.24	150.14	150.11	150.16	19339.90	839		
KS_15 C (PG 64-22)	1	98.00	98.04	98.13	98.06	150.33	150.27	150.20	150.27	18533.48	801	809	75
	3	98.02	98.17	97.99	98.06	150.21	150.27	150.32	150.27	16318.82	705		
	4	98.14	98.16	98.03	98.11	150.16	150.27	150.21	150.21	21341.95	922		
KS_15 UC (PG 64-22)	2	98.00	97.99	97.91	97.97	150.14	150.30	150.15	150.20	21358.41	924	1075	
	5	97.92	97.87	97.86	97.88	150.20	150.20	150.03	150.14	28007.28	1213		
	6	98.15	98.30	97.97	98.14	150.14	150.11	150.10	150.12	25148.99	1087		
KS_35 C (PG 70-22)	1	97.98	97.86	97.72	97.85	150.41	150.38	150.41	150.40	18650.91	807	813	88
	3	97.63	97.75	97.61	97.66	150.59	150.36	150.21	150.39	19757.13	856		
	5	97.75	97.93	97.81	97.83	150.48	150.37	150.13	150.33	17925.88	776		
KS_35 UC (PG 70-22)	2	97.67	97.65	97.67	97.66	150.12	150.21	150.23	150.19	21752.05	944	926	
	4	97.71	97.70	97.70	97.70	150.10	150.22	150.26	150.19	21490.07	932		
	6	97.93	97.64	97.63	97.73	150.17	150.25	150.22	150.21	20810.86	902		
KS_25 C (PG 70-22)	2	97.72	97.61	97.61	97.65	150.14	150.20	150.35	150.23	19097.93	829	803	94
	3	97.76	97.96	97.82	97.85	150.35	150.27	150.19	150.27	18573.96	804		
	4	97.54	97.57	97.61	97.57	150.23	150.38	150.21	150.27	17854.27	775		
KS_25 UC (PG 70-22)	1	97.47	97.48	97.63	97.53	150.15	150.17	150.18	150.17	18872.86	820	854	
	5	97.73	97.69	97.71	97.71	150.27	150.24	150.11	150.21	20158.78	874		
	6	97.57	97.62	97.62	97.60	150.28	150.19	150.15	150.21	19952.39	866		
KS_15 C (PG 70-22)	1	98.06	98.01	98.06	98.04	150.12	150.16	150.12	150.13	19560.97	846	880	95
	3	98.00	98.01	97.99	98.00	150.11	150.10	150.27	150.16	19859.88	859		
	4	97.98	98.04	97.89	97.97	150.20	150.29	150.15	150.21	21643.52	936		
KS_15 UC (PG 70-22)	2	98.12	98.09	97.93	98.05	150.18	150.17	150.11	150.15	19911.47	861	930	
	5	97.95	97.97	97.78	97.90	150.13	150.10	150.08	150.10	21880.60	948		
	6	97.94	97.93	97.88	97.92	150.09	150.10	150.10	150.10	22655.00	981		

Table B.19 Thickness, Diameter, and Indirect Tensile Strength of KT-56, K-25 Laboratory Mixes

Sample ID		Thickness, T (mm)			AVG. T, (mm)	Diameter, D (mm)			AVG. D, (mm)	Load (N)	Tensile Strength, S_t (kPa)	AVG. S_t, (kPa)	TSR, (%)
KS_35 C (PG 64-22)	1	97.69	97.69	97.57	97.65	150.4	151	150.4	150.47	28131.82	1219	1167	74
	2	97.5	97.6	97.52	97.54	150.5	150	150.4	150.44	27626.53	1199		
	5	97.78	97.84	97.78	97.80	150.5	151	150.5	150.50	25081.38	1085		
KS_35 UC (PG 64-22)	3	97.59	97.65	97.57	97.60	150.1	150	150	150.04	35483.03	1543	1588	
	4	97.54	97.55	97.5	97.53	150.2	150	150	150.07	36897.05	1605		
	6	97.66	97.66	97.65	97.66	150	150	149.9	149.93	37151.48	1615		
KS_25 C (PG 64-22)	1	97.91	97.88	97.89	97.89	150.6	151	150.4	150.51	24331.45	1051	1156	73
	5	97.91	97.98	98	97.96	150.2	150	150.4	150.29	28922.68	1251		
	6	98.17	97.81	97.81	97.93	150.3	151	150.4	150.43	27010.92	1167		
KS_25 UC (PG 64-22)	2	97.67	97.86	97.6	97.71	150	150	150.1	150.06	37004.69	1607	1592	
	3	97.68	97.68	97.65	97.67	150	150	150	149.98	37910.30	1648		
	4	97.73	97.6	97.63	97.65	149.9	150	149.9	149.92	35009.76	1522		
KS_15 C (PG 64-22)	1	97.78	97.74	97.68	97.73	150.3	150	150.2	150.24	25028.01	1085	1120	81
	2	97.76	97.67	97.69	97.71	150.2	150	150.1	150.16	22706.15	985		
	4	97.81	97.92	97.87	97.87	150.7	150	150.2	150.36	29842.08	1291		
KS_15 UC (PG 64-22)	3	97.63	97.63	97.66	97.64	150.2	150	150.1	150.15	27914.31	1212	1380	
	5	97.73	97.78	97.85	97.79	150	150	149.9	149.89	33747.42	1466		
	6	97.7	97.8	97.68	97.73	149.9	150	150	149.95	33654.01	1462		
KS_35 C (PG 70-22)	1	97.65	97.66	97.69	97.67	150.3	150	150.3	150.27	26250.76	1139	1037	82
	4	97.73	97.78	97.66	97.72	150.4	150	150.4	150.41	23296.84	1009		
	6	97.85	97.75	97.73	97.78	150.4	150	150.1	150.29	22203.53	962		
KS_35 UC (PG 70-22)	2	97.65	97.87	97.64	97.72	150	150	150	150.02	30140.54	1309	1265	
	3	97.71	97.82	97.75	97.76	150	150	149.9	149.94	30612.03	1329		
	5	97.72	97.65	97.74	97.70	150	150	150	150.03	26648.41	1157		
KS_25 C (PG 70-22)	3	97.66	97.63	97.74	97.68	150.2	151	150.3	150.38	23835.05	1033	983	74
	4	97.63	97.73	97.61	97.66	150.4	150	150.5	150.46	22302.27	966		
	5	97.65	97.61	97.73	97.66	150.5	150	150.2	150.32	21905.51	950		
KS_25 UC (PG 70-22)	1	97.71	97.63	97.68	97.67	150	150	150	149.99	24274.96	1055	1325	
	2	97.66	97.65	97.7	97.67	150	150	150	150.03	33556.60	1458		
	6	97.59	97.56	97.59	97.58	150.1	150	150	150.07	33604.20	1461		
KS_15 C (PG 70-22)	1	97.76	97.66	97.66	97.69	150.5	151	150.4	150.47	25850.44	1120	1053	81
	4	97.06	97.71	97.81	97.53	150.4	150	150.3	150.27	22599.40	982		
	6	97.94	97.72	97.72	97.79	150.3	150	150.1	150.22	24432.86	1059		
KS_15 UC (PG 70-22)	2	97.56	97.68	97.56	97.60	150	150	149.9	149.97	33399.14	1453	1307	
	3	97.72	97.64	97.62	97.66	150	150	150	150.03	26671.54	1159		
	5	97.56	97.54	97.67	97.59	150.1	150	150.1	150.08	30111.63	1309		

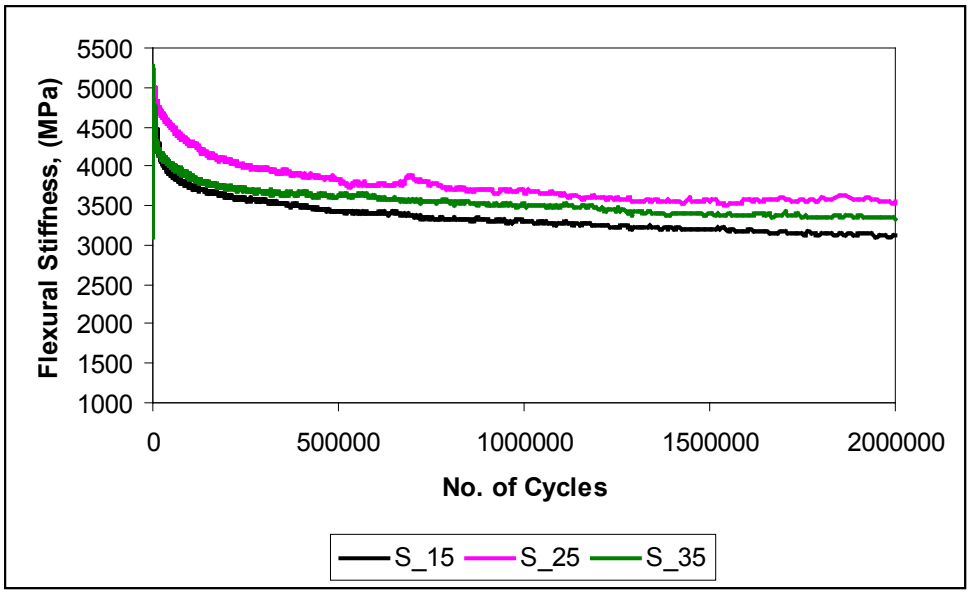

Figure B.7 Flexural stiffness variation of K-25 mixes with PG 64-22 in fatigue-beam test

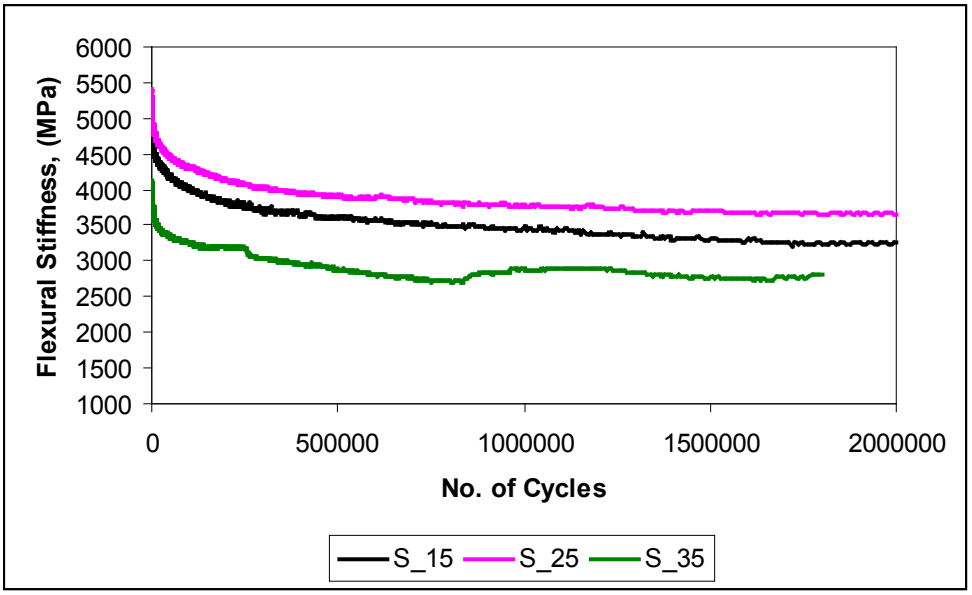

Figure B.8 Flexural stiffness variation of K-25 mixes with PG 70-22 in fatigue-beam test

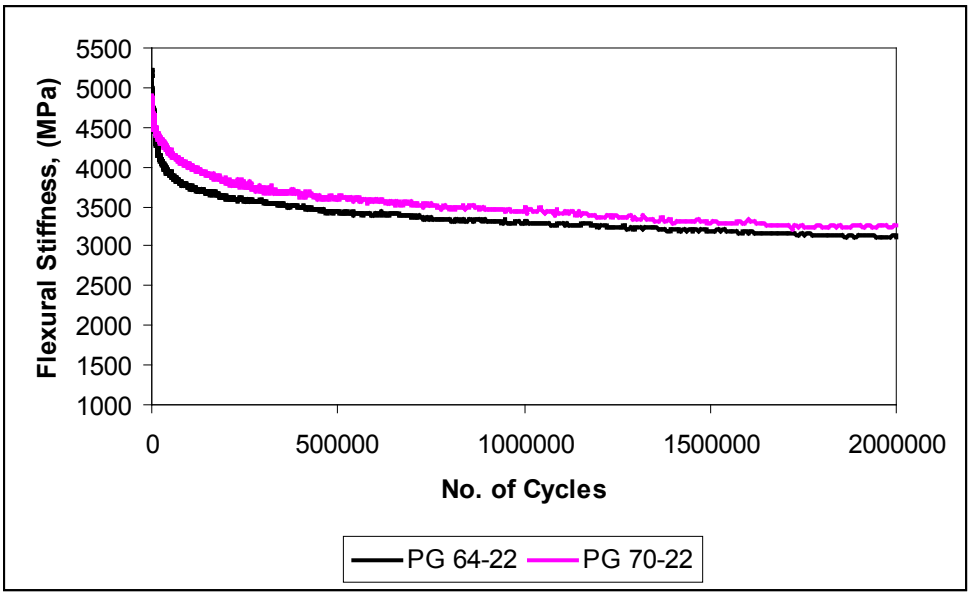

Figure B.9 Flexural stiffness variation of K-25 mixes with 15% river sand in fatigue-beam test

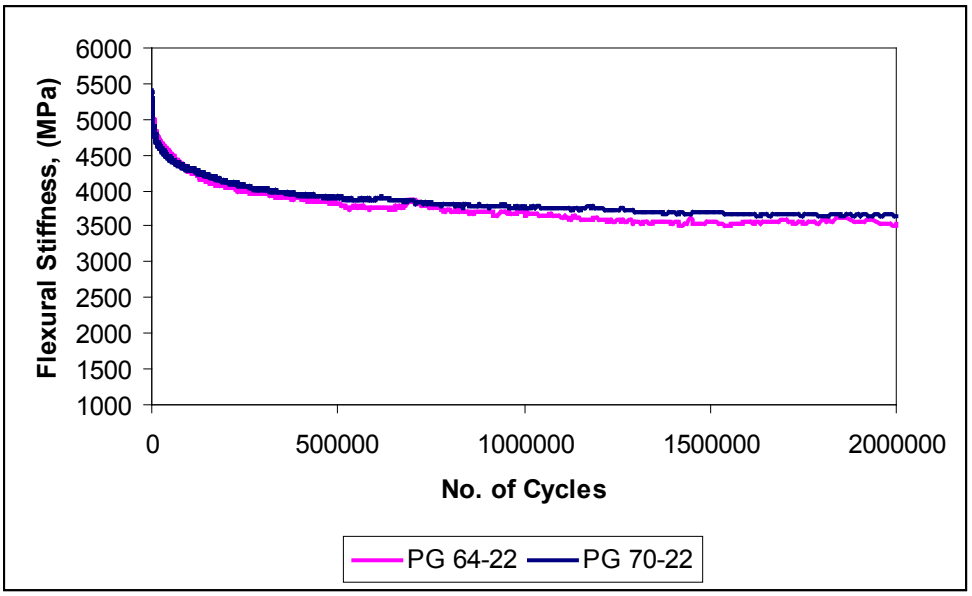

Figure B.10 Flexural stiffness variation of K-25 mixes with 25% river sand in fatigue-beam test

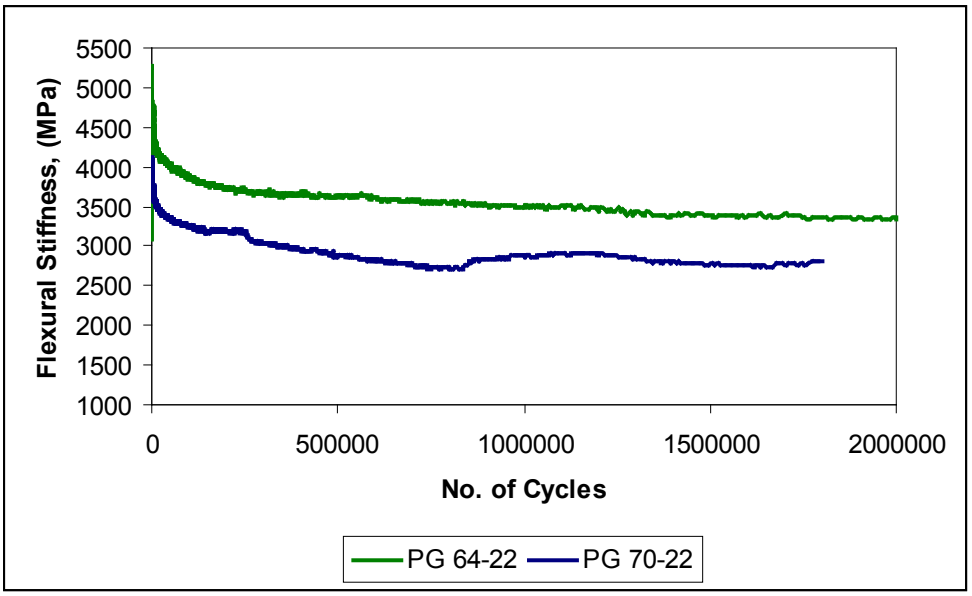

Figure B.11 Flexural stiffness variation of K-25 mixes with 25% river sand in fatigue-beam test

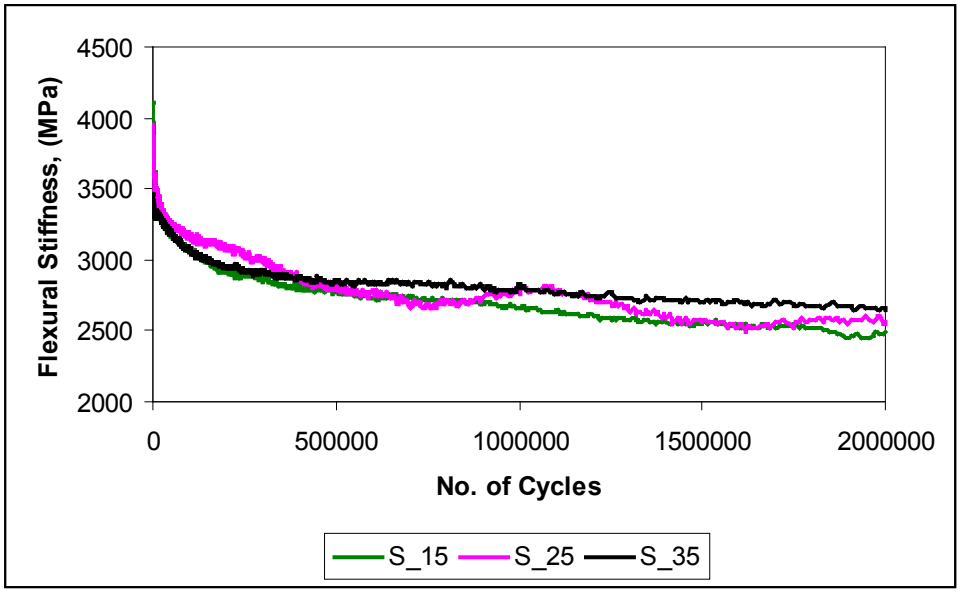

Figure B.12 Flexural stiffness variation of US-160 mixes with PG 64-22 in fatigue-beam test

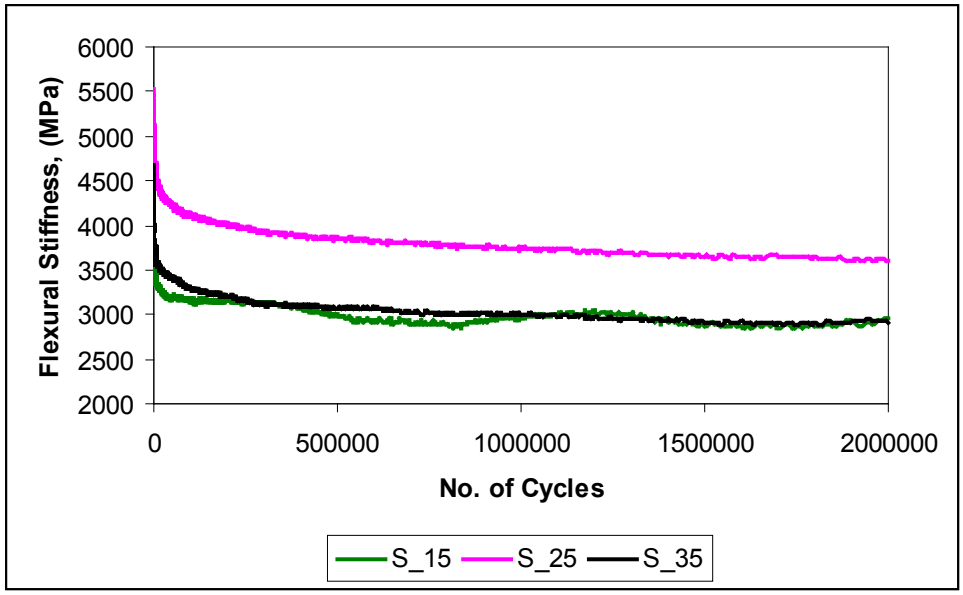

Figure B.13 Flexural stiffness variation of US-160 mixes with PG 70-22 in fatigue-beam test

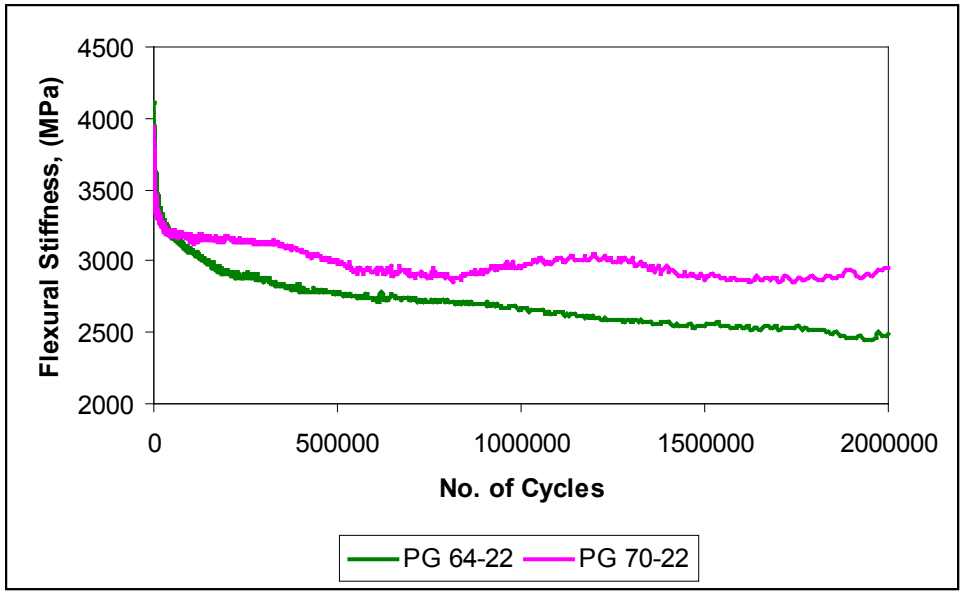

Figure B.14 Flexural stiffness variation of US-160 mixes with 15% river sand in fatigue-beam

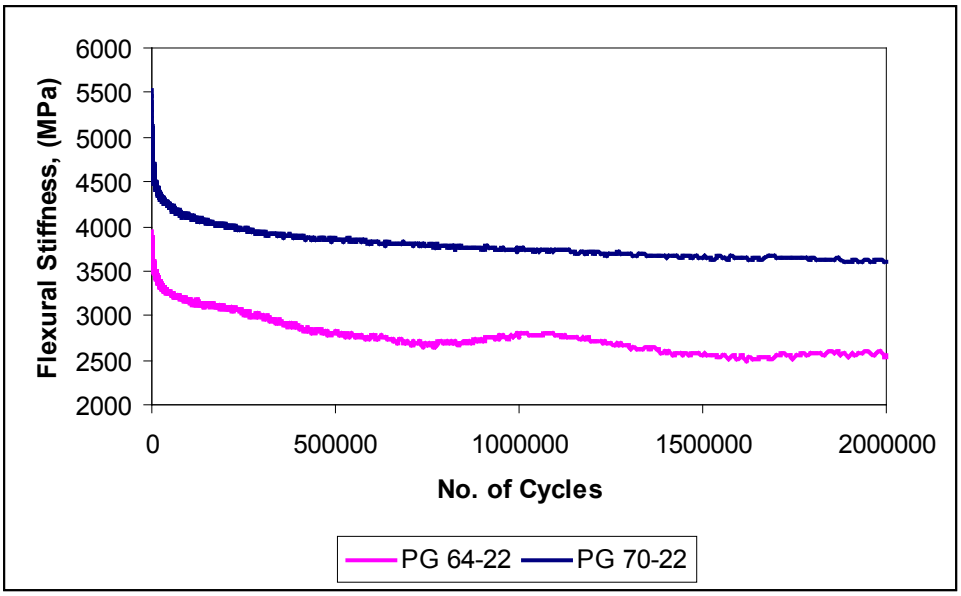

Figure B.15 Flexural stiffness variation of US-160 mixes with 25% river sand in fatigue-beam

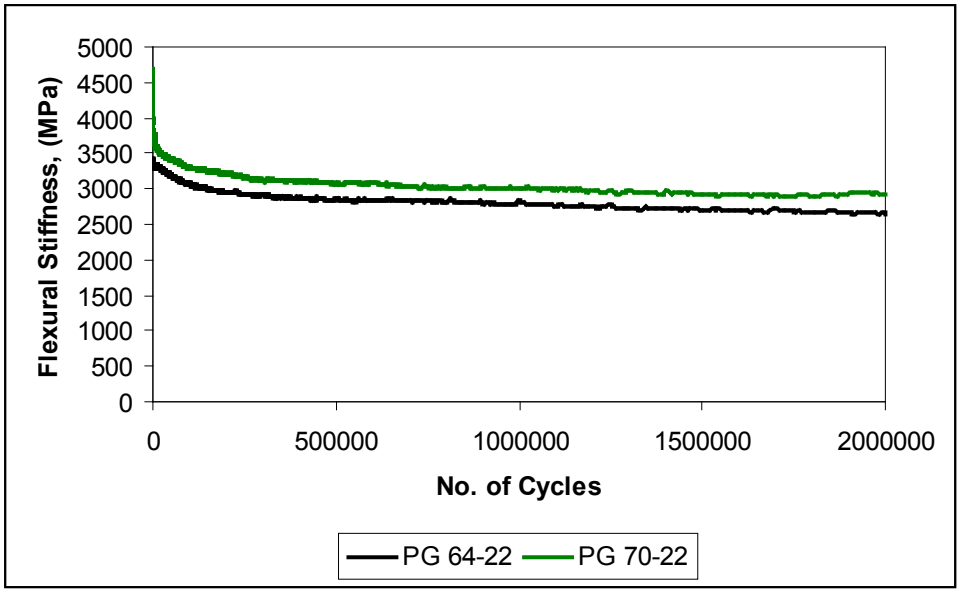

Figure B.16 Flexural stiffness variation of US-160 mixes with 35% river sand in fatigue-beam

Appendix C - Statistical Analysis of Laboratory 4.75-mm NMAS Mixture (SAS Input/Output Files)

Determination of Significant Volumetric Parameter by ANOVA

```
data;
input AGG PG NSR AC;
cards;
1 3 35 7.00
1 3 25 6.80
1 3 15 6.75
1 4 35 6.80
1 4 25 6.60
1 4 15 6.60
2 3 35 6.10
2 3 25 5.60
2 3 15 5.40
2 4 35 5.70
2 4 25 5.50
2 4 15 5.40
;
proc glm;
title ‘GLM W Interaction’;
class AGG PG NSR;
model AC = AGG PG NSR AGG*PG PG*NSR NSR*AGG;
run;

proc glm;
title ‘GLM W/O Interaction’;
class AGG PG NSR;
model AC = AGG PG NSR;
run;
```

ANOVA Output File for Design Asphalt Content

The SAS System 16:11 Sunday, July 30, 2006 11

The REG Procedure
Model: MODEL1
Dependent Variable: AC

Number of Observations Read 12
Number of Observations Used 12

Analysis of Variance

Source	DF	Sum of Squares	Mean Square	F Value	Pr > F
Model	3	4.26490	1.42163	107.57	<.0001
Error	8	0.10573	0.01322		
Corrected Total	11	4.37062			

Root MSE	0.11496	R-Square	0.9758
Dependent Mean	6.18750	Adj R-Sq	0.9667
Coeff Var	1.85796		

Parameter Estimates

Variable	DF	Parameter Estimate	Standard Error	t Value	Pr > |t|
Intercept	1	6.39271	0.11674	54.76	<.0001
AGG	1	-1.14167	0.06637	-17.20	<.0001
PG	1	-0.17500	0.06637	-2.64	0.0299
NSR	1	0.01812	0.00406	4.46	0.0021

Determination of Significant Volumetric Parameter by MANOVA

```
data;
input AGG PG NSR AC VMA VFA Gmm DP EAC;
cards;
0   0   35  7    16.123 73.136 89.315 0.996   5.322
0   0   25  6.8 15.32   74.243 87.837 1.099   5.096
0   0   15  6.75     15.643 73.397 85.533 1.211   4.79
0   1   35  6.8 15.631 73.993 89.431 1.019   5.2
0   1   25  6.6 15.265 74.016 87.891 1.105   5.069
0   1   15  6.6 15.279 73.346 85.599 1.153   5.029
1   0   35  6.1 16.491 78.87   89.993 1.197   5.847
1   0   25  5.6 16.036 75.093 89.354 1.478   5.478
1   0   15  5.4 15.651 74.716 88.956 1.526   5.243
1   1   35  5.7 15.472 78  90.373 1.299   5.388
1   1   25  5.5 16.266 70.734 88.394 1.541   5.191
1   1   15  5.4 15  75.7     89.577 1.589   5.033
;
proc print;
run;

proc reg;
model AC VMA VFA Gmm DP EAC = AGG PG NSR;
mtest / details print;
run;
```

MANOVA Output File

The SAS System 16:11 Sunday, July 30, 2006 1

Obs	AGG	PG	NSR	AC	VMA	VFA	Gmm	DP	EAC
1	0	0	35	7.00	16.123	73.136	89.315	0.996	5.322
2	0	0	25	6.80	15.320	74.243	87.837	1.099	5.096
3	0	0	15	6.75	15.643	73.397	85.533	1.211	4.790
4	0	1	35	6.80	15.631	73.993	89.431	1.019	5.200
5	0	1	25	6.60	15.265	74.016	87.891	1.105	5.069
6	0	1	15	6.60	15.279	73.346	85.599	1.153	5.029
7	1	0	35	6.10	16.491	78.870	89.993	1.197	5.847
8	1	0	25	5.60	16.036	75.093	89.354	1.478	5.478
9	1	0	15	5.40	15.651	74.716	88.956	1.526	5.243
10	1	1	35	5.70	15.472	78.000	90.373	1.299	5.388
11	1	1	25	5.50	16.266	70.734	88.394	1.541	5.191
12	1	1	15	5.40	15.000	75.700	89.577	1.589	5.033

The SAS System 16:11 Sunday, July 30, 2006 2

The REG Procedure
Model: MODEL1
Dependent Variable: AC

Number of Observations Read 12
Number of Observations Used 12

Analysis of Variance

Source	DF	Sum of Squares	Mean Square	F Value	Pr > F
Model	3	4.26490	1.42163	107.57	<.0001
Error	8	0.10573	0.01322		
Corrected Total	11	4.37062			

Root MSE	0.11496	R-Square	0.9758
Dependent Mean	6.18750	Adj R-Sq	0.9667
Coeff Var	1.85796		

Parameter Estimates

Variable	DF	Parameter Estimate	Standard Error	t Value	Pr > |t|
Intercept	1	6.39271	0.11674	54.76	<.0001
AGG	1	-1.14167	0.06637	-17.20	<.0001
PG	1	-0.17500	0.06637	-2.64	0.0299
NSR	1	0.01812	0.00406	4.46	0.0021

The REG Procedure
Model: MODEL1
Dependent Variable: VMA

Number of Observations Read	12
Number of Observations Used	12

Analysis of Variance

Source	DF	Sum of Squares	Mean Square	F Value	Pr > F
Model	3	1.26344	0.42115	3.26	0.0806
Error	8	1.03353	0.12919		
Corrected Total	11	2.29698			

Root MSE	0.35943	R-Square	0.5500
Dependent Mean	15.68142	Adj R-Sq	0.3813
Coeff Var	2.29209		

Parameter Estimates

Variable	DF	Parameter Estimate	Standard Error	t Value	Pr > |t|
Intercept	1	15.06942	0.36501	41.29	<.0001
AGG	1	0.27583	0.20752	1.33	0.2204
PG	1	-0.39183	0.20752	-1.89	0.0957
NSR	1	0.02680	0.01271	2.11	0.0680

The REG Procedure
Model: MODEL1
Dependent Variable: VFA

Number of Observations Read	12
Number of Observations Used	12

Analysis of Variance

Source	DF	Sum of Squares	Mean Square	F Value	Pr > F
Model	3	17.01852	5.67284	1.29	0.3425
Error	8	35.18665	4.39833		
Corrected Total	11	52.20517			

Root MSE	2.09722	R-Square	0.3260
Dependent Mean	74.60367	Adj R-Sq	0.0732
Coeff Var	2.81115		

Parameter Estimates

Variable	DF	Parameter Estimate	Standard Error	t Value	Pr > |t|
Intercept	1	71.85650	2.12974	33.74	<.0001
AGG	1	1.83033	1.21083	1.51	0.1691
PG	1	-0.61100	1.21083	-0.50	0.6274
NSR	1	0.08550	0.07415	1.15	0.2822

The REG Procedure
Model: MODEL1
Dependent Variable: Gmm

Number of Observations Read	12
Number of Observations Used	12

Analysis of Variance

Source	DF	Sum of Squares	Mean Square	F Value	Pr > F
Model	3	21.32076	7.10692	9.35	0.0054
Error	8	6.07983	0.75998		
Corrected Total	11	27.40059			

Root MSE	0.87177	R-Square	0.7781
Dependent Mean	88.52108	Adj R-Sq	0.6949
Coeff Var	0.98481		

Parameter Estimates

Variable	DF	Parameter Estimate	Standard Error	t Value	Pr > |t|
Intercept	1	84.62573	0.88528	95.59	<.0001
AGG	1	1.84017	0.50332	3.66	0.0064
PG	1	0.04617	0.50332	0.09	0.9292
NSR	1	0.11809	0.03082	3.83	0.0050

The REG Procedure
Model: MODEL1
Dependent Variable: DP

Number of Observations Read	12
Number of Observations Used	12

Analysis of Variance

Source	DF	Sum of Squares	Mean Square	F Value	Pr > F
Model	3	0.46961	0.15654	38.88	<.0001
Error	8	0.03221	0.00403		
Corrected Total	11	0.50182			

Root MSE	0.06345	R-Square	0.9358
Dependent Mean	1.26775	Adj R-Sq	0.9117
Coeff Var	5.00531		

Parameter Estimates

Variable	DF	Parameter Estimate	Standard Error	t Value	Pr > |t|
Intercept	1	1.38308	0.06444	21.46	<.0001
AGG	1	0.34117	0.03664	9.31	<.0001
PG	1	0.03317	0.03664	0.91	0.3917
NSR	1	-0.01210	0.00224	-5.39	0.0007

The REG Procedure
Model: MODEL1
Dependent Variable: EAC

Number of Observations Read	12
Number of Observations Used	12

Analysis of Variance

Source	DF	Sum of Squares	Mean Square	F Value	Pr > F
Model	3	0.64130	0.21377	11.17	0.0031
Error	8	0.15314	0.01914		
Corrected Total	11	0.79444			

Root MSE	0.13836	R-Square	0.8072
Dependent Mean	5.22383	Adj R-Sq	0.7349
Coeff Var	2.64858		

Parameter Estimates

Variable	DF	Parameter Estimate	Standard Error	t Value	Pr > |t|
Intercept	1	4.63712	0.14050	33.00	<.0001
AGG	1	0.27900	0.07988	3.49	0.0082
PG	1	-0.14433	0.07988	-1.81	0.1084
NSR	1	0.02078	0.00489	4.25	0.0028

The REG Procedure
Model: MODEL1
Multivariate Test 1

L Ginv(X'X) L' LB-cj

0.3333333333	0	0	-1.141666667	0.2758333333
0	0.3333333333	0	-0.175	-0.391833333
0	0	0.00125	0.018125	0.0268

L Ginv(X'X) L' LB-cj

1.8303333333	1.8401666667	0.3411666667	0.279
-0.611	0.0461666667	0.0331666667	-0.144333333
0.0855	0.1180875	-0.0121	0.020775

Inv(L Ginv(X'X) L') Inv()(LB-cj)

3	0	0	-3.425	0.8275
0	3	0	-0.525	-1.1755
0	0	800	14.5	21.44

Inv(L Ginv(X'X) L') Inv()(LB-cj)

5.491	5.5205	1.0235	0.837
-1.833	0.1385	0.0995	-0.433
68.4	94.47	-9.68	16.62

Error Matrix (E)

0.1057291667	0.0791791667	0.8730666667	-0.355747917	-0.038329167	0.0510375
0.0791791667	1.03353475	-3.852139667	-1.603139417	0.02946125	0.0748545
0.8730666667	-3.852139667	35.186651333	2.7551046667	-0.833873667	0.8191033333
-0.355747917	-1.603139417	2.7551046667	6.079826625	0.0815220833	-0.131961417
-0.038329167	0.02946125	-0.833873667	0.0815220833	0.0322120833	-0.047940833
0.0510375	0.0748545	0.8191033333	-0.131961417	-0.047940833	0.1531418333

Hypothesis Matrix (H)

4.2648958333	-0.350416667	-4.708366667	-4.614539583	-1.361358333	-0.5785625
-0.350416667	1.2634441667	4.0659513333	4.000265	-0.016096	0.8459523333
-4.708366667	4.0659513333	17.018523333	18.096916667	0.9849116667	3.217562
-4.614539583	4.000265	18.096916667	21.320760292	0.7449171667	3.4828435833
-1.361358333	-0.016096	0.9849116667	0.7449171667	0.4696121667	0.0700933333
-0.5785625	0.8459523333	3.217562	3.4828435833	0.0700933333	0.6412998333

Hypothesis + Error Matrix (T)

4.370625	-0.2712375	-3.8353	-4.9702875	-1.3996875	-0.527525
-0.2712375	2.2969789167	0.2138116667	2.3971255833	0.01336525	0.9208068333
-3.8353	0.2138116667	52.205174667	20.852021333	0.151038	4.0366653333
-4.9702875	2.3971255833	20.852021333	27.400586917	0.82643925	3.3508821667
-1.3996875	0.01336525	0.151038	0.82643925	0.50182425	0.0221525
-0.527525	0.9208068333	4.0366653333	3.3508821667	0.0221525	0.7944416667

Eigenvectors

0.243979	-0.110439	-0.031477	0.004513	-0.580765	-0.046767
-0.197483	0.377403	0.016454	0.125761	-1.288153	-0.250994
2.269154	0.125070	0.090357	-0.020242	6.265459	0.967357
1.107248	-1.400498	-0.190507	-0.090427	3.114795	3.952835
-0.002553	-0.243655	0.140810	-0.067212	-0.204455	0
1.746831	-0.368005	0.006203	0.281421	4.591861	0

Eigenvalues

0.996143
0.946077
0.594356
3.408888E-16
-3.96586E-17
-1.09774E-15

Multivariate Statistics and F Approximations

S=3 M=1 N=0.5

Statistic	Value	F Value	Num DF	Den DF	Pr > F
Wilks' Lambda	0.00008436	13.24	18	8.9706	0.0002
Pillai's Trace	2.53657669	4.56	18	15	0.0024
Hotelling-Lawley Trace	277.30195843	61.62	18	2.6667	0.0051
Roy's Greatest Root	258.29179012	215.24	6	5	<.0001

NOTE: F Statistic for Roy's Greatest Root is an upper bound.

SAS Input File for Rutting Prediction Model

```
data abc1;
input PG CA1 CA2 NSC NWP Block$;
PGCA1 = PG*CA1;
PGCA2 = PG*CA2;
PGNSC = PG*NSC;
logNWP = log(NWP);
recipNWP = 1/NWP;
CA1sq = CA1*CA1;
PGCA1sq = PG*CA1sq;
cards;
0  32 26 35 8650  B1
0  40 28 25 20000 B1
0  45 33 15 20000 B1
1  32 26 35 6070  B1
1  40 28 25 5428  B1
1  45 33 15 11600 B1
0  32 26 35 8500  B2
0  40 28 25 20000 B2
0  45 33 15 15750 B2
1  32 26 35 5950  B2
1  40 28 25 6200  B2
1  45 33 15 7950  B2
0  32 26 35 4600  B3
0  40 28 25 20000 B3
0  45 33 15 16450 B3
1  32 26 35 5750  B3
1  40 28 25 7550  B3
1  45 33 15 7950  B3
;
proc reg data=abc1;
   model NWP = PG CA1/selection = forward;
   model NWP = PG CA2/selection = forward;
   model NWP = PG NSC/selection = forward;
run;
proc reg data=abc1;
   model NWP = PG CA1;
run;
proc reg data=abc1;
   model NWP = PG CA1 PGCA1;
run;
proc reg data=abc1;
   model NWP = PG CA2 PGCA2;
run;
proc reg data=abc1;
   model NWP = PG NSC PGNSC;
run;
proc reg data=abc1;
   model logNWP = PG CA1 PGCA1;
run;
proc reg data=abc1;
   model recipNWP = PG CA1 PGCA1;
run;
proc reg data=abc1;
   model NWP = PG CA1 PGCA1sq CA1sq;
run;
```

SAS Input File for Moisture Damage Prediction Model

```
data abc1;
input PG CA1 CA2 NSC TSR;
PGCA1 = PG*CA1;
PGCA2 = PG*CA2;
PGNSC = PG*NSC;
logTSR = log(TSR);
recipTSR = 1/TSR;
CA2sq = CA2*CA2;
PGCA2sq = PG*CA2sq;
cards;
0  32 26 35 103
0  40 28 25 95
0  45 33 15 75
1  32 26 35 88
1  40 28 25 94
1  45 33 15 95
;
proc reg data=abc1;
  model TSR = PG CA1/selection = forward;
  model TSR = PG CA2/selection = forward;
   model TSR = PG NSC/selection = forward;
run;
quit;
proc reg data=abc1;
   model TSR = PG;
   *plot r.*p.;
run;
proc reg data=abc1;
   model TSR = PG CA1 PGCA1;
   *plot r.*p.;
run;
proc reg data=abc1;
   model TSR = PG CA2;
   *plot r.*p.;
run;
proc reg data=abc1;
   model TSR = PG CA2 PGCA2;
   *plot r.*p.;
run;
proc reg data=abc1;
   model TSR = PG NSC PGNSC;
   *plot r.*p.;
run;
proc reg data=abc1;
   model logTSR = PG CA2 PGCA2;
   *plot r.*p.;
run;
proc reg data=abc1;
   model recipTSR = PG CA2 PGCA2;
   *plot r.*p.;
run;
proc reg data=abc1;
   model TSR = PG CA2 CA2sq PGCA2sq;
   *plot r.*p.;
run;
```

SAS Input File for Moisture Damage Prediction Model

```
data abc1;
input PG CA1 CA2 NSC FS Block$;
PGCA1 = PG*CA1;
PGCA2 = PG*CA2;
PGNSC = PG*NSC;
logFS = log(FS);
recipFS = 1/FS;
NSCsq = NSC*NSC;
PGNSCsq = PG*NSCsq;
cards;
0  30 33 35 25 B1
0  34 39 25 31 B1
0  40 43 15 40 B1
1  30 33 35 30 B1
1  34 39 25 28 B1
1  40 43 15 31 B1
0  30 33 35 25 B2
0  34 39 25 32 B2
0  40 43 15 35 B2
1  30 33 35 30 B2
1  34 39 25 31 B2
1  40 43 15 31 B2
;
proc reg data=abc1;
   model FS = PG CA1/selection = forward;
   model FS = PG CA2/selection = forward;
   model FS = PG NSC/selection = forward;
   run;
   quit;
proc reg data=abc1;
   model FS = PG CA1 PGCA1;
run;
proc reg data=abc1;
   model FS = PG CA2 PGCA2;
run;
proc reg data=abc1;
   model FS = PG NSC PGNSC;
run;
proc reg data=abc1;
   model FS = PG NSC;
run;
proc reg data=abc1;
   model logFS = PG NSC PGNSC;
run;

proc reg data=abc1;
   model recipFS = PG NSC PGNSC;
   *plot r.*p.;
run;
proc reg data=abc1;
   model FS = PG NSC PGNSC NSCsq PGNSCsq;
run;
quit;
```

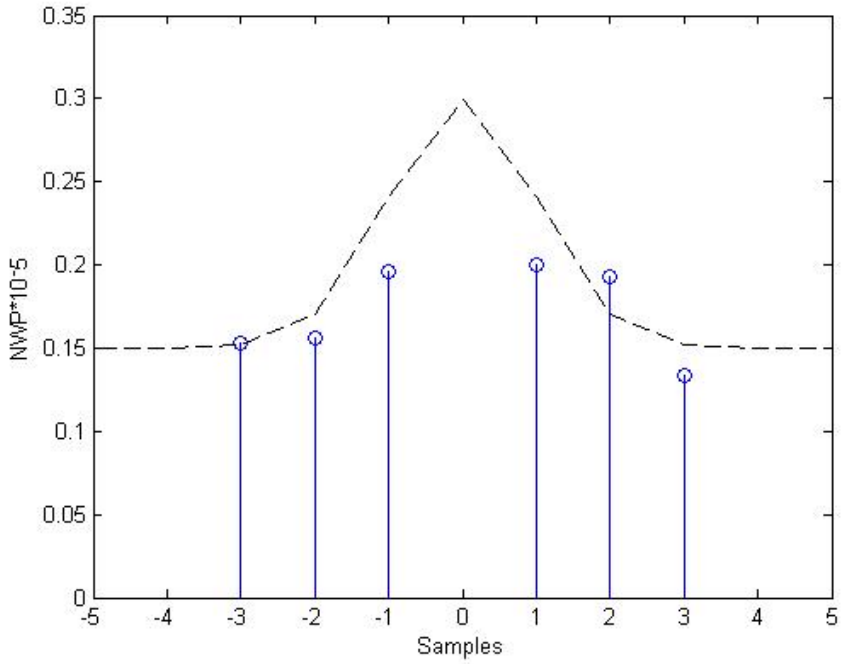

Figure C 1 Gaussian distribution of Hamburg Wheel Testing Device laboratory data with respect to aggregate subsets and binder grades on K-25

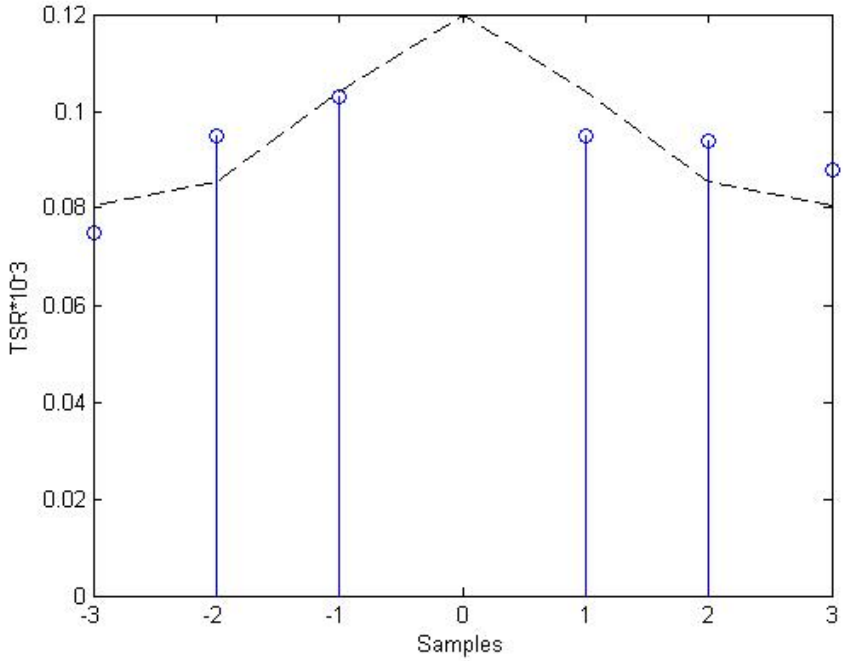

Figure C 3 Gaussian distribution of laboratory moisture susceptibility test data with respect to aggregate subsets and binder grades US-160

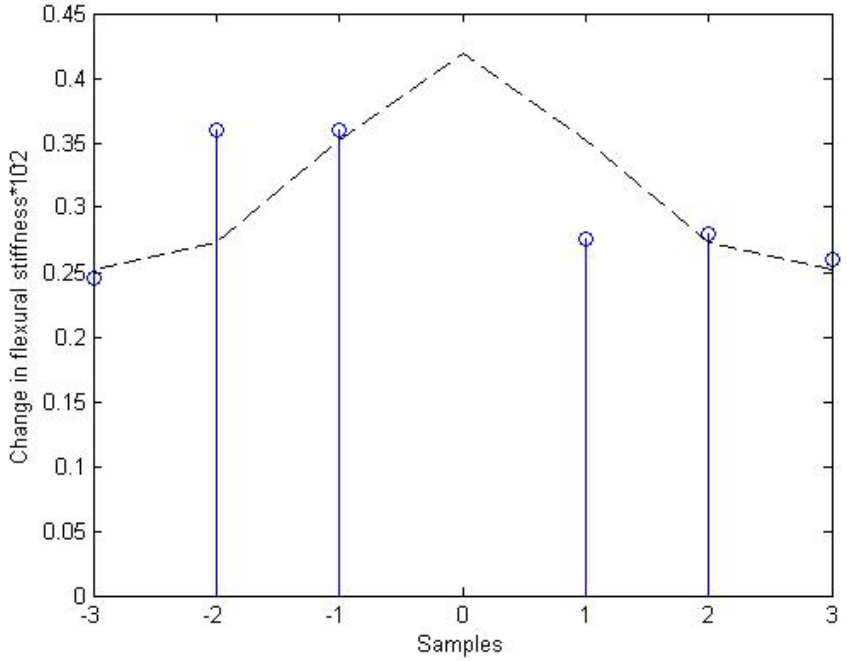

Figure C 3 Gaussian distribution of laboratory beam fatigue test data with respect to aggregate subsets and binder grades US-160

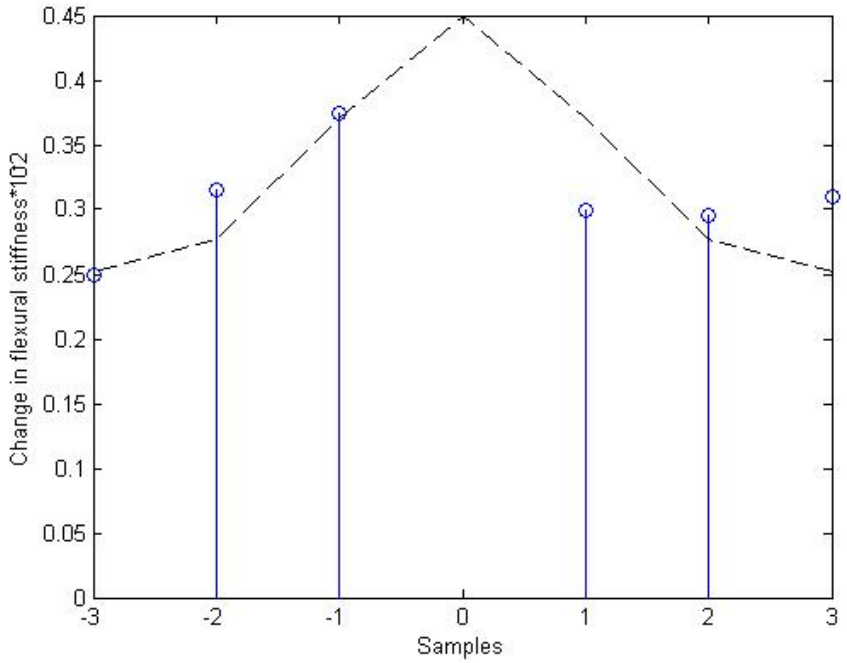

Figure C 4 Gaussian distribution of laboratory beam fatigue test data with respect to aggregate subsets and binder grades K-25

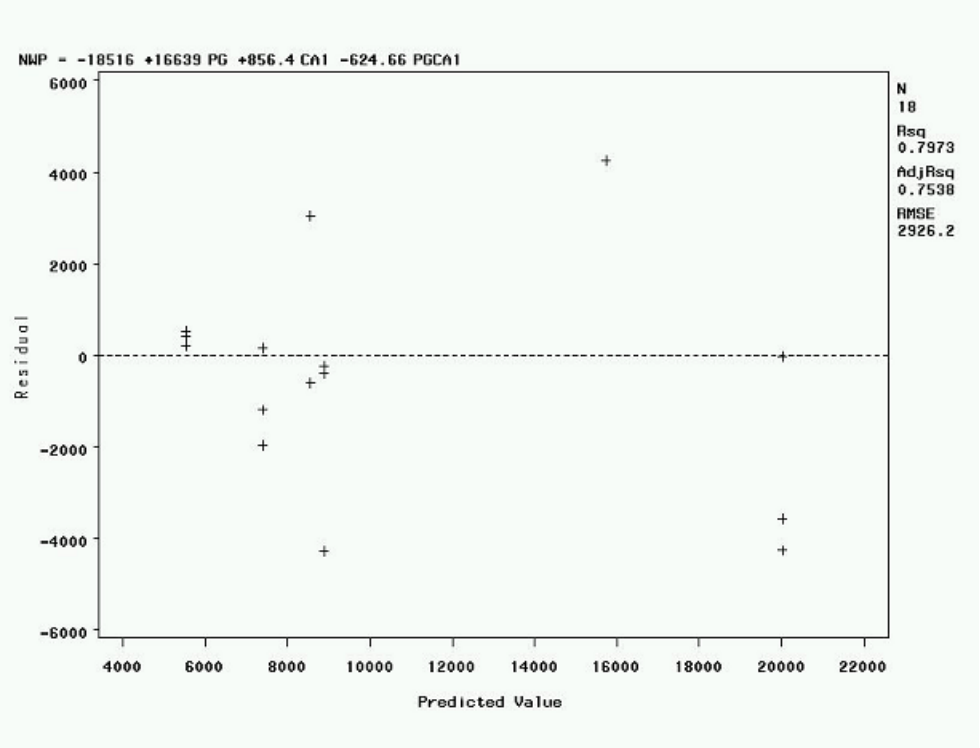

Figure C 5 Residual plot of rutting prediction model equation for US-160 mixes

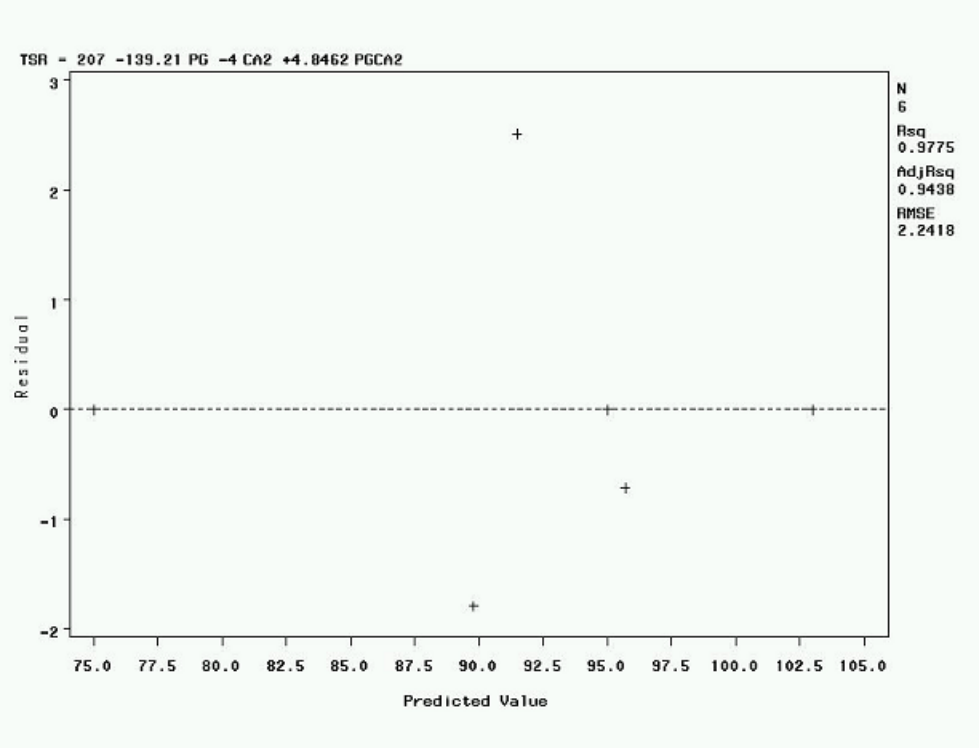

Figure C 6 Residual plot of moisture damage prediction equation for US-160 mixes

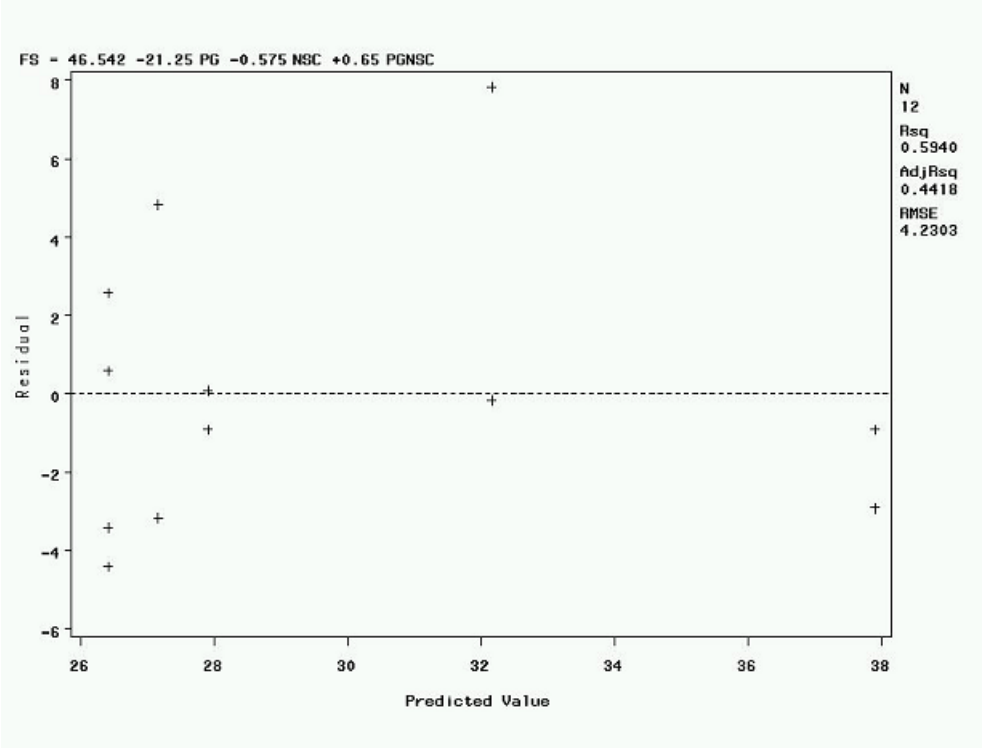

Figure C 7 Residual plot of fatigue life prediction equation for US-160 mixes

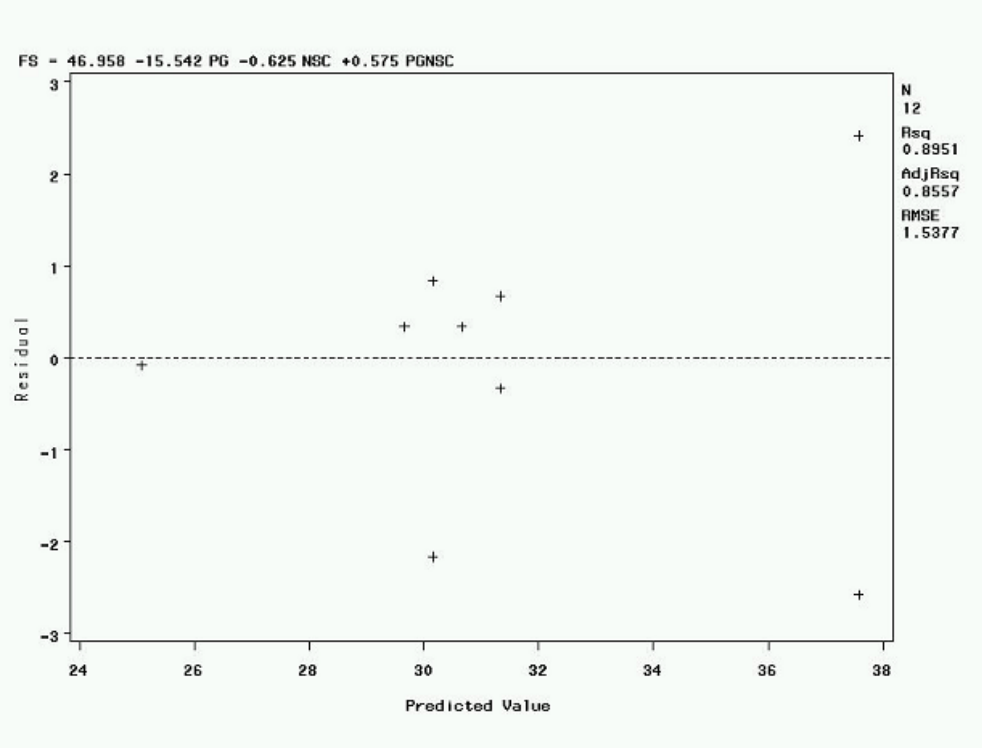

Figure C 8 Residual plot of fatigue life prediction equation for K-25 mixes

Appendix D - Multi-Objective Optimization of 4.75-mm NMAS Mixture

Optimization Input File for US-160 Mixes

```
namespace SM_475
{
   public partial class Form1 : Form
   {
      public Form1()
      {
         InitializeComponent();
      }

      private void btnOptimize_Click(object sender, EventArgs e)
      {
         //Optimize_v2();
         Optimize();
      }

      private void Optimize()
      {
         int[] upperBounds = new int[] { 1, 45, 33, 35 };
         int[] lowerBounds = new int[] { 0, 32, 26, 15 };

         int totalValue = 93;

         double minNWP = 20000;
         double minTSR = 80;
         //double maxTSR = 100;
         double maxFS = 50;
         //double minFS = 0;

         StreamWriter writer = new StreamWriter("output.txt");
         writer.WriteLine("PG, CA1, CA2, NSC, TSR, NWP, FS, TSR_Accept, NWP_Accept, FS_Accept, ALL_Accept");

         for (int pgCount = lowerBounds[0]; pgCount <= upperBounds[0]; pgCount = pgCount + 1)
```

```
        {
            for (int ca1Count = lowerBounds[1]; ca1Count <= upperBounds[1]; ca1Count++)
            {
                for (int ca2Count = lowerBounds[2]; ca2Count <= upperBounds[2]; ca2Count++)
                {
                    for (int nscCount = lowerBounds[3]; nscCount <= upperBounds[3]; nscCount++)
                    {
                        if (ca1Count + ca2Count + nscCount != totalValue) continue;

                        //double TSR = 207 - 139.205 * pgCount - 4 * ca2Count + 4.846 * pgCount * ca2Count;
                        //double NWP = -18516 + 16639 * pgCount + 856.395 * ca1Count - 624.66 * pgCount * ca1Count;
                        //double FS = 46.4167 - 21.25 * pgCount - 0.575 * nscCount + 0.65 * pgCount * nscCount;

                        double TSR = 207 - 139.205 * pgCount - 4 * ca2Count + 4.846 * pgCount * ca2Count;
                        double NWP = -18516 + 16639 * pgCount + 856.395 * ca1Count - 624.66 * pgCount * ca1Count;
                        double FS = 46.54 - 21.25 * pgCount - 0.575 * nscCount + 0.65 * pgCount * nscCount;

                        int NWP_Accept = (NWP >= minNWP) ? 1 : 0;
                        int TSR_Accept = (TSR >= minTSR) ? 1 : 0;
                        int FS_Accept = (FS <= maxFS) ? 1 : 0;

                        int ALL_Accept = ((NWP_Accept == 1) && (TSR_Accept == 1) && (FS_Accept == 1)) ? 1 : 0;

                        writer.WriteLine("{0}, {1}, {2}, {3}, {4}, {5}, {6}, {7}, {8}, {9}, {10}",
                            pgCount, ca1Count, ca2Count, nscCount, TSR, NWP, FS, TSR_Accept, NWP_Accept, FS_Accept,
ALL_Accept);
                    }
                }
            }
        }
        writer.Close();

    }
```

Optimization Input File for K-25 Mixes

```
private void Optimize_v2()
      {
         int[] upperBounds = new int[] { 1, 40, 43, 35 };
         int[] lowerBounds = new int[] { 0, 30, 33, 15 };

         int totalValue = 98;

         double minNWP = 20000;
         //double minTSR = 80;
         //double maxTSR = 100;
         double maxFS = 50;
         //double minFS = 0;

         StreamWriter writer = new StreamWriter("output_v2.txt");
         writer.WriteLine("PG, CA1, CA2, NSC, NWP, FS, NWP_Accept, FS_Accept, ALL_Accept");

         for (int pgCount = lowerBounds[0]; pgCount <= upperBounds[0]; pgCount = pgCount + 1)
         {
            for (int ca1Count = lowerBounds[1]; ca1Count <= upperBounds[1]; ca1Count++)
            {
               for (int ca2Count = lowerBounds[2]; ca2Count <= upperBounds[2]; ca2Count++)
               {
                  for (int nscCount = lowerBounds[3]; nscCount <= upperBounds[3]; nscCount++)
                  {
                     if (ca1Count + ca2Count + nscCount != totalValue) continue;

                     //double TSR = 207 - 139.205 * pgCount - 4 * ca2Count + 4.846 * pgCount * ca2Count;
                     //double NWP = 24056 - 274.75 * nscCount;
                     //double FS = 46.95833 - 15.54167 * pgCount - 0.625 * nscCount + 0.575 * pgCount * nscCount;
                     double NWP = -3791.03 + 547.26 * ca2Count;
                     double FS = 46.95833 - 15.54167 * pgCount - 0.625 * nscCount + 0.575 * pgCount * nscCount;
```

```
                    int NWP_Accept = (NWP >= minNWP) ? 1 : 0;
                    //int TSR_Accept = (TSR >= minTSR) ? 1 : 0;
                    int FS_Accept = (FS <= maxFS) ? 1 : 0;

                    int ALL_Accept = ((NWP_Accept == 1) && (FS_Accept == 1)) ? 1 : 0;

                    writer.WriteLine("{0}, {1}, {2}, {3}, {4}, {5}, {6}, {7}, {8}",
                       pgCount, ca1Count, ca2Count, nscCount, NWP, FS, NWP_Accept, FS_Accept, ALL_Accept);
                }
            }
        }
    }
    writer.Close();

  }
 }
}
```

Optimization Output File for US-160 Mixes

SL_NO	PG	CA1	CA2	NSC	TSR	NWP	FS	TSR Accept	NWP Accept	FS Accept	ALL Accept
105	0	45	26	22	103	20021.78	33.767	1	1	1	1
106	0	45	27	21	99	20021.78	34.342	1	1	1	1
107	0	45	28	20	95	20021.78	34.917	1	1	1	1
108	0	45	29	19	91	20021.78	35.492	1	1	1	1
109	0	45	30	18	87	20021.78	36.067	1	1	1	1
110	0	45	31	17	83	20021.78	36.642	1	1	1	1
111	0	45	32	16	79	20021.78	37.217	0	1	1	0
112	0	45	33	15	75	20021.78	37.792	0	1	1	0
97	0	44	26	23	103	19165.38	33.192	1	0	1	0
98	0	44	27	22	99	19165.38	33.767	1	0	1	0
99	0	44	28	21	95	19165.38	34.342	1	0	1	0
100	0	44	29	20	91	19165.38	34.917	1	0	1	0
101	0	44	30	19	87	19165.38	35.492	1	0	1	0
102	0	44	31	18	83	19165.38	36.067	1	0	1	0
103	0	44	32	17	79	19165.38	36.642	0	0	1	0
104	0	44	33	16	75	19165.38	37.217	0	0	1	0
89	0	43	26	24	103	18308.99	32.617	1	0	1	0
90	0	43	27	23	99	18308.99	33.192	1	0	1	0
91	0	43	28	22	95	18308.99	33.767	1	0	1	0
92	0	43	29	21	91	18308.99	34.342	1	0	1	0
93	0	43	30	20	87	18308.99	34.917	1	0	1	0
94	0	43	31	19	83	18308.99	35.492	1	0	1	0
95	0	43	32	18	79	18308.99	36.067	0	0	1	0
96	0	43	33	17	75	18308.99	36.642	0	0	1	0
81	0	42	26	25	103	17452.59	32.042	1	0	1	0
82	0	42	27	24	99	17452.59	32.617	1	0	1	0
83	0	42	28	23	95	17452.59	33.192	1	0	1	0
84	0	42	29	22	91	17452.59	33.767	1	0	1	0
85	0	42	30	21	87	17452.59	34.342	1	0	1	0
86	0	42	31	20	83	17452.59	34.917	1	0	1	0
87	0	42	32	19	79	17452.59	35.492	0	0	1	0
88	0	42	33	18	75	17452.59	36.067	0	0	1	0
73	0	41	26	26	103	16596.2	31.467	1	0	1	0
74	0	41	27	25	99	16596.2	32.042	1	0	1	0
75	0	41	28	24	95	16596.2	32.617	1	0	1	0
76	0	41	29	23	91	16596.2	33.192	1	0	1	0
77	0	41	30	22	87	16596.2	33.767	1	0	1	0
78	0	41	31	21	83	16596.2	34.342	1	0	1	0

79	0	41	32	20	79	16596.2	34.917	0	0	1	0
80	0	41	33	19	75	16596.2	35.492	0	0	1	0
65	0	40	26	27	103	15739.8	30.892	1	0	1	0
66	0	40	27	26	99	15739.8	31.467	1	0	1	0
67	0	40	28	25	95	15739.8	32.042	1	0	1	0
68	0	40	29	24	91	15739.8	32.617	1	0	1	0
69	0	40	30	23	87	15739.8	33.192	1	0	1	0
70	0	40	31	22	83	15739.8	33.767	1	0	1	0
71	0	40	32	21	79	15739.8	34.342	0	0	1	0
72	0	40	33	20	75	15739.8	34.917	0	0	1	0
57	0	39	26	28	103	14883.41	30.317	1	0	1	0
58	0	39	27	27	99	14883.41	30.892	1	0	1	0
59	0	39	28	26	95	14883.41	31.467	1	0	1	0
60	0	39	29	25	91	14883.41	32.042	1	0	1	0
61	0	39	30	24	87	14883.41	32.617	1	0	1	0
62	0	39	31	23	83	14883.41	33.192	1	0	1	0
63	0	39	32	22	79	14883.41	33.767	0	0	1	0
64	0	39	33	21	75	14883.41	34.342	0	0	1	0
49	0	38	26	29	103	14027.01	29.742	1	0	1	0
50	0	38	27	28	99	14027.01	30.317	1	0	1	0
51	0	38	28	27	95	14027.01	30.892	1	0	1	0
52	0	38	29	26	91	14027.01	31.467	1	0	1	0
53	0	38	30	25	87	14027.01	32.042	1	0	1	0
54	0	38	31	24	83	14027.01	32.617	1	0	1	0
55	0	38	32	23	79	14027.01	33.192	0	0	1	0
56	0	38	33	22	75	14027.01	33.767	0	0	1	0
41	0	37	26	30	103	13170.62	29.167	1	0	1	0
42	0	37	27	29	99	13170.62	29.742	1	0	1	0
43	0	37	28	28	95	13170.62	30.317	1	0	1	0
44	0	37	29	27	91	13170.62	30.892	1	0	1	0
45	0	37	30	26	87	13170.62	31.467	1	0	1	0
46	0	37	31	25	83	13170.62	32.042	1	0	1	0
47	0	37	32	24	79	13170.62	32.617	0	0	1	0
48	0	37	33	23	75	13170.62	33.192	0	0	1	0
33	0	36	26	31	103	12314.22	28.592	1	0	1	0
34	0	36	27	30	99	12314.22	29.167	1	0	1	0
35	0	36	28	29	95	12314.22	29.742	1	0	1	0
36	0	36	29	28	91	12314.22	30.317	1	0	1	0
37	0	36	30	27	87	12314.22	30.892	1	0	1	0
38	0	36	31	26	83	12314.22	31.467	1	0	1	0
39	0	36	32	25	79	12314.22	32.042	0	0	1	0

40	0	36	33	24	75	12314.22	32.617	0	0	1	0
25	0	35	26	32	103	11457.83	28.017	1	0	1	0
26	0	35	27	31	99	11457.83	28.592	1	0	1	0
27	0	35	28	30	95	11457.83	29.167	1	0	1	0
28	0	35	29	29	91	11457.83	29.742	1	0	1	0
29	0	35	30	28	87	11457.83	30.317	1	0	1	0
30	0	35	31	27	83	11457.83	30.892	1	0	1	0
31	0	35	32	26	79	11457.83	31.467	0	0	1	0
32	0	35	33	25	75	11457.83	32.042	0	0	1	0
17	0	34	26	33	103	10601.43	27.442	1	0	1	0
18	0	34	27	32	99	10601.43	28.017	1	0	1	0
19	0	34	28	31	95	10601.43	28.592	1	0	1	0
20	0	34	29	30	91	10601.43	29.167	1	0	1	0
21	0	34	30	29	87	10601.43	29.742	1	0	1	0
22	0	34	31	28	83	10601.43	30.317	1	0	1	0
23	0	34	32	27	79	10601.43	30.892	0	0	1	0
24	0	34	33	26	75	10601.43	31.467	0	0	1	0
9	0	33	26	34	103	9745.035	26.867	1	0	1	0
10	0	33	27	33	99	9745.035	27.442	1	0	1	0
11	0	33	28	32	95	9745.035	28.017	1	0	1	0
12	0	33	29	31	91	9745.035	28.592	1	0	1	0
13	0	33	30	30	87	9745.035	29.167	1	0	1	0
14	0	33	31	29	83	9745.035	29.742	1	0	1	0
15	0	33	32	28	79	9745.035	30.317	0	0	1	0
16	0	33	33	27	75	9745.035	30.892	0	0	1	0
1	0	32	26	35	103	8888.64	26.292	1	0	1	0
2	0	32	27	34	99	8888.64	26.867	1	0	1	0
3	0	32	28	33	95	8888.64	27.442	1	0	1	0
4	0	32	29	32	91	8888.64	28.017	1	0	1	0
5	0	32	30	31	87	8888.64	28.592	1	0	1	0
6	0	32	31	30	83	8888.64	29.167	1	0	1	0
7	0	32	32	29	79	8888.64	29.742	0	0	1	0
8	0	32	33	28	75	8888.64	30.317	0	0	1	0
217	1	45	26	22	89.791	8551.075	26.817	1	0	1	0
218	1	45	27	21	90.637	8551.075	26.742	1	0	1	0
219	1	45	28	20	91.483	8551.075	26.667	1	0	1	0
220	1	45	29	19	92.329	8551.075	26.592	1	0	1	0
221	1	45	30	18	93.175	8551.075	26.517	1	0	1	0
222	1	45	31	17	94.021	8551.075	26.442	1	0	1	0
223	1	45	32	16	94.867	8551.075	26.367	1	0	1	0
224	1	45	33	15	95.713	8551.075	26.292	1	0	1	0

209	1	44	26	23	89.791	8319.34	26.892	1	0	1	0
210	1	44	27	22	90.637	8319.34	26.817	1	0	1	0
211	1	44	28	21	91.483	8319.34	26.742	1	0	1	0
212	1	44	29	20	92.329	8319.34	26.667	1	0	1	0
213	1	44	30	19	93.175	8319.34	26.592	1	0	1	0
214	1	44	31	18	94.021	8319.34	26.517	1	0	1	0
215	1	44	32	17	94.867	8319.34	26.442	1	0	1	0
216	1	44	33	16	95.713	8319.34	26.367	1	0	1	0
201	1	43	26	24	89.791	8087.605	26.967	1	0	1	0
202	1	43	27	23	90.637	8087.605	26.892	1	0	1	0
203	1	43	28	22	91.483	8087.605	26.817	1	0	1	0
204	1	43	29	21	92.329	8087.605	26.742	1	0	1	0
205	1	43	30	20	93.175	8087.605	26.667	1	0	1	0
206	1	43	31	19	94.021	8087.605	26.592	1	0	1	0
207	1	43	32	18	94.867	8087.605	26.517	1	0	1	0
208	1	43	33	17	95.713	8087.605	26.442	1	0	1	0
193	1	42	26	25	89.791	7855.87	27.042	1	0	1	0
194	1	42	27	24	90.637	7855.87	26.967	1	0	1	0
195	1	42	28	23	91.483	7855.87	26.892	1	0	1	0
196	1	42	29	22	92.329	7855.87	26.817	1	0	1	0
197	1	42	30	21	93.175	7855.87	26.742	1	0	1	0
198	1	42	31	20	94.021	7855.87	26.667	1	0	1	0
199	1	42	32	19	94.867	7855.87	26.592	1	0	1	0
200	1	42	33	18	95.713	7855.87	26.517	1	0	1	0
185	1	41	26	26	89.791	7624.135	27.117	1	0	1	0
186	1	41	27	25	90.637	7624.135	27.042	1	0	1	0
187	1	41	28	24	91.483	7624.135	26.967	1	0	1	0
188	1	41	29	23	92.329	7624.135	26.892	1	0	1	0
189	1	41	30	22	93.175	7624.135	26.817	1	0	1	0
190	1	41	31	21	94.021	7624.135	26.742	1	0	1	0
191	1	41	32	20	94.867	7624.135	26.667	1	0	1	0
192	1	41	33	19	95.713	7624.135	26.592	1	0	1	0
177	1	40	26	27	89.791	7392.4	27.192	1	0	1	0
178	1	40	27	26	90.637	7392.4	27.117	1	0	1	0
179	1	40	28	25	91.483	7392.4	27.042	1	0	1	0
180	1	40	29	24	92.329	7392.4	26.967	1	0	1	0
181	1	40	30	23	93.175	7392.4	26.892	1	0	1	0
182	1	40	31	22	94.021	7392.4	26.817	1	0	1	0
183	1	40	32	21	94.867	7392.4	26.742	1	0	1	0
184	1	40	33	20	95.713	7392.4	26.667	1	0	1	0
169	1	39	26	28	89.791	7160.665	27.267	1	0	1	0

170	1	39	27	27	90.637	7160.665	27.192	1	0	1	0
171	1	39	28	26	91.483	7160.665	27.117	1	0	1	0
172	1	39	29	25	92.329	7160.665	27.042	1	0	1	0
173	1	39	30	24	93.175	7160.665	26.967	1	0	1	0
174	1	39	31	23	94.021	7160.665	26.892	1	0	1	0
175	1	39	32	22	94.867	7160.665	26.817	1	0	1	0
176	1	39	33	21	95.713	7160.665	26.742	1	0	1	0
161	1	38	26	29	89.791	6928.93	27.342	1	0	1	0
162	1	38	27	28	90.637	6928.93	27.267	1	0	1	0
163	1	38	28	27	91.483	6928.93	27.192	1	0	1	0
164	1	38	29	26	92.329	6928.93	27.117	1	0	1	0
165	1	38	30	25	93.175	6928.93	27.042	1	0	1	0
166	1	38	31	24	94.021	6928.93	26.967	1	0	1	0
167	1	38	32	23	94.867	6928.93	26.892	1	0	1	0
168	1	38	33	22	95.713	6928.93	26.817	1	0	1	0
153	1	37	26	30	89.791	6697.195	27.417	1	0	1	0
154	1	37	27	29	90.637	6697.195	27.342	1	0	1	0
155	1	37	28	28	91.483	6697.195	27.267	1	0	1	0
156	1	37	29	27	92.329	6697.195	27.192	1	0	1	0
157	1	37	30	26	93.175	6697.195	27.117	1	0	1	0
158	1	37	31	25	94.021	6697.195	27.042	1	0	1	0
159	1	37	32	24	94.867	6697.195	26.967	1	0	1	0
160	1	37	33	23	95.713	6697.195	26.892	1	0	1	0
145	1	36	26	31	89.791	6465.46	27.492	1	0	1	0
146	1	36	27	30	90.637	6465.46	27.417	1	0	1	0
147	1	36	28	29	91.483	6465.46	27.342	1	0	1	0
148	1	36	29	28	92.329	6465.46	27.267	1	0	1	0
149	1	36	30	27	93.175	6465.46	27.192	1	0	1	0
150	1	36	31	26	94.021	6465.46	27.117	1	0	1	0
151	1	36	32	25	94.867	6465.46	27.042	1	0	1	0
152	1	36	33	24	95.713	6465.46	26.967	1	0	1	0
137	1	35	26	32	89.791	6233.725	27.567	1	0	1	0
138	1	35	27	31	90.637	6233.725	27.492	1	0	1	0
139	1	35	28	30	91.483	6233.725	27.417	1	0	1	0
140	1	35	29	29	92.329	6233.725	27.342	1	0	1	0
141	1	35	30	28	93.175	6233.725	27.267	1	0	1	0
142	1	35	31	27	94.021	6233.725	27.192	1	0	1	0
143	1	35	32	26	94.867	6233.725	27.117	1	0	1	0
144	1	35	33	25	95.713	6233.725	27.042	1	0	1	0
129	1	34	26	33	89.791	6001.99	27.642	1	0	1	0
130	1	34	27	32	90.637	6001.99	27.567	1	0	1	0

131	1	34	28	31	91.483	6001.99	27.492	1	0	1	0
132	1	34	29	30	92.329	6001.99	27.417	1	0	1	0
133	1	34	30	29	93.175	6001.99	27.342	1	0	1	0
134	1	34	31	28	94.021	6001.99	27.267	1	0	1	0
135	1	34	32	27	94.867	6001.99	27.192	1	0	1	0
136	1	34	33	26	95.713	6001.99	27.117	1	0	1	0
121	1	33	26	34	89.791	5770.255	27.717	1	0	1	0
122	1	33	27	33	90.637	5770.255	27.642	1	0	1	0
123	1	33	28	32	91.483	5770.255	27.567	1	0	1	0
124	1	33	29	31	92.329	5770.255	27.492	1	0	1	0
125	1	33	30	30	93.175	5770.255	27.417	1	0	1	0
126	1	33	31	29	94.021	5770.255	27.342	1	0	1	0
127	1	33	32	28	94.867	5770.255	27.267	1	0	1	0
128	1	33	33	27	95.713	5770.255	27.192	1	0	1	0
113	1	32	26	35	89.791	5538.52	27.792	1	0	1	0
114	1	32	27	34	90.637	5538.52	27.717	1	0	1	0
115	1	32	28	33	91.483	5538.52	27.642	1	0	1	0
116	1	32	29	32	92.329	5538.52	27.567	1	0	1	0
117	1	32	30	31	93.175	5538.52	27.492	1	0	1	0
118	1	32	31	30	94.021	5538.52	27.417	1	0	1	0
119	1	32	32	29	94.867	5538.52	27.342	1	0	1	0
120	1	32	33	28	95.713	5538.52	27.267	1	0	1	0

Optimization Output File for K-25 Mixes

SL_NO	PG	CA1	CA2	NSC	NWP	FS	NWP_Accept	FS_Accept	ALL_Accept
121	0	40	43	15	19934.75	37.58333	0	1	0
242	1	40	43	15	19934.75	30.66666	0	1	0
110	0	39	43	16	19660	36.95833	0	1	0
120	0	40	42	16	19660	36.95833	0	1	0
231	1	39	43	16	19660	30.61666	0	1	0
241	1	40	42	16	19660	30.61666	0	1	0
99	0	38	43	17	19385.25	36.33333	0	1	0
109	0	39	42	17	19385.25	36.33333	0	1	0
119	0	40	41	17	19385.25	36.33333	0	1	0
220	1	38	43	17	19385.25	30.56666	0	1	0
230	1	39	42	17	19385.25	30.56666	0	1	0
240	1	40	41	17	19385.25	30.56666	0	1	0
88	0	37	43	18	19110.5	35.70833	0	1	0
98	0	38	42	18	19110.5	35.70833	0	1	0
108	0	39	41	18	19110.5	35.70833	0	1	0
118	0	40	40	18	19110.5	35.70833	0	1	0
209	1	37	43	18	19110.5	30.51666	0	1	0
219	1	38	42	18	19110.5	30.51666	0	1	0
229	1	39	41	18	19110.5	30.51666	0	1	0
239	1	40	40	18	19110.5	30.51666	0	1	0
77	0	36	43	19	18835.75	35.08333	0	1	0
87	0	37	42	19	18835.75	35.08333	0	1	0
97	0	38	41	19	18835.75	35.08333	0	1	0
107	0	39	40	19	18835.75	35.08333	0	1	0
117	0	40	39	19	18835.75	35.08333	0	1	0
198	1	36	43	19	18835.75	30.46666	0	1	0
208	1	37	42	19	18835.75	30.46666	0	1	0
218	1	38	41	19	18835.75	30.46666	0	1	0
228	1	39	40	19	18835.75	30.46666	0	1	0
238	1	40	39	19	18835.75	30.46666	0	1	0
66	0	35	43	20	18561	34.45833	0	1	0
76	0	36	42	20	18561	34.45833	0	1	0
86	0	37	41	20	18561	34.45833	0	1	0
96	0	38	40	20	18561	34.45833	0	1	0
106	0	39	39	20	18561	34.45833	0	1	0
116	0	40	38	20	18561	34.45833	0	1	0
187	1	35	43	20	18561	30.41666	0	1	0
197	1	36	42	20	18561	30.41666	0	1	0

207	1	37	41	20	18561	30.41666	0	1	0
217	1	38	40	20	18561	30.41666	0	1	0
227	1	39	39	20	18561	30.41666	0	1	0
237	1	40	38	20	18561	30.41666	0	1	0
55	0	34	43	21	18286.25	33.83333	0	1	0
65	0	35	42	21	18286.25	33.83333	0	1	0
75	0	36	41	21	18286.25	33.83333	0	1	0
85	0	37	40	21	18286.25	33.83333	0	1	0
95	0	38	39	21	18286.25	33.83333	0	1	0
105	0	39	38	21	18286.25	33.83333	0	1	0
115	0	40	37	21	18286.25	33.83333	0	1	0
176	1	34	43	21	18286.25	30.36666	0	1	0
186	1	35	42	21	18286.25	30.36666	0	1	0
196	1	36	41	21	18286.25	30.36666	0	1	0
206	1	37	40	21	18286.25	30.36666	0	1	0
216	1	38	39	21	18286.25	30.36666	0	1	0
226	1	39	38	21	18286.25	30.36666	0	1	0
236	1	40	37	21	18286.25	30.36666	0	1	0
44	0	33	43	22	18011.5	33.20833	0	1	0
54	0	34	42	22	18011.5	33.20833	0	1	0
64	0	35	41	22	18011.5	33.20833	0	1	0
74	0	36	40	22	18011.5	33.20833	0	1	0
84	0	37	39	22	18011.5	33.20833	0	1	0
94	0	38	38	22	18011.5	33.20833	0	1	0
104	0	39	37	22	18011.5	33.20833	0	1	0
114	0	40	36	22	18011.5	33.20833	0	1	0
165	1	33	43	22	18011.5	30.31666	0	1	0
175	1	34	42	22	18011.5	30.31666	0	1	0
185	1	35	41	22	18011.5	30.31666	0	1	0
195	1	36	40	22	18011.5	30.31666	0	1	0
205	1	37	39	22	18011.5	30.31666	0	1	0
215	1	38	38	22	18011.5	30.31666	0	1	0
225	1	39	37	22	18011.5	30.31666	0	1	0
235	1	40	36	22	18011.5	30.31666	0	1	0
33	0	32	43	23	17736.75	32.58333	0	1	0
43	0	33	42	23	17736.75	32.58333	0	1	0
53	0	34	41	23	17736.75	32.58333	0	1	0
63	0	35	40	23	17736.75	32.58333	0	1	0
73	0	36	39	23	17736.75	32.58333	0	1	0
83	0	37	38	23	17736.75	32.58333	0	1	0
93	0	38	37	23	17736.75	32.58333	0	1	0

103	0	39	36	23	17736.75	32.58333	0	1	0
113	0	40	35	23	17736.75	32.58333	0	1	0
154	1	32	43	23	17736.75	30.26666	0	1	0
164	1	33	42	23	17736.75	30.26666	0	1	0
174	1	34	41	23	17736.75	30.26666	0	1	0
184	1	35	40	23	17736.75	30.26666	0	1	0
194	1	36	39	23	17736.75	30.26666	0	1	0
204	1	37	38	23	17736.75	30.26666	0	1	0
214	1	38	37	23	17736.75	30.26666	0	1	0
224	1	39	36	23	17736.75	30.26666	0	1	0
234	1	40	35	23	17736.75	30.26666	0	1	0
22	0	31	43	24	17462	31.95833	0	1	0
32	0	32	42	24	17462	31.95833	0	1	0
42	0	33	41	24	17462	31.95833	0	1	0
52	0	34	40	24	17462	31.95833	0	1	0
62	0	35	39	24	17462	31.95833	0	1	0
72	0	36	38	24	17462	31.95833	0	1	0
82	0	37	37	24	17462	31.95833	0	1	0
92	0	38	36	24	17462	31.95833	0	1	0
102	0	39	35	24	17462	31.95833	0	1	0
112	0	40	34	24	17462	31.95833	0	1	0
143	1	31	43	24	17462	30.21666	0	1	0
153	1	32	42	24	17462	30.21666	0	1	0
163	1	33	41	24	17462	30.21666	0	1	0
173	1	34	40	24	17462	30.21666	0	1	0
183	1	35	39	24	17462	30.21666	0	1	0
193	1	36	38	24	17462	30.21666	0	1	0
203	1	37	37	24	17462	30.21666	0	1	0
213	1	38	36	24	17462	30.21666	0	1	0
223	1	39	35	24	17462	30.21666	0	1	0
233	1	40	34	24	17462	30.21666	0	1	0
11	0	30	43	25	17187.25	31.33333	0	1	0
21	0	31	42	25	17187.25	31.33333	0	1	0
31	0	32	41	25	17187.25	31.33333	0	1	0
41	0	33	40	25	17187.25	31.33333	0	1	0
51	0	34	39	25	17187.25	31.33333	0	1	0
61	0	35	38	25	17187.25	31.33333	0	1	0
71	0	36	37	25	17187.25	31.33333	0	1	0
81	0	37	36	25	17187.25	31.33333	0	1	0
91	0	38	35	25	17187.25	31.33333	0	1	0
101	0	39	34	25	17187.25	31.33333	0	1	0

111	0	40	33	25	17187.25	31.33333	0	1	0
132	1	30	43	25	17187.25	30.16666	0	1	0
142	1	31	42	25	17187.25	30.16666	0	1	0
152	1	32	41	25	17187.25	30.16666	0	1	0
162	1	33	40	25	17187.25	30.16666	0	1	0
172	1	34	39	25	17187.25	30.16666	0	1	0
182	1	35	38	25	17187.25	30.16666	0	1	0
192	1	36	37	25	17187.25	30.16666	0	1	0
202	1	37	36	25	17187.25	30.16666	0	1	0
212	1	38	35	25	17187.25	30.16666	0	1	0
222	1	39	34	25	17187.25	30.16666	0	1	0
232	1	40	33	25	17187.25	30.16666	0	1	0
10	0	30	42	26	16912.5	30.70833	0	1	0
20	0	31	41	26	16912.5	30.70833	0	1	0
30	0	32	40	26	16912.5	30.70833	0	1	0
40	0	33	39	26	16912.5	30.70833	0	1	0
50	0	34	38	26	16912.5	30.70833	0	1	0
60	0	35	37	26	16912.5	30.70833	0	1	0
70	0	36	36	26	16912.5	30.70833	0	1	0
80	0	37	35	26	16912.5	30.70833	0	1	0
90	0	38	34	26	16912.5	30.70833	0	1	0
100	0	39	33	26	16912.5	30.70833	0	1	0
131	1	30	42	26	16912.5	30.11666	0	1	0
141	1	31	41	26	16912.5	30.11666	0	1	0
151	1	32	40	26	16912.5	30.11666	0	1	0
161	1	33	39	26	16912.5	30.11666	0	1	0
171	1	34	38	26	16912.5	30.11666	0	1	0
181	1	35	37	26	16912.5	30.11666	0	1	0
191	1	36	36	26	16912.5	30.11666	0	1	0
201	1	37	35	26	16912.5	30.11666	0	1	0
211	1	38	34	26	16912.5	30.11666	0	1	0
221	1	39	33	26	16912.5	30.11666	0	1	0
9	0	30	41	27	16637.75	30.08333	0	1	0
19	0	31	40	27	16637.75	30.08333	0	1	0
29	0	32	39	27	16637.75	30.08333	0	1	0
39	0	33	38	27	16637.75	30.08333	0	1	0
49	0	34	37	27	16637.75	30.08333	0	1	0
59	0	35	36	27	16637.75	30.08333	0	1	0
69	0	36	35	27	16637.75	30.08333	0	1	0
79	0	37	34	27	16637.75	30.08333	0	1	0
89	0	38	33	27	16637.75	30.08333	0	1	0

130	1	30	41	27	16637.75	30.06666	0	1	0
140	1	31	40	27	16637.75	30.06666	0	1	0
150	1	32	39	27	16637.75	30.06666	0	1	0
160	1	33	38	27	16637.75	30.06666	0	1	0
170	1	34	37	27	16637.75	30.06666	0	1	0
180	1	35	36	27	16637.75	30.06666	0	1	0
190	1	36	35	27	16637.75	30.06666	0	1	0
200	1	37	34	27	16637.75	30.06666	0	1	0
210	1	38	33	27	16637.75	30.06666	0	1	0
8	0	30	40	28	16363	29.45833	0	1	0
18	0	31	39	28	16363	29.45833	0	1	0
28	0	32	38	28	16363	29.45833	0	1	0
38	0	33	37	28	16363	29.45833	0	1	0
48	0	34	36	28	16363	29.45833	0	1	0
58	0	35	35	28	16363	29.45833	0	1	0
68	0	36	34	28	16363	29.45833	0	1	0
78	0	37	33	28	16363	29.45833	0	1	0
129	1	30	40	28	16363	30.01666	0	1	0
139	1	31	39	28	16363	30.01666	0	1	0
149	1	32	38	28	16363	30.01666	0	1	0
159	1	33	37	28	16363	30.01666	0	1	0
169	1	34	36	28	16363	30.01666	0	1	0
179	1	35	35	28	16363	30.01666	0	1	0
189	1	36	34	28	16363	30.01666	0	1	0
199	1	37	33	28	16363	30.01666	0	1	0
7	0	30	39	29	16088.25	28.83333	0	1	0
17	0	31	38	29	16088.25	28.83333	0	1	0
27	0	32	37	29	16088.25	28.83333	0	1	0
37	0	33	36	29	16088.25	28.83333	0	1	0
47	0	34	35	29	16088.25	28.83333	0	1	0
57	0	35	34	29	16088.25	28.83333	0	1	0
67	0	36	33	29	16088.25	28.83333	0	1	0
128	1	30	39	29	16088.25	29.96666	0	1	0
138	1	31	38	29	16088.25	29.96666	0	1	0
148	1	32	37	29	16088.25	29.96666	0	1	0
158	1	33	36	29	16088.25	29.96666	0	1	0
168	1	34	35	29	16088.25	29.96666	0	1	0
178	1	35	34	29	16088.25	29.96666	0	1	0
188	1	36	33	29	16088.25	29.96666	0	1	0
6	0	30	38	30	15813.5	28.20833	0	1	0
16	0	31	37	30	15813.5	28.20833	0	1	0

26	0	32	36	30	15813.5	28.20833	0	1	0
36	0	33	35	30	15813.5	28.20833	0	1	0
46	0	34	34	30	15813.5	28.20833	0	1	0
56	0	35	33	30	15813.5	28.20833	0	1	0
127	1	30	38	30	15813.5	29.91666	0	1	0
137	1	31	37	30	15813.5	29.91666	0	1	0
147	1	32	36	30	15813.5	29.91666	0	1	0
157	1	33	35	30	15813.5	29.91666	0	1	0
167	1	34	34	30	15813.5	29.91666	0	1	0
177	1	35	33	30	15813.5	29.91666	0	1	0
5	0	30	37	31	15538.75	27.58333	0	1	0
15	0	31	36	31	15538.75	27.58333	0	1	0
25	0	32	35	31	15538.75	27.58333	0	1	0
35	0	33	34	31	15538.75	27.58333	0	1	0
45	0	34	33	31	15538.75	27.58333	0	1	0
126	1	30	37	31	15538.75	29.86666	0	1	0
136	1	31	36	31	15538.75	29.86666	0	1	0
146	1	32	35	31	15538.75	29.86666	0	1	0
156	1	33	34	31	15538.75	29.86666	0	1	0
166	1	34	33	31	15538.75	29.86666	0	1	0
4	0	30	36	32	15264	26.95833	0	1	0
14	0	31	35	32	15264	26.95833	0	1	0
24	0	32	34	32	15264	26.95833	0	1	0
34	0	33	33	32	15264	26.95833	0	1	0
125	1	30	36	32	15264	29.81666	0	1	0
135	1	31	35	32	15264	29.81666	0	1	0
145	1	32	34	32	15264	29.81666	0	1	0
155	1	33	33	32	15264	29.81666	0	1	0
3	0	30	35	33	14989.25	26.33333	0	1	0
13	0	31	34	33	14989.25	26.33333	0	1	0
23	0	32	33	33	14989.25	26.33333	0	1	0
124	1	30	35	33	14989.25	29.76666	0	1	0
134	1	31	34	33	14989.25	29.76666	0	1	0
144	1	32	33	33	14989.25	29.76666	0	1	0
2	0	30	34	34	14714.5	25.70833	0	1	0
12	0	31	33	34	14714.5	25.70833	0	1	0
123	1	30	34	34	14714.5	29.71666	0	1	0
133	1	31	33	34	14714.5	29.71666	0	1	0
1	0	30	33	35	14439.75	25.08333	0	1	0
122	1	30	33	35	14439.75	29.66666	0	1	0